GENETIC REGULATION OF VERTEBRATE RETINAL DEVELOPMENT

by

Jamie Lauren Zagozewski,

A thesis submitted in partial fulfillment of the requirements for the degree of

Doctor of Philosophy

Medical Sciences – Medical Genetics

University of Alberta

Abstract

Development of the vertebrate ocular structures requires the cooperative interactions of transcription factors, signalling proteins, external growth factors, and epigenetic regulatory factors. Consequently, misregulation of these cues can result in a number of developmental and functional defects. We were interested in the roles of the distal-less homeobox transcription factors (Dlx) *Dlx1* and *Dlx2*, and the transmembrane receptor neuropilin-2 (Nrp2) in the development of the vertebrate retina and ocular vasculature. In the retina, Dlx genes are known to be involved in the differentiation of retinal ganglion cells (RGC) by transactivating expression of genes required for both differentiation and survival of RGC. The role of Nrp2 in the developing retina, on the other hand, is unknown.

In addition to defects in RGC differentiation and survival in *Dlx1*/*Dlx2* double knockout (DKO) retinas, an increase in expression of a critical photoreceptor gene, *Crx* has been reported. This led us to hypothesize that *Dlx* genes are required to make binary cell fate decisions between RGC and photoreceptors through transcriptional repression of genes critical for photoreceptor development, including the basic helix-loop-helix transcription factor *Olig2*. We identified Olig2 as a transcriptional target of DLX2 both *in vivo* and *in vitro*. We determined that *Olig2* expression is limited to photoreceptor precursors and excluded from mature photoreceptors. Utilizing *Dlx1*/*Dlx2* DKO animals we observed strain-dependent ectopic expression of OLIG2 in the ganglion cell layer (GCL). We suggest that *Dlx1*/*Dlx2* expression is required for retinal progenitors to adopt an RGC fate and restrict the specification of photoreceptor cell fate. We also carried out studies of the role of *Dlx1*/*Dlx2* in neuronal differentiation in the developing forebrain, which provided further insight into the mechanisms by which *Dlx* genes regulate differentiation in the central nervous system (CNS).

Nrp2 is widely known for its role in axonal guidance in the CNS. Neuropilins have also been shown to be critical for both developmental and pathological angiogenesis. However, the function of *Nrp2* in the developing retina has not been previously explored. We postulated that

Nrp2 would also be critical for developmental angiogenesis and axonal guidance during ocular development. *Nrp2* expression was observed in the choroid and hyaloid vessels starting at early retinal development and in the RGC during later developmental stages. We observed increased expression of amacrine cell markers in the embryonic and adult *Nrp2* knockout eye, resulting in an expanded inner plexiform layer (IPL) in postnatal stages of retinal development. In addition, the hyaloid vasculature persisted into much later developmental stages when compared with wildtype (WT) littermate controls, which is reminiscent of the human ocular disease known as persistent fetal vasculature (PFV). In addition, the *Nrp2* null mice had a number of secondary ocular pathologies that are concurrent with PFV including retinal folding and microphthalmia. Our results indicated that *Nrp2* plays a critical role in both transient embryonic vascular development and amacrine cell genesis in the developing retina.

Collectively, we found that both *Dlx1*/*Dlx2* and *Nrp2* have critical roles in the development of early-born cells of the inner retina including RGC and amacrine cells, respectively. In addition, we discovered a novel role for *Nrp2* in hyaloid vasculature development. Future work clarifying the functional consequence of PFV and IPL expansion in the *Nrp2* knockout eye will be of great interest, as will the role of *Dlx* genes in postnatal retina development.

Preface

All procedures utilizing animals were approved by the University of Alberta Animal Care and Use Committee (ACUC) and the Canadian Council on Animal Care (CCAC), protocol number AUP00001115.

Chapter 3 contains primarily original unpublished work carried out by Jamie Zagozewski. Figure 3.12 is modified from an article published in *Development* on which Jamie Zagozewski is the second author (Zhang et al. 2017). Images of DLX2 immunostaining in *Atoh7* null retinas in Figure 3.12 were generated by Dr. Qi Zhang. Additional DLX2 staining in *Atoh7* null retinas for the purpose of cell counting, and statistical analysis was performed by Jamie Zagozewski. Figure Figure 3.9 is also adapted from our *Development* article.

Chapter 4 contains original work carried out primarily by Jamie Zagozewski. Marino Novel performed the p107 luciferase reporter gene assays, and Jamie Zagozewski prepared the vectors required for the reporter assay. Xiaohua Song carried out the *Dlx2* gain of function and knockdown experiments. Shaohong Cheng performed the ChIP-chip experiments.

Chapter 5 contains original unpublished work carried out by Jamie Zagozewski. Pranidhi Baddam from Dr. Daniel Graf's laboratory assisted with the H&E staining.

This thesis is dedicated to Iris Zagozewski and Leslie Gislason. Out of all they would have been the most proud to see “Dr.” attached to my name

Acknowledgements

It is said that it takes a village to raise a child. While I am willfully ignorant regarding the process of child rearing, I believe that replacing the word “child” with “higher degree” in this proverb would also reflect an absolutely true statement. There are so many people that contributed to this process in a number of ways both academically and in sanity maintenance.

I would firstly like to thank my supervisor, Dr. David Eisenstat for not only offering me the opportunity to come to Edmonton to pursue this degree, but for also being a consistent champion for me. For this, I am truly grateful.

I would also like to thank my committee members Dr. Ordan Lehmann, Dr. Andrew Waskiewicz, and Dr. Roseline Godbout for all of your invaluable advice and guidance.

To Dr. Mike Walter and Dr. Sarah Hughes: Thank you very much for your guidance. I am very grateful for the amazing jobs you do for the students in the department.

Thanks to Drs. Yves Sauvé and Daniel Graf for collaborating with us on the Nrp2 project. A huge “thank you” to Pranidhi Baddam for all of your hard work on the Nrp2 project.

Thanks to Dr. Andrew Simmonds for teaching me very valuable life lessons.

Thank you to Nichole, Shelley, and Collette from Health Sciences Laboratory Animal services for the daily care of our mice.

Thank you to Eisenstat lab 2.0 for all the support and friendship they have provided over the last few years.

I would also like to thank all the wonderful friends I made in the Department of Medical Genetics. I never would have expected I would meet such a great group of people in one small department. Every day in the department halls as well as evenings out and about in Edmonton with you guys was truly the highlight of this whole experience. I will miss you incredibly.

Alli: I’m so disappointed that you didn’t join the department earlier to make my time here that much more fun and enjoyable. Thanks for all the fun evenings you and Adrian hosted. Thanks for being my co-gym bro. We really killed it. Let’s just say there are other things I would like to say here, but it would probably be inappropriate to put in text.

Vanessa: The care and love you have for your friends is unmatched. I am so lucky to count myself as one of those friends. You are absolutely selfless and incredibly sweet (but you have just the right amount of sass too). You’re a very talented and hard-working student regardless of what you may think about that statement! Be safe around sofas and when I’m gone.

Maryam: You are quite possibly the nicest human that ever lived. Thanks for your help in the lab and being a great friend. I can honestly say there is nobody quite like you. Team retina forever!

Ping: Thank you for reluctantly becoming my friend. We both know you really didn't need to rotate your tires that night. Thanks for sharing all your chips with me, which in addition to your friendship is so excellent of you. A true friend shares their chips.

Lance: I'm so happy to have become your "little buddy" during my time here, even if Marino replaced my "little buddy" status shortly after you met him. I'm cool with it. Thank you for all your advice both in science and non-science things. Thanks for yelling "YOU'LL BE FINE" in my face while I prepared for my candidacy exam. It was much needed and very funny.

I would like to extend a thank you to the ladies ball hockey team, the Scibabes (formerly Medgene, The Mutants, and The Mutant Disasters). How awesome it was to win our intramurals division in my final season after six years with you ladies! I expect to be invited to a ceremony in the future where you retire my jersey to the rafters.

I would like to thank for family for helping to move me to Edmonton to start this journey. Your support means a lot to me. A special thank you to my brother Matthew, who is the superior genetic specimen of the Zagozewski F1 generation. Your annual visits to Edmonton were always so much fun and way too short. Thanks for being my best friend.

Finally, I would like to thank Marino. Words seem so inadequate to express what you mean to me. Thank you for the weekly Skype dates while you were in Poland. Thank you for always encouraging me, believing in me, and most of all for loving me. For those few hours a week when we spoke, it felt like I was home. I cannot wait to start this next chapter of our lives together and finally get to be together permanently. I love you immeasurably.

Since it is not like me to end on a serious note, I would also like to say that despite all these years in oil country, my loyalties have never wavered. Go Jets go.

Jamie Zagozewski
Edmonton, Alberta
2017

Table of Contents

ABSTRACT ..... **II**

PREFACE ..... **IV**

ACKNOWLEDGEMENTS ..... **VI**

TABLE OF CONTENTS ..... **VIII**

LIST OF TABLES ..... **XI**

LIST OF FIGURES ..... **XII**

LIST OF ABBREVIATIONS AND SYMBOLS ..... **XV**

1 CHAPTER 1: GENERAL INTRODUCTION **2**

1.1 OVERVIEW OF OCULAR DEVELOPMENT 2

1.2 SPECIFICATION AND BISECTION OF THE EYE FIELD 6

1.3 OPTIC VESICLE 6

1.4 OPTIC CUP: NEURAL RETINA AND RETINAL PIGMENTED EPITHELIUM 8

1.5 OVERVIEW OF RETINAL ANATOMY AND FUNCTION 10

1.5.1 Retinal progenitor cells *13*

1.5.2 Retinal ganglion cells *14*

1.5.3 Horizontal cells *15*

1.5.4 Amacrine cells *16*

1.5.5 Cone and rod photoreceptors *17*

1.5.6 Bipolar cells *18*

1.5.7 Müller glia cells *19*

2 CHAPTER 2: MATERIALS AND METHODS **22**

2.1 ANIMALS 22

2.2 TISSUE COLLECTION AND CRYOPRESERVATION 23

2.3 TISSUE IMMUNOFLUORESCENCE 24

2.3.1 Cell counting and statistical analysis *24*

2.4 HISTOLOGICAL STAINING 26

2.5 X-GAL STAINING 27

2.6 WHOLE-MOUNT ZEBRAFISH *IN SITU* HYBRIDIZATION 28

2.6.1 Generation of in situ hybridization probes *28*

2.6.2 In situ hybridization *28*

2.7 CHROMATIN IMMUNOPRECIPITATION 29

2.7.1 ChIP-chip *30*

2.7.2 ChIP-reChIP *31*

2.8 ELECTROPHORETIC MOBILITY SHIFT ASSAY 31

2.8.1 Deletion mutagenesis EMSA *32*

2.8.2 Production and affinity purification of rDLX2 ..... *33*

2.9 REPORTER GENE ASSAYS 33

2.9.1 Constructs for reporter assays *33*

2.9.2 Transfection and reporter gene assays *34*
2.10 *DLX2* GAIN-OF-FUNCTION AND *DLX2* KNOCKDOWN 35
2.11 QUANTITATIVE REAL-TIME PCR 36
2.12 RETINAL FLATMOUNTS AND INTRARETINAL RGC AXON LABELLING 39
2.13 *IN UTERO* RETINAL ELECTROPORATION 40
2.14 OPTICAL COHERENCE TOMOGRAPHY 41
2.15 FUNDUS IMAGING AND FLUORESCEIN ANGIOGRAPHY 42

3 CHAPTER 3: THE ROLE OF DLX GENES IN REGULATION OF RETINAL CELL FATE DECISIONS 44
3.1 INTRODUCTION 44
3.1.1 Role of invertebrate Dlx orthologue, Distal-less, in Drosophila development *44*
3.1.2 Organization and regulation of vertebrate Dlx genes *44*
3.1.3 Structure and function of DLX proteins *45*
3.1.4 Dlx expression and function in the developing retina *46*
3.1.5 Olig2: a neural progenitor factor in the CNS and retina *47*
3.2 RESULTS 49
3.2.1 dlx orthologues are not expressed in the zebrafish retina retina *49*
3.2.2 DLX2 and OLIG2 are expressed in distinct retinal cell populations in the retina *51*
3.2.3 OLIG2 co-localizes with photoreceptor precursors *56*
3.2.4 DLX2 binds to Olig2 regulatory chromatin elements *61*
3.2.5 Loss of Dlx1/Dlx2 results in ectopic expression of Olig2 in the GCL *67*
3.2.6 Exogenous Dlx2 drives expression of Brn3b, but photoreceptor gene expression excluded from cells ectopically expressing Dlx2 ..... *69*
3.2.7 Increase in Olig2 expressing cells in the Atoh7 null retina *75*
3.2.8 Olig2 transcript levels in the DKO retina are unchanged compared to controls in an inbred CD-1 background *81*
3.3 DISCUSSION 83
3.3.1 dlx is not observed in the developing zebrafish retina *83*
3.3.2 Dlx2 regulates the expression of Olig2 in the developing retina *84*
3.3.3 Dlx2 regulates binary retinal cell fate decisions by restricting Olig2 expression *86*
3.3.4 Background strain significantly affects photoreceptor differentiation in the absence of Dlx1/Dlx2 expression *93*

4 CHAPTER 4. REGULATION OF NEURAL DIFFERENTIATION IN THE DEVELOPING CENTRAL NERVOUS SYSTEM THOUGH TRANSCRIPTIONAL REGULATION OF *P107* 97
4.1 INTRODUCTION 97
4.1.1 Expression and function of Dlx genes in forebrain development *97*
4.1.2 Retinoblastoma family *100*
4.2 RESULTS 101
4.2.1 Identification and characterization of p107 as a transcriptional target for DLX2 ..... *101*
4.2.2 TAAT/ATTA homeodomain binding motifs in p107 regulatory elements are critical for DLX2 binding in vitro *103*
4.2.3 p107 expression is reduced in the SVZ of Dlx1/Dlx2 DKO forebrains *107*

4.2.4 Notch signalling is upregulated in the Dlx1/Dlx2 DKO GE but is unchanged in the retinas of Dlx1/Dlx2 DKO mice. *109*
4.2.5 Dlx2 gain-of-function in WERI-Rb-1 cells drives p107 expression whereas Dlx2 knockdown reduces p107 expression in vitro *111*
4.3 DISCUSSION 113
4.3.1 Dlx1/Dlx2 indirectly regulates Notch signalling through activation of p107 to promote neuronal differentiation in the subpallium *113*
4.3.2 Rb family regulates GABAergic interneuron differentiation both up- and downstream of Dlx1/Dlx2 ..... *118*
4.3.3 Reduction of p107 in the MGE may lead to specific reduction in cortical interneurons *119*

5 CHAPTER 5. PERSISTENT FETAL VASCULATURE IN THE *NRP2* KNOCKOUT EYE 122
5.1 INTRODUCTION 122
5.1.1 Ocular vascular systems *122*
5.1.2 Hyaloid vasculature and persistent fetal vasculature *124*
5.1.3 Neuropilins *129*
5.2 RESULTS 133
5.2.1 Expression of Neuropilins in the developing retina *133*
5.2.2 PFV and inner retina expansion in the embryonic Nrp2 null eye *137*
5.2.3 Reduced vitreal space and retinal folding in the Nrp2 null eye *142*
5.2.4 Optical coherence tomography also shows aberrations in the retinal cell layers *152*
5.2.5 Persistent pupillary membrane in the Nrp2 heterozygous eye *152*
5.2.6 Retrolental mass contains vascular and neural crest cells *156*
5.2.7 Nrp2 negatively regulates amacrine cell differentiation *165*
5.2.8 Intraretinal axonal guidance defects in the Nrp2 null retina *174*
5.2.9 Shh signalling is not affected in the absence of Nrp2 expression in the retina *176*
5.3 DISCUSSION 178
5.3.1 Nrp2 is critical for the development of the hyaloid vasculature *178*
5.3.2 Increased RGC may be due to lack of apoptosis through Semaphorin signalling. *184*
5.3.3 Increased amacrine cells/IPL in the Nrp2 null retina may be due to misregulation of TgfβII signalling *185*
5.3.4 Neuropilins may play a role in intraretinal axon guidance *186*

6 CHAPTER 6. OVERALL DISCUSSION AND CONCLUSIONS 190

7 BIBLIOGRAPHY 195

8 APPENDIX 235
8.1 CHARACTERIZATION OF THE *DLX1* AND *DLX2* SINGLE KNOCKOUT RETINAS 235

List of Tables

Table 1: Tissue fixation times for immunofluorescence or histological analysis..... 23

Table 2: List of antibodies used in the study 25

Table 3: List of primers used in the study 37

Table 4: Putative DLX2 transcriptional targets in the E13 forebrain 102

Table 5: Genetic models with phenotypes similar to Nrp2 KO.....183

List of Figures

Figure 1.1: Development of Retina. 5

Figure 1.2: Retinal competency model. 12

Figure 3.1: Absence of *dlx* expression in the developing zebrafish retina. 50

Figure 3.2 DLX2 and OLIG2 are expressed in distinct RPC and retinal cell populations. 54

Figure 3.3 DLX2 is expressed in RPC during early retinal development. 55

Figure 3.4 OLIG2 is expressed in photoreceptor precursors. 59

Figure 3.5 OLIG2 expression is not observed in differentiated amacrine cells. 60

Figure 3.6 DLX2 negatively regulates *Olig2* expression *in vivo*. 63

Figure 3.7 DLX2 binds to and restricts *Olig2* expression *in vitro*. 66

Figure 3.8 Strain-specific ectopic expression of OLIG2 in the *Dlx1*/*Dlx2* DKO retina. 68

Figure 3.9 *Dlx2* drives ectopic expression of BRN3B *in vivo* 72

Figure 3.10 Photoreceptor gene expression is excluded from cells ectopically expressing *Dlx2 in vivo*. 74

Figure 3.11 Increase in OLIG2 positive cells in the *Atoh7* knockout 78

Figure 3.12 DLX2 expression is reduced at the peak of RGC genesis in the *Atoh7* knockout. 80

Figure 3.13 No change in *Olig2* expression in the CD-1 *Dlx1/Dlx2* DKO retina 82

Figure 3.14 Proposed model of *Dlx1*/*Dlx2* regulation of retinal cell fate. 92

Figure 4.1 Expression pattern of *Dlx* genes in the subpallium 99

Figure 4.2 Several ATTA/TAAT homeodomain binding motifs are critical for DLX2 binding to *p107 in vitro*. 106

Figure 4.3 P107 expression is reduced in the *Dlx1*/*Dlx2* DKO forebrain. 108

Figure 4.4 Significant elevation of Notch signalling in the *Dlx1*/*Dlx2* DKO forebrain. 110

Figure 4.5 p107 expression is increased upon *Dlx2* gain of function and reduced with *Dlx2* knockdown. 112

Figure 4.6 Proposed model for Dlx1/Dlx2 regulation of *p107* expression and interneuron differentiation during forebrain development. 117

Figure 5.1 Hyaloid vasculature and PFV. 128

Figure 5.2 Neuropilin receptors and ligands. 132

Figure 5.3 Neuropilin expression during embryonic ocular development. 135

Figure 5.4 *Nrp2* is expressed in the inner cell layers of the adult retina. 136

Figure 5.5 Expanded inner retina and retrolental mass in the embryonic *Nrp2* null eye..... 140

Figure 5.6 Lens differentiation is unaffected in the absence of *Nrp2*..... 141

Figure 5.7 *Nrp2* knockout mice are significantly smaller than WT littermate controls at P28. .144

Figure 5.8 Microphthalmia, retinal folding, and PFV in the *Nrp2* knockout eye at P7. 146

Figure 5.9 Microphthalmia and retinal folding in the *Nrp2* knockout eye at P14..... 148

Figure 5.10 Microphthalmia, retinal folding, and PFV in the *Nrp2* knockout eye at P28. 150

Figure 5.11 Increased corneal thickness in the *Nrp2* knockout eye. 151

Figure 5.12 OCT imagining shows expanded IPL in *Nrp2* knockout retinas. 154

Figure 5.13 PFV in the *Nrp2* heterozygous eye. 155

Figure 5.14 Retrolental mass in the *Nrp2* knockout eye contains IB4 positive endothelial cells. 159

Figure 5.15 Collagen IV is expressed in *Nrp2* knockout retrolental mass. 161

Figure 5.16 Co-localization of NRP1 and Collagen IV in the vitreal mass in the *Nrp2* knockout. 163

Figure 5.17 Accumulation of non-functional NRP2 positive cells in the vitreous of the *Nrp2* knockout mouse. 164

Figure 5.18 No change in RGC and amacrine cells is observed during early retinal development in the *Nrp2* knockout. 168

Figure 5.19 Increased amacrine and RGC in the *Nrp2* knockout retina at E18. 170

Figure 5.20 Increased amacrine cells in the P7 *Nrp2* knockout retina. 171

Figure 5.21 Increased amacrine cells in the P14 *Nrp2* knockout retina. 172

Figure 5.22 Increased amacrine cells in the P28 *Nrp2* knockout retina. 173

Figure 5.23 Intraretinal axonal guidance defects may be present in the *Nrp2* null retina. 175

Figure 5.24 Shh signalling is not affected in the absence of *Nrp2* during early retinal development. 177

Figure 8.1 *Dlx2* SKO retina resembles *Dlx1*/*Dlx2* DKO. 238

List of Abbreviations and Symbols

°C	Degrees Celsius
µM	Micrometer
µl	Microliter
AMD	Age-related macular degeneration
αDLX2	High affinity DLX2 antibody
bHLH	Basic helix-loop-helix
Bp	Base pair
BrdU	5-bromo 2'-deoxyuridine
cDNA	Complementary deoxyribonucleic acid
ChIP	Chromatin immunoprecipitation
CNS	Central Nervous System
CV	Cresyl Violet
CO2	Carbon dioxide
DAPI	4′,6-diamidine-2-phenylindole
DKO	Double knockout
Dlx2	Distal-less homebox (gene)
DLX2	Distal-less homeobox (protein)
dlx	Distal-less homeobox gene (zebrafish)
DNA	Deoxyribonucleic acid
DMEM	Dulbecco's modified Eagle's medium
E	Embryonic day
E.coli	*Escherichia coli*
EGFP	Enhanced green fluorescent protein

EMSA	Electrophoretic mobility shift assay
FBS	Fetal bovine serum
FEVR	Familial exudative vitreoretinopathy
Gapdh	Glyceraldehyde 3-phosphate dehydrogenase
GCL	Ganglion cell layer
gDNA	Genomic deoxyribonucleic acid
GE	Ganglionic eminence
GFP	Green fluorescent protein
GTP [α-^{32}P]	Guanosine triphosphate labelled with ^{32}P
H&E	Hematoxylin and eosin
INL	Inner nuclear layer
IPL	Inner plexiform layer
ISH	In situ hybridization
LB	Lysogeny broth
LGE	Lateral ganglionic eminence
MG	Müller glia
MGE	Medial ganglionic eminence
ML	Millilitre
NBL	Neuroblastic layer
Nrp1	Neuropilin-1
Nrp2	Neuropilin-2
OCT	Optical coherence tomography
ONL	Outer nuclear layer
O/N	Overnight
OPL	Outer plexiform layer

P	Postnatal day
PBS	Phosphate buffered saline
PCR	Polymerase chain reaction
PFA	Paraformaldehyde
qRT-PCR	Quantitative real-time polymerase chain reaction
Rb	Retinoblastoma gene
rDLX2	Recombinant DLX2 protein
RGC	Retinal ganglion cells
RNA	Ribonucleic acid
RPC	Retinal progenitor cell
RPE	Retinal pigment epithelium
RPM	Revolutions per minute
RT	Room temperature
Shh	Sonic hedgehog
SVZ	Subventricular zone
VEGF	Vascular endothelial growth factor
VZ	Ventricular zone
WT	Wildtype

CHAPTER 1: GENERAL INTRODUCTION

1 Chapter 1: General introduction

The utilization of reverse genetics approaches has led to the discovery of genes and gene networks that are critical for the specification, differentiation, and function of the ocular cells and structures. The goal of our study was to determine the roles of *Dlx* homeobox genes, and the semaphorin ligand receptor, *Nrp2* in the development of the vertebrate retina and the transient ocular vasculature. In addition, we carried out studies on the role of *Dlx1*/*Dlx2* in the developing forebrain, which further unravel the role of *Dlx* genes in cell fate decisions and differentiation in the central nervous system. To this end, we examined knockout mouse models for *Dlx1*/*Dlx2* and *Nrp2*, and subsequently performed a number of molecular and biochemical assays in order to determine their functional role in ocular development. In this thesis, I will describe our findings and demonstrate how *Dlx1*/*Dlx2* and *Nrp2* integrate into the regulatory networks that are required for the proper development of the vertebrate retina and ocular vasculature.

1.1 Overview of ocular development

The foundation of the future ocular structures is first established during gastrulation when a single eye field is specified centrally in the anterior neural plate. The eye field is then bisected at the midline allowing for the generation of the bilateral optic vesicles, which arise as lateral projections of the diencephalic neuroectoderm (Chow and Lang 2001, Kim and Kim 2012, Zagozewski, Zhang, and Eisenstat 2014). The optic vesicles are the first visible ocular structures in the developing murine embryo, which grow and extend laterally toward the surface ectoderm (Figure 1.1). Concurrent with the generation of the optic vesicles, the surface ectoderm thickens giving rise to the lens placode. The optic vesicles then come into close contact with the overlying lens placode, initiating the invagination of the lens placode into the optic vesicle. From this invagination, generation of the optic cup and prospective lens begins. As the surface ectoderm closes, the lens vesicles and optic cups are formed. The optic cup is then separated into anterior neural retina and posterior retinal pigment epithelium (RPE). Retinal progenitor

cells (RPC) of the neural retina will then begin to differentiate into the neural and glia cells of the retina and will be described in more detail below.

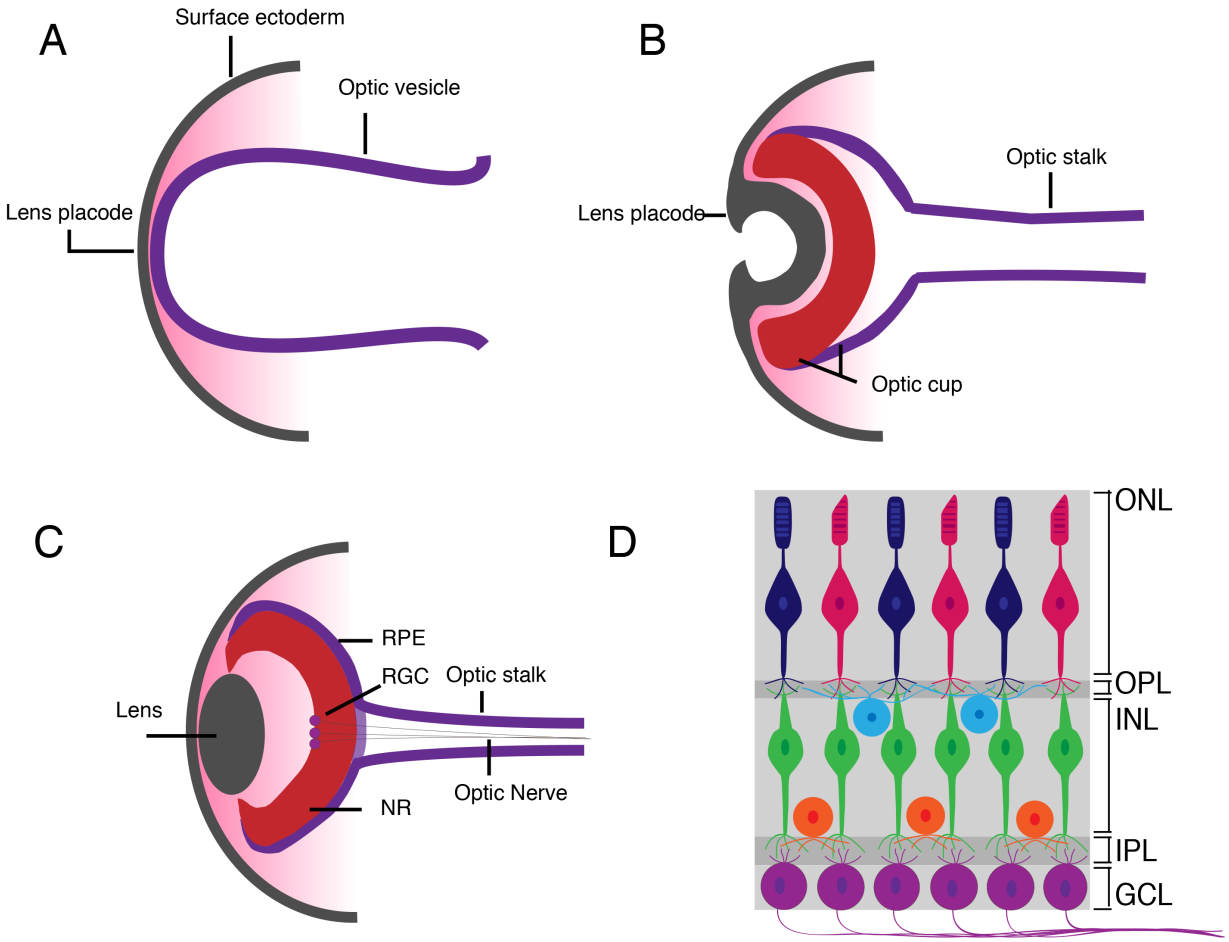
A
Surface ectoderm
Optic vesicle
Lens placode
B
Optic stalk
Lens placode
Optic cup
C
RPE
RGC
Optic stalk
Lens
Optic Nerve
NR
D
ONL
OPL
INL
IPL
GCL

Figure 1.1: Development of Retina.

(A) The first structures discernable as ocular structures during early ocular development are the bilateral optic vesicles. The optic vesicles extend laterally toward the thickening surface ectoderm, which will give rise to the lens placode. (B) Close contact of the optic vesicle with the surface ectoderm initiates the invagination of the lens placode into the optic vesicle. This initiates the development of the prospective lens and optic cup structures. (C) The optic cup is separated into neural retina tissue and the posteriorly localized RPE, and the lens placode pinches off to form the lens. When neural retina development is initiated, the RGC are the first neural retina cell to differentiate. RGC project their axons from the retina through the optic tract and into the superior colliculus. (D) The mature retina contains six neural retina cell types and one macroglial cell class (glial cells not shown). The mature retina is organized into three cellular layers including the innermost GCL, INL, and ONL. The organization is such that light entering the eye is converted to electrical signals by the photoreceptors in the ONL, which is then transmitted to the cells of the INL, and then finally to the cells in the GCL where the RGC then transmits the signal to the brain for processing.

[GCL; ganglion cell layer, INL; inner nuclear layer, IPL, inner plexiform layer, NR; neural retina, ONL; outer nuclear layer, OPL; outer plexiform layer, RGC; retinal ganglion cells, RPE; retinal pigment epithelium. Figure modified from (Zagozewski, Zhang, and Eisenstat 2014), reproduced with permission]

1.2 Specification and bisection of the eye field

Prior to the specification of the vertebrate eye field, Wnt signalling is required to establish the anterior-posterior polarity of the neural ectoderm (Erter et al. 2001, Lekven et al. 2001). Wnt expression specifies posterior neural fates and must be suppressed for development of anterior neural structures including the prospective eye field (Erter et al. 2001, Kiecker and Niehrs 2001, Lekven et al. 2001). Hyper-activation of Wnt signalling leads to the expansion of the posterior neural structures at the expense of the anterior neural tissue resulting in the absence of eye development. The specification of the eye field requires the cooperative expression of a number of eye field transcription factors. These eye field transcription factors include *Pax6*, *Rax*, *Lhx2*, *Six3*, *tll/Tlx*, *Six6,* and *Tbx3* (Zuber et al. 2003). *Otx2* also plays a permissive role in specification of the eye field where *Otx2* expression is required for forebrain specification. As will become apparent throughout the introduction chapter, these transcription factors have a number of roles in ocular development, from early eye field specification to retinal cell specification. Following specification of the forebrain by *Otx2*, the anterior neural plate is now competent to specify the eye field (Zuber et al. 2003). Mice with mutations in eye field transcription factors, including LIM homeobox 2 (*Lhx2*), Paired box 6 (*Pax6*), Retina and anterior fold homeobox gene (*Rax*), and SIX homeobox 3 (*Six3*), have abnormal eye development or fail to form visible ocular structures (Carl, Loosli, and Wittbrodt 2002, Hill et al. 1991, Mathers et al. 1997, Porter et al. 1997). During establishment of the midline, the eye field is bisected to enable the generation of the bilateral optic vesicles. Sonic hedgehog (Shh) expression is critical for this process. Mice lacking Shh expression fail to establish the midline and split the eye field into two bilateral components resulting in the development of holoprosencephaly and a single midline eye or “cyclops” phenotype (Chiang et al. 1996).

1.3 Optic Vesicle

The optic vesicles are the first visible ocular structures. Following its early role in eye field specification, *Rax* (formerly *Rx*) is critical for development of the optic vesicles (Bailey et

al. 2004). *Rax* mutations have been described in humans, mice and zebrafish, which resulted in the lack visible ocular structures (Abouzeid et al. 2012, Furukawa, Kozak, and Cepko 1997, Loosli et al. 2003, Voronina et al. 2004). As the name suggests, *Rax* is also expressed in the cephalic neural folds (Furukawa, Kozak, and Cepko 1997). Therefore, in addition to anophthalmia, *Rax* mutants also lack forebrain structures. The *Rax* zebrafish orthologue *rx3* is critical for the lateral evagination of optic vesicles from the neural ectoderm (Loosli et al. 2003). In the *rx3* null zebrafish, retinal cells converge at the midline and fail to migrate laterally and optic vesicles fail to form. Transcriptional targets of *rx3* have been identified that could contribute to the lack of lateral migration observed including *cxcr4a* and *nlcam*, which are chemokine signalling receptors and cell adhesion proteins, respectively, each having known roles in cellular migration (Loosli et al. 2003).

Lhx2 is also critical for the proper development and patterning of the optic vesicles. Like *Rax*, *Lhx2* expression is first observed in the neural ectoderm of the eye field and is later expressed in the optic vesicles. In *Lhx2* null mice, eye field specification is unaffected, but the transition of the optic vesicle to the optic cup fails, thereby results in anophthalmia (Hagglund, Dahl, and Carlsson 2011, Yun et al. 2009). Therefore, unlike *Rax* mutants that do not generate visible optic vesicles, the optic vesicles in *Lhx2* mutants develop and evaginate toward the lens placode but subsequently fail to generate the optic cups. Despite the anophthalmia observed in the *Lhx2* mutant mice, no human anophthalmic cases resulting from *LHX2* mutation have been identified to date. The dorsal-ventral patterning of the developing optic vesicle is also disrupted in *Lhx2* null mice. *Lhx2* mutant optic vesicles become dorsalized as *Pax6* expression extends ventrally at the expense of the ventral patterning transcription factor *Vax2* (Yun et al. 2009). In addition, expression of the ventral patterning markers *Tbx5* and *Bmp4* is absent, and ventral expression of *Pax2* while initiated normally, fails to be maintained in the *Lhx2* mutant optic vesicle (Yun et al. 2009).

In addition to establishing the midline of the anterior neural plate, Shh is also critical for ventral specification of the optic vesicles. The transcription factors Ventral anterior homeobox (Vax), *Vax1*, *Vax2* and Paired box 2 (*Pax2*) are all driven by Shh in the ventral optic vesicle (Sasagawa et al. 2002, Take-uchi, Clarke, and Wilson 2003). In addition to the ventral identity of the optic vesicle, *Pax2* also patterns the optic vesicle on the proximal-distal axis, specifying the prospective optic stalk (Puschel, Westerfield, and Dressler 1992). The ventral optic stalk is the location of the transient choroid fissure through which blood vessels enter the developing eye and RGC axons can exit. In *Pax2* mutants, this fissure fails to close leading to the development of optic nerve coloboma (Sanyanusin et al. 1995). *Pax2* loss also results in the ventral expansion of *Pax6* in the optic vesicle. *Pax6* is required to pattern the dorsal-distal region of the optic vesicle as prospective neural retina (Walther and Gruss 1991, Grindley, Davidson, and Hill 1995). Dorsal expansion of *Pax2* is observed in *Pax6* mutant optic vesicles. Therefore, the boundary between the prospective optic stalk and neural retina and dorso-ventral patterning of the optic stalk is maintained by reciprocal repression of *Pax2* and *Pax6* (Schwarz et al. 2000, Chow and Lang 2001, Zagozewski, Zhang, and Eisenstat 2014, Zagozewski et al. 2014).

1.4 Optic cup: neural retina and retinal pigmented epithelium

Pax6 is often referred to as the "master regulator" of eye development. Indeed, *Pax6* plays a number of critical roles throughout multiple stages of ocular development. As described above, *Pax6* is one of many eye field transcription factors that specify the vertebrate eye field, patterns the prospective neural retina at the optic vesicle stage, is critical for lens development, and maintains retina progenitor cell (RPC) multipotency (Macdonald et al. 1995, Ashery-Padan et al. 2000, Schwarz et al. 2000, Ashery-Padan and Gruss 2001, Marquardt et al. 2001). Not surprisingly, PAX6 mutations give rise to a number of ocular disorders including aniridia, coloboma, cataracts, Peters' anomaly, optic nerve hypoplasia, and foveal hypoplasia (Brown et al. 1998, Tzoulaki, White, and Hanson 2005, Zagozewski, Zhang, and Eisenstat 2014). Pax6 null

mice fail to develop eyes, a phenotype that was first described in *Drosophila* almost 70 years ago (Sturtevant 1951).

Similar to the *Lhx2* null eye, development fails at the optic vesicle stage in *Pax6* null mice (Grindley, Davidson, and Hill 1995, Hill et al. 1991). Despite this, the prospective neural retina and retinal pigment epithelium (RPE) are still established in the *Pax6* null mouse, suggesting that *Pax6* is dispensable for early optic vesicle generation. The neural retina and the RPE form the inner layer and outer layer of the developing optic cup, respectively. In the RPE, combined *Pax2*/*Pax6* expression is required to drive expression of microphthalmia associated transcription factor (*Mitf*) in the RPE (Baumer et al. 2003). *Mitf* is a critical factor for RPE specification where it prevents the RPE from adopting a neural retina fate (Bumsted and Barnstable 2000, Mochii et al. 1998). In addition to *Mitf*, *Otx2* is also a significant factor for RPE differentiation. Similar to *Mitf*, mutation in *Otx2* results in aberrant patterning of RPE into neural retina (Martinez-Morales et al. 2003, Martinez-Morales et al. 2001). *Mitf* and *Otx2* each transactivate the expression of a number of genes involved in RPE differentiation including *QNR71*, *Trp1*, *Trp2* and *Tyr* (Goding 2000, Martinez-Morales et al. 2003).

A number of extrinsic factors are also critical for the patterning of the optic cup including transforming growth factor β (Tgfβ) Wnt, fibroblast growth factor (Fgf) and bone morphogenetic protein (Bmp) signalling. At the initiation of optic cup formation, Tgfβ, Wnt and Bmp originating from the ocular mesenchyme surrounding the optic cup contribute to RPE specification by inducing the expression of *Mitf* and *Otx2* (Fuhrmann, Levine, and Reh 2000, Fujimura et al. 2009). Loss-of-function mutations in these signalling proteins result in upregulation of *Vsx2* (formerly *Chx10*) expression at the expense of *Mitf* and *Otx2*, which then re-specifies the RPE as neural retina (Nguyen and Arnheiter 2000, Pittack, Grunwald, and Reh 1997, Fujimura et al. 2009, Fuhrmann 2010).

FGF is highly expressed in the surface ectoderm and contact of the optic vesicle with the overlying surface ectoderm is thought to initiate neural retina specification. Neural retina identity is maintained by expression of Vsx2 (Liu et al. 1994). Removal of the surface ectoderm or blockage of FGF signalling fails to upregulate Vsx2 expression and consequently specification of the neural retina fails (Pittack, Grunwald, and Reh 1997). FGF expression also restricts the alternative RPE fate as the absence of surface ectoderm/FGF expression also leads to ectopic expression of *Mitf* in the prospective neural tissue (Horsford et al. 2005, Nguyen and Arnheiter 2000). Following the specification of the neural retina in the optic cup, multipotent RPC begin proliferating to allow for the subsequent specification and differentiation of all retinal cell types. Retinogenesis will be discussed in detail below.

1.5 Overview of retinal anatomy and function

The mature retina is populated by seven retinal cell types including six neural cell and one glial cell type. These cell types, in order of their birth, are retinal ganglion cells (RGC), horizontal cells, cone photoreceptors, amacrine cells, rod photoreceptors, bipolar cells and Müller glia (MG) cells, born in highly conserved overlapping temporal windows of development (Marquardt and Gruss 2002, Young 1985). All retinal cells are derived form a common pool of multipotent RPC competent to generate all retinal cell types (Figure 1.2) (Turner and Cepko 1987). The mature retina is organized into three cellular layers, which include the innermost GCL, the inner nuclear layer (INL), and the outer nuclear layer (ONL). These cellular layers are separated by synaptic plexiform layers, and bordered on the outer retina by the RPE, and the nerve fibre layer on the inner retina (Dowling 1970). As the name suggests, the GCL contains the cell bodies of the RGC but also contains displaced amacrine cells. The INL contains the cell bodies of the amacrine cells, bipolar cells, and horizontal cells. The ONL contains the cell bodies of the rod and cone photoreceptors. The organization of these layers establishes the visual system from which visual information is transported from the outermost layers of the retina to the brain for interpretation of this information. First, light enters the eye and is converted to electrical signals

in the outer segments of the photoreceptors via a process called phototransduction. This information is carried to the outer plexiform layer (OPL) and relayed to the horizontal and bipolar cells. Bipolar cells in the INL then synapse the information onto amacrine cells and RGC terminals in the inner plexiform layer (IPL). Finally, RGC in the GCL relay the visual information along their axons, through the optic nerve, and finally to the brain.

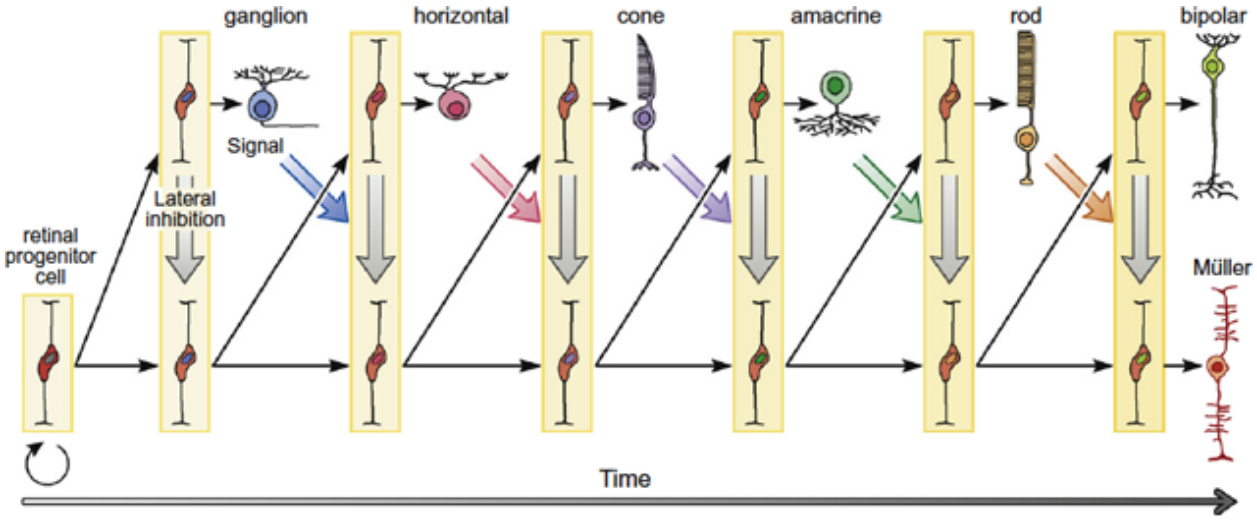

Figure 1.2: Retinal competency model.

Retinal cells are generated from a pool of multipotent RPC that are competent to generate all retinal cell types, which are born in a highly conserved, temporally overlapping windows of development. At the start of neural retinogenesis, the multipotent RPC pool expands by self-renewing (symmetrical) divisions (far left curved arrow). Early proneural gene expression then increases to promote the RPC to adopt early retinal cell fates. Newly committed retinal cells (grey arrows) restrict RPC from adopting the same fate (lateral inhibition). Intrinsic factors expressed in newly differentiating retinal cells also restrict the RPC from specifying the same retinal cell fate (coloured arrows), restricting RPC competency, and allowing for unidirectional acquisition of retinal cell fates.

[RPC; retinal progenitor cell. Figure from (Reese 2011), reproduced with permission]

1.5.1 Retinal progenitor cells

Development of all retinal cells requires a large pool of multipotent RPC (Turner and Cepko 1987). A number of intrinsic factors are required to keep the progenitors in a multipotent state. As development progresses, the competency of RPC becomes temporally restricted allowing for unidirectional differentiation of early to late born retinal cells (Figure 1.2). This restriction in competency primarily comes from signals arising from the differentiating retinal cells, signalling to the RPC to stop producing the same retinal cell types.

One important factor for RPC multipotency is *Vsx2*. *Vsx2* is critical for the proliferation of RPC, increasing the progenitor pool so the correct retinal size is achieved and all retinal cell types can be generated (Burmeister et al. 1996, Liu et al. 1994). Mutations in *Vsx2* were first described in the ocular retardation mouse model, or^{J} (Burmeister et al. 1996). This model contains a mutation that introduces a premature stop codon disrupting the function of Vsx2. As a result of this mutation, a significant reduction in the size of the eye is observed owing to dramatically reduced proliferation of RPC.

Pax6 also contributes to RPC proliferation in early retinogenesis. *Pax6* is required to maintain RPC multipotency during early retinogenesis (Marquardt et al. 2001). In *Pax6* null eyes, RPC competency is restricted dramatically, leading to the production of amacrine cells only. Pro-neural gene expression, including atonal bHLH transcription factor 7 (*Atoh7*, previously *Math5*) and neurogenin-2, are not upregulated in the *Pax6* null retina, contributing to the failure to generate non-amacrine retinal cell types (Marquardt et al. 2001, Riesenberg et al. 2009).

In addition to its role in early ocular development, *Rax* is also an important factor maintaining RPC identity. *Rax* is expressed throughout the neural retina in the RPC population and decreases in expression upon retinal cell differentiation (Mathers et al. 1997). Loss of Rax decreases RPC proliferation, and RPC multipotency through reduced expression of *Pax6* (Nelson, Park, and Stenkamp 2009, Zhang, Mathers, and Jamrich 2000).

1.5.2 Retinal ganglion cells

RGC are the first retinal cell types to differentiate in the neural retina. The RGC are the terminal cells in the cellular chain that transmits visual information from the retina to the brain. The RGC transmits the visual information to the brain via their axons, which form the optic nerve. There are currently 25 distinct types of RGC described based on molecular, physiological, and morphological criteria (Sanes and Masland 2015).

As is required for differentiation of all retinal cells, RPC must be competent to specify RGC. The bHLH transcription factor *Atoh7* is critical for RPC to become competent to generate RGC (Brown et al. 2001, Wang et al. 2001). *Atoh7* is atop the genetic regulatory network for RGC differentiation. In the absence of *Atoh7* expression RGC are not formed, and an increase in cone photoreceptors is observed. In addition, as a result of significant RGC loss, optic nerves are not formed. The increase in cones in the absence of Atoh7 expression indicates an overlapping temporal window of RGC and cone genesis in early retinal development, and a shift in progenitor cell fate in the absence of *Atoh7* expression. Following RGC specification, Atoh7 upregulates the expression of a number of genes that are critical for RGC differentiation (Gao et al. 2014). Two transcription factors critical for RGC differentiation include *Brn3b* and *Isl1*. In *Brn3b* null adult retinas approximately 80% of RGC are lost (Erkman et al. 1996, Gan et al. 1996). As development progresses in *Brn3b* null mice, the RGC axons become defasciculated, project abnormally, and undergo apoptosis beginning at E15.5. However, early RGC specification and migration occurs normally in the absence of *Brn3b* and therefore, *Brn3b* is dispensable for these processes. In parallel to *Brn3b*, *Isl1* is also a critical factor for differentiation of RGC. Much like that observed in the *Brn3b* null retina, RGC in *Isl1* mutant retinas are specified and migrate normally, but at late embryonic retinogenesis, defects in axon pathfinding are observed as well as a significant increase in RGC apoptosis (Mu et al. 2008, Pan et al. 2008). The defects in RGC differentiation and survival observed in the *Brn3b* and *Isl1* mutants arise from a lack of transcriptional control of target genes required for RGC genesis,

and the lack of neurotropic support to the RGC in aberrant axonal pathfinding. Compound mutants of *Brn3b* and *Isl1* have even greater RGC apoptosis where 95% of RGC are lost (Pan et al. 2008). *Brn3b* and *Isl1*, share a number of downstream transcriptional targets and can each bind to the regulatory DNA to control transcription of these genes (Mu et al. 2008, Pan et al. 2008). Some of these shared targets include *Shh*, *Gap43*, *L1cam* and *Isl1*, which play roles in RGC development, axonal guidance and fasciculation.

The remaining 5% of RGC found in the compound *Brn3b;Isl1* mutant indicate that additional factors are required for complete RGC genesis. Other factors that are important for RGC genesis are the distal-less homeobox genes (*Dlx*), *Dlx1* and *Dlx2*. Like *Brn3b* and *Isl1*, RGC loss is observed at later embryonic RGC genesis in the *Dlx1*/*Dlx2* DKO retina. Because the *Dlx1*/*Dlx2* DKO mouse dies at birth, the consequence of RGC loss in the absence of *Dlx1*/*Dlx2* is unknown. This loss of RGC can partially be attributed to a reduction in *TrkB* expression. *TrkB* is a transcriptional target for DLX2 in the embryonic retina (de Melo et al. 2008). *TrkB* is a neurotrophic receptor expressed in RGC and has known roles in neuronal survival through its interaction with the neurotrophic ligand Brain Derived Neurotrophic Factor (BDNF) (Pollock et al. 2003, Rohrer et al. 2001). DLX2 also transactivates expression of *Brn3b* thereby contributing to RGC differentiation through activation of *Brn3b* (Zhang et al. 2017). The role of *Dlx* genes in development and retinogenesis will be discussed further in Chapter 3 and Chapter 4.

1.5.3 Horizontal cells

Horizontal cells are located in the outer INL where they relay visual signals from the photoreceptors laterally along the OPL. There are three subtypes in the vertebrate retina, which like the RGC are classified based on morphological and molecular criteria..

Formation of horizontal cells requires the expression of *FoxN4* and *Ptf1a* (Boije et al. 2016, Li et al. 2004, Fujitani et al. 2006). Deletion of either of these two genes abolishes the generation of horizontal cells and also significantly reduces amacrine cell genesis in the retina. Significant loss of horizontal cells is also observed in the Onecut1 (*Oc1*) null retina (Wu et al.

2013). Approximately 80% of horizontal cells are lost in the absence of *Oc1* expression. Compound mutants of *Oc1*/*Oc2* are completely missing horizontal cells in the mature retina; however, initial horizontal cell specification is not affected (Klimova et al. 2015). In the horizontal cell gene regulatory network, *Oc1* is downstream of *FoxN4* and parallel to *Ptf1a* (Wu et al. 2013). Recently, *Pax6* was also identified as an upstream regulator of *Oc1*/*Oc2* in the horizontal cell gene regulatory network (Klimova et al. 2015). Additional factors that play an important role in horizontal cell genesis downstream of *Oc1* are *Lhx1* and *Prox1*. Horizontal cell specification is established normally in *Lhx1*$^{-/-}$ retinas but later, horizontal cells fail to establish their correct laminar positing (Poche et al. 2007). *Prox1* mutant retinas are also devoid of horizontal cells (Dyer et al. 2003).

1.5.4 Amacrine cells

Amacrine cells are the most diverse cell population in the retina. Amacrine cells integrate electrical signals from bipolar cells onto RGC. Amacrine cells can be classified into 33 distinct subtypes based on their stratification and dendritic morphology (Boije et al. 2016). Amacrine cells can also be classified into two major groups based on which inhibitory neurotransmitter they express. FOXN4 promotes amacrine cell genesis by upregulating expression of *Neurod1* and *Neurod4* (Li et al. 2004). *Neurod1* and *Neurod4* redundantly regulate amacrine cell differentiation, as amacrine cell numbers are unaffected in single mutants of either gene (Inoue et al. 2002, Balasubramanian and Gan 2014). Compound mutations of *Neurod1* and *Neurod4,* however, are completely devoid of amacrine cells. Specification of the amacrine cell subtypes requires the expression of several transcription factors. *Barhl2* promotes glycinergic amacrine cell differentiation and restricts the alternative GABAergic amacrine cell fate (Mo et al. 2004, Ding et al. 2009, Balasubramanian and Gan 2014). *Bhlhb5* and *Lmo4* conversely are critical for GABAergic amacrine cell genesis, as reduction in GABAergic amacrine cell numbers is observed in retinas lacking expression of either of these genes (Feng et al. 2006, Huang et al. 2014, Balasubramanian and Gan 2014).

1.5.5 Cone and rod photoreceptors

Cones and rods are the light sensing cells of the retina. Cones are formed during early retinogenesis while peak rod genesis occurs postnatally. Rhodopsin is the lone rod photopigment (opsin). Humans have three cone opsins (S opsin, L opsin, and M opsin) that each respond to different wavelengths of light. Mice only have S and M cone opsins. In early photoreceptor genesis, inhibition of Notch signalling is required to drive RPC to commit to photoreceptor fates (Yaron et al. 2006, Jadhav, Mason, and Cepko 2006, Swaroop, Kim, and Forrest 2010, Brzezinski and Reh 2015). Upon *Notch1* inhibition, *Otx2* is upregulated in precursor cells that make binary cell fate decisions between photoreceptors and bipolar cells. Photoreceptors and bipolar cells are both absent in the *Otx2* conditional null retina (Koike et al. 2007, Nishida et al. 2003, Wang, Sengel, et al. 2014). OTX2 regulates the expression of a number of downstream genes that are critical for photoreceptor differentiation. OTX2 directly activates expression of *Prdm1*, driving the *Otx2* positive precursors to adopt photoreceptor fate over bipolar cell fate (Brzezinski, Lamba, and Reh 2010, Brzezinski, Uoon Park, and Reh 2013, Katoh et al. 2010, Wang, Sengel, et al. 2014). *Crx* lies downstream of *Otx2* and while it is not required for photoreceptor specification, it transactivates genes that are critical for terminal differentiation of photoreceptors (Chen, Wang, et al. 1997, Freund et al. 1997, Furukawa, Morrow, and Cepko 1997). Mutations in *CRX* have been implicated in several human diseases including Leber congenital amaurosis, cone-rod dystrophy and retinitis pigmentosa (Freund et al. 1997, Rivolta et al. 2001, Sohocki et al. 1998). Several genes have been identified that drive committed *Otx2* positive photoreceptor precursors to adopt either cone or rod photoreceptor fates. *Nrl* and *Rorβ* are two factors that are critical for *Otx2* positive precursors to adopt rod fates (Swaroop, Kim, and Forrest 2010, Akimoto et al. 2006, Fu et al. 2014, Kautzmann et al. 2011, Roger et al. 2014). In *Nrl* or *Rorβ* mutants, photoreceptor precursors generate S-opsin expressing cones at the expense of rods (Brzezinski and Reh 2015, Fu et al. 2014, Mears et al. 2001). The activation of the *Nrl* target gene *Nr2e3* is also necessary for rod versus S-opsin cell

fate decisions (Akhmedov et al. 2000, Corbo and Cepko 2005). Much less is known regarding the genetic regulatory network required for photoreceptor precursors to adopt cone fates. *Thrβ2* and *Rxrγ* are each involved in cone subtype specification, but play no part in initial cone genesis (Ng et al. 2001, Roberts et al. 2006, Ng et al. 2011, Roberts et al. 2005). It is believed that *Otx2* positive photoreceptor precursors will adopt a cone fate by default in the absence of *Nrl*.

1.5.6 Bipolar cells

Bipolar cells are the critical cells linking light-responsive photoreceptors to the RGC visual output. There are 13 subtypes of bipolar cells in the mouse retina, 12 of which are cone bipolar cells and one rod bipolar cell. The cone bipolar cells are primarily classified based on their morphology and IPL stratification. Bipolar cells can be further divided in two groups, either OFF or ON bipolar cells based on their response to glutamate release from the photoreceptors (Ghosh et al. 2004, Cheng et al. 2005, Euler et al. 2014). *Vsx2* is critical for the specification of bipolar cells as bipolar cells are absent from the *Vsx2* null retina (Bone-Larson et al. 2000, Burmeister et al. 1996, Green, Stubbs, and Levine 2003). *Otx2* expressing precursor cells specify bipolar cells in the absence of photoreceptor-specific gene expression. *Prdm1* is one such factor pushing *Otx2* positive precursors to adopt a photoreceptor cell fate. *Otx2* positive precursors shifted their fate proportionally from photoreceptors to bipolar cells in *Prdm1* null retinas (Brzezinski, Lamba, and Reh 2010, Katoh et al. 2010). Several additional transcription factors are involved in the differentiation of the bipolar cell subtypes. For instance, *Vsx1* is required for the terminal differentiation of a subset of OFF cone bipolar cells and type 7 ON bipolar cells (Chow et al. 2004, Shi et al. 2011). Members of the *Irx* family are also critical for bipolar cell subtype differentiation. *Irx5* is required for type 2 and type 3 OFF bipolar cells while *Irx6* expression restricts type 3a bipolar cells from adopting type 2 bipolar cell identity (Star et al. 2012, Cheng et al. 2005).

1.5.7 Müller glia cells

Müller glia (MG) cells are the lone glia cell type in the retina derived from RPC. They are born in a late temporal developmental window spanning E18 to P21 (Rapaport et al. 2004, Jadhav, Roesch, and Cepko 2009). MG span the entire length of the retina from the vitreal to ventricular surface making contact with the retinal neurons. MG cells provide both structural and functional supports to the retina including maintaining homeostasis, supporting neuron function, and providing metabolic support (Bringmann et al. 2006). Many factors that are critical for the maintenance of RPC are also required for MG development. For instance, *Lhx2* is required both for RPC maintenance and competence, and is also critical for the development of MG (de Melo, Clark, and Blackshaw 2016, de Melo et al. 2016, Gordon et al. 2013). *Lhx2* appears to have a central role in MG development as reintroduction of several known MG developmental factors in a *Lhx2* null background were unable to completely rescue MG development (de Melo, Clark, and Blackshaw 2016). Active Notch signalling is also shared between RPC and MG cells, and is positively regulated by *Lhx2* expression in MG (de Melo, Clark, and Blackshaw 2016, de Melo et al. 2016). Downstream of Notch in MG genesis, a number of Sry-related HMG-box (*Sox*) family transcription factors, including *Sox2*, *Sox8*, and *Sox9,* are also shared RPC/MG transcription factors. Reduction of MG is observed in the knockout/knockdown of the aforementioned *Sox* transcription factors in the developing retina (Lin et al. 2009, Muto et al. 2009).

In the mature retina, MG have the unique ability to respond to injury in a process called reactive gliosis. In reactive gliosis, MG can protect the retinal neurons by releasing neuroprotective factors (Bringmann et al. 2009, Bringmann et al. 2006, Goldman 2014). However, prolonged gliosis can also be detrimental due to the reduced capacity of the MG to maintain retinal homeostasis. In line with the shared molecular signatures of RPC and MG, the MG have to ability to regenerate retinal neurons in response to injury in the teleost retina. While mammalian MG can proliferate in response to injury, they are unable to reprogram MG into

RPC (Goldman 2014, Jadhav, Roesch, and Cepko 2009). However, in teleost fish MG can be reprogrammed into a proliferating population of multipotent RPC, which can then repair the damaged neurons, and consequently restore vision (Fausett and Goldman 2006, Goldman 2014). Not surprisingly, the study of mechanisms enabling retinal regeneration in the teleost retina is being actively pursued to develop novel regenerative therapies for retinal diseases.

CHAPTER 2: MATERIALS AND METHODS

2 Chapter 2: Materials and Methods

2.1 Animals

All animal protocols were carried out in the Eisenstat and Sauvé laboratories in accordance with the guidelines set by the Canadian Council on Animal Care and the University of Alberta. All daily colony maintenance tasks, breeding, and biopsy collection was provided by Health Sciences Laboratory Animal Services at the University of Alberta.

The *Dlx1/Dlx2* DKO mice were originally produced by Dr. John Rubenstein (UCSF, San Francisco, CA, USA) and heterozygous mice were kindly provided to our laboratory to generate a *Dlx1*/*Dlx2* DKO colony (Anderson, Qiu, et al. 1997, Qiu et al. 1997). *Dlx1/Dlx2* mice were maintained on a CD-1 background. Heterozygous animals were maintained for breeding as the *Dlx1*/*Dlx2* DKO dies at birth. Genotyping of ear biopsy samples was carried out by first extracting the genomic DNA (gDNA) using a common phenol/chloroform technique followed by PCR amplification (Hotstar Plus DNA polymerase, Qiagen) using *Dlx2* and *Neo*-specific primers (Table 3). In addition, we also utilized *Dlx1*/*Dlx2* DKO tissue sections derived from mice maintained on a mixed CD-1;C57BL/6 background, which had been collected from our previous laboratory at the University of Manitoba when *Dlx1*/*Dlx2* DKO CD-1 mice were unavailable at the University of Alberta.

Nrp2 knockout mice were provided by Dr. Marc Tessier-Lavigne (The Rockefeller University, New York, NY, USA) and maintained on a CD-1 background. Homozygous mutant mice are viable and fertile (Chen et al. 2000) and therefore, heterozygous and mutant animals were both maintained for breeding and colony maintenance. Genotyping was performed on tail biopsies by first extracting whole RNA using Trizol (Invitrogen) followed by PCR amplification of cDNA. Whole RNA was used to generate complementary DNA (cDNA) using *Nrp2* gene-specific primers and SuperScript III Reverse Transcriptase (Invitrogen). PCR amplification was

then carried out on the cDNA template to determine genotype (Hotstar Plus polymerase). Primers used for *Nrp2* colony genotyping are listed in Table 3.

Timed-pregnant WT CD-1 mice for chromatin immunoprecipitation experiments, and juvenile mice for the purposes of colony out-crossing were received from Charles River Laboratories.

2.2 Tissue collection and cryopreservation

In order to obtain embryonic mouse tissues, breeding animals of the appropriate genotype was carried out and pregnancy was determined by the presence of a vaginal plug on the selected dam. Pregnant dams were sacrificed by cervical dislocation when the appropriate embryonic age was reached. Embryos were sacrificed by decapitation. Retinas and forebrains were collected and cross-linked with 4% paraformaldehyde (PFA) (Sigma) at 4°C for times specific to the embryonic age being examined (Table 1). Retinas aged E13 and earlier were not dissected from whole embryos. Instead, embryos were decapitated leaving the eyes in place during cross-linking. Following cross-linking, tissue was cryopreserved using a sucrose gradient ranging from 10-30% sucrose. Cryopreserved tissue was then frozen in optimal cutting temperature compound (VWR) and stored at -80°C. Cryosections were cut at 10-12 µm on a Leica Cryostat, and tissues were mounted on Superfrost Plus Microscope slides (Fisher).

Table 1: Tissue fixation times for immunofluorescence or histological analysis

Tissue/Age	**Fixation time in 4% PFA**
Retina/E11 *(in situ)*	2 hours
Retina/E13 (*in situ*)	3 hours
Retina/E18 (dissected)	30 minutes
Retina/Adult (dissected)	1 hour
Forebrain/E13 (*in situ*)	3 hours

2.3 Tissue immunofluorescence

Cryosections were blocked for 1-2 hours at room temperature (RT) with 5% serum blocking solution (0.1% bovine serum albumin (BSA), 0.2% Triton-X 100, 5% horse or goat Serum in 1X PBS). Following the blocking step, primary antibodies were diluted in the same blocking solution and tissues were incubated with the primary antibody dilution overnight (O/N) at 4°C. After O/N incubation, tissues were washed 3x for 5 minutes with 1x PBS/0.05% Triton-X 100. Secondary fluorescent antibodies were diluted to 1/200 in blocking solution, placed on the tissue and incubated for 1-2 hours in the dark at RT. The secondary antibody solution was then washed 3x for 5 minutes with PBS/0.05% Triton-X 100. Slides were mounted with VectaShield Mounting Medium containing DAPI (Vector), and coverslips were then applied and sealed using a clear lacquer. Fluorescent images were captured with a Nikon Eclipse TE2000U platform and NIS Elements software. Images were prepared for presentation using Adobe Photoshop CC. When necessary, image pseudocolouring was carried out using Image-J. Primary and secondary antibodies and their dilutions used in this project are listed in Table 2

2.3.1 Cell counting and statistical analysis

For counting immunopositive cells in the retina, the slide that contained the widest section through the optic nerve was identified and designated the starting slide (slide zero) to be utilized for counting and to serve as a guide to ensure similar regions of the retina were being counted between different litters of mice. Four selected slides were ±4 and ±8 sections from slide zero. The slides were then stained with the appropriate antibodies and immunopositive cells were counted using Image-J software. The mean of the counts from the four slides was then calculated. Tissues from three independent litters of mice were utilized to perform cell counting (three biological replicates) and the mean calculations from the different litters were calculated. When cell counts between WT and mutant slides were analyzed, the average counts from WT and mutant littermates from three litters of mice were used to carry out unpaired t-test to

determine the statistical significance of the changes in cell numbers observed between WT and mutant tissues.

Table 2: List of antibodies used in the study

Antibody	**Source**	**Catalogue number**	**Dilution**	**Host species**
Immunostaining				
Alexa Fluor 488	Invitrogen	A21206, A11055	1/200	Donkey
Alexa Fluor 594	Invitrogen	A11058, A21207	1/200	Donkey
Biotinylated anti-mouse	Vector Labs	BA-2000	1/200	Horse
Brn3b	Santa Cruz Biotechnology	sc-6026	1/200	Goat
Collagen IV	Millipore	AB756P	1/400	Rabbit
Calretinin	Chemicon	AB5054	1/1000	Rabbit
Crx	Gift from Dr. Craft (University of USC)	N/A	1/1000	Rabbit
Dlx2	Prepared by Dr. Eisenstat	N/A	1/200	Rabbit
Dkk3	Santa Cruz Biotechnology	sc-14959	1/200	Goat
IB4	Vector	B-1205	1/400	Biotin
Nrp1	R&D Systems	AF566	1/400	Goat
Nrp2	R&D Systems	AF567	1/400	Goat
Olig2	Millipore	AB9610	1/800	Rabbit
Olig2	Santa Cruz Biotechnology	sc-19969	1/200	Goat
Otx2	Santa Cruz Biotechnology	sc-30659	1/200	Goat
P107	Santa Cruz Biotechnology	sc-318	1/200	Rabbit
Pax6	Covance	PRB-278P	1/400	Rabbit

Prox1	Millipore	MAB5654	1/200	Mouse
Rxrγ	Santa Cruz Biotechnology	sc-555	1/800	Rabbit
Syntaxin	Sigma	S0664	1/200	Mouse
Streptavidin 488	Invitrogen	S32354	1/200	N/A
Streptavidin 594	Invitrogen	S32356	1/200	N/A
Tuj1	Sigma	T2200	1/400	Rabbit
ChIP				
DLX2	Prepared by Dr. Eisenstat	N/A	10 µg	Rabbit
H3K27me3	Millipore	07-449	10 µg	Rabbit
PAX6	Covance	PRB-278P	10 µg	Rabbit

2.4 Histological Staining

Both cresyl violet (CV) and hematoxylin and eosin (H&E) staining were performed on frozen and paraffin embedded retinal tissues, respectively. For CV staining, frozen sections were first allowed to dry at RT for 30 minutes. Sections were then incubated in CV staining solution (0.1% CV acetate prepared in glacial acetic acid) for two minutes, followed by one minute incubations in 75% ethanol, 95% ethanol and 100% ethanol. Slides were then incubated in xylene for two minutes. CV staining sections were then air dried in a fume hood and mounted with Permount (Fisher). For H&E staining, paraffin embedded slides were first placed in a 60°C oven for 10 minutes to melt the paraffin. Next, the sections are deparaffinised and rehydrated by the following treatments: Two xylene treatments for 2 minutes each, decreasing ethanol gradients for one minute each starting with 100% ethanol followed by an additional 100% ethanol treatment, 95% ethanol, and 70% ethanol. Finally, slides are submerged in a cool water bath with gently running tap water. Next, the rehydrated slides were dipped in hematoxylin staining solution (Fisher) 3-5 times then rinsed in a running water bath for one minute. Slides

were then dipped in 0.5% acid alcohol solution (1 mL concentrated HCl, 199 mL 70% ethanol) three times and then rinsed in a running water bath for one minute. Slides were then submerged in a saturated (1.5%) lithium carbonate Bluing solution for one minute. Slides were then rinsed in a running water bath for five minutes. Slides were next submerged in eosin staining solution (1% eosin stock dissolved in 80% ethanol and 1 ML glacial acetic acid) for two minutes. Slides were then finally cleared and dehydrated in 95% ethanol (slides dipped 3-5 times), followed by two 100% ethanol treatments (one minute each). Slides were then twice submerged in xylene for three minutes each. Following clearing and dehydration, slides were mounted (Permount) and brightfield images were then captured with a Nikon Eclipse TE2000U platform and NIS Elements software.

2.5 X-gal staining

β-galactosidase gene expression from the *Nrp2* secretory gene trap was detected using X-gal staining and used to report *Nrp2* expression in retina sections. Frozen sections were first air-dried at RT for 30 minutes. Sections were then incubated in ice-cold X-gal fixative solution (4% PFA, 0.5% glutaraldehyde, 0.1 M Na phosphate buffer (pH 7.2)) for 4 minutes. Following fixation, sections were washed twice with 1x PBS for 1 minute and 10 minutes, respectively. X-gal stock solution (40 mg/mL in N, N Dimethylformamide) was then diluted in X-gal staining solution (5 M K4[Fe(CN)6] · 3H2O, 5 M K3[Fe(CN)6], 2 M $MgCl_2$) to a final concentration of 1 mg/mL and placed on the tissue and covered with a parafilm “coverslip”. The tissue was incubated at 37°C in a humidity chamber for 2 hours or until optimal colour development was observed. Following optimal colour development, the tissue was rinsed briefly in 1x PBS then briefly air-dried at RT. Slides were then mounted in Permount mounting medium and imaged on Nikon Eclipse TE2000U platform using NIS Elements software.

2.6 Whole-mount zebrafish *in situ* hybridization

2.6.1 Generation of in situ hybridization probes

Plasmids containing cDNA of zebrafish orthologues of murine *Dlx* genes (*dlx2a*, *dlx2b*, *dlx3b*, *dlx5a*, *dlx1a*, *dlx4a*, *dlx4b*, and *dlx6a*) were kindly provided by Dr. Marc Ekker (University of Ottawa, Ottawa, ON, CA). Plasmids were linearized using restriction enzymes and purified using phenol/chloroform extraction followed by ethanol precipitation. Antisense RNA probes were generated using a T7 primer that binds upstream of the linearized cDNA sequences, the SP6/T7 Transcription Kit (Roche), and a DIG-RNA Labelling Mix (Roche) and performed according to the protocol for the SP6/T7 Transcription Kit. RNA probes were then purified using SigmaSpin Post-Reaction Clean-Up Columns (Sigma) and stored at -80°C until needed.

2.6.2 In situ hybridization

Whole mount zebrafish *in situ* hybridization (ISH) was carried out as described previously (Thisse and Thisse 2008). Briefly, embryos were fixed in 4% PFA for 4 hours. Embryos were then washed 5x for 5 minutes (0.1% PBST) and dechorionated. Next, the embryos were permeabilized with Proteinase-K for 2 minutes and 30 minutes for 28 hours post fertilization (hpf) embryos and 48 hpf embryos, respectively. Embryo permeabilization was stopped by incubating the embryos in 4% PFA for 20 minutes, followed by 4x 5 minute washes in 1x PBST. Embryos were then prehybridized in hybridization solution (50% formamide, 50 µg/ml heparin, 0.1% Tween, 0.092 M citric acid, 5x SCC) with tRNA for 1 hour at 65°C. ISH probes were diluted in hybridization solution and were then added to embryos and incubated at 65°C O/N. The following day, embryos were washed with 66% hybridization solution/33% 2x SCC, 33% hybridization solution/66% 2x SCC, and 2x SCC for 5 minutes each at 65°C. These washes were then followed by additional washes with 0.2x SCC/0.1 % Tween and 0.1x SCC/0.1% Tween for 20 minutes each at 65°C. Embryos were then washed 3x for 5 minutes at RT in 66% 0.2x SCC/33% PBST, 33% 0.2x SCC/66% PBST, and PBST. Next, embryos were blocked in 2% sheep

serum solution for 1 hour then incubated with 1/5000 dilution of anti-Digoxigenin antibody for 2 hours. After 3x 15 minutes washes in PBST, staining was carried out with a solution of 4-Nitro blue tetrazolium chloride and 5-Bromo-4-chloro-3-indolyl phosphate. Embryos were incubated in the staining solution until optimal colour development was achieved, then washed in stop solution. Whole embryos were then imaged on an Olympus SZX12 platform and QCapture Suite Plus software.

2.7 Chromatin Immunoprecipitation

Embryonic retinas were collected for chromatin immunoprecipitation experiments (ChIP) from timed-pregnant WT CD-1 mice obtained from Charles River Laboratories. WT embryonic hindbrains were also collected as a negative tissue expression control since *Dlx* genes are not expressed in the hindbrain. After retinal tissues were collected, retinal cells were mechanically dissociated and washed 2x with 1X PBS. Tissues were then cross-linked with a solution of freshly prepared 1% PFA plus 1X protease inhibitor cocktail (Roche) for 30 minutes at 4°C. Cross-linked cells were then resuspended in freshly prepared lysis buffer (1% SDS, 10 mM Tris-HCl pH 8.1, 10 mM EDTA) and sonicated on ice to generate soluble chromatin complexes between 100-500 base pairs (bp) in size. The sonicated chromatin was then topped up to 1 mL total with dilution buffer (0.01X SDS, 1.1 X Triton X-100, 1.2 mM EDTA, 16.7 mM Tris-HCl (pH 7.0), 167 mM NaCL). The lysate was then pre-cleared with Protein A/G sepharose beads (Thermo Fisher) to reduce antibody binding to non-specific background IgG. To the pre-cleared lysate anti-DLX2 antibody, tRNA and BSA was added and incubated O/N at 4°C. Negative antibody (no primary antibody) controls for both the retina and the hindbrain were also carried forward. The following day, sepharose beads primed with tRNA and BSA were added to lysates and incubated at 4°C O/N to precipitate out DLX2/chromatin/antibody complexes. Once complexes were precipitated, the beads were then washed with increasingly stringent wash buffers, starting with a low salt wash buffer (0.1% SDS, 1% Triton, 2 mM EDTA, 20 mM Tris-HCl, 150 mM NaCl), high salt wash buffer (0.1% SDS, 1% Triton, 2 mM EDTA, 20

mM Tris-HCl, 500 mM NaCl) and LiCl wash buffer (0.25 M LiCl, 1% deoxycholate, 1 mM EDTA, 10 mM Tris-HCl, 1% NP-40). Chromatin/DLX2-bound beads were then briefly washed with Tris-EDTA (pH 8.0). Chromatin complexes were eluted from beads using an elution buffer pre-heated to 65°C. The elution step was repeated to ensure maximal enrichment of chromatin complexes from the sepharose beads. Cross-linking was reversed at 65°C O/N by addition of 5 M NaCl. RNase A was also added to remove RNA contamination. Finally, Proteinase K was added to the samples for 2 hours and followed by DNA purification using the PCR Clean-up kit (Qiagen). Purified chromatin was then PCR amplified using primers designed to flank putative DLX2 binding sites identified in the regulatory region of the target gene, and Phusion Taq Polymerase (NEB). Positive DLX2 binding to chromatin elements was identified by the presence of a band on a DNA gel of the correct bp size when compared to a gDNA PCR control. Primers used for amplification of enriched DLX2-bound chromatin are listed in Table 3. All ChIP-positive PCR products were sequence verified (TAGC, University of Alberta).

2.7.1 ChIP-chip

To identify DLX2 gene targets in the developing forebrain, we carried out a DLX2-ChIP and then hybridized the enriched chromatin to a CpG island DNA microarray. The ChIP was carried out as described above. The isolated chromatin was amplified using linker-mediated PCR. The PCR products were then labelled with Cy3 or Cy5 using indirect labelling with aminoallyl dUTP and random primers. DNA isolated from DLX2 ChIP and negative antibody control ChIP were then hybridized to a Mouse MCGI 4.6k1 CpG island spotted arrays (UHN-Microarray Centre, Toronto). Chips were scanned using an Axon Scanner and the GenePix Pro 4 software. Spots for which the ratio of the antibody-treated: -antibody control was >1.5 (having a signal >2 x background) were considered significant.

2.7.2 ChIP-reChIP

ChIP-reChIP was utilized to identify binding of two different proteins at the same region of chromatin. The ChIP protocol above was modified slightly for this purpose. The ChIP protocol was carried out as described above up to the chromatin elution step. Following the elution step the chromatin was diluted 10x with dilution buffer. The diluted chromatin was then incubated at 65°C for 10 minutes. The second primary antibody was then added to the diluted chromatin and the immunoprecipitation, reverse cross-linking, and purification was carried out as described above. Again, the enriched chromatin that was bound by both primary antibodies was PCR amplified with primers specific for chromatin regions containing putative DLX2 binding sites. Phusion Taq Polymerase (NEB) was used for PCR amplification of enriched chromatin. Controls for H3K27me3 ChIP-reChIP included H3K27me3 ChIP followed by PCR for *Otx2* (identified as a target repressed by DLX2 in the retina in our laboratory) and *TrkB* (identified as a target activated by DLX2 in the retina in our laboratory). All ChIP-reChIP positive products were sequence verified (TAGC, University of Alberta).

2.8 Electrophoretic mobility shift assay

Specific binding of DLX2 at DNA regulatory elements was identified using electrophoretic mobility shift assays (EMSA). First, ChIP-positive regions of DLX2 binding were cloned into pGL3 reporter vectors (for use in both 3' termini labeling of DNA probes for EMSA and for subsequent reporter gene assays). Plasmid maxi-preps were first performed (Qiagen Maxiprep kit) to generate large amounts of plasmid. Next, 30 μg of plasmid was restriction digested using the appropriate enzymes and buffers to generate 5' overhangs on DLX2 binding-positive DNA fragments. The digested plasmid was then resolved on a 1% agarose DNA gel and the DLX2-positive DNA region was extracted and gel purified (Qiagen). Purified DNA fragments were then radiolabelled using dGTP [α-^{32}P] (Perkin Elmer) and DNA Polymerase I (Klenow) (Invitrogen) to fill in recessed 3' DNA probe termini. Labelled probes were then purified using GE Healthcare Illustra MicroSpin G-25 Columns. Probe radioactivity

levels were measured in a Beckman LS 6500 series scintillation counter and subsequently diluted to 80, 000 counts per million/µl. Binding reactions were then carried out with labelled probes, 1x binding buffer (Promega), poly(dI-dC) •poly(dI-dC), and recombinant DLX2 (rDLX2) protein and incubated for 1 hour at RT. Controls include free probe (no rDLX2 added to overall binding solution), supershift (anti-DLX2 antibody added to overall binding solution), a non-specific antibody control (anti-IgG antibody added to overall binding solution), and cold competitor (excess unlabelled probes added to overall binding solution). Binding reactions were then resolved on a non-denaturing vertical 4% acrylamide gel (60:1 acrylamide:bisacrylamide). Resolved gels were then dried onto filter paper using a Biorad Gel drying and HydraTech vacuum pump system (Biorad) for 1 hour at 80°C. Dried gels were next exposed to X-ray film (Kodak) in a Biorad cassette with an photointensifying screen for 2 hours at RT. Films were developed in a dark room using an AFP Imaging Mini-Medical 90 film developer.

2.8.1 Deletion mutagenesis EMSA

Further validation of DLX2 binding sites identified in the DLX2 ChIP-positive chromatin was carried out by deleting putative DLX2 binding sites in ChIP/EMSA positive DNA regions and re-running EMSA experiments with WT and deletion-mutant probes. Deletion of DLX2 binding sites was performed using the overlap extension PCR method (Lee et al. 2010). For the splice overlap method, two separate PCR steps are required to generate the mutant probes. For the first step, two independent PCR reactions were carried out in order to generate two templates that overlap at the deletion site. This first step requires mutagenic primers that are designed to exclude the deletion site, but continue priming past the deletion site, and outside flanking primers containing restriction sites for subsequent cloning and radiolabelling. The PCR products from the first step were then used as the template for a second PCR step. The PCR products from the first step contain a large area of overlap in the deleted region and become annealed in the second PCR step and filled in during the PCR reaction. The same outside flanking primers used in the first step were used in the second step to amplify the newly

annealed template containing the region of deletion. Phusion Taq polymerase (NEB) was used for all PCR steps. The PCR template containing the deleted region were cloned into pGL3 vectors and submitted for sequence verification (TAGC, University of Alberta). The plasmids containing the deleted DLX2 binding elements were then maxi-prepped (Qiagen) and radiolabelled as described above. Labelled deletion mutant probes were then added to a binding reaction, resolved on a non-denaturing 4% acrylamide gel, and then imaged as described above. Primers used to generate deletion probes are listed in Table 3.

2.8.2 Production and affinity purification of rDLX2

The C-terminal domain of DLX2 including the homeodomain was sub-cloned into pET11d (Novagen) and transformed into BL21DE3pLysS *Escherichia coli*. Lysogeny Broth (LB) containing carbenicillin and chloramphenicol was inoculated with an O/N culture of the transformed bacteria. Isopropyl-β-thiogalactopyranoside (IPTG) was then added to induce expression of rDLX2 from the *lac* promoter in the pET11d vector. Finally, HisTrap FF columns (GE Healthcare) were used to affinity purify the rDLX2 protein as described previously (Porteus et al. 1994).

2.9 Reporter gene assays

2.9.1 Constructs for reporter assays

Dlx2 expression vectors were generated previously by sub-cloning *Dlx2* cDNA into the mammalian expression vector pCDNA3 (Invitrogen), placing *Dlx2* downstream of a CMV promoter. *Dlx2*-pCDNA3 plasmids were kindly provided by Dr. John Rubenstein, UCSF, California, USA. Regulatory DNA regions identified to be DLX2 targets by ChIP were sub-cloned into pGL3-basic reporter vectors (Promega) upstream of the luciferase gene. Primers were designed which introduced restriction sites onto the 5' and 3' ends of the regulatory DNA regions which were to be used for cloning into the pGL3 multiple cloning site (as described in EMSA methods above). These primers were then used to amplify the DLX2 binding positive

regulatory DNA regions and followed by restriction digestion with the appropriate restriction enzymes. The digested DNA fragments were then gel purified according to the QIAquick Gel Extraction kit protocol (Qiagen). Concurrent to regulatory DNA digestion, empty pGL3 vectors were also restriction digested using the same restriction enzymes. Digested regulatory DNA regions were then ligated to digested pGL3 vectors using T4 DNA ligase (Invitrogen). All primers used for cloning experiments are listed in Table 3. Plasmids were then transformed into chemically competent DH5α *E.Coli* (Invitrogen) using a standard heat-shock transformation protocol. Briefly, plasmids were added to chemically competent DH5α *E.Coli* and incubated for 30 minutes on ice. The DH5α *E.Coli*/plasmid mixture was then heat-shocked for 1 minute at 42°C then immediately put on ice. Transformed cells were then grown in LB (no antibiotics) for 2 hours at 37°C, 250 RPM in a New Brunswick Scientific Excella E25 Console shaker. The cultures were then spread on LB agar plates (carbenicillin) and grown at 37°C O/N. The following day, isolated colonies were picked and used to inoculate LB (carbenicillin) that was then incubated at 37°C O/N at 250 RPM. Plasmids were isolated and purified the following day using Qiagen Spin Miniprep Kits. All plasmids were sequence verified (TAGC, University of Alberta) prior to use.

2.9.2 Transfection and reporter gene assays

Dlx2 expression vectors (1 μg), reporter vectors (120 ng) and transfection control vectors (pRL-SV40, 4 ng) were co-transfected into HEK 293 cells seeded in a 12 well plate at a density of $1.7x10^5$ cells/well (three different wells of HEK 293 cells were transfected for three biological replicates). Transfection was performed with Lipofectamine 2000 (Invitrogen) at a DNA to Lipofectamine ratio of 1:1. Cells were cultured for 48 hours post-transfection in DMEM (10% fetal bovine serum (FBS), no antibiotics) at 37°C, 5% CO_2. The transfection media was then aspirated and cells were washed in ice-cold 1x PBS. Reporter lysis buffer (Promega) was then applied to the cells, incubated at -80°C for at least 15 minutes (or stored at -80°C until measurement of bioluminescence), and then thawed at RT for maximum cell lysis. Cell lysates

were then collected and spun at 2000 RPM for 5 minutes at 4°C. While samples were incubating at -80°C, the SpectraMax L luminometer substrate injectors were washed with 70% ethanol and water before finally priming with Firefly and Renilla luciferase substrates (Promega). Two 96-well plates were prepared with the cell lysates plated in duplicate (technical replicates) for the reading of Firefly luciferase activity and Renilla luciferase activity. Firefly luciferase bioluminescence is the measure of the expression of the reporter gene in the presence or absence of DLX2, while Renilla luciferase output is a measure of the plasmid transfection efficiency. Statistical analysis and graphing was performed using GraphPad Prism 7 using unpaired t-tests.

2.10 *Dlx2* gain-of-function and *Dlx2* knockdown

Human WERI-Rb-1 retinoblastoma cells were used to assess *p107* expression following *Dlx2* gain-of-function. WERI-Rb-1 cells were cultured with RPMI-1640 supplemented with 10% FBS. Cells were seeded 24 hours prior to transfection at 6 x 10^6 cells/well in 12 well plates to achieve approximately 80% confluency prior to transfection. Cells were transfected with *Dlx2*-GFP or empty GFP control plasmids using WERI-Rb-1 transfection reagent (Altogen Biosystems). Cells were collected by centrifugation 48 hours post transfection. Following cell collection, whole RNA extraction using RNA isolation kits (Qiagen) was performed. cDNA was then generated from whole RNA using Oligo(dT) primers and SuperScript III reverse transcriptase (Invitrogen). Quantitative real-time PCR (qRT-PCR) was then carried out on a Roche Lightcycler 96 system, using Roche FastStart SYBR Green Master and *p107* cDNA-specific primers to amplify *p107* transcript. Glyceraldehyde 3-phosphate dehydrogenase (*Gapdh*) amplification was carried out as an internal control. Graphical representation was generated using GraphPad Prism 7. *Dlx2* transient knockdown experiments were performed with SK-N-BE(2) neuroblastoma cells. SK-N-BE(2) cells were cultured in F12 medium supplemented with 10% FBS. Cells were seeded at a density of 1.5 x 10^5 cells/well in 6 well plates. Cells were transfected with *Dlx2* and scramble siRNA complexes using Lipofectamine

2000 (Invitrogen). Two different siRNA duplexes were tested with similar knockdown efficiencies. The sequences for the *Dlx2* siRNA duplexes are as follows: *Dlx2* duplex 1: Sense 5'-GGAAGACCUUGAGCCUGAATT -3', Antisense 5'–UUCAGGCUCAAGGUCUUCCTT-3. *Dlx2* duplex 2: Sense 5'-CCUGAAUCCGAAUAGUGATT-3', Antisense 5'–UCACUAUUCGGAUUUCAGGCT-3'. Cells were cultured in transfection medium for 48 hours. Following collection, RNA was extracted using RNA isolation kits (Qiagen) and cDNA was generated using Oligo(dT) primers and SuperScript III reverse transcriptase (Invitrogen). To quantify changes in *p107* expression following *Dlx2* gain and loss of function, qRT-PCR was carried out using a Roche Lightcycler as described in 2.11 below and primers for human *P107* and *GAPDH* transcript, as listed in Table 3.

2.11 Quantitative real-time PCR

Quantification of transcripts in WT and mutant tissues was carried out using qRT-PCR. The ΔΔCq method was utilized to calculate relative gene expression. Tissues were dissected and whole RNA was extracted using Trizol (Invitrogen). Whole RNA was then used to generate cDNA templates of mRNA transcripts using SuperScript III (Invitrogen) and Oligo(dT) primers (Invitrogen). The cDNA templates were then amplified using Roche FastStart SYBR Green Master system, and coding sequence-specific primers (i.e primers that span exon-exon junctions). Three biological replicates (WT and *Dlx1*/*Dlx2* DKO littermate pairs from three independent litters of mice) were examined, and Cq measurements were carried out in triplicate (technical replicates) for each litter. Cq values were collected for the reference gene (*Gapdh*) and gene targets using a Roche LightCycler 96 system. The Cq values for the technical replicates were averaged, then ΔCq was calculated by subtracting the average Cq (target gene) from the average Cq. The resultant ΔCq values were then exponentially transformed to calculate ΔCq expression. The mean ΔCq expression of the biological replicates was then calculated. ΔΔCq expression and ΔΔCq standard deviation was then calculated by normalizing ΔCq expression to the WT control. Data was collected using the corresponding Roche LightCycler software.

Statistical analysis was performed using GraphPad Prism 7 using unpaired t-tests. Graphical analysis was also performed with GraphPad Prism 7. Primers used for qRT-PCR are listed in Table 3.

Table 3: List of primers used in the study

Primer Name	Sequence (5' to 3')
Genotyping Primers	
Dlx2-F	TCCGAATAGTGAACGGGAAGCCAAAG
Dlx2-R	CAGGGTGCTGCTCGGTGGGTATCTC
Neo-F	CAAGATGGATTGCACGCAG
Neo-R	CATCCTGATCGACAAGAC
Nrp2-F	AGACTACCACCCCATATCCCATGG
Nrp2-RV	CTTGAGCCTCTGGAGCTGCTCAGC
Nrp2-RC	CTGCCCTGGTCCTCACGGATGAC
ChIP Primers	
P107-R1F	TACTGAGCCTCTACTATTTTATC
P107-R1R	CGTCACAACTGCTGGAATATAG
P107-R8F	GAAGTTAGGTGTCAGCTTATA
P107-R8R	CACTCAGAATCCTGCACGAG
Olig2-R6F	GAGCCAGGTTCTCCTCCG
Olig2-R6R	GACCGGAGATCTGAATAGAG
Luciferase (cloning) primers	
5'-p107	GACACGCGTTACTGAGCCTCTACTATTTTATC

3'-p107	GACCTCGAGCACTCAGAATCCTGCACGAG
Olig2-R6F	GACACGCGTGAGCCAGGTTCTCCTCCG
Olig2-R6R	GACCTCGAGGACCGGAGATCTGAATAGAG
EMSA deletion primers	
P107-R1delF	GGTCCCTCCTATACTGTAAAGAGAAGT
P107-R1delR	TATAACTTCTCTTTACAGTATAGGAGGGA
P107-R8S1delF	GCTTATAGATGTACTGCTCAGGGCCTG
P107-R8S1delR	CTAATTTTAACCTTCTCAGGCCCTGAG
P107-R8S2delF	GTAATGGCCTGAGAAGGTTAAAGACTT
P107-R8S2delR	CTTGCTCTTCATCATTTAAGTCTTTAAC
P107-R8S3delF	TACCTGGTGCATCTGAATGCTTTTTTC
P107-R8S3delR	CATTTTTTGTCTTTAAAATACAGAAAA
qRT-PCR primers	
Gapdh-F	ACCATCCGGGTTCCTATAAAT
Gapdh-R	CAATACGGCCAAATCCGTT
P107-F	CCGAAGCCCTGGATGACTT
P107-R	GCATGCCAGCCAGTGTATAACTT
Hes1-F	GTGGGTCCTAACGCAGTGTC
Hes1-R	ACAAAGGCGCAATCCAATATG
Hes5-F	GCTCCGCTCGCTAATCGCCT
Hes5-R	CCGGCTTCCGCAGTCGGTTTTT
Notch1-F	TCAATGTTCGAGGACCAGATG
Notch1-R	TCACTGTTGCCTGTCTCAAG

Olig2-F	GGCGGTGGCTTCAAGTCATC
Olig2-R	TCGGGCTCAGTCATCTGCTTC
Crx-F	ACCCAGTACCCGGATGTGTA
Crx-R	CTTGAACCAGACCTGGACCC
Brn3b-F	CGATGCGGAGAGCTTGTCTTC
Brn3b-R	GATGGTGGTGGTGGCTCTTACTCT
Dlx2-F	GCCTCACCCAAACTCAGGT
Dlx2-R	AGGCACAAGGAGGAGAAGC
Gli1-F	CGGAGTTCAGTCAAATTAAC
Gli1-R	CATCTGAGGTTGGGAATCC
Gli2-F	AGCCTTCACCCACCTTCTTG
Gli2-R	TGGGCGCAGGCCCTCAGC
Gli3-F	CCTTCTGAGTCCTCACAGAG
Gli3-R	GACTAGGGTTGTTCCTTCCG
***Dlx2* gain and loss of function**	
P107-F (human)	CTCTTTGCCTATAGCTCACCTC
P107- R (human)	GCGGATCACCACCTCAATAA
Gapdh-F (human)	GGTGTGAACCATGAGAAGTATGA
Gapdh-R (human)	GAGTCCTTCCACGATACCAAAG

2.12 Retinal Flatmounts and intraretinal RGC axon labelling

E18 and adult retinas were flat mounted and immunostained to detect intraretinal RGC axons. Eyes were first enucleated and placed in a 12 well plate containing 4% PFA at room temperature for 10 minutes. The eyes were then transferred to wells containing cold 1x PBS to

wash for 5 minutes. Following fixation, the sclera and lens were carefully removed to preserve the retinal cup structure. Any visible hyaloid vessels were also removed to prevent them from obscuring the immunostaining. Four small cuts were then made into the retina from the periphery toward the optic disc. The PBS was then carefully drawn away from the well using a transfer pipette to facilitate flattening of the retina into a flower-like structure. Ice-cold methanol (-20°C) was then added in drops to the retina, which facilitates crosslinking, permeabilization, and flattens the retina into a rigid structure. Detection of the RGC axons is then performed by immunostaining using an antibody to neuron-specific tubulin, Tuj1. Immunostaining was performed as described in section 2.3 above, but with the blocking and antibody incubations occurring in a microfuge tube rather than on tissue cryosections. Immunostained retinas were then carefully transferred to Superfrost Plus microscope slides (Fisher Scientific) using plastic transfer pipets with the nerve fibre layer facing up. Coverslips were then gently laid over the tissues and sealed with clear lacquer. Images were then captured with a Nikon Eclipse TE2000U platform and NIS Elements software. Images were prepared for presentation using Adobe Photoshop CC.

2.13 *In utero* retinal electroporation

Dlx2 gain of function experiments were performed by ectopic gene delivery using *in utero* retinal electroporation. *Dlx2* expression plasmids for the gene delivery were generated by sub-cloning *Dlx2* cDNA into the pCIG2 expression vector. This cloning places *Dlx2* downstream of a CMV enhancer and β-actin promoter, and upstream of an internal ribosome entry site (IRES) EGFP cassette or mCherry cassette. Empty pCIG2 reporter vectors were used as a control. Electroporation was carried out as described previously (Dixit et al. 2011). Briefly, C57BL/6 timed-pregnant dams were bred and pregnancy was followed until embryos reached E13, at which point pregnant mice were utilized for gene delivery. Pregnant dams were anesthetised with 5% isofluorane and oxygen and then prepared for surgery. The forelimbs of the dams were gently taped down onto a heating pad and a thick layer of depilatory cream was

applied to the abdomen to remove the fur. After the fur was removed, the skin was cleaned and sterilized with chlorhexidine. Next, an incision was made into the skin. The skin was then gently pulled away from the abdominal wall and a small (~1 cm) cut was made into the skin. An incision was then made into the peritoneum and another small cut was made. A cut was made into sterile gauze though which the uterus will be pulled through. The gauze laid over the skin/peritoneal incision and was dampened with warmed sterile saline. Using round-tipped forceps the uterine horns were externalized. Plasmids were diluted to 3 μg/μl and mixed with Fast Green FCF dye for visualization of electroporated DNA. Injection of the DNA was performed with a Femtojet microinjector (Eppendorf) into the sub-retinal space of E13 embryos. Using an ECM8300 BTX electroporation system, an electric pulse was delivered with the positive electrodes placed dorsal to the DNA injection site to ensure introduction of the exogenous DNA into the RPC of the embryonic retina (five square pulse of 40-50V). Following injection and electroporation of the *Dlx2* plasmids, the uterus was replaced into abdomen, the incision sutured, and skin stapled. The embryos were then allowed to develop for an additional five days (until E18). The dam was then euthanized and the embryonic tissues were collected and processed as described in 2.2 above.

2.14 Optical Coherence Tomography

Non-invasive *in vivo* imaging of the adult (3 months of age) *Nrp2* knockout retina was performed by optical coherence tomography (OCT) using the Bioptigen spectral domain ophthalmic imaging system (Bioptigen SDOIS). Adult mice from the *Nrp2* knockout colony were anaesthetized with a mixture of ketamine and xylazine (150 mg/kg and 10 mg/kg, respectively) injected into the peritoneum. When the mice were fully anesthetized, pupils were dilated using a mixture of phenylephrine and tropicamide (2.5% and 1%, respectively). Lubricant eye drops were then applied to prevent drying of the cornea during the procedure. Mice were then placed and secured into a stereotactic rotational cassette allowing for the proper positioning of the mouse in relation to the imaging system. The animal was then rotated in the cassette to position

the eye in close proximity to the OCT probe. Scanning of the retina and image acquisition was performed using InVivoVue Clinic software.

2.15 Fundus imaging and fluorescein angiography

Fundus imaging was performed when the mice were 4 weeks of age on WT and *Nrp2* heterozygous mice. Mice were anaesthetized as described for the acquisition of OCT imaging above. When performing fluorescent angiography, mice were injected with 10% sodium fluorescein intraperitoneally prior to imaging. Fundus and angiographic imaging was performed on a Micron III retina imaging system (Phoenix Research Laboratories). Images were captured with StreamPix 5 software.

CHAPTER 3: THE ROLE OF DLX GENES IN REGULATION OF RETINAL CELL FATE DECISIONS

3 Chapter 3: The role of Dlx genes in regulation of retinal cell fate decisions

3.1 Introduction

3.1.1 Role of invertebrate Dlx orthologue, Distal-less, in Drosophila development

The invertebrate orthologue of *Dlx*, Distal-less (*Dll*) has been identified in several arthropods including crustaceans and insects (Williams, Nulsen, and Nagy 2002, Williams and Nagy 1996, Chen, Piel, and Monteiro 2016, Pechmann et al. 2010) and also in *Caenorhabditis elegans* (Aspock and Burglin 2001, Panganiban et al. 1997) and Planarian flatworms (Lapan and Reddien 2011). Of these invertebrates, the role of *Dll* in *Drosophila* has been the most widely studied. One *Dll* gene has been identified in *Drosophila* where it plays a critical role in the development of the distal appendages. *Drosophila Dll* mutants are embryonic lethal due to the absence of rudimentary larval limbs (Cohen and Jurgens 1989). *Drosophila* carrying one functional *Dll* allele or one hypomorphic *Dll* allele have partial homeotic transformation of antenna to legs (Sunkel and Whittle 1987, Cohen and Jurgens 1989, Dong, Chu, and Panganiban 2000). Conversely, ectopic *Dll* expression results in the ectopic formation of limbs that were dependent on the localization along the body axis where ectopic antenna were observed on head elements and ectopic legs on wing elements (Gorfinkiel, Morata, and Guerrero 1997, Dong, Chu, and Panganiban 2000, Chen, Piel, and Monteiro 2016). *Dll* expression has also been observed in the medulla cortex of adult optic lobes in *Drosophila*; however the specific role of *Dll* in the development of the *Drosophila* optic lobe remains unknown (Morante, Erclik, and Desplan 2011).

3.1.2 Organization and regulation of vertebrate Dlx genes

The *Dlx* family of homeobox transcription factors are critical for the development of the CNS, craniofacial structures, and retina. In mouse and humans, there are three convergently transcribed pairs of *Dlx* genes with each gene containing intergenic regulatory elements and

each linked to a *Hox* gene cluster. These pairs include *Dlx1*/*Dlx2* (linked to *HoxD*), *Dlx3*/*Dlx4* (linked to *HoxB*), and *Dlx5*/*Dlx6* (linked to *HoxA*). Of these pairs, *Dlx1*/*Dlx2* and *Dlx5*/*Dlx6* are expressed in the developing CNS. The role of *Dlx1*/*Dlx2* in the developing forebrain will be described in Chapter 4. Cross-regulation of *Dlx* genes occurs where DLX1 and DLX2 bind to the *Dlx5*/*Dlx6* intergenic enhancer (I56i) *in vivo* where it upregulates expression of *Dlx5*/*Dlx6* in the forebrain (Zhou et al. 2004, Anderson, Qiu, et al. 1997). DLX2, but not DLX1 was also shown to bind to I56i in the P0 retina (Zhou et al. 2004). In addition to the intergenic enhancer elements, upstream regulatory elements (URE) URE1 and URE2 have been identified upstream of the *Dlx1*/*Dlx2* bigene cluster which is active by E11.5 in the developing telencephalon (Ghanem et al. 2007). In zebrafish, owing to the mammalian genome duplication event in zebrafish, there are eight *Dlx* orthologues (Amores et al. 1998, Robinson-Rechavi et al. 2001, Ekker et al. 1992). Similar to that observed in mammals, six zebrafish *dlx* genes are organized into three convergently transcribed pairs also linked to *hox* genes. The remaining two *Dlx* orthologues are not apparently linked to other *Dlx* genes.

3.1.3 Structure and function of DLX proteins

Dll and *Dlx* encode homeodomain-containing transcription factors, which bind to DNA and regulate transcription (Liu et al. 1997, Panganiban and Rubenstein 2002, Stuhmer, Anderson, et al. 2002, de Melo et al. 2008, Le et al. 2007). The *Dlx* and *Dll* encoded homeodomains are highly conserved and comprised of 61 amino acids that are flanked by proline rich areas both up- and downstream of the homeodomain (Panganiban and Rubenstein 2002, Zerucha and Ekker 2000). The homeodomains of *Drosophila* DLL, vertebrate DLX proteins DLX1, DLX2, DLX3, DLX4, DLX5, and DLX6 share 79% amino acid homology. The *Dlx* genes can be organized into two distinct subgroups or clades based amino acid conservation in the homeodomain and flanking C-terminal regions. These clades include Dlx1/Dlx4/Dlx6 and Dlx2/Dlx3/Dlx5. The Dlx2/Dlx3/Dlx5 subgroup also contains a DllA domain upstream of the homeodomain of unknown functional significance (Akimenko et al. 1994, Panganiban and

Rubenstein 2002, Zerucha and Ekker 2000). Expression of DLX1 and DLX2 in both the developing forebrain and retina significantly overlap in the subpallium and the GCL and INL, respectively. This overlapping temporal and spatial expression in addition to the increased phenotypic severity observed in the *Dlx1*/*Dlx2* DKO mice compared to the *Dlx1* and *Dlx2* single null mice suggests partial redundancy exists between DLX1 and DLX2.

3.1.4 Dlx expression and function in the developing retina

The earliest expression of *Dlx2* is observed in the central E11 retina while the earliest documented expression of *Dlx1* is E12.5 (Eisenstat et al. 1999, de Melo et al. 2008). By E13, DLX2 expressing cells co-localize with VSX2, BRN3B, and PAX6 expressing cells, which are indicative of RPC, RGC, and amacrine cells, respectively (de Melo et al. 2003). At late stages of embryonic retinal development and into adulthood, co-localization of DLX2 with BRN3B and PAX6 is maintained, and co-localization of DLX2 with calbindin positive horizontal cells is also observed. By P0 and into adulthood, DLX1 expression is significantly reduced compared to DLX2. *Dlx5* expression is observed in the E16, P0, and adult retina where it co-localizes with DLX2 expressing cells in the GCL and INL (Zhou et al. 2004). The role of *Dlx5*/*Dlx6* in retinogenesis has not been examined to date.

Dlx1/*Dlx2* DKO retinas have been characterized to determine the role of this convergent gene pair in the developing retina. In the absence of *Dlx1*/*Dlx2* there is a 33% loss of late-born RGC and a consequent thinning of the optic nerve due to a significant increase in apoptosis (de Melo et al. 2005). The postnatal role of *Dlx1*/*Dlx2* in the developing and mature retina is unknown as the DKO mouse dies shortly following birth. The single knockouts for *Dlx1* and *Dlx2* also die at birth, but the phenotype of the single knockout retinas has yet to be fully characterized (Qiu et al. 1995). We have, however, begun initial characterization of the *Dlx1* and *Dlx2* single knockout retinas (Appendix). In addition to the loss of RGC in the *Dlx1*/*Dlx2* DKO retina, there was also increased and ectopic expression of *Crx* observed in the NBL and the GCL, respectively (de Melo et al. 2005). This suggests that *Dlx1*/*Dlx2* may be involved in binary

retinal cell fate decisions between RGC and photoreceptors. It is likely that the RPC can be competent for the generation of RGC or cones as the temporal developmental windows of these cells overlap in prenatal retinal development. Due to the death of *Dlx1*/*Dlx2* DKO mice at P0, however, we cannot rule out whether rods may also be affected, as peak genesis of rods occurs during postnatal retinal development. Therefore, we hypothesize that *Dlx1*/*Dlx2* restricts RPC from adopting photoreceptor cell fates by restricting expression of genes critical for photoreceptor genesis while concomitantly promoting RGC cell fate decisions by upregulating expression of genes required for differentiation and survival of RGC.

3.1.5 Olig2: a neural progenitor factor in the CNS and retina

Olig2, along with its related family member *Olig1,* were first identified for their role in oligodendrocyte differentiation in the spinal cord (Zhou, Wang, and Anderson 2000, Takebayashi et al. 2000, Lu et al. 2000). *Olig2* murine mutants die at birth lacking oligodendrocytes and motor neurons. In the CNS, *Olig2* is critical for the commitment of multipotent neural progenitors into oligodendrocyte precursors, and for the differentiation and myelination of oligodendrocytes (Lu et al. 2002, Yue et al. 2006, Zhou, Wang, and Anderson 2000). Despite the complete lack of myelin in the vertebrate neural retina, *Olig2* expression has been observed in the vertebrate retina (Shibasaki et al. 2007, Nakamura et al. 2006, Hafler et al. 2012). Similar to the remainder of the CNS, *Olig2* appears to be critical for cell fate decisions in the developing retina. However, there are disagreements as to which mature retinal cells are generated from *Olig2* positive progenitor cells or express *Olig2*. Where all studies are in agreement is the fact that *Olig2* is expressed in embryonic RPC (Shibasaki et al. 2007, Nakamura et al. 2006, Hafler et al. 2012). Expression of *Olig2* in the embryonic retina is confined to the proliferative NBL and co-localizes with Ki67 (proliferation marker) expressing cells and S-phase cells which have incorporated BrdU. With respect to the mature retinal cells generated from RPC that express *Olig2*, one study indicates that in the postnatal retina, *Olig2* expression is observed in RGC, bipolar cells, and MG cells (Shibasaki et al. 2007). A different

group, however, used lineage tracing to follow RPC with *Olig2* expression histories and determined that RGC and MG cells were never generated from RPC that express *Olig2* (Hafler et al. 2012). The retinal cells most represented in the lineage tracing analysis were photoreceptors, horizontal cells, and amacrine cells. The authors did not observe expression of *Olig2* in the mature retina, but however they noted that expression of *Olig2* in mature bipolar cells and RGC was rarely observed (Hafler et al. 2012). It is unclear as to why differences in *Olig2* expression were observed between the various groups. Perhaps the expression of *Olig2* expression differs depending on the genetic background of the mice examined (discussed later in this chapter). The genetic background of the mice utilized by Hafler and colleagues was unclear while the Nakamura and Shibasaki groups utilized C57Bl/6 animals. The tools utilized to examine *Olig2* expression may also contribute to the differences observed where lineage tracing was used in Hafler's study to identify retinal cells with Olig2 expression history while other groups utilized immunostaining with OLIG2 antibodies.

In the developing telencephalon, *Dlx1*/*Dlx2* inhibits progenitors from acquiring oligodendrocyte cell fates by restricting expression of *Olig2* (Petryniak et al. 2007). These *Dlx1*/*Dlx2* positive progenitors then adopt GABAergic interneuron fates. We questioned whether *Dlx1*/*Dlx2* could also be instrumental in regulating retinal cell fate decisions by regulating expression of *Olig2* in the developing retina. Because of the *Olig2* expression history observed in photoreceptors, and the increased/ectopic photoreceptor gene expression in the *Dlx1*/*Dlx2* DKO retina, we hypothesized that *Dlx1*/*Dlx2* is critical for establishment of binary cell fate decisions in the retina where *Dlx* gene expression promotes RGC cell fate while at the same time restricts cells from adopting photoreceptor cells fates, in part by restricting the expression of *Olig2*.

3.2 Results

3.2.1 dlx orthologues are not expressed in the zebrafish retina retina

We were interested in utilizing an additional model system along with our established mouse models to examine the role of *Dlx* genes in regulating retinal cell fate. We chose to examine whether zebrafish would be a suitable system for this purpose. Zebrafish were chosen since the expression pattern and function of *Dlx* genes in the zebrafish and mouse forebrains are highly conserved (Ghanem et al. 2003, MacDonald et al. 2010, Yu et al. 2011). We generated *in situ* probes for the zebrafish *dlx* orthologous and examined 28 hpf and 48 hpf embryos for *dlx* gene expression. Strong expression of *dlx1a*, *dlx2a*, and *dlx2b* was observed in the telencephalon of zebrafish embryos, as expected (Figure 3.1). However, there was no evidence of *dlx* gene expression in the retina at either developmental time point examined. Expression of all *dlx* orthologues was observed in the pharyngeal arches of the zebrafish embryos (Figure 3.1). The murine *Dlx* genes are critical for the patterning of the branchial arches, and mutations in *Dlx* genes result in defects in craniofacial development. For instance, *Dlx1*/*Dlx2* DKO mice lack maxillary molars and have cleft palates while the *Dlx5*/*Dlx6* DKO mouse develops a homeotic transformation of the lower jaws into upper jaw (Depew et al. 2005, Depew, Lufkin, and Rubenstein 2002). Expression of *dlx* orthologues in the pharyngeal arches (the structures homologous to the branchial arches in jawed vertebrates) has been previously reported and is suggested to play a conserved role in patterning of the pharyngeal arches in zebrafish (Gillis, Modrell, and Baker 2013, Talbot, Johnson, and Kimmel 2010). Therefore, our results interestingly suggest that during evolution of the zebrafish, *dlx* gene expression was lost in the developing zebrafish retina, but expression and function was conserved in the forebrain and pharyngeal arches. Given that *dlx* gene expression was not conserved in the developing zebrafish retina, we pursued our study of *Dlx* gene function in the developing retina solely utilizing mice models.

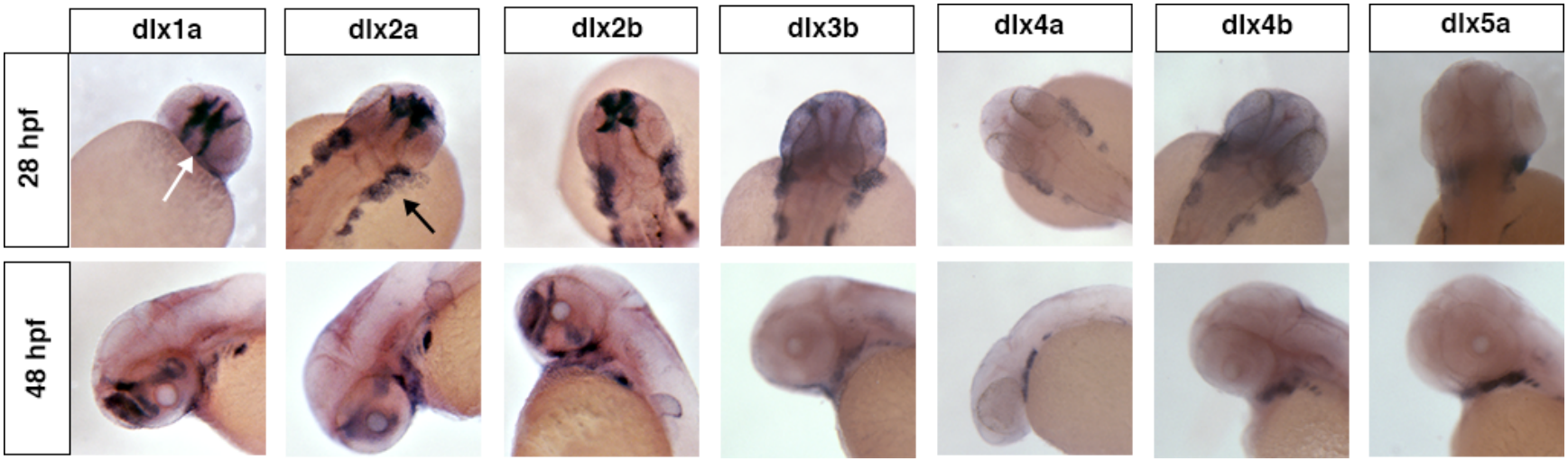

Figure 3.1: Absence of *dlx* expression in the developing zebrafish retina.

To determine if expression of the zebrafish *dlx* orthologues was present in the retina, we performed ISH on zebrafish embryos at two developmental time points including 28 and 48 hpf. While *dlx1a*, and *dlx2a* and *dlx2b*, which are the zebrafish orthologues for *Dlx1* and *Dlx2*, respectively, are highly expressed in the zebrafish telencephalon (white arrow), expression was not observed in the retina. Expression of the remaining orthologues, including *dlx3b*, *dlx4a*, *dlx4b*, and *dlx5a* was also not observed in the retina or the developing telencephalon. Expression of all *dlx* orthologues was observed in the pharyngeal arches (black arrow).

[ISH; *in situ* hybridization, HPF; hours post fertilization]

3.2.2 DLX2 and OLIG2 are expressed in distinct retinal cell populations in the retina

The temporal and spatial expression pattern of OLIG2 and DLX2 was examined throughout the development of the retina by immunostaining frozen retinal sections at several developmental time points. In previous studies, the earliest expression of *Olig2* was identified at E12.5 in the NBL using ISH (Hafler et al. 2012). We determined that OLIG2 expression could be identified as early as E11 in a few cells localized in the NBL (Figure 3.2A). By E13, the number of cells expressing OLIG2 has increased and OLIG2 expressing cells maintain their NBL localization (Figure 3.2B). OLIG2 expressing cells are notably absent from the inner NBL, which contains differentiating RGC/amacrine cells of the presumptive GCL at this developmental time point. At E18, the restriction of OLIG2 expressing cells from the differentiated GCL is even more apparent (Figure 3.2C). OLIG2 expressing cells at E18 are localized throughout the NBL. In accordance with previous ISH findings (Hafler et al. 2012), we did not observe OLIG2 expression in the adult retina (Figure 3.2D, Di). The exclusion of OLIG2 expression from the differentiated GCL in embryonic retinas and absence of OLIG2 expression in the adult retina indicate that OLIG2 is expressed in RPC and/or proliferating precursor cells as has been described previously, but not maintained in any differentiated retinal cell types (Nakamura et al. 2006, Shibasaki et al. 2007, Hafler et al. 2012). DLX2 expression is also observed as early as E11 in the NBL (Figure 3.2E). At E13, expression of DLX2 increases throughout the NBL (Figure 3.2F). We also examined co-expression of DLX2 and DKK3 at E11 and E13 to demonstrate that DLX2 is expressed in RPC at these early embryonic developmental time points (Sato et al. 2007) (Figure 3.3). DLX2 expression in VSX2 positive RPC was previously observed by our laboratory (de Melo et al. 2003). DKK3, a secreted inhibitor of Wnt signalling (Krupnik et al. 1999), is expressed in RPC and has been utilized to drive *Cre* expression in RPC for the generation of neural retina-specific gene knockouts (Iida et al. 2011, Ogata-Iwao et al. 2011, Sato et al. 2007). At E11, DKK3 expression is observed throughout the NBL (Figure 3.3A). As described above, DLX2 expression is localized in a few RPC in the central NBL (Figure 3.3B). Merged images

show that DLX2 positive cells co-localize with DKK3 positive RPC (Figure 3.3C, D). Similarly, at E13 DKK3 and DLX2 positive cells co-localize in the proliferative NBL (Figure 3.3E-H). Here, we utilized wide-field fluorescent microscopy to analyze co-localization of DLX2 and DKK3 which has disadvantages compared to laser scanning confocal microscopy, including image obstruction from out of focus light outside the focal plane. Confocal microscopy reduces/eliminates this obstruction and therefore should be considered to re-evaluate co-localization of DLX2 and DKK3 in future experiments. At E18, expression of DLX2 is localized to the GCL and the inner NBL where differentiated RGC and amacrine cells reside, respectively (Figure 3.2G). DLX2 expression is also observed in several cells in the central NBL. Based on the laminar positioning of these cells they are likely horizontal cells, which we have shown previously to express DLX2 (de Melo et al. 2003). We next carried out dual expression analysis of DLX2 and OLIG2 in the developing retina at E13 and E18 to determine if DLX2 and OLIG2 are expressed in shared retinal cell types. At E13, DLX2 and OLIG2 expressing cells did not co-localize with OLIG2 positive cells (Figure 3.2H). At E18, the lack of DLX2 and OLIG2 co-localization was more apparent with DLX2 expression observed in the differentiated NBL and the inner NBL, while OLIG2 expressing cells were found throughout the proliferative NBL with strict exclusion from the GCL (Figure 3.2I). These findings demonstrate that while DLX2 and OLIG2 are both expressed in RPC during early retinal development, DLX2 and OLIG2 are not expressed in the same RPC (expressed in distinct RPC subsets) and OLIG2 expression is excluded from differentiated retinal cell populations.

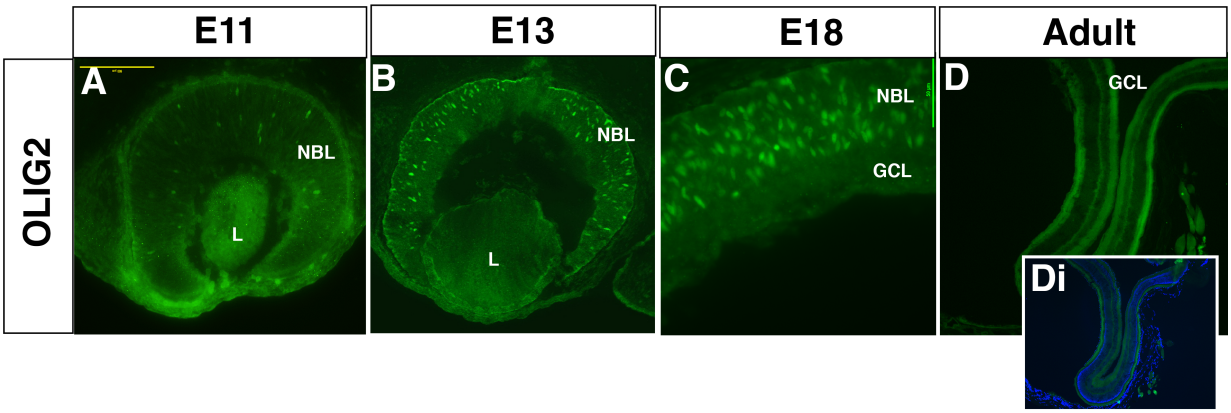
E11
E13
E18
Adult
OLIG2
A
B
C
D
Di
NBL
L
GCL

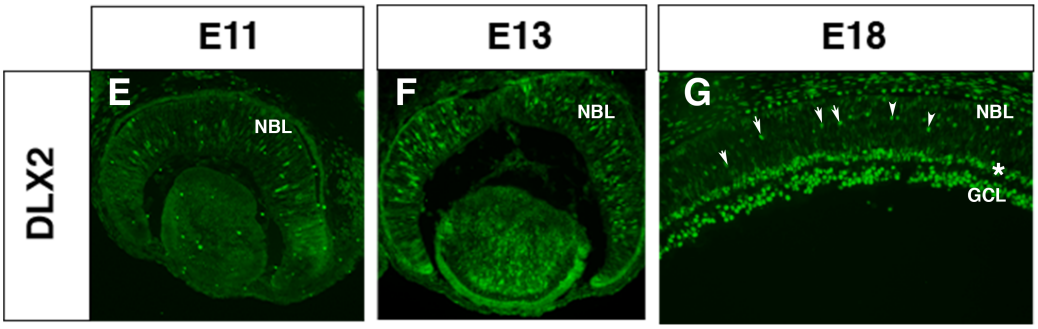
E11
E13
E18
DLX2
E
F
G
NBL
GCL

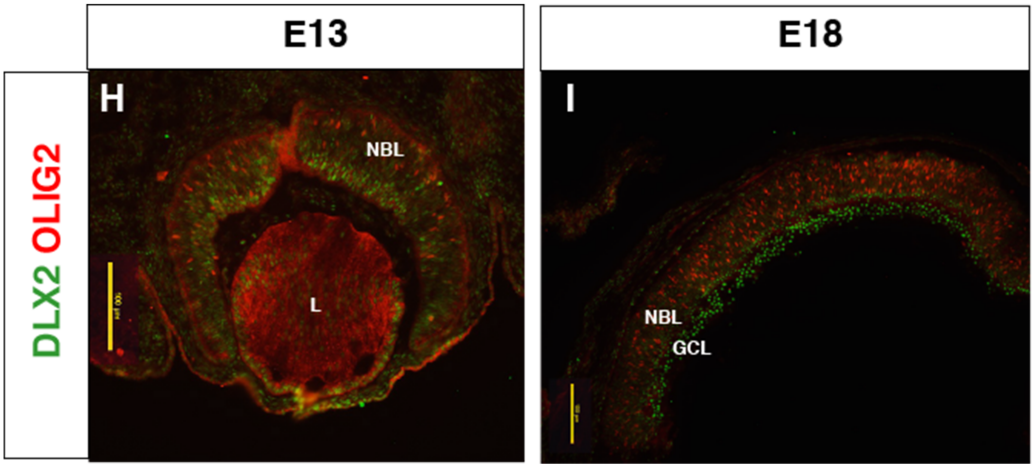
E13
E18
DLX2 OLIG2
H
I
NBL
L
GCL

Figure 3.2 DLX2 and OLIG2 are expressed in distinct RPC and retinal cell populations.

(A-D) OLIG2 expression was examined at numerous stages of retinal development. (A) OLIG2 expression is observed in RPC of the central NBL at E11. (B) At E13 OLIG2 is restricted from the inner NBL but expressed throughout the remainder of the central and outer NBL. (C) OLIG2 expression is restricted from the differentiated GCL at E18, but expressed throughout the proliferative NBL. (D) OLIG2 expression is not observed in the adult retina. (Di) The negative control for OLIG2 expression in the adult retina co-stained with DAPI is shown for comparison to the OLIG2 staining in D. (E-G) DLX2 expression was also examined during retinal development. (E) DLX2 expression was observed in a few RPC in the central NBL the E11 retina. (F) At E13 expression of DLX2 is localized to the inner NBL. (G) By E18, DLX2 expression is observed in the GCL, inner NBL amacrine cells (asterisk), and a few cells in the central NBL which were previously identified by our laboratory to be amacrine cells (arrows). (H-I) Double immunofluorescence analysis of DLX2 and OLIG2 expression at E13 (H) and E18 (I) demonstrate that co-localization of DLX2 and OLIG2 expressing cells is not observed during retinal development.

[GCL; ganglion cell layer, L; lens, NBL; neuroblastic layer. Scale = 100 μm]

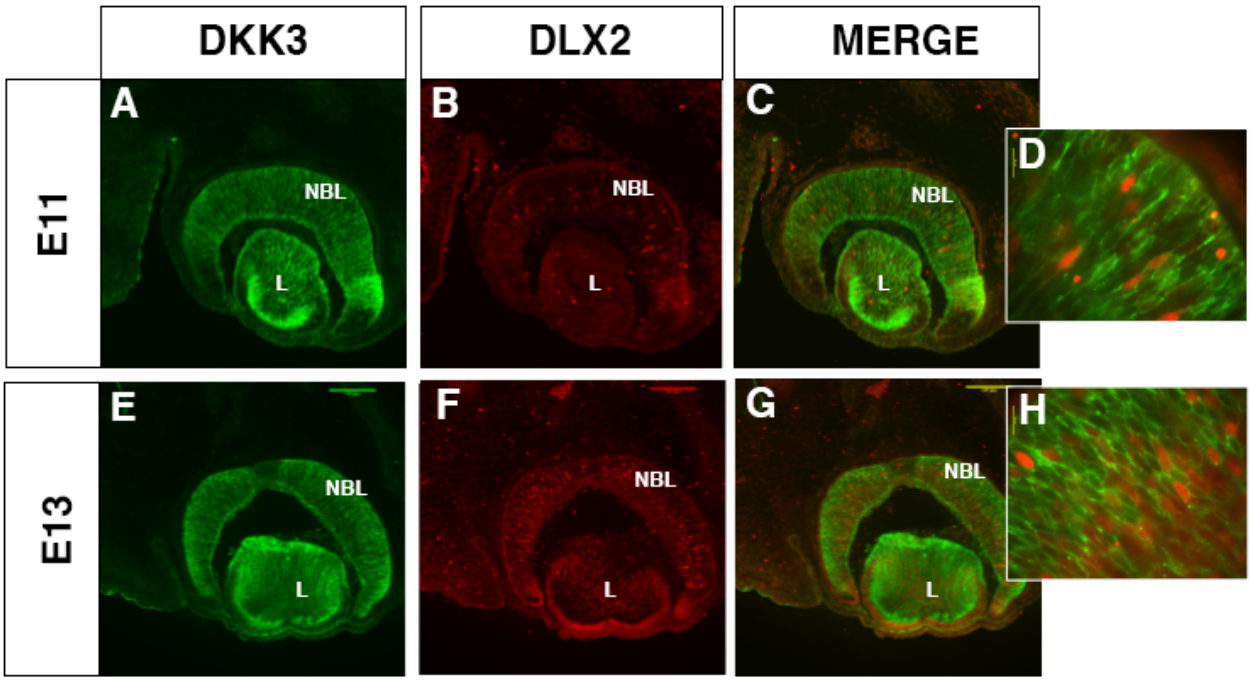

Figure 3.3 DLX2 is expressed in RPC during early retinal development.

To examine if DLX2 is expressed in early RPC, we carried out double immunostaining with DLX2 and the RPC marker DKK3. (A-C) At E11, DLX2 and DKK3 co-localization was observed in the NBL. (D) Co-localization of DLX2 and DKK3 positive cells merged at E11, magnified 100x. (E-H) DLX2 and DKK3 co-localization was also observed in RPC at E13. (H) 100x magnification of the E13 retina demonstrating DLX2 and DKK3 co-localization.

[L; lens, NBL; neuroblastic layer. Scale bar = 100 μm]

3.2.3 OLIG2 co-localizes with photoreceptor precursors

Lineage tracing studies have shown that photoreceptors are the most represented retinal cells generated from RPC with *Olig2* expression histories (Hafler et al. 2012). Because we observed OLIG2 expression in the embryonic NBL, we sought to determine if OLIG2 expression co-localized with photoreceptor precursors and/or mature photoreceptor markers at late embryonic retinal development. We performed double immunostaining on E18 retinas with OLIG2 and OTX2 antibodies to determine if OLIG2 is expressed in photoreceptor precursors. *Otx2* is expressed in photoreceptor precursors and is critical for the specification of photoreceptors (Martinez-Morales et al. 2001, Koike et al. 2007, Swaroop, Kim, and Forrest 2010). We determined that the majority of OLIG2 positive cells also co-express OTX2 (79%), while approximately half (53%) of OTX2 positive cells also expressed OLIG2 (Figure 3.4A-C). OTX2 positive cells that did not also express OLIG2 are likely bipolar cell precursors since bipolar cells very rarely arise from RPC with an *Olig2* expression history and *Otx2* is also important for the development of bipolar cells (Hafler et al. 2012, Koike et al. 2007, Swaroop, Kim, and Forrest 2010). Again, confocal microscopy could be considered to re-examine co-localization of OLIG2 with other retinal markers for improved image resolution. Next, we carried out double immunostaining of OLIG2 and CRX to examine if OLIG2 expression was maintained in further differentiated photoreceptors. *Crx* is critical for transactivating the expression of a number of genes critical for the terminal differentiation of photoreceptors (Chen, Wang, et al. 1997, Freund et al. 1997, Furukawa, Morrow, and Cepko 1997). CRX expressing photoreceptors are localized to the outer NBL at E18 (Figure 3.4D-F). Only 19% of CRX positive cells also expressed OLIG2. In the central NBL, CRX expression was observed in 31% of OLIG2 positive cells. However, this CRX antibody does have cross reactivity with OTX2 (personal communication with Dr. Craft, USC). Therefore, these OLIG2/CRX co-expressing cells likely represent OLIG2/OTX2 expressing cells based on their location in the NBL. Amacrine cells were also determined to have *Olig2* expression history (Hafler et al. 2012). Therefore, we also

performed double expression studies of the amacrine cell marker, PAX6 with OLIG2 to examine if any OLIG2 positive cells are amacrine cells at E18. PAX6 was highly expressed in differentiated amacrine cells localized to the inner NBL, as expected (Figure 3.5B,E). No co-localization of OLIG2 and PAX6 was observed in the inner NBL (Figure 3.5C,F). There were however, a few OLIG2 positive cells that also expressed PAX6 in the central NBL. Based on the localization of these OLIG2/PAX6 positive cells in the central NBL, these cells may represent amacrine cells that have not yet terminally differentiated and migrated to the inner NBL. Collectively, these results demonstrate that while amacrine cells and photoreceptors were previously shown to have *Olig2* history, we determined that OLIG2 is expressed in more primitive photoreceptor and amacrine cell precursors while OLIG2 expression is absent from differentiated photoreceptors and amacrine cells. Our results suggest that the function of *Olig2* is to specify RPC to adopt photoreceptor or amacrine cells fates, but is dispensable for terminal differentiation of these cell types.

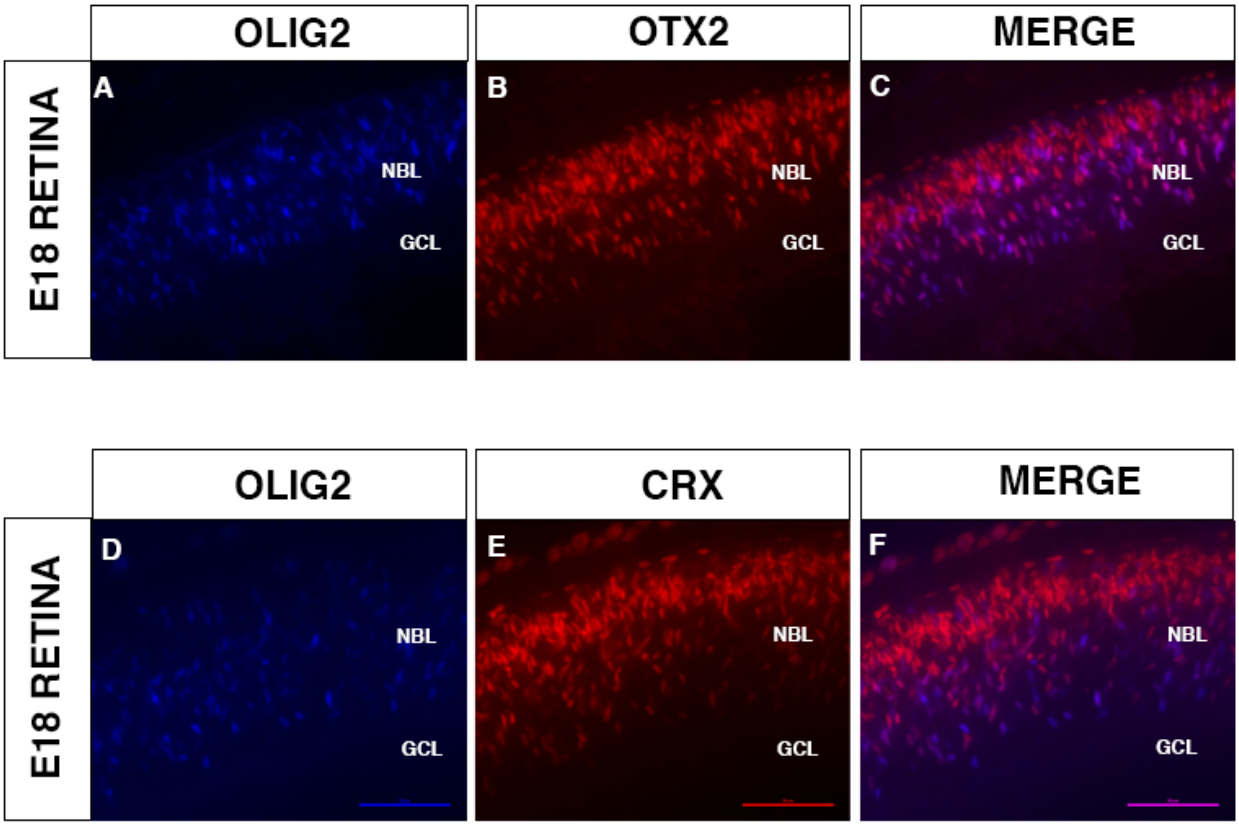
OLIG2
OTX2
MERGE
E18 RETINA
A
B
C
NBL
GCL
NBL
GCL
NBL
GCL
OLIG2
CRX
MERGE
E18 RETINA
D
E
F
NBL
GCL
NBL
GCL
NBL
GCL

Figure 3.4 OLIG2 is expressed in photoreceptor precursors.

(A-C) Co-localization of OLIG2 with the photoreceptor precursor marker OTX2 was examined in E18 retinas. (A) OLIG2 was expressed throughout the NBL and excluded from the GCL. (B) OTX2 was highly expressed in differentiated photoreceptors localized in the presumptive photoreceptor layer and in photoreceptor precursor in the central NBL. (C) Co-localization analysis determined that 79% of OLIG2 positive cells (blue) also expressed OTX2 (red). (D-F) Co-localization of OLIG2 and CRX was also examined to determine if OLIG2 positive cell were expressed in differentiated photoreceptors. (E) The majority of CRX positive cells are localized to the outer NBL where the differentiated photoreceptors are located (F) Only 19% of CRX positive cells (red) also expressed OLIG2 (blue). Based on localization of OLIG2 expression in the central NBL and exclusion from the presumptive photoreceptor layer in the outer NBL, the OLIG2 positive cells that also express CRX in the central NBL (31%) are likely OTX2 positive cells as the CRX antibody has cross reactively to OTX2. Percentages of cells co-expressing OLIG2 and OTX2/CRX were calculated by first carrying out cell counts as described in 2.3.1. Briefly, four sections of OLIG2 and OTX2/CRX stained slides were counted and the average cell counts for each protein were calculated. The total number of cells that co-expressed OLIG2/OTX2 and OLIG2/CRX were then counted and averaged. To calculate the percentage of cells that express OLIG2 and OTX2/CRX the number of cells that co-express OLIG2 and OTX2/CRX is divided by the total number of OLIG2 expressing cells.

[GCL; ganglion cell layer, NBL; neuroblastic layer. Scale = 100 μm]

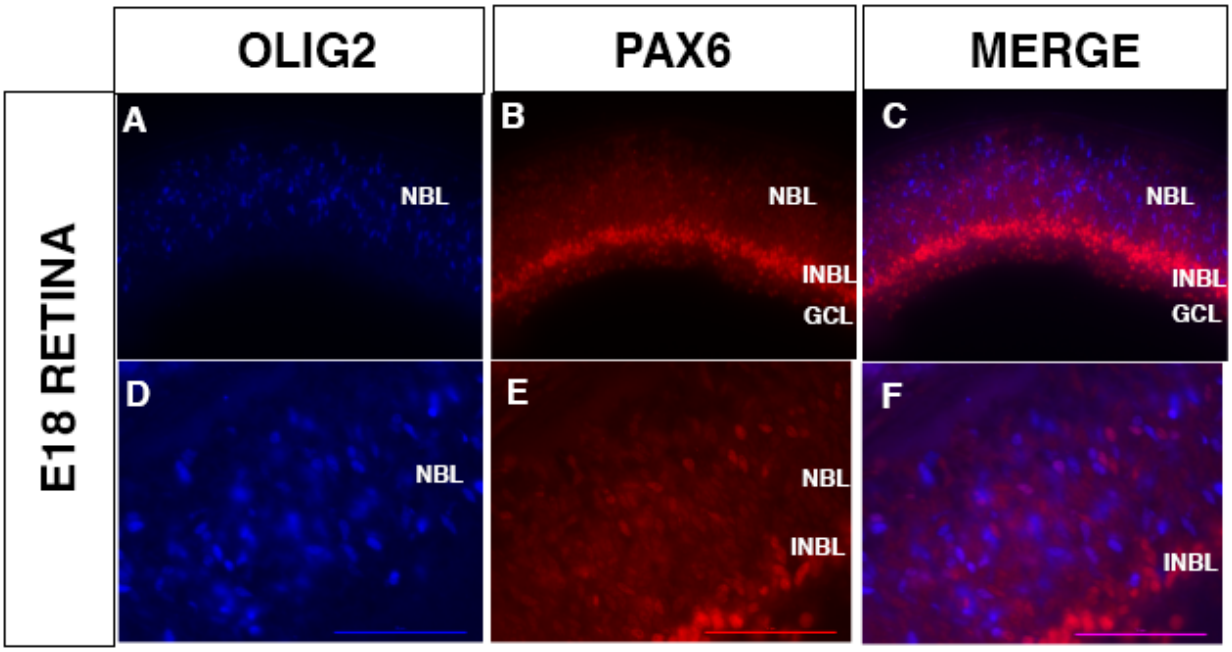

Figure 3.5 OLIG2 expression is not observed in differentiated amacrine cells.

We assessed whether OLIG2 immunoreactivity was also observed in amacrine cells. Previous lineage tracing studies identified amacrine cells to have *Olig2* expression histories. We examined co-localization of OLIG2 with PAX6 to see if OLIG2 was observed in amacrine cells. (A) As described above, OLIG2 is expressed throughout the NBL. (B) PAX6 expression is observed in the inner NBL, where differentiated amacrine cells localize. A few cells expressing PAX6 in the central NBL were also observed, likely representing immature amacrine cells. (D) Dual expression of OLIG2 and PAX6 was observed in a few cells in the NBL, while OLIG2 was restricted from the inner NBL where the majority of PAX6 positive cell were located. (D-F) Higher magnification demonstrates the absence of OLIG2 expression from the inner NBL, and co-localization of OLIG2 with PAX6 in several cell in the NBL.

[GCL; ganglion cell layer, INBL; inner neuroblastic layer, NBL; neuroblastic layer. Scale = 50 μm]

3.2.4 DLX2 binds to Olig2 regulatory chromatin elements

We expected that DLX2 restricted expression of *Olig2* in RPC to promote RGC cell fates. To determine if DLX2 was localized at *Olig2* regulatory elements *in vivo*, we carried out ChIP using E18 embryonic retinas and a high-affinity DLX2 antibody to isolate DLX2-bound chromatin. The resultant enriched chromatin was PCR amplified with primers designed to amplify *Olig2* regulatory elements that contained putative DLX2 binding sites (conserved ATTA/TAAT homeodomain binding motifs). We found that DLX2 is bound to a regulatory element proximal to the transcriptional start site of *Olig2 in vivo*, which we denoted as *Olig2*-R6 (Figure 3.6A). This region of DLX2 binding corresponded with DNAseI hypersensitive chromatin areas upstream of *Olig2* (Figure 3.6B) DNAseI hypersensitivity is an indicator of chromatin accessibility that allows for the binding of tissue specific transcription factors, chromatin modifiers, and regulatory machinery (Sabo et al. 2006). Following DLX2 ChIP, we performed ChIP-reChIP experiments in order to examine the co-localization of DLX2 and the chromatin marker H3K27me3 at *Olig2* regulatory elements *in vivo*. Inactive or "closed" chromatin can be identified based on the presence of modifications on histones including H3K27me3 located in the regulatory chromatin (Bernstein, Meissner, and Lander 2007, Kouzarides 2007, Li, Carey, and Workman 2007). Therefore, we expected that DLX2 would co-localize with H3K27me3 at *Olig2* regulatory elements *in vivo*, further supporting DLX2 as a negative transcriptional regulator of *Olig2* expression *in vivo*. First, we determined that H3K27me3 was not present at *TrkB* regulatory elements that we previously identified to be occupied and transactivated by DLX2 in the developing retina (Figure 3.6C) (de Melo et al. 2008). H3K27me3 ChIP followed by DLX2 re-ChIP demonstrated that both proteins were present at *Olig2* regulatory elements *in vivo* (Figure 3.6D), further supporting that DLX2 is involved in the negative regulation of *Olig2* expression in the developing retina *in vivo*.

A

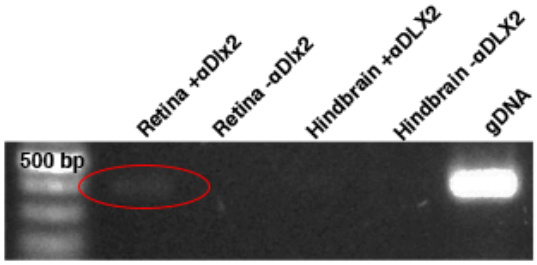

Olig2-Region 6

B

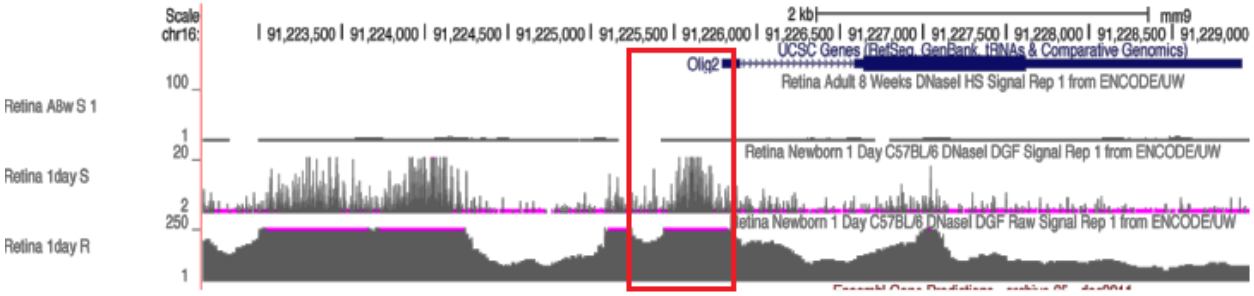

C

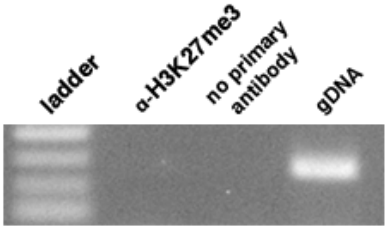

TrkB

D

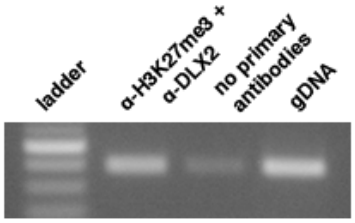

Olig2

Figure 3.6 DLX2 negatively regulates *Olig2* expression *in vivo*.

ChIP was utilized to examine binding of DLX2 to the regulatory region of *Olig2 in vivo*. (A) DLX2 ChIP was performed on E18 retinas. DLX2 binding was observed at two regulatory elements proximal to the transcriptional start site in *Olig2*, denoted as *Olig2*-R6 and *Olig2*-R7. (data not shown). Both negative antibody (-αDLX2) and ChIP on HB tissue, which is negative for DLX2 expression, were carried out as controls. (B) Regulatory regions identified to be positive for DLX2 binding correspond to regions of open chromatin in the 1 day old retina as indicated by DNase I hypersensitive sites (bottom two tracks, red boxed region). At 8 weeks, DNase I hypersensitivity is no longer observed in the retina (top track, red boxed in region). (C-D) DLX2 co-localizes with repressive chromatin marks at *Olig2* regulatory elements. (C) We first examined a DLX2 target gene that is transcriptionally activated in the retina (TrkB) to determine if the repressive chromatin mark H3K27me3 was observed. As expected, there was no binding of H3K27me3 at TrkB. (D) DLX2 and H3K27me3 ChIP-reChIP was performed to examine co-localization of DLX2 and H3K27me3 at *Olig2* regulatory elements. Both DLX2 and H3K27me3 bind to *Olig2 in vivo*, further supporting that DLX2 binding leads to the transcriptional repression of *Olig2* in the developing retina *in vivo*.

[bp; base pair, gDNA; genomic DNA. DNAse I hypersensitivity sites in the *Olig2* regulatory region identified using the UCSC genome browser NCB137/mm9 assembly]

Next we next carried out EMSA using *Olig2*-R6 radiolabelled DNA probes to investigate the nature of DLX2 binding to *Olig2 in vitro* (i.e direct binding to DNA). Labelled probes were incubated with recombinant DLX2 (rDLX2) protein and rDLX2/probe complexes were then resolved on a non-denaturing acrylamide gel. rDLX2 was found to directly bind to *Olig2*-R6 *in vitro* (Figure 3.7A). To examine the specification of DLX2 binding to *Olig2*-R6, cold competition and supershift binding experiments were carried out using excess unlabelled probe and a DLX2 antibody, respectively. In cold competition experiments the excess unlabelled probe out-competes the labelled probe for binding to rDLX2. In the supershift binding reactions, the DLX2 antibody will specifically bind to DLX2/probe complexes, creating larger molecular weight complexes that will migrate more slowly in the vertical gel compared to free probes and rDLX2 bound probes. These experiments demonstrated that the shift observed for *Olig2*-R6 is specifically due to binding by rDLX2. Collectively, these findings indicate that DLX2 is binding to regulatory elements in *Olig2* upstream of the transcriptional start site *in vivo* and *in vitro*.

To determine the functional consequence of DLX2 binding to *Olig2* regulatory elements *in vitro*, we performed reporter gene assays where *Dlx2* expression plasmids were co-transfected into HEK 293 cells with luciferase reporter vectors that contained the *Olig2*-R6 regulatory element cloned upstream of the luciferase gene or with empty reporter gene controls. Binding of DLX2 to *Olig2*-R6 regulatory elements *in vitro* resulted in significant repression of luciferase expression compared to empty vector controls (Figure 3.7B) (N=3). This *in vitro* reporter gene assay further supports that DLX2 is important for the transcriptional repression of *Olig2* expression.

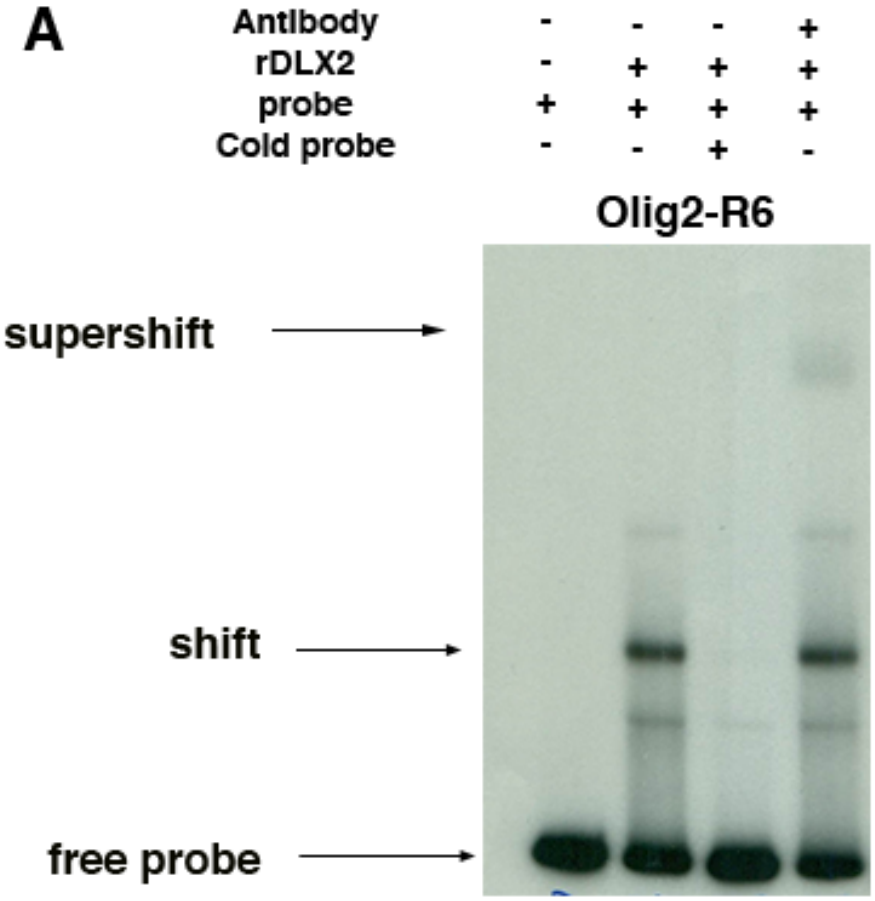
A
Antibody - - - +
rDLX2 - + + +
probe + + + +
Cold probe - - + -
Olig2-R6
supershift
shift
free probe

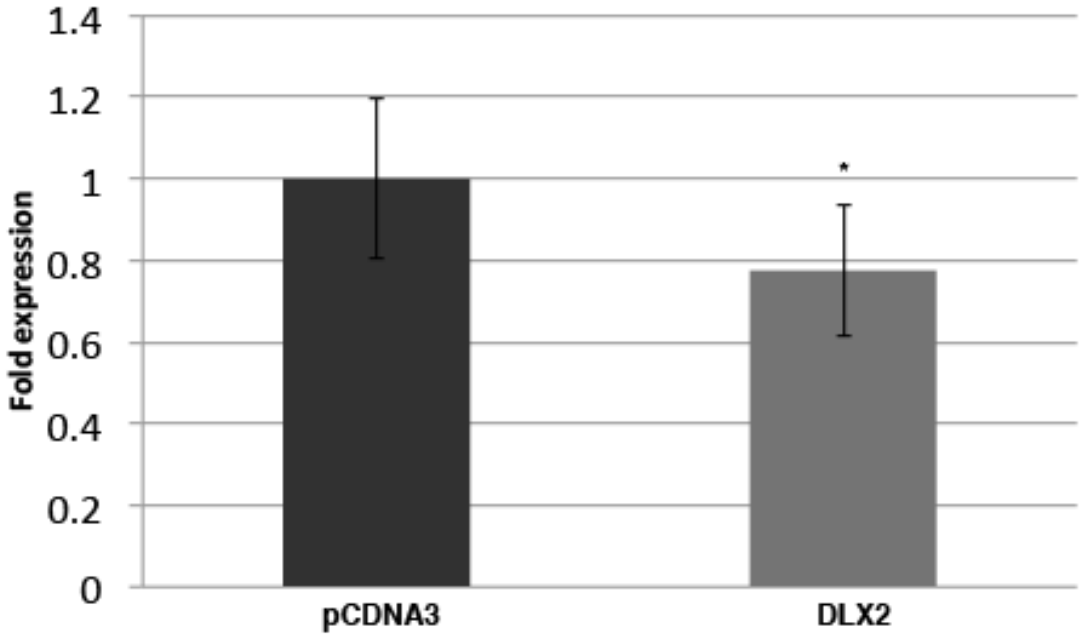
B
1.4
1.2
1
0.8
0.6
0.4
0.2
0
Fold expression
*
pCDNA3
DLX2

Figure 3.7 DLX2 binds to and restricts *Olig2* expression *in vitro*.

To examine direct binding of DLX2 to *Olig2* and the functional consequence of DLX2 binding to *Olig2 in vitro*, we performed EMSA and reporter gene assays, respectively. (A) Incubation of radiolabelled *Olig2*-R6 probes with rDLX2 protein resulted in a shift of probe/protein complexes in the non-denaturing polyacrylamide gel (compare gel lane 1 to lane 2). Addition of excess unlabelled probe to the labelled probe/rDLX2 reaction out competes labelled probe for binding to rDLX2, abolishing the observed shift in the gel (lane 3). Addition of an αDLX2 antibody to the labelled probe/rDLX2 reaction generates a supershift in the gel due to the production of a higher molecular weight complex generated upon αDLX2 binding (lane 4). (B) The functional consequence of DLX2 binding to *Olig2* regulatory elements *in vitro* was examined using reporter gene assays (N=3). Co-transfection of *Dlx2* expression vectors and *Olig2*-R6 reporter vectors resulted in a significant reduction in luciferase expression *in vitro* compared to empty vector (pCDNA3) controls as determined by unpaired t-tests. EMSA and luciferase assays were performed by Q. Jiang.

[rDLX2; recombinant DLX2 protein, *= $P<0.05$]

3.2.5 Loss of Dlx1/Dlx2 results in ectopic expression of Olig2 in the GCL

Dlx1/*Dlx2* is required for the terminal differentiation of late-born RGC in the developing retina (de Melo et al. 2005). We expected that loss of *Dlx1*/*Dlx2* expression would result in the increased expression of photoreceptor-specific gene expression including *Olig2*. To determine the functional consequence of *Dlx1*/*Dlx2* loss on *Olig2* expression *in vivo*, we first carried out immunostaining on E18 retinal cryosections on a mixed CD-1;C57Bl/6 background. To our surprise, in *Dlx1*/*Dlx2* DKO retinas we observed ectopic expression of *Olig2* in the GCL, coupled with a concomitant decrease in *Olig2* expression in the NBL (Figure 3.8A, B) (N=2). These findings may suggest a cell fate switch from RGC to photoreceptors and defects in photoreceptor lamination. However, these phenotypic findings appear to be genetic background strain-specific. We also examined OLIG2 expression in *Dlx1*/*Dlx2* DKO retinas maintained on the inbred CD-1 genetic background. Unlike our observations in the *Dlx1*/*Dlx2* DKO retinas on the mixed CD-1;C57Bl/6 background, there is no change in OLIG2 expression observed in the *Dlx1*/*Dlx2* DKO retina compared to WT littermate controls (Figure 3.8D, E) (N=3). Overall, these findings suggest that *Dlx* genes are playing a role in restricting the expression of *Olig2* in RPC fated to become RGC in a strain-dependent manner. In the absence of *Dlx1*/*Dlx2* expression, those precursors that would become RGC may now express markers of early photoreceptors and migrate ectopically to the GCL. Additional replicates of OLIG2 staining and additional photoreceptor marker staining, including OTX2 and CRX in the CD-1;C57Bl/6 *Dlx1*/*Dlx2* DKO retina, will need to be carried out in the future to confirm if photoreceptor gene expression is ectopically expressed in the GCL following *Dlx1*/*Dlx2* loss.

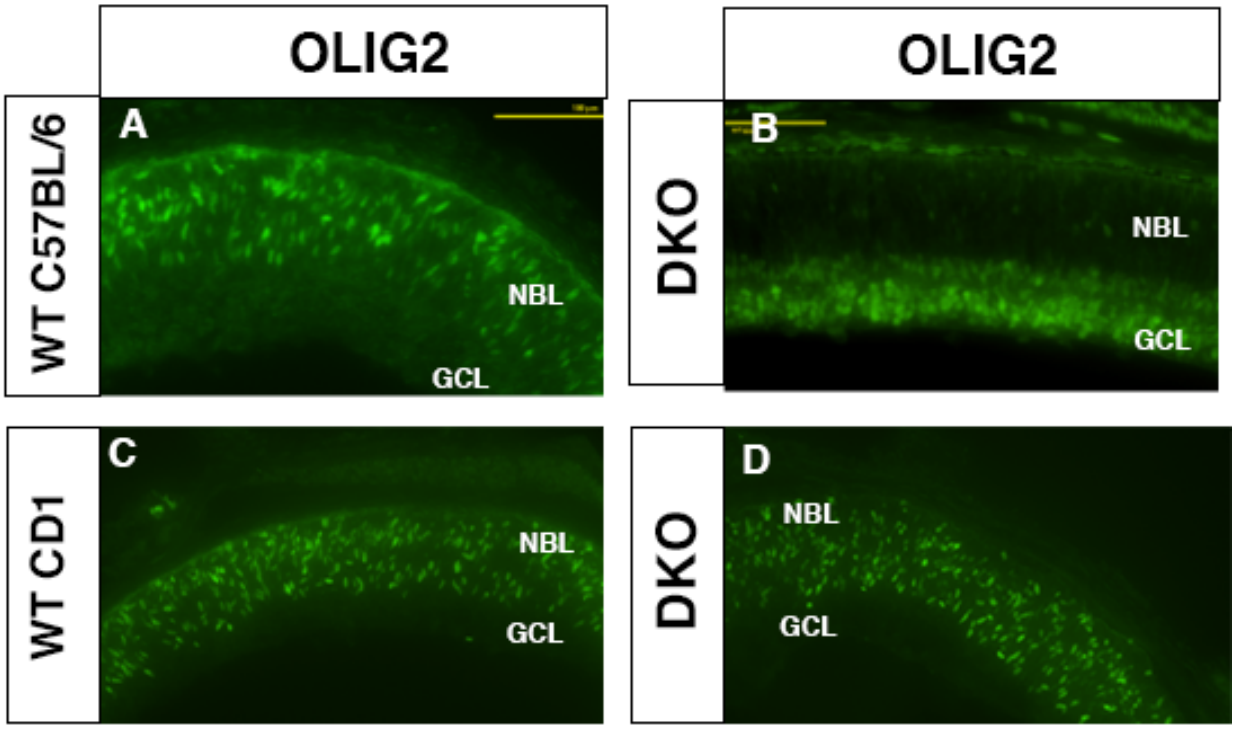

Figure 3.8 Strain-specific ectopic expression of OLIG2 in the *Dlx1*/*Dlx2* DKO retina.

Expression of OLIG2 in the absence of *Dlx1*/*Dlx2* expression was examined in the E18 retina. (A) In the WT E18 retina OLIG2 is expressed in the NBL (B) Expression of OLIG2 in the *Dlx1*/*Dlx2* DKO retina on a mixed CD-1;C57Bl/6 background showed ectopic localization of OLIG2 in the GCL and the inner NBL, corresponding to regions of RGC and amacrine cell localization (N=2). (C, D) On the CD-1 background, however, no change in OLIG2 expression was observed in the *Dlx1*/*Dlx2* DKO retina compared to WT controls (N=3).

[GCL; ganglion cell layer, NBL; neuroblastic layer. Scale = 100 μm]

3.2.6 Exogenous Dlx2 drives expression of Brn3b, but photoreceptor gene expression excluded from cells ectopically expressing Dlx2

Loss of *Dlx1*/*Dlx2* expression experiments were complemented with *Dlx2* gain of function experiments. *Dlx2* gain of function was carried out by *in utero* retinal electroporation of pCIG2-*Dlx2*-mCherry or pCIG-2*Dlx2*-EGFP expression plasmids into the sub-retinal space of embryonic mice. Electroporation was carried out at E13 and embryos were collected at E18. Cells ectopically expressing DLX2 were identified by the presence of mCherry (Figure 3.9A, B) or EGFP expression (Figure 3.10A). We also carried out additional validation of DLX2 expression from the pCIG2-*Dlx2*-mCherry and pCIG2-*Dlx2*-EGFP expression vectors by performing immunostaining using a DLX2 antibody and examining the co-localization of mCherry (Figure 3.9C, D) or EGFP positive cells (Figure 3.10B-D) and DLX2 immuno-positive cells in retinas electroporated with *Dlx2*-mCherry or *Dlx2*-EGFP. RPC that have taken up exogenous pCIG2-*Dlx2*-mCherry ectopically expressed BRN3B, demonstrating *Dlx2* expression is sufficient to drive *Brn3b* expression in the developing retina *in vivo* (Figure 3.9E-G). RPC that have taken up empty pCIG2-mCherry control vectors were unable to drive ectopic expression of Brn3b (Figure 3.9H-J). We next sought to determine if cells ectopically expressing *Dlx2* also expressed photoreceptor genes including OLIG2, OTX2, and CRX. As expected, cells expressing exogenous *Dlx2*-EGFP did not co-localize with photoreceptor gene expression (Figure 3.10E-G). The lack of co-localization of DLX2-EGFP with photoreceptor markers in electroporated retinas supports that DLX2 has a restrictive transcriptional role on photoreceptor gene expression in the developing retina. RPC that have taken up empty pCIG2-EGFP control vectors were unable to drive ectopic expression of BRN3B *in vivo* (Figure 3.10H-J) These findings support a role for Dlx2 in promoting the expression of *Brn3b* in the developing retina *in vivo* and restricting the acquisition of photoreceptor cell fate in RPC fated to become RGC by restricting expression of photoreceptor specific genes during retinogenesis in these cells. We also attempted *Dlx2*-shRNA knockdown in developing retinas utilizing *in utero* retinal electroporation to determine

if an increase in photoreceptor gene expression would be observed from RPC in which *Dlx2* expression was inhibited. However, due to technical limitations, electroporation of pCIG2-*Dlx2*-shRNA into the embryonic retina was not successful and will be re-examined in future studies.

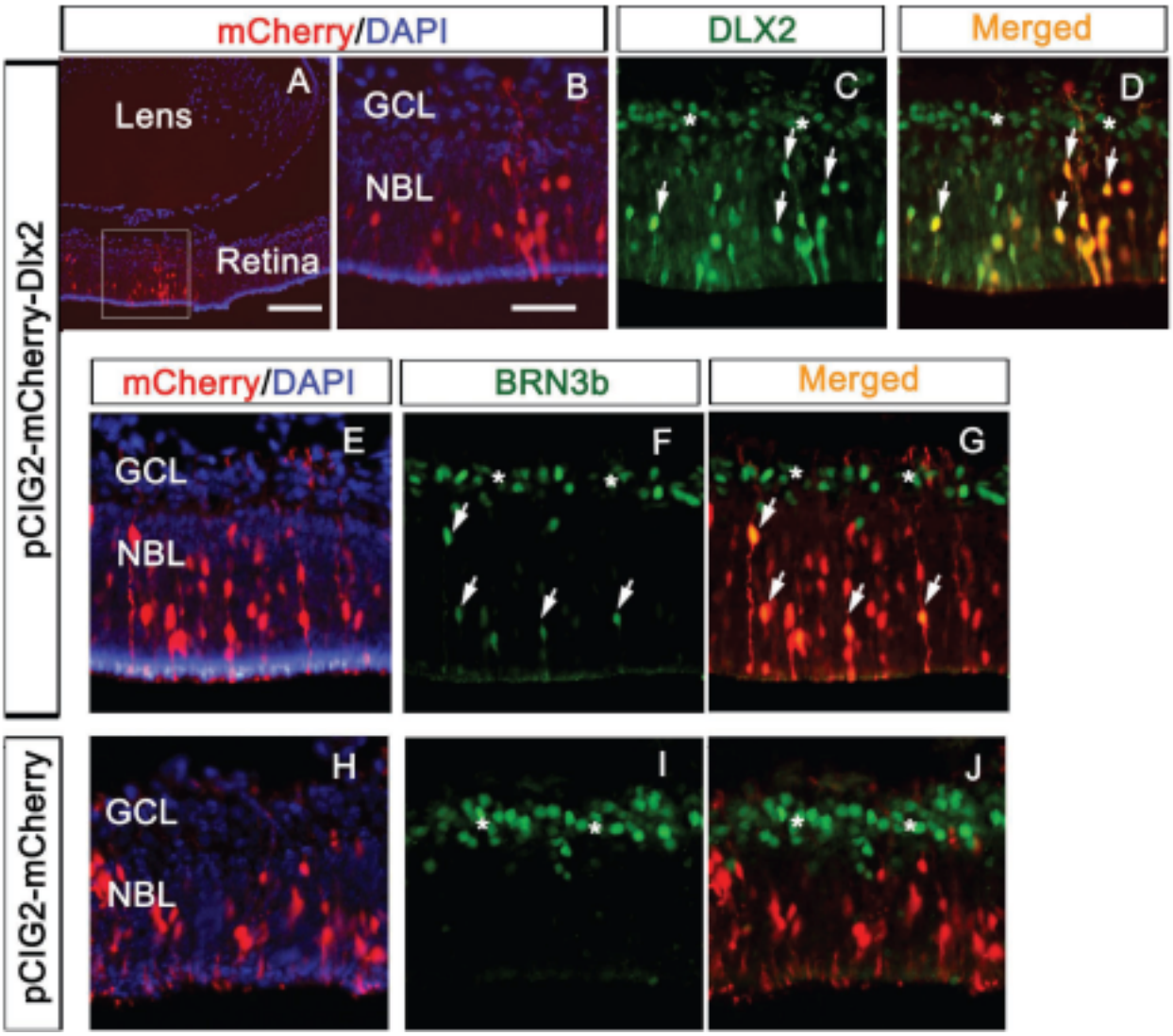
mCherry/DAPI
DLX2
Merged
pCIG2-mCherry-Dlx2
A
Lens
Retina
B
GCL
NBL
C
D
mCherry/DAPI
BRN3b
Merged
E
GCL
NBL
F
G
pCIG2-mCherry
H
GCL
NBL
I
J

Figure 3.9 *Dlx2* drives ectopic expression of BRN3B *in vivo*.

Dlx2 gain of function was carried out using *in utero* retinal electroporation to drive ectopic expression of *Dlx2* in RPC at E13. (A, B) Cells ectopically expressing *Dlx2* were visualized by mCherry expression from the *Dlx2* expression plasmid (red). (C, D) Ectopic expression of DLX2 from the pGIG2-*Dlx2* expression vector was verified by DLX2 immunostaining where merged mCherry and DLX2 expression demonstrate expression of DLX2 from the pCIG2-*Dlx2* vector. (E-G) Exogenous *Dlx2* expression in RPC that have taken up pCIG2-*Dlx2*-mCherry expression vectors drive ectopic expression of BRN3B (arrows in panel F, merged with pCIG2-*Dlx2*-mCherry in panel G). (H-J) Empty pCIG2-mCherry expression vectors were electroporated as a negative control. The lack of co-localization observed with mCherry (H) and BRN3B (I) observed in panel J demonstrate that RPC that have taken up pCIG2-mCherry are unable to drive ectopic expression of BRN3B. Figure adapted from (Zhang et al. 2017), reproduced with permission.

[GCL; ganglion cell layer, NBL; neuroblastic layer. Scale bar in panel A = 50 μm. Scale bar in panel B = 20 μm]

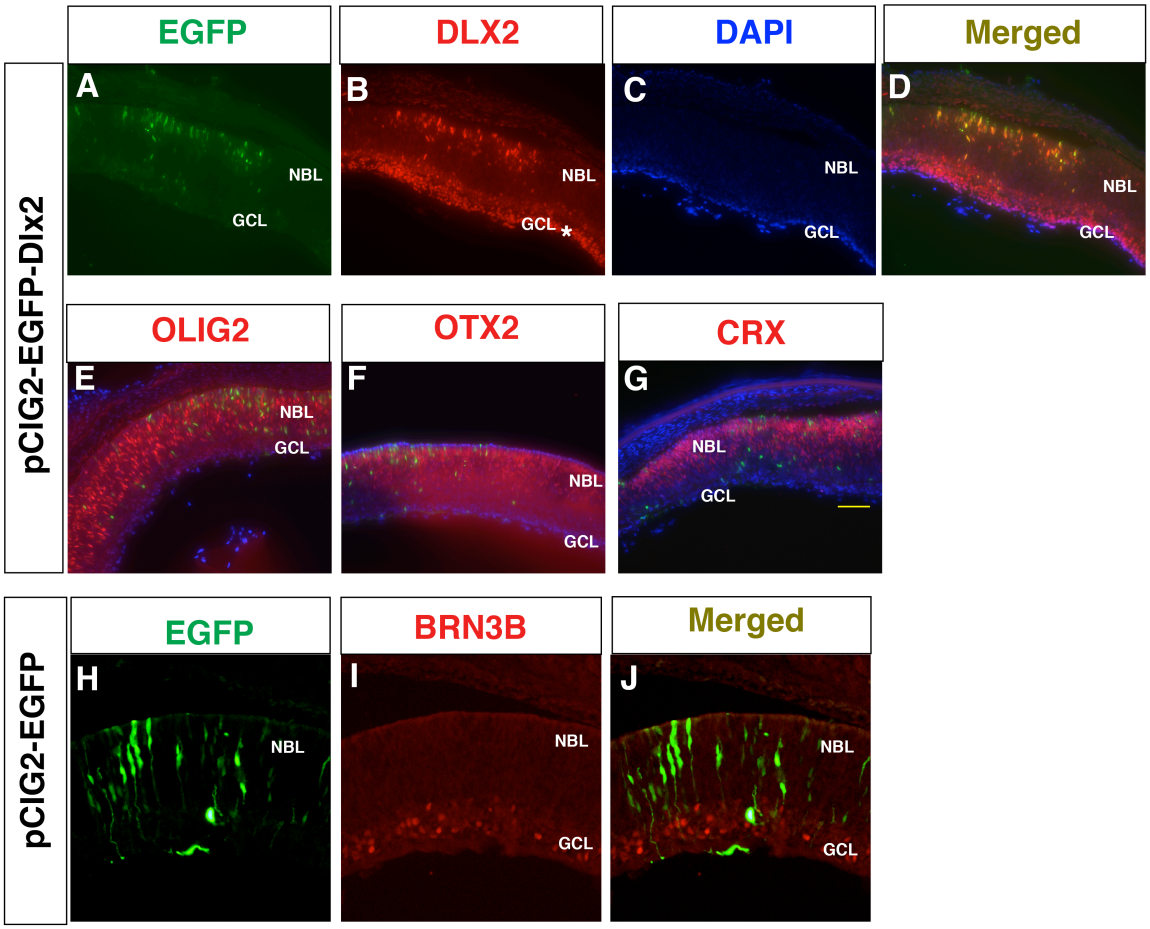
pCIG2-EGFP-Dlx2
EGFP
DLX2
DAPI
Merged
A
B
C
D
NBL
GCL
OLIG2
OTX2
CRX
E
F
G
pCIG2-EGFP
EGFP
BRN3B
Merged
H
I
J

Figure 3.10 Photoreceptor gene expression is excluded from cells ectopically expressing *Dlx2 in vivo*.

Dlx2 gain of function was carried out using *in utero* retinal electroporation to drive ectopic expression of *Dlx2* in RPC at E13. (A-D) Cells ectopically expressing DLX2 were visualized by EGFP expression from the pCIG2-*Dlx2* expression plasmid (green). (B) Verification of ectopic DLX2 expression was performed by immunostaining with a DLX2 antibody. Endogenous DLX2 expression in the GCL is indicated with an asterisk (*). (D) Merged EGFP and DLX2 immunostaining verify that EGFP positive cells ectopically express DLX2. (E-F) Photoreceptor gene expression was examined in the *Dlx2* gain of function retina. (E) OLIG2, (F) OTX2, and (G) CRX expressing cells did not co-localize with cells ectopically expressing DLX2. (H) Empty pCIG2-EGFP controls demonstrate cells that have taken up empty EGFP vector. (I) BRN3B expression in pCIG2-EGFP electroporated retina. (J) Merged image demonstrating lack of upregulation of Brn3b expression in cells that have taken up empty control pGIC2-EGFP vectors.

[EGFP; enhanced green fluorescent protein, GCL; ganglion cell layer, NBL; neuroblastic layer. Scale = 100 μm]

3.2.7 Increase in Olig2 expressing cells in the Atoh7 null retina

Atoh7 is critical for RPC to acquire RGC fate. *Atoh7* null retinas are devoid of RGC, and cone photoreceptors increase at the expense of RGC (Brown et al. 2001). These findings suggest that RPC make binary cell fate decisions between RGC and cone photoreceptors, which are born in overlapping temporal developmental windows. We therefore questioned whether *Olig2* positive photoreceptor precursors would be increased in the *Atoh7* null retina at the expense of RGC. We also examined DLX2 expression in the absence of *Atoh7* as DLX2 expression has not been previously examined in the *Atoh7* knockout retina. We examined the expression of DLX2 and OLIG2 in *Atoh7*$^{-/-}$ retinas at time points near peak RGC and cone genesis (E13), and near the cessation of *Atoh7* expression (E16). OLIG2 expression was significantly elevated at both developmental time points examined (Figure 3.11) (N=3). DLX2 expression, on the other hand, was significantly reduced at peak RGC genesis at E13 (Figure 3.12) (N=3). At the later stage of retinogenesis, however, no significant change in DLX2 expressing cells was observed between the WT and *Atoh7* null retina (Figure 3.12) (N=3). The elevation in retinal OLIG2 expression in the absence of *Atoh7* provides further evidence that *Olig2* is a marker of early photoreceptor precursors. In addition, these results demonstrate that *Atoh7* initiates early expression of *Dlx2* during RGC development, which has not been previously observed by our laboratory. Interestingly, the lack of significant loss of DLX2 expression at late retinogenesis in the *Atoh7* null retina may suggest that additional RGC specific transcription factors, such as Brn3b, Isl1 and/or others, while reduced in the *Atoh7* null retina, may be sufficient to drive expression of *Dlx2* at late stages of retinal development. Alternatively, the remaining DLX2 expressing cells at E16 could be DLX2 positive amacrine cells, which like cones are elevated in the *Atoh7* null retina (Wang et al. 2001). Co-localization analysis with DLX2 and amacrine markers, such as PAX6, as well as with other RGC markers such as BRN3B and BRN3A, could help clarify the identify of the DLX2 expressing cells in the E16 retina of the *Atoh7* null mouse. The increase in OLIG2 expression and concurrent reduction in DLX2 expression in the *Atoh7* null retina support the

previous findings that RPC are re-specified to generate photoreceptors in the absence of *Atoh7* at the expense of RGC.

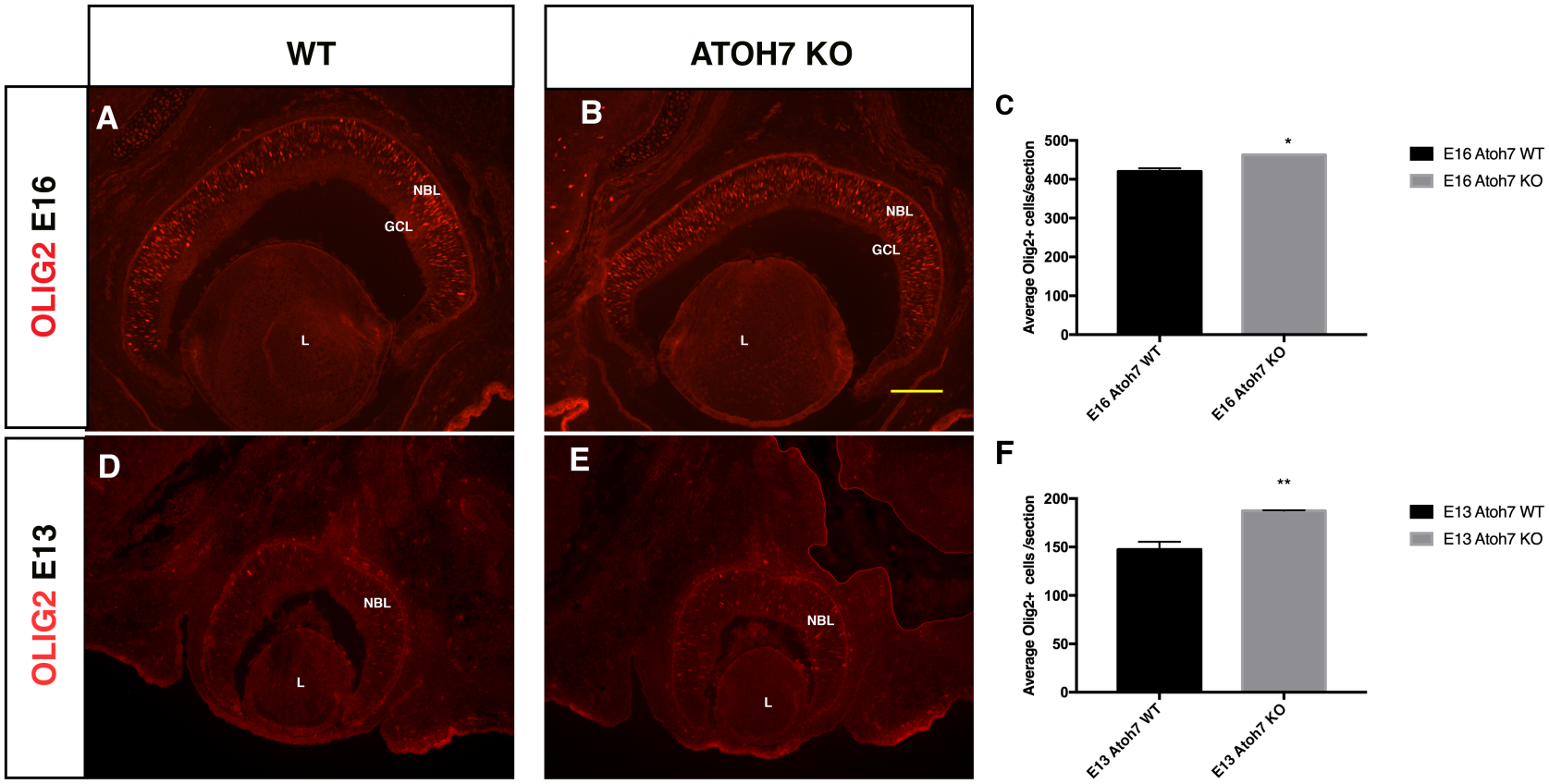
WT
ATOH7 KO
OLIG2 E16
OLIG2 E13
A
B
C
D
E
F
NBL
GCL
L
Average Olig2+ cells/section
E16 Atoh7 WT
E16 Atoh7 KO
E13 Atoh7 WT
E13 Atoh7 KO
*
**
0
100
200
300
400
500
50
150

Figure 3.11 Increase in OLIG2 positive cells in the *Atoh7* knockout.

OLIG2 expression was examined in the *Atoh7* knockout (KO) retina to further validate *Olig2* as a photoreceptor precursor as cone photoreceptors are elevated in the *Atoh7* null retina. (A-C) The number of OLIG2 expressing cells was increased in the absence of *Atoh7* in the E16 retina compared to WT controls. (D-F) At E13, at the peak of RGC genesis, a significant increase in OLIG2 positive cells was also observed in the *Atoh7* null retina compared to WT controls as determined by unpaired t-tests (N=3).

[GCL; ganglion cell layer, L; lens, NBL; neuroblastic layer. Scale = 100 μm. *= $P<0.05$, **= $P<0.01$]

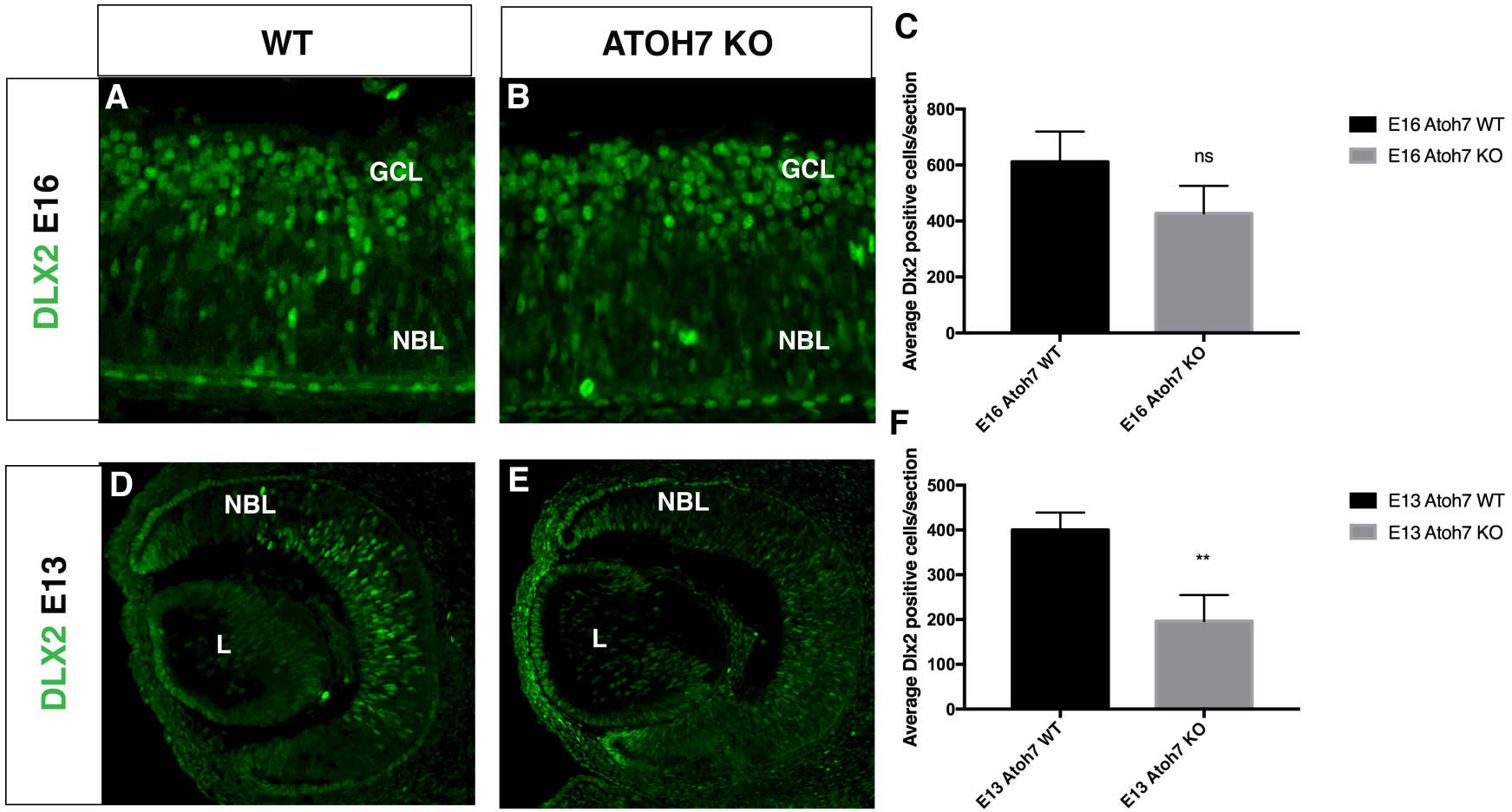
WT
ATOH7 KO
DLX2 E16
DLX2 E13
A
B
C
D
E
F
GCL
NBL
L
Average Dlx2 positive cells/section
800
600
400
200
0
ns
E16 Atoh7 WT
E16 Atoh7 KO
500
300
100
**
E13 Atoh7 WT
E13 Atoh7 KO

Figure 3.12 DLX2 expression is reduced at the peak of RGC genesis in the *Atoh7* knockout.

(A-C) During late embryonic retinogenesis (E16), there is no significant change in DLX2 positive cells in the retinas of *Atoh7* null mice compared to WT littermate controls. (D-F) During early embryonic retinogenesis, however, and near the peak of RGC genesis, a significant reduction in DLX2 expressing cells is observed in the *Atoh7* knockout compared to WT littermate controls as determined by unpaired t-tests (N=3). DLX2 immunostaining performed by Q. Zhang.

[L; lens, GCL; ganglion cell layer, NBL; neuroblastic layer, NS; not significant. **P=<0.01]

3.2.8 Olig2 transcript levels in the DKO retina are unchanged compared to controls in an inbred CD-1 background

To quantify the *Olig2* transcript levels in the *Dlx1*/*Dlx2* DKO retinas, we carried out qRT-PCR. In addition, *Crx* expression in the DKO was also quantified to examine the influence of *Dlx1/Dlx2* loss in the expression of mature photoreceptor target genes. *Dlx2* and *Brn3b* expression was also examined as additional controls for loss of *Dlx2* expression and reduction of Brn3b expression, respectively, in the *Dlx1*/*Dlx2* DKO retina, which we have demonstrated previously (Zhang et al. 2017). Surprisingly, we found that there was no significant change in the expression of *Olig2* or *Crx* in the DKO retina compared to controls while *Dlx2* and *Brn3b* were both significantly reduced verifying the loss of *Dlx2* and decrease in Brn3b expression expected in the *Dlx1*/*Dlx2* retina (Figure 3.13) (N=3). However, these qRT-PCR experiments were carried out on whole retinas isolated from mice from the CD-1 genetic background strain. As described above, the genetic background strain appears to play a critical role in the phenotype and gene expression in the *Dlx1*/*Dlx2* DKO mice. We have performed preliminary qRT-PCR utilizing *Dlx1*/*Dlx2* DKO mice that were crossed into a C57Bl/6 genetic background to generate mixed CD-1;C57Bl/6 background. Preliminary results show a two-fold increase in *Olig2* expression in the absence of *Dlx1*/*Dlx2* compared to WT controls (Figure 3.13) (N=2). Collectively, these results suggest that *Olig2* is de-repressed in the absence of *Dlx1*/*Dlx2* expression in the developing retina on a mixed genetic background, supporting a repressive transcriptional role for *Dlx1/Dlx2* on *Olig2* expression *in vivo*. More importantly, these preliminary qPCR results on the mixed genetic background combined with the immunostaining results on the mixed genetic background in 3.2.5 above demonstrate the critical importance of genetic background strain in the examination of photoreceptor gene expression in a murine mouse model. It will be important to cross the CD-1 *Dlx1*/*Dlx2* heterozygous mice to a C57Bl/6 background to generate a mixed background moving forward with further examination of photoreceptor gene expression in the *Dlx1*/*Dlx2* DKO retina.

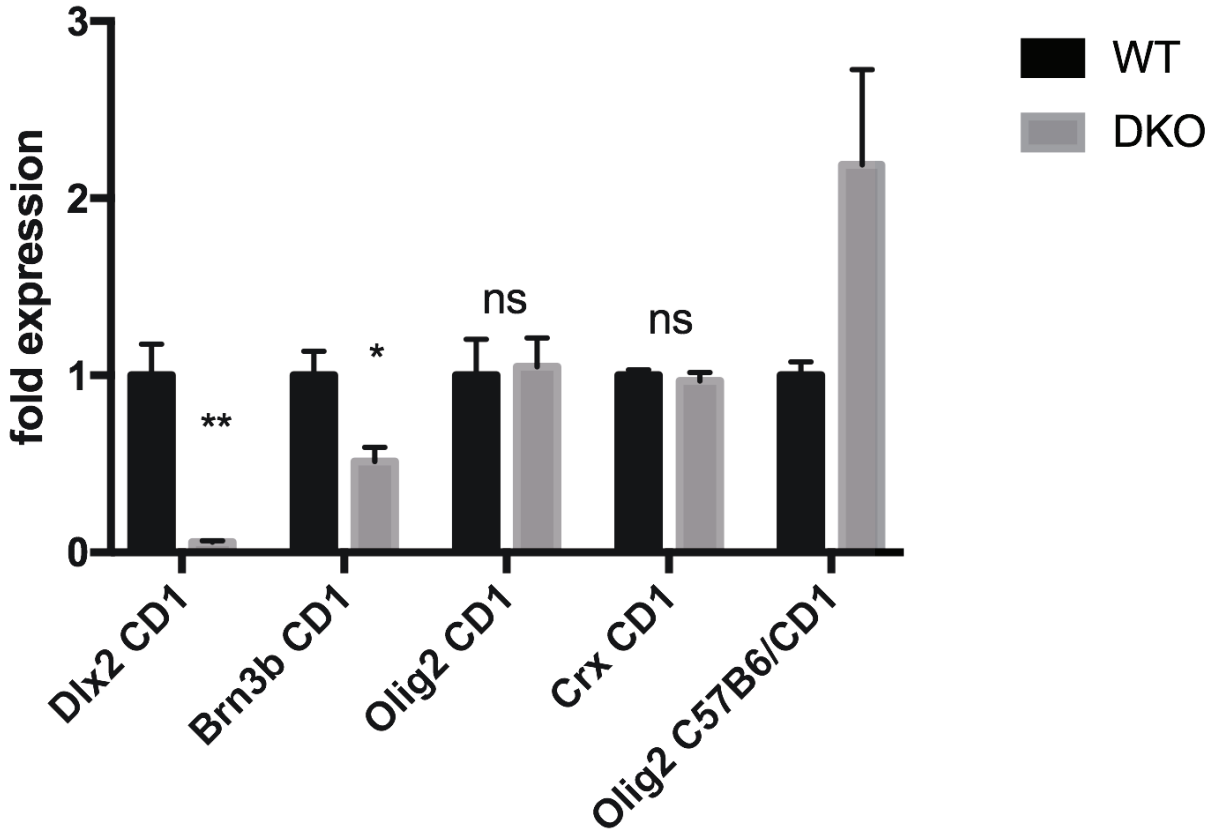

Figure 3.13 No change in *Olig2* expression in the CD-1 *Dlx1/Dlx2* DKO retina.

Olig2 transcripts were quantified along with *Crx* to determine if photoreceptor gene expression was decreased in the absence of *Dlx1/Dlx2*. *Dlx2* and *Brn3b* expression was also examined as controls for *Dlx2* knockout and *Brn3b* reduction. While significant reduction in *Dlx2* and *Brn3b* expression was observed as expected (N=3), no change in *Olig2* and *Crx* was observed in the CD-1 retina (N=3). Preliminary analysis of *Olig2* expression in *Dlx1/Dlx2* DKO mice on a mixed genetic background, however, appears to be elevated in the DKO compared to controls (N=2). Significant reductions in *Dlx2* and *Brn3b* expression were determined by carrying out unpaired t-tests.

[ns; not significant. * = P<0.05, ** =P<0.01]

3.3 Discussion

3.3.1 dlx is not observed in the developing zebrafish retina

Dlx genes have been identified in a number of vertebrates including humans (Simeone et al. 1994), mice (Porteus et al. 1991, Price et al. 1991, Robinson, Wray, and Mahon 1991), chick (Ferrari et al. 1995), *Xenopus* (Asano et al. 1992), and zebrafish (Ekker et al. 1992). *Dlx* gene expression in the developing forebrain and craniofacial/pharyngeal structures is widely conserved in vertebrates. (Gordon et al. 2010, Marcucio et al. 2005, Brox et al. 2003). However, zebrafish appear to be one of the few vertebrates that do not express *Dlx* genes in the developing retina. We have observed *Dlx2* expression in the developing human retina (Bush and Eisenstat, unpublished observations) and the mouse retina (de Melo et al. 2005, de Melo et al. 2003, Eisenstat et al. 1999). It also appears that *Xenopus Dlx2* (which is an orthologue of mouse and human *Dlx3*) is expressed in the developing retina; however its role in the development of the *Xenopus* retina has not been explored (Square et al. 2015). *Dlx3* has also been observed in the chick retina (Dhawan, Schoen, and Beebe 1997). Invertebrate organisms including planaria and *Drosophila* also express *dlx*/*Dll* in the optic cup and optic lobes, respectively (Lapan and Reddien 2011, Morante, Erclik, and Desplan 2011). We did not observe expression of *dlx* genes in the developing zebrafish retina at 24 hpf and 48 hpf, which are time points corresponding to developmental time points where RGC first become post mitotic and enter the tectum of zebrafish, respectively (Avanesov and Malicki 2010, Burrill and Easter 1994, Hu and Easter 1999). However, a recent article described lineage tracing of *dlx1a*/*dlx2a* and *dlx5a*/*dlx6a* expressing cells in zebrafish. The authors showed that *dlx5a*/*dlx6a* expression was observed in the juvenile retina at 45 days post fertilization in the GCL, INL, and ONL (Solek et al. 2017). These findings suggest that unlike murine *Dlx* genes, *dlx* genes in the zebrafish may not be required for early retina cell fate determination and development, but perhaps have unique functions in retinal cell maintenance/function. It is unclear from this recent study if *dlx1a*/*dlx2a*

are expressed in the juvenile retina. It will therefore be interesting to examine the role of *dlx* genes in maintenance/function of the zebrafish retina in future studies, particularly given that *dlx5a/dlx6a* was observed in the ONL.

3.3.2 Dlx2 regulates the expression of Olig2 in the developing retina

Olig2 expression in the retina was first described nearly a decade ago. However, little is known about the transcriptional regulation of *Olig2* during retinal development. We determined that DLX2 occupies regulatory elements of *Olig2* and restricts *Olig2* expression in the developing retina *in vivo*. This is the first report, to our knowledge, investigating the transcriptional regulation of *Olig2* expression in the developing retina. The presence of both H3K27me3 and DLX2 at *Olig2* regulatory elements further supports a negative regulatory role for DLX2 in restricting *Olig2* expression in the retina. We have also shown that OLIG2 expression is limited to photoreceptor precursors but excluded from mature photoreceptors, which has not been explicitly demonstrated previously. Recently, a retina OTX2 ChIP followed by high throughput sequencing (ChIP-seq) experiments have determined that *Olig2* regulatory elements are also occupied by OTX2 (Samuel et al. 2014), suggesting that OTX2 may also regulate the expression of *Olig2*. Interestingly, however, OTX2 binding to *Olig2* in the ChIP-seq experiments was observed in the adult retina where *Olig2* expression is no longer observed (Figure 3.2) (Hafler et al. 2012). As we have shown during embryonic retinal development (E18) the majority of OLIG2 expressing cells also express OTX2, but OLIG2 is excluded from differentiated photoreceptors expressing CRX. Considering the critical role of *Otx2* in photoreceptor development and the co-localization of OTX2 and OLIG2 in photoreceptor precursors, this may suggest that OTX2 positively regulates *Olig2* expression in the developing retina. Therefore, our findings when combined with the OTX2 ChIP-seq data suggest that OTX2 may both negatively and positively regulate *Olig2* expression depending on the stage of photoreceptor development. In medulloblastoma, OTX2 has been shown to be critical in maintaining OTX2-bound promoters in a bivalent state where both activating and repressing

chromatin marks are present at gene promoters poising the gene for transcriptional activation or repression (Bunt et al. 2013). Bivalent promoters are widely observed in developmental genes in embryonic stem cells, where they are silenced to maintain pluripotency and then quickly activated during differentiation (Bernstein et al. 2006). Therefore, it is possible that during early retinogenesis, OTX2 may bind to *Olig2* and promote *Olig2* expression in photoreceptor precursors, but then during postnatal retinogenesis OTX2 binding restricts *Olig2* expression in mature photoreceptors to maintain photoreceptors in a differentiated state. In order to activate *Olig2* expression during early photoreceptor specification, perhaps OTX2 recruits and/or interacts with transcriptional co-activators at *Olig2* regulatory elements or promoters to drive *Olig2* expression in the photoreceptor precursors. To restrict *Olig2* expression in mature photoreceptors, OTX2 may recruit and/or interact with transcriptional co-repressors at *Olig2* regulatory elements in mature photoreceptors in order to maintain photoreceptors in a terminally differentiated state. Certainly transcription factors are capable of transcriptional regulation at the level of histone modifications. The Forkhead box (Fox) family are a well-known example of transcription factors with this ability (Wang et al. 2009, Wang, Wang, et al. 2014, Koo, Muir, and Lam 2012, Lam et al. 2013). Fox transcription factors can recruit the transcriptional activator CBP/p300 and chromatin remodelling proteins to responsive elements to promote gene expression, while conversely, Fox transcription factors can also recruit chromatin remodelling proteins that condense chromatin and silence gene expression (Lam et al. 2013). In the future, it would be of interest to carry out OTX2 ChIP on embryonic retinas to determine if OTX2 binding to *Olig2* is also observed in the embryonic retinas *in vivo*.

Despite the finding that OTX2 binds to the promoter of *Olig2 in vivo*, *Olig2* expression has not been identified in transcriptome analysis of *Otx2* conditional knockout retinas (Omori et al. 2011). However, it is worth noting that the transcriptome analysis of the *Otx2* conditional knockout retinas was examined utilizing a microarray (Omori et al. 2011). RNA-sequencing (RNA-seq) may be a more attractive approach to carry out transcriptome analysis of the *Otx2*

conditional knockout retina as this technology has a broader dynamic range, the ability to detect small amounts of transcript, and less technical limitations than microarray technology (Zhao et al. 2014). Therefore, by utilizing RNA-seq technology in the future, we may still determine that *Olig2* expression is reduced in the absence of *Otx2*, which we would be expected since photoreceptors are lost in *Otx2* knockout retinas.

3.3.3 Dlx2 regulates binary retinal cell fate decisions by restricting Olig2 expression

The few studies that have examined expression of *Olig2* in the retina demonstrate that *Olig2* is expressed in a subset of RPC (Nakamura et al. 2006, Shibasaki et al. 2007, Hafler et al. 2012). Lineage tracing has revealed that over 60% of photoreceptors are derived from RPC that express *Olig2* (Hafler et al. 2012). Our study revealed that *Olig2* is expressed in photoreceptor precursors expressing OTX2, but is absent from further differentiated (CRX positive) and mature photoreceptors, which suggests that *Olig2* is required for the specification of photoreceptors (Figure 3.4). Upregulation of *Olig2* expression in *Atoh7* null retinas further supported *Olig2* as a marker for photoreceptor precursors as cone photoreceptors increase at the expense of RGC in the absence of *Atoh7* expression (Figure 3.11) (Brown et al. 2001). While the expression of *Olig2* in photoreceptor precursors may indicate that *Olig2* is critical for photoreceptor specification but is dispensable for photoreceptor differentiation, this has yet to be explicitly demonstrated. *Olig2* knockout mice die shortly after they are born and lack motor neurons and oligodendrocytes (Lu et al. 2000, Takebayashi et al. 2000, Zhou, Wang, and Anderson 2000). The retinas of these mice have not been examined. Conditional *Olig2*-flox mice have also been generated (Yue et al. 2006). A retina-specific *Olig2* knockout generated by breeding *Olig2*-flox mice with RPC-specific *Cre* mice would be a useful tool to study *Olig2* function in the retina, as it would circumvent lethality thereby allowing for the study of postnatal photoreceptor development. We are also currently exploring *Olig2*-shRNA knockdowns and *Olig2* open reading frame gain of function in our laboratory using *in vitro* retinal explant models to determine the effect of *Olig2* loss and ectopic expression on

photoreceptor differentiation. Based on previous findings by others and our current results, we expect that loss of *Olig2* in RPC would lead to a significant reduction in photoreceptors. Conversely, we expect that ectopic expression of *Olig2* during early stages of retinal development will drive RPC to specify photoreceptors at the expense of early born retinal cell types. Because RGC were not generated from RPC with *Olig2* expression history (Hafler et al. 2012), it would be interesting to see if DLX2 expression and/or RGC genesis is increased in the *Olig2* knockout/knockdown retinas due to altered RPC competency to generate RGC in the absence of *Olig2* expression. *Dlx1* and *Dlx2* transcripts are increased in *Otx2* conditional knockout retinas and therefore may also be elevated in *Olig2* null retinas (Omori et al. 2011). If an increase in *Dlx2* expression/RGC genesis is observed, it may suggest a regulatory feedback loop whereby *Olig2* expression in RPC restricts RGC fate by restricting *Dlx2* expression, while *Dlx2* restricts *Olig2* expression and photoreceptor cell fate.

Based on our current, previous, and ongoing findings, we propose that *Dlx1*/*Dlx2* regulates binary cell fate decisions, promoting RGC differentiation and restricting photoreceptor development in part though the restriction of *Olig2* expression in RPC (Figure 3.14). Future studies will examine if *Olig2* is able to restrict RPC from adopting RGC fate by restricting expression of *Dlx1* and *Dlx2*. The absence of *Olig2*, *Otx2*, and *Crx* expression in cells ectopically expressing pCIG2-*Dlx2*-EGFP supports our model of *Dlx2* restricting photoreceptor gene expression; however, additional experiments where *Dlx2* is knocked down using shRNA will need to be carried out to determine if photoreceptor gene expression is de-repressed in the absence of *Dlx2* expression in RPC. We expect that knocking down *Dlx2* expression in RPC will result in upregulated expression of *Olig2*, *Otx2*, and *Crx*.

Contrary to our previous suggestions (de Melo et al. 2005), we have determined *Dlx2* is downstream of *Atoh7* in the hierarchy of RGC genesis. Recent *Atoh7* transcriptome analysis (Gao et al. 2014), combined with our DLX2 immunostaining on *Atoh7* null retina sections (Figure 3.12) led us to this conclusion. Our previous suggestion that *Dlx2* expressing RGC are

generated independently from *Atoh7* positive RPC was likely due to not having access to *Atoh7* null tissue to examine at the time of our previous publication, the lack of ATOH7 antibodies for double immunostaining experiments with DLX2, and the observation that *Dlx1*/*Dlx2* expressing cells are derived from RPC expressing *Vsx2* (de Melo et al. 2005). In addition to our finding that DLX2 expression is reduced in the *Atoh7* null retina, more recent studies have shown that *Atoh7* expression is upregulated in RPC that have recently reduced *Vsx2* expression (Vitorino et al. 2009, Jusuf et al. 2011), which demonstrates that a *Vsx2*/*Atoh7*/*Dlx2* expression history for RGC is a possibility. The loss of DLX2 in the E13 *Atoh7* null retina, but unchanged number of DLX2 expressing cells at later developmental stages (E16) suggests that *Dlx1*/*Dlx2* expression may be maintained by RGC transcription factors downstream of *Atoh7*. Indeed, while Brn3b and Isl1 positive cells are rarely observed in an *Atoh7* null retina at E13, by E17 a number of cells expressing Brn3b, Isl1, or both transcription factors are found in the GCL and could potentially upregulate *Dlx2* in the absence of *Atoh7* (Wu et al. 2015). Furthermore, ectopic expression of *Brn3b* and *Isl1* on a *Atoh7* null background are able to specify RGC fate and regulate RGC differentiation in the absence of *Atoh7* expression, lending support for the ability of these factors to drive *Dlx2* expression independent of *Atoh7* (Wu et al. 2015). Alternatively, the unchanged expression of DLX2 observed in the *Atoh7* null retina at E16 could possibly be due to elevated DLX2 positive amacrine cells (Wang et al. 2001).

Our previous work has shown that *Dlx1*/*Dlx2* contributes to RGC genesis and survival in part though promoting the expression of *Brn3b* and *TrkB*, respectively (de Melo et al. 2008, Zhang et al. 2017). In addition to *Dxl1*/*Dlx2*, *Brn3b* and *Isl1* are also critical factors for RGC genesis. Loss of *Brn3b* or *Isl1* results in ~80% RGC loss (Erkman et al. 1996, Gan et al. 1996, Mu et al. 2008, Pan et al. 2008), while *Dlx1*/*Dlx2* loss results in ~33% RGC loss (de Melo et al. 2005), demonstrating distinct genetic pathways utilized for RGC differentiation. There is also cooperation and cross-regulation between the RGC genetic regulatory pathways (Figure 3.14). *Brn3b* and *Isl1* share a number of genetic targets and compound mutants of *Brn3b*/*Isl1* lack 95%

of RGC (Mu et al. 2008, Pan et al. 2008). Triple mutants of *Dlx1*/*Dlx2*/*Brn3b* also have 95% RGC loss (Zhang et al. 2017). These findings further demonstrate that despite substantial RGC loss in compound mutants, maintained RGC genesis in these mutants shows additional genetic pathways can promote RGC development. It has been shown that *Brn3b* and *Isl1* also regulate distinct, non-overlapping gene targets in RGC development (Mu et al. 2008). It would be of great interest to carry out DLX2 ChIP-sequencing, coupled with RNA-sequencing, to examine the overlapping and distinct genetic targets of DLX2, which we could then compare to Brn3b and Isl1 to further define the genetic network of RGC development.

The cross-regulation and co-expression of combinations of transcription factors involved in RGC development are likely required for the specification of distinct RGC subtypes during retinal development. There are currently 25 known RGC subtypes that differ based on molecular, physiological, and morphological criteria (Sanes and Masland 2015). However, unlike bipolar cell development where a great deal is known about the transcription factors which define bipolar cell subtypes (Cheng et al. 2005, Chow et al. 2004, Shi et al. 2011, Star et al. 2012), little is known regarding the molecular criteria that specify RGC subtypes. *Brn3b* null retinas transiently upregulate *Dlx1* and *Dlx2* expression, suggesting Brn3b restricts *Dlx1*/*Dlx2* expression during retinal development, but not through direct protein-DNA interactions (Mu et al. 2004, Zhang et al. 2017). This may suggest that RGC subtypes exist where BRN3B restricts the expression of *Dlx1*/*Dlx2* in that subtype, while additional subtypes required the coordinated expression of both *Brn3b* and *Dlx1*/*Dlx2*. In addition, the distinct genetic targets of Isl1 and Brn3b may promote specification of distinct RGC subtypes, while combined expression of *Brn3b*/*Isl1* could specify alternative subtypes. Certainly, the specification of distinct RGC subtypes is very complex and further studies utilizing lineage tracing of *Dlx1*/*Dlx2*, *Brn3b* and *Isl1* expressing RGC populations will need to be performed. Furthermore, utilizing known criteria for RGC subtype specification, including neurotransmitters expressed, stratification, and morphology, specific retina knockouts of *Dlx1*/*Dlx2*, *Brn3b*, and *Isl1* will need to examined to

evaluate specific RGC subtypes that are lost upon genetic deletion. These studies will contribute much needed knowledge regarding the molecular criteria required for RGC subtype specification.

Taken together, we propose that *Dlx2* is downstream of *Atoh7* in the RGC gene regulatory network, where cross regulation occurs between *Dlx2* and other RGC transcription factors including *Brn3b* (Figure 3.14). *Dlx1*/*Dlx2* expression also inhibits RPC from adopting an alternative photoreceptor fate by restricting expression of *Olig2*, while reciprocal repression of *Dlx1*/*Dlx2* may occur in *Otx2* positive photoreceptor precursors to restrict cells from acquiring RGC identities.

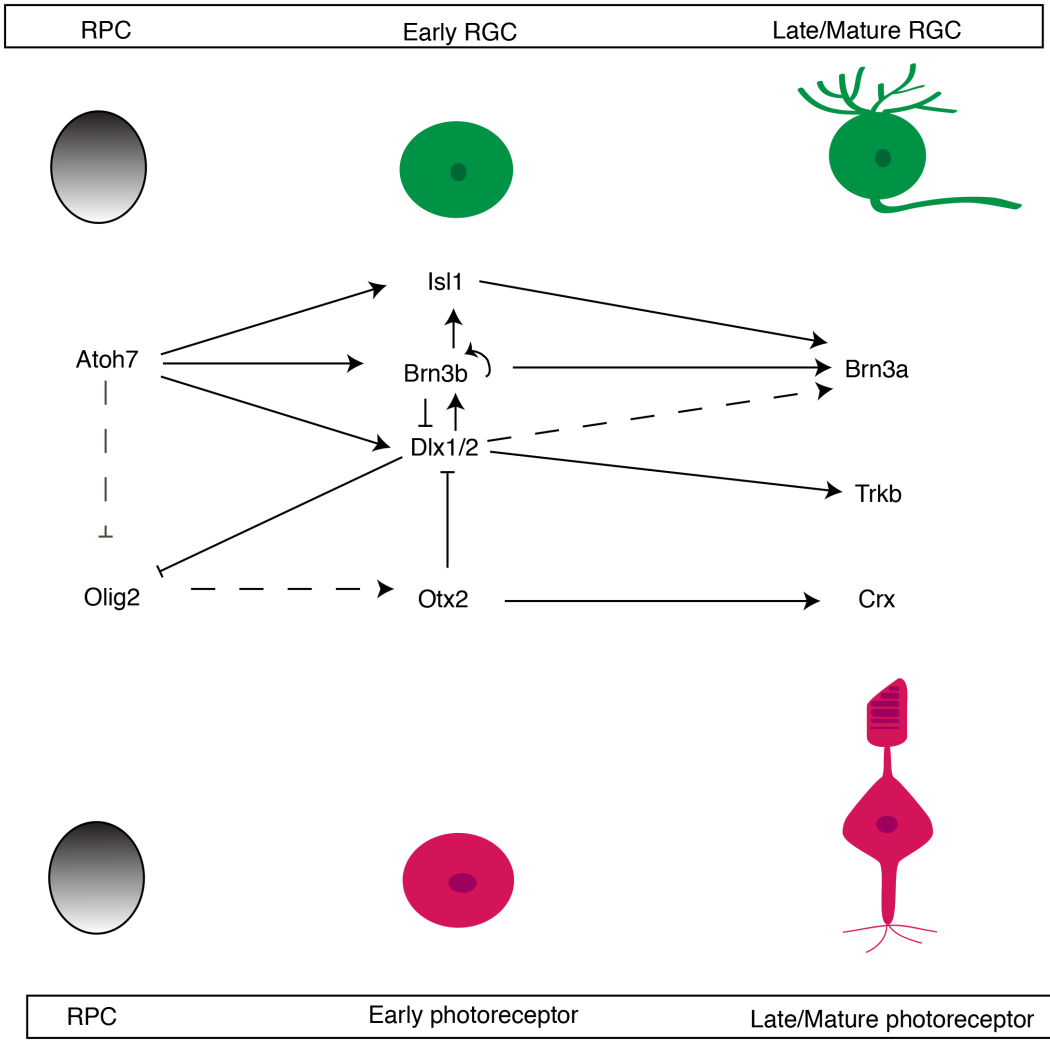
RPC
Early RGC
Late/Mature RGC
Isl1
Atoh7
Brn3b
Brn3a
Dlx1/2
Trkb
Olig2
Otx2
Crx
RPC
Early photoreceptor
Late/Mature photoreceptor

Figure 3.14 Proposed model of *Dlx1/Dlx2* regulation of retinal cell fate.

We propose that *Dlx1/Dlx2* is playing a central role in regulating binary retinal cell fate decisions. Early expression of *Atoh7* enables RPC to become competent to specify RGC fate. A number of critical intrinsic factors including *Dlx1/Dlx2*, *Brn3b*, and *Isl1* are upregulated to promote RGC differentiation and survival by driving the expression of genes required for RGC differentiation and survival including *Brn3a* and *TrkB*. In the absence of *Atoh7*, expression of *Dlx1/Dlx2*, *Brn3b*, and *Isl1* is significantly reduced and RGC are lost, while cone and amacrine cell genesis increases at the expense of RGC. *Olig2* expression is elevated in *Atoh7* mutants, suggesting *Atoh7* restricts *Olig2* expression, and the promotion of cone genesis in RPC fated to generate RGC. In RGC differentiation, cross regulation of transcription factors occurs, including *Dlx1/Dlx2* promoting *Brn3b* expression, and *Brn3b* restricting *Dlx1/Dlx2* expression, which perhaps indicates the differentiation of RGC subtypes governed by varied expression of transcription factors involved in RGC differentiation (Zhang et al. 2017). Further studies, as detailed above, will need to be performed to understand the complexities of RGC subtype specification driven by combined expression of these transcription factors In addition to promoting RGC differentiation and survival, *Dlx1/Dlx2* may inhibit RPC from adopting photoreceptor cell fate by restricting expression of *Olig2*. *Otx2* knockout data support *Otx2* restriction of the expression of *Dlx1/Dlx2*, suggesting that reciprocal repression occurs between *Dlx1/Dlx2* and *Otx2* where *Otx2* promotes photoreceptor cell fate over RGC fate by inhibiting *Dlx1/Dlx2* expression in postmitotic OTX2-positive precursors (Omori et al. 2011). OLIG2 and OTX2 are co-expressed in photoreceptor precursors. Therefore, OLIG2 may also drive OTX2 expression in postmitotic photoreceptor precursors and will need to be evaluated in *Olig2* mutant models. Dotted lines indicate hypothesized regulation while solid lines indicate studied/published regulatory interactions.

3.3.4 Background strain significantly affects photoreceptor differentiation in the absence of Dlx1/Dlx2 expression

There are numerous articles that describe the substantial influence of the mouse genetic background strain in expressivity, phenotype variability, and penetrance. The first instances of strain-related difference were documented two decades ago with several knockout models. In keratin-8 knockout animals, the phenotype ranges from mid-gestational lethality on one genetic background, to colorectal hyperplasia during adulthood on a different genetic background (Baribault et al. 1993, Doetschman 2009). Another example is the *Tgfβ1* knockout. *Tgfβ1* null mutations in inbred animals are lethal at the preimplantation stage (Bonyadi et al. 1997, Kallapur, Ormsby, and Doetschman 1999, Doetschman 2009). On mixed genetic backgrounds however, *Tgfβ1* null mice are variably penetrant with survival to birth ranging from 0-80% depending on the mixed background. Unsurprisingly, genetic background has also been shown to significantly influence the phenotypes observed in the murine retina. For example, the disease phenotypes of the retinal degeneration mouse model (*Nr2e3*$^{rd7/rd7}$) and the ocular retardation model (*Chx10*$^{or\text{-}J}$) are significantly impacted by the genetic background (Akhmedov et al. 2000, Haider et al. 2008, Wong, Conger, and Burmeister 2006). A study by Jelcick and colleagues examined gene expression in the retinas of normal WT mice from four different genetic backgrounds (Jelcick et al. 2011). Over 3000 genes were variably expressed in the retinas of these mice, which included genes associated with retinal and photoreceptor development, and genes associated with retinal diseases including *Foxc1* and *Vsx1*. In our studies, *Dlx1*/*Dlx2* DKO mice from two different genetic backgrounds were utilized. *Dlx1*/*Dlx2* DKO retinas on a mixed CD-1;C57BL/6 had ectopic expression of OLIG2 in the GCL (Figure 3.8) while qRT-PCR carried out on the *Dlx1*/*Dlx2* DKO CD-1 mice showed no change in photoreceptor gene expression in the absence of *Dxl1*/*Dlx2* (Figure 3.8, Figure 3.13). In addition, OLIG2 immunostaining on DKO retinal sections from the CD-1 background showed no change in OLIG2 expression. It is worthwhile noting that previous *Crx* ISH carried out in our

laboratory previously were performed on *Dlx1*/*Dlx2* DKO retinas from mice maintained on a CD-1;C57BL/6 mixed genetic background. These *Dlx1*/*Dlx2* DKO mice had elevated expression of *Crx* in the NBL compared to controls, and were the basis for our hypothesis that *Dlx1*/*Dlx2* restricts photoreceptor cell fate (de Melo et al. 2005) (Qi Zhang, unpublished observations). It is therefore plausible that no change was observed in *Olig2* and *Crx* expression in the *Dlx1*/*Dlx2* DKO CD-1 retina as measured by qRT-PCR due to the differences in genetic background. Preliminary qRT-PCR experiments on *Dlx1*/*Dlx2* DKO mice on a mixed CD-1;C57Bl/6 background and the immunostaining results for OLIG2 in the *Dlx1/Dlx2* DKO support the conclusion that the genetic background is critical for *Olig2* expression in the absence of *Dlx1*/*Dlx2*. (Figure 3.13). In future studies, examination of amacrine cell genesis in the absence of *Dlx1*/*Dlx2* could also be considered. In addition to photoreceptors, RPC that express *Olig2* generate amacrine cells (Hafler et al. 2012). Certainly, the expression pattern of OLIG2 in the GCL and the inner NBL of the CD-1;C57Bl/6 *Dlx1*/*Dlx2* DKO retina resembles the expression pattern of amacrine cells (Figure 3.8). Therefore, in the absence of *Dlx1*/*Dlx2* on a CD-1;C57Bl/6 background, perhaps RPC that were fated to generate RGC now upregulate *Olig2* and generate amacrine cells, which are also produced in temporally overlapping windows with RGC (Young 1985). Co-expression analysis of OLIG2 and PAX6 in the CD-1;C57Bl/6 *Dlx1*/*Dlx2* DKO retina could be carried out to determine if these OLIG2 expressing cells are in fact amacrine cells. While increased amacrine cell genesis was not previously observed in the *Dlx1*/*Dlx2* DKO retina (de Melo et al. 2005, Zhang et al. 2017), *Dlx1*/*Dlx2* DKO die at P0 and perhaps amacrine cell genesis would increase postnatally. Examination of *Olig2* expression and amacrine cell genesis the *Dlx1*/*Dlx2* conditional knockout (Silbereis et al. 2014) mouse retina would help us answer this question. We have also observed that a *Dlx1*/*Dlx2*/*Brn3b* triple knockout retina had a near complete loss of RGC and increased amacrine cells in the GCL compared to controls, suggesting that cells fated to generate RGC in the absence of *Dlx1*/*Dlx2*/*Brn3b* undergo apoptosis or adopt amacrine cells fates, highlighting a complex role for *Dlx1*/*Dlx2* and *Brn3b* in early retinal cell

fate differentiation (Zhang et al. 2017). Additional photoreceptor marker staining in the CD-1;C57Bl/6 retina in the absence of *Dlx1*/*Dlx2*, including OTX2 and CRX in addition to repetition of OLIG2 staining, are ongoing in our laboratory to further evaluate a possible increase in photoreceptor genesis in the *Dlx1*/*Dlx2* null retina.

One of the key differences between the CD-1 and C57Bl/6 mice is the presence of a pigmented RPE. The C57Bl/6 mice have a pigmented RPE while CD-1 mice are albino and lack melanin in the RPE. Certainly, the location of the RPE in relation to the neural retina may suggest that there are cellular interactions between these two tissues that could influence the development of neural retina. Recent studies have begun examining the effect of RPE pigmentation on RPE cellular morphology and cellular communication and how these factors could potentially contribute to neural retina differentiation (Iwai-Takekoshi et al. 2016, Bhansali et al. 2014). Given our findings, it will be critical to utilize mouse models maintained on a mixed genetic background for the study of photoreceptor development in the absence of *Dlx1/Dlx2*. Importantly, future directions in our laboratory include the examination of a *Dlx1*/*Dlx2* and/or *Dlx2* conditional knockout mouse to study the role of *Dlx2* in postnatal retinal development and retinal function. Because of the impact genetic background has on gene expression, it will be important to keep this in mind when comparing data collected from the conditional *Dlx1*/*Dlx2* and *Dlx2* knockout to the *Dlx1/Dlx2* DKO as the conditional knockout may be on a mixed background after crossing the *Dlx1/Dlx2*-flox and *Dlx2*-flox animals to RPC-specific *Cre* drivers. We have secured *Dkk3*-Cre mice to excise *Dlx* genes specifically in RPC and these mice are maintained on a C57Bl/6 background.

CHAPTER 4: REGULATION OF NEURAL DIFFERENTIATION IN THE DEVELOPING CENTRAL NERVOUS SYSTEM THROUGH TRANSCRIPTIONAL REGULATION OF P107

4 Chapter 4. Regulation of neural differentiation in the developing central nervous system though transcriptional regulation of *p107*

4.1 Introduction

4.1.1 Expression and function of Dlx genes in forebrain development

The vertebrate prosencephalon or forebrain, similar to the retina, arises from the anterior neural ectoderm. The forebrain can be divided into two distinct anatomical structures, the telencephalon, which gives rise to the cortex and subpallium, and the diencephalon giving rise to the prethalamus, thalamus, and the pretectum (Rubenstein and Beachy 1998, Wilson and Houart 2004). The *Dlx* genes are highly expressed in the subpallium during early forebrain development. There are four (out of a total of six) *Dlx* genes expressed in the subpallium with overlapping expression patterns in the ganglionic eminences (GE) structures, which include the medial and lateral ganglionic eminences (MGE and LGE, respectively) (Figure 4.1). Interneurons generated in the MGE primarily migrate to the cortex and striatum, while the interneurons born in the LGE primarily populate the olfactory bulbs (Anderson et al. 2001). *Dlx2* is highly expressed in the highly proliferative subventricular zone (SVZ) and ventricular zone (VZ) of the GE (Panganiban and Rubenstein 2002, Eisenstat et al. 1999). *Dlx1* has a similar expression pattern but with fewer cells expressing *Dlx1* in the VZ compared to *Dlx2*. *Dlx5* and *Dlx6* are also expressed in the SVZ, but are more highly expressed in differentiated cells in the mantle zone (Figure 4.1). In vertebrate systems, *Dlx1* and *Dlx2* have been primarily studied for their role in the development of the forebrain. While *Dlx1* and *Dlx2* single knockouts die at birth they have very subtle forebrain defects, suggesting that partial redundancy exists between the convergent *Dlx* gene pair (Anderson, Qiu, et al. 1997, Eisenstat et al. 1999). The overlapping temporal domains of *Dlx* gene expression are further evidence of their redundant role in forebrain development. Therefore, in order to characterize the function of *Dlx* genes in the

developing forebrain, DKO mutants of *Dlx1*/*Dlx2* were generated and subsequently analyzed. *Dlx1*/*Dlx2* DKO mutants also die at birth but have significant defects in interneuron differentiation and migration (Anderson, Eisenstat, et al. 1997, Anderson, Qiu, et al. 1997). *Dlx1*/*Dlx2* expression is observed in nearly all interneurons utilizing the inhibitory γ-amino butyric acid (GABA) neurotransmitter (Stuhmer, Puelles, et al. 2002). In addition, *Dlx* drives expression of glutamic acid decarboxylase (Gad) genes, which are critical for GABA biosynthesis (Stuhmer, Anderson, et al. 2002). Differentiation and tangential migration of GABAergic interneurons born in the subpallium is impaired in the *Dlx1*/*Dlx2* DKO (Anderson, Eisenstat, et al. 1997, Anderson, Qiu, et al. 1997). Failed differentiation of GABAergic interneurons may be partially due to a lack of *Gad* upregulation. The Notch pathway has also been implicated in the failure of GABAergic interneurons to differentiate in the *Dlx1*/*Dlx2* DKO forebrain (Yun et al. 2002) and will be explored further in this study. Failed tangential migration of interneurons is partially due to increased response of the *Dlx1*/*Dlx2* DKO interneurons to the Semaphorin (Sema) 3 repulsive guidance ligands that are expressed in the striatum of developing forebrains (Le et al. 2007). DLX2 binds to and restricts the expression of *Nrp2* in the developing forebrain (Le et al. 2007). The lack of *Dlx1*/*Dlx2* expression in GABAergic interneurons results in a failure to inhibit expression of *Nrp2*, which thereby allows NRP2+ receptors to bind Sema3 ligands in the striatum and promote repulsive axonal guidance signalling through interaction with Plexin (He and Tessier-Lavigne 1997).

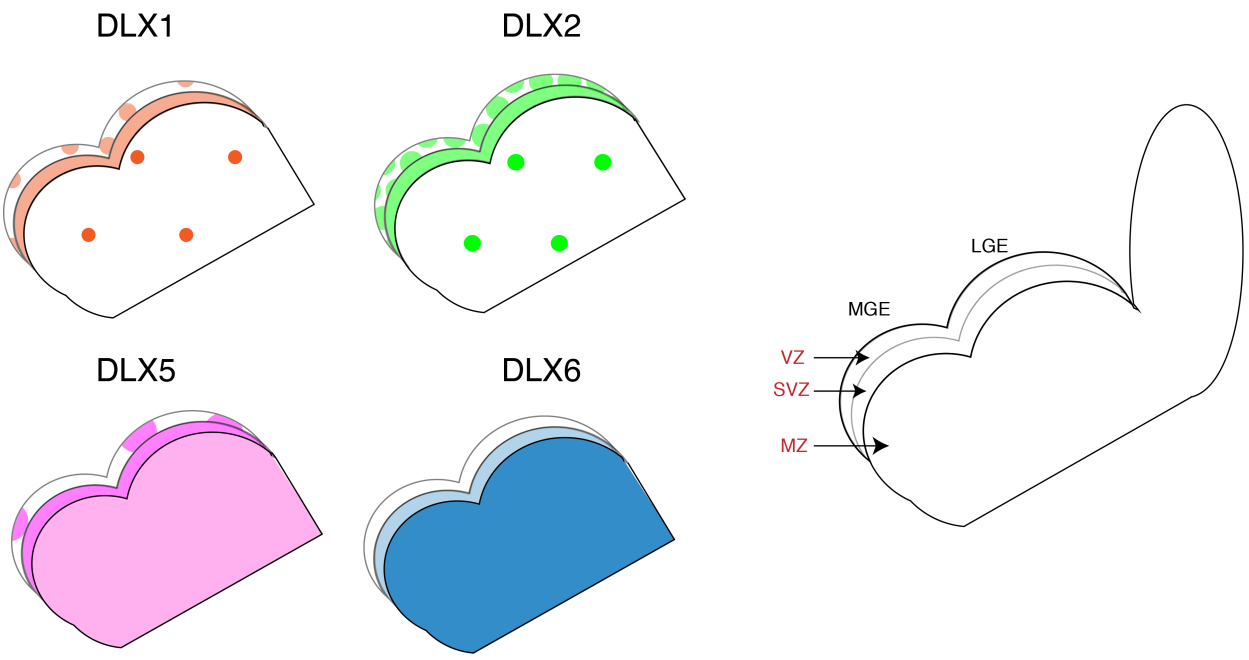

Figure 4.1 Expression pattern of *Dlx* genes in the subpallium.

The *Dlx* genes are expressed in overlapping domains in the GE of the ventrally localized subpallium. *Dlx2* is highly expressed in progenitors in the SVZ (solid green), a number of cells of the VZ (tightly clustered green polka dots), and a few scattered cells in the MZ (sparse green polka dots). *Dlx1* expression resembles that of *Dlx2* where *Dlx1* is highly expressed in the SVZ (solid orange) and few cells in the VZ. Fewer *Dlx1* expressing cells are present in the VZ compared to *Dlx2* (clustered orange dots, less than that observed for *Dlx2*). *Dlx5* expression is present in both the SVZ (solid dark pink) and in few VZ cells (sparse pink dots), but also at decreased levels in the differentiated cells of the MZ (solid light pink). *Dlx6* is primarily expressed in the MZ (solid dark blue), expressed at lower levels in the SVZ (light blue), and absent from the VZ.

[LGE; lateral ganglionic eminence, MGE; medial ganglionic eminence, MZ; mantle zone, SVZ; subventricular zone, VZ; ventricular zone]

4.1.2 Retinoblastoma family

The retinoblastoma protein (Rb), p107, and p130 (also referred to as retinoblastoma-like (Rbl) 1 and Rbl2, respectively) are the members of the pocket protein family colloquially referred to as the retinoblastoma protein family. They are so named due to the presence of a bipartite "pocket" through which they interact with members of the E2F transcription factor family (Classon and Dyson 2001). The retinoblastoma protein family members have been primarily investigated for their role in the cell cycle where they negatively regulate transition of G1 to S phase by restricting the E2F transcription factors from upregulating expression of genes required for DNA replication and S-phase progression, and/or by recruiting repressor E2F and chromatin remodelling proteins to genes required for DNA replication and S-phase progression (Cao et al. 1992, Zhu et al. 1993, Chellappan et al. 1991, Classon and Dyson 2001). *Rb* was discovered over three decades ago as the first tumour suppressor gene, which when mutated leads to the formation of the intraocular cancer Retinoblastoma for which the gene was named (Dryja, Friend, and Weinberg 1986, Friend et al. 1986, Lee et al. 1987). More recently, the retinoblastoma family has been shown to participate in neuronal differentiation and maturation, and transcriptional control of non-cell cycle target genes (Andrusiak et al. 2011, Ghanem et al. 2012, McClellan et al. 2007, McClellan and Slack 2006, Naser et al. 2016, Vanderluit et al. 2007). Elevated repressor E2F in the *Rb* null brain restricts expression of *Dlx1/Dlx2* via the I12b intergenic enhancer, leading to severe disruptions in the differentiation and migration of interneurons (Ghanem et al. 2012). *Rb* null brains also have elevated expression of the repulsive guidance molecule neogenin (Andrusiak et al. 2011, McClellan et al. 2007). Neuronal migration is impaired upon elevation of neogenin due to increased interaction with the negative guidance ligand netrin-1 (Andrusiak et al. 2011, Le et al. 2007). In addition to Rb, P107 has also been shown to be involved in neural differentiation (Vanderluit et al. 2004, Vanderluit et al. 2007). *P107* deletion in the developing cortex results in elevated expression of *Hes1*, which consequently leads to expansion of the progenitor pool and reduction in the number of mature

cortical neurons (Vanderluit et al. 2007). In addition, P107 represses *Hes1* expression in reporter gene assays (Vanderluit et al. 2007).

We sought to identify DLX2 target genes that could contribute to the differentiation defect observed in the *Dlx1*/*Dlx2* forebrain. Upon analysis of the transcriptional targets of DLX2 following a ChIP-chip assay we discovered *p107* as a putative target of DLX2 in the developing forebrain. Because of the previously identified role of p107 in restricting Notch signalling, we hypothesized that DLX2 regulates the transcription of *p107* to promote neural differentiation in the developing forebrain through control of Notch signalling.

4.2 Results

4.2.1 Identification and characterization of p107 as a transcriptional target for DLX2

We were interested in identifying DLX2 target genes that could contribute to the decreased differentiation of GABAergic interneurons observed in the developing *Dlx1*/*Dlx2* DKO forebrain. Chromatin enriched from DLX2 forebrain ChIP was used to hybridize a CpG island microarray (DLX2 ChIP-chip) to identify target genes potentially regulated by DLX2. CpG islands are indicative of transcriptional initiation sites and are associated with many annotated developmental regulatory gene promoters (Deaton and Bird 2011, Saxonov, Berg, and Brutlag 2006, Larsen et al. 1992). A number of putative downstream DLX2 targets were identified in the DLX2 ChIP-chip (Table 4). Among the targets identified, *p107* has previously been associated with the regulation of Notch signalling (Vanderluit et al. 2007). *In situ* hybridization experiments have previously demonstrated an increase in Notch signalling in the *Dlx1*/*Dlx2* DKO forebrain (Yun et al. 2002). Notch is a well-known pathway that promotes self-renewal of neural progenitors and restricts neural differentiation (Artavanis-Tsakonas, Rand, and Lake 1999, Gaiano and Fishell 2002, Selkoe and Kopan 2003). The downstream effectors of Notch signalling are bHLH transcription factors from the Hes family, which include *Hes1* and *Hes5*. Hes transcription factors inhibit the expression of pro-neural genes including *Ascl1* and

Neurogenin2 to restrict neuronal differentiation (Hatakeyama et al. 2004, Ishibashi et al. 1994, Ohtsuka et al. 1999). Interestingly, however, Notch pathway genes were not identified in the ChIP-chip as transcriptional targets of DLX2 suggesting that DLX2 may regulate Notch signalling indirectly. Based on the previous studies detailing the role of *p107* in the regulation of Notch signalling combined with the observation that Notch pathway gene expression (*Hes5* and *Dll1*, specifically) is elevated in *Dlx1*/*Dlx2* DKO brains *in situ*, we postulated that *Dlx1*/*Dlx2* promotes expression of *p107*, which subsequently regulates Notch signalling. We have previously validated *p107* as a transcriptional target of DLX2 in both the developing retina and forebrain *in vivo* and determined that DLX2 was associated with chromatin at two sites in *p107* regulatory region, which we termed *p107*-R1 and *p107*-R8 (Zagozewski, et al., prepared for *J Biol Chem*, J Zagozewski MSc thesis, 2011). In our previous study, we also confirmed that rDLX2 bound directly to the *p107*-R1 and *p107*-R8 chromatin elements *in vitro*. Taken together, we have determined that *p107* is a direct transcriptional target of DLX2 in the developing forebrain.

Table 4: Putative DLX2 transcriptional targets in the E13 forebrain

Putative transcriptional targets of DLX2					
Als2cr7	*Anxa5*	*Arhgef15*	*AY705449*	*B3gnt1*	*BC026682*
Cct4	*Centb2*	*Cog8*	*Commd1*	*Copa*	*Cpxm1*
Cpz	*Crispld1*	*Cxcr4*	*Cxxc1*	*Cygb*	*Ear1*
Ebf4	*Fabp5*	*Fzd7*	*Gal3st1*	*Gna14*	*Gnaq*
Gpr103	*Gramd2*	*Gtf2e2*	*Hspb8*	*Idh3b*	*Irx1*
Irx2	*Nefl*	*Odf4*	*Pcdha4*	*Pmp2*	***Rbl1 (p107)***
Sox5	*Tbl2*	*Tmed6*	*Ttc4*	*Wdr42a*	*Znrf4*

4.2.2 TAAT/ATTA homeodomain binding motifs in p107 regulatory elements are critical for DLX2 binding in vitro

We have previously confirmed that DLX2 directly binds to *p107* regulatory elements *in vitro* (Zagozewski et al., prepared for J Biol Chem, J Zagozewski MSc thesis). These elements were referred to as *p107*-R1 and *p107*-R8. *P107*-R1 is located distally to the *p107* transcriptional start site while *p107*-R8 is located proximal to the transcriptional start (Figure 4.2A). To confirm that direct binding of rDLX2 was specific to putative DLX2 (homeodomain) binding motifs (ATTA/TAAT) identified in the ChIP-positive *p107* regulatory elements, we deleted these motifs and repeated EMSA to determine if direct binding to labelled probes was lost. *P107*-R1 contains one putative DLX2 binding site, which was deleted using PCR-based methods (Lee et al. 2010). *P107*-R8 contains three putative DLX2 binding sites (Figure 4.2A, site most distal to the transcription start site indicated with superscript number 1 while the more proximal site indicated with superscript number 3) and therefore a number of deletion mutants of *p107*-R8 were generated. We deleted each site individually (single deletions), a combination of two sites (double deletion), and all three putative sites (triple deletion). As was done with WT probes described for *Olig2* experiments described in Chapter 3, the mutant probes with ATTA/TAAT sites deleted were radiolabelled, incubated with rDLX2, and resolved on a non-denaturing polyacrylamide gel. Deletion of the lone site in *p107*-R1 reduced the binding of rDLX2 compared to WT probe control (Figure 4.2B). In *p107*-R8 single deletions, deletion of the most distal (distal to the transcription start site of *p107*) putative DLX2 binding site (mA in Figure 4.2C) did not affect binding of rDLX2 compared to WT controls (Figure 4.2C). Deletion of the central (mB) or proximal DLX2 binding site in *p107*-R8 (mC) reduced rDLX2 binding to labelled probes (Figure 4.2C). Double deletions also reduced rDLX2 binding (mD-mF), with deletion of the central and proximal binding site having the greatest influence on rDLX2 binding (mF) (Figure 4.2C) Deletion of all three putative DLX2 binding sites (triple deletion) resulted in the most significant loss of rDLX2 binding to *p107*-R8 (Figure 4.2C). These findings confirm that binding

of rDLX2 to *p107* probes occurs through ATTA/TAAT motifs present in the *p107* regulatory elements, *in vitro*. Our findings also potentially eliminate the most distal TAAT motif in *p107*-R8 as a DLX2 binding motif. All transcription factors containing a homeodomain recognize core ATTA/TAAT motifs, which are frequently found in the genome. Therefore, it is unsurprising that not all ATTA/TAAT motifs identified in the *p107* regulatory region are recognized by DLX2.

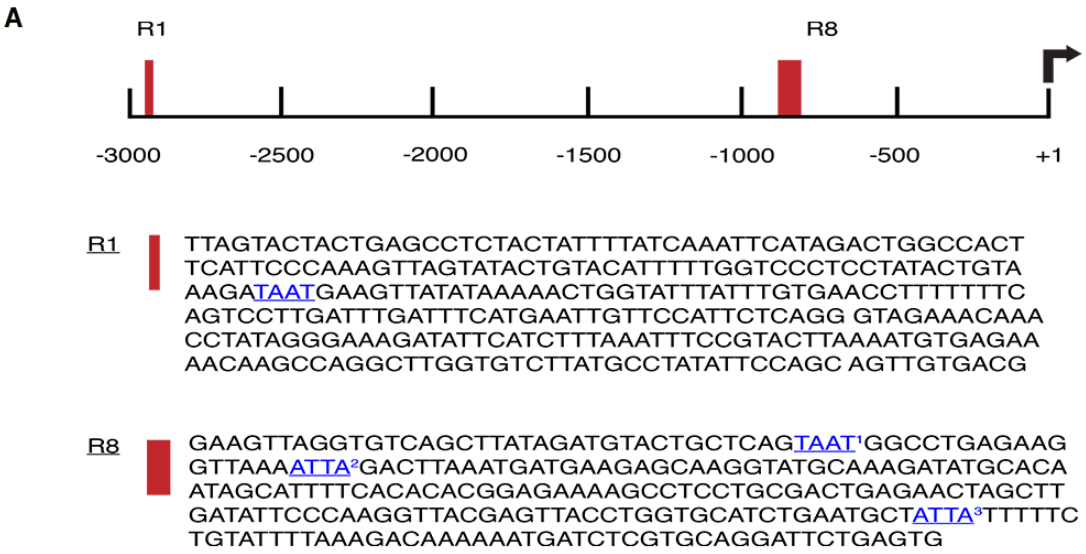
A
R1
R8
-3000
-2500
-2000
-1500
-1000
-500
+1
R1
TTAGTACTACTGAGCCTCTACTATTTTATCAAATTCATAGACTGGCCACT
TCATTCCCAAAGTTAGTATACTGTACATTTTTGGTCCCTCCTATACTGTA
AAGATAATGAAGTTATATAAAAACTGGTATTTATTTGTGAACCTTTTTTTC
AGTCCTTGATTTGATTTCATGAATTGTTCCATTCTCAGG GTAGAAACAAA
CCTATAGGGAAAGATATTCATCTTTAAATTTCCGTACTTAAAATGTGAGAA
AACAAGCCAGGCTTGGTGTCTTATGCCTATATTCCAGC AGTTGTGACG
R8
GAAGTTAGGTGTCAGCTTATAGATGTACTGCTCAGTAAT1GGCCTGAGAAG
GTTAAAATTA2GACTTAAATGATGAAGAGCAAGGTATGCAAAGATATGCACA
ATAGCATTTTCACACACGGAGAAAAGCCTCCTGCGACTGAGAACTAGCTT
GATATTCCCAAGGTTACGAGTTACCTGGTGCATCTGAATGCTATTA3TTTTTC
TGTATTTTAAAGACAAAAAATGATCTCGTGCAGGATTCTGAGTG

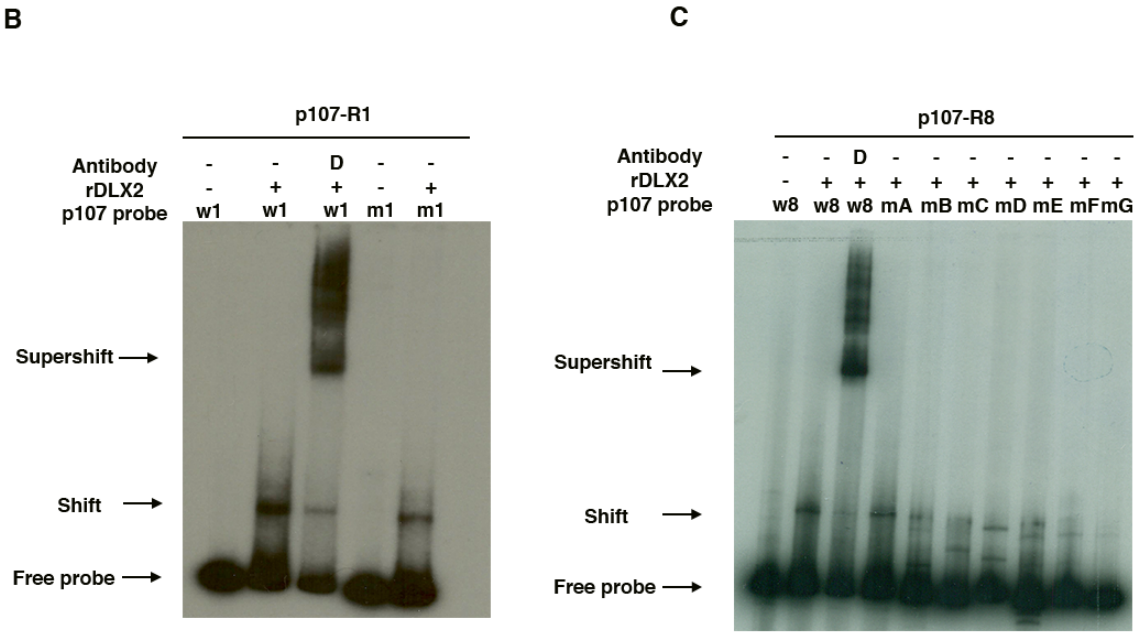
B
p107-R1
Antibody
rDLX2
p107 probe
- - D - -
- + + - +
w1 w1 w1 m1 m1
Supershift
Shift
Free probe
C
p107-R8
Antibody
rDLX2
p107 probe
- - D - - - - - - -
- + + + + + + + + +
w8 w8 w8 mA mB mC mD mE mF mG
Supershift
Shift
Free probe

Figure 4.2 Several ATTA/TAAT homeodomain binding motifs are critical for DLX2 binding to *p107 in vitro*.

(A) p107 is directly regulated by DLX2 at *p107*-R1 and *p107*-R8 elements located in the *p107* regulatory region upstream of the *p107* transcriptional start site (+1). *P107*-R1 contains one putative DLX2 binding site (highlighted in blue) while *p107*-R8 contains three putative DLX2 binding sites (highlighted in blue). (B) rDLX2 binds to the *p107*-R1 WT labelled probe (w1) *in vitro* (compare lane 1 to lane 2). Addition of a DLX2 antibody to the rDLX2/w1 probe binding reaction results in a supershifted band (lane 3). Deletion of the DLX2 binding motif creating a deletion probe (m1) reduced binding of rDLX2 to labelled mutant probes (compare lane 2 to lane 5). (C) rDLX2 binds to WT *p107*-R8 labelled probe (w8) *in vitro* (compare lane 1 to lane 2). Addition of a DLX2 antibody to the rDLX2/w8 probe binding reaction results in a supershifted band (lane 3). Deletion of the most distal binding site in p107-R8 (mA) did not affect rDLX2 binding to p107-R8 (compare w8, lane 2 to mA, lane 4). Single deletions of the central and proximal putative DLX2 binding motifs reduced binding to *p107*-R8 (compare w8, lane 2 with mB and mC, lane 5 and lane 6, respectively). Deletion of two putative DLX2 binding sites further reduced rDLX2 binding (mD, mE, mF in lanes 7, 8, and 9, respectively). The most dramatic reduction in rDLX2 binding to *p107*-R8 was observed when all three (triple deletion) DLX2 binding sites were deleted (compare w8, lane 2 with mG, lane 10). The presence of multiple bands may indicate the formation of DLX2 monomers and dimers (Diamond et al. 2006).

4.2.3 p107 expression is reduced in the SVZ of Dlx1/Dlx2 DKO forebrains

We have established that *p107* is a transcriptional target for DLX2 in the developing forebrain, as well as the developing retina *in vivo*. We then sought to determine the functional consequence of DLX2 binding to p107 both *in vivo* and *in vitro*. First, we examined the expression of DLX2 in the WT E13 GE. As has been demonstrated in previous studies, DLX2 is highly expressed in the SVZ and less so in the VZ in the MGE and LGE of the basal telencephalon (Figure 4.3A) (Anderson, Eisenstat, et al. 1997, Anderson, Qiu, et al. 1997, Eisenstat et al. 1999, Le et al. 2007). P107 expression was observed in the SVZ and VZ of the MGE, and the VZ of the LGE in the WT forebrain (Figure 4.3B). In the absence of *Dlx1*/*Dlx2*, P107 expression is specifically reduced in the SVZ of the MGE (Figure 4.3C). We next carried out luciferase reporter gene assays to determine the transcriptional consequence of DLX2 binding to *p107* regulatory elements *in vitro*. We cloned 4 kb of the *p107* regulatory region upstream of the transcriptional start site into luciferase reporter vectors, and co-transfected these vectors along with *Dlx2* expression plasmids into HEK293 cells. Upon co-transfection, we observed a significant increase in luciferase expression compared to empty vector controls *in vitro* (Figure 4.3D). We then utilized qRT-PCR to quantify changes in *p107* transcript in the GE of E13 *Dlx1*/*Dlx2* DKO GE. We observed a significant ~30% reduction in *p107* expression in the *Dlx1*/*Dlx2* DKO GE compared to WT controls (Figure 4.3E). These results demonstrate that DLX2 is a transcriptional activator of *p107* expression in the developing forebrain.

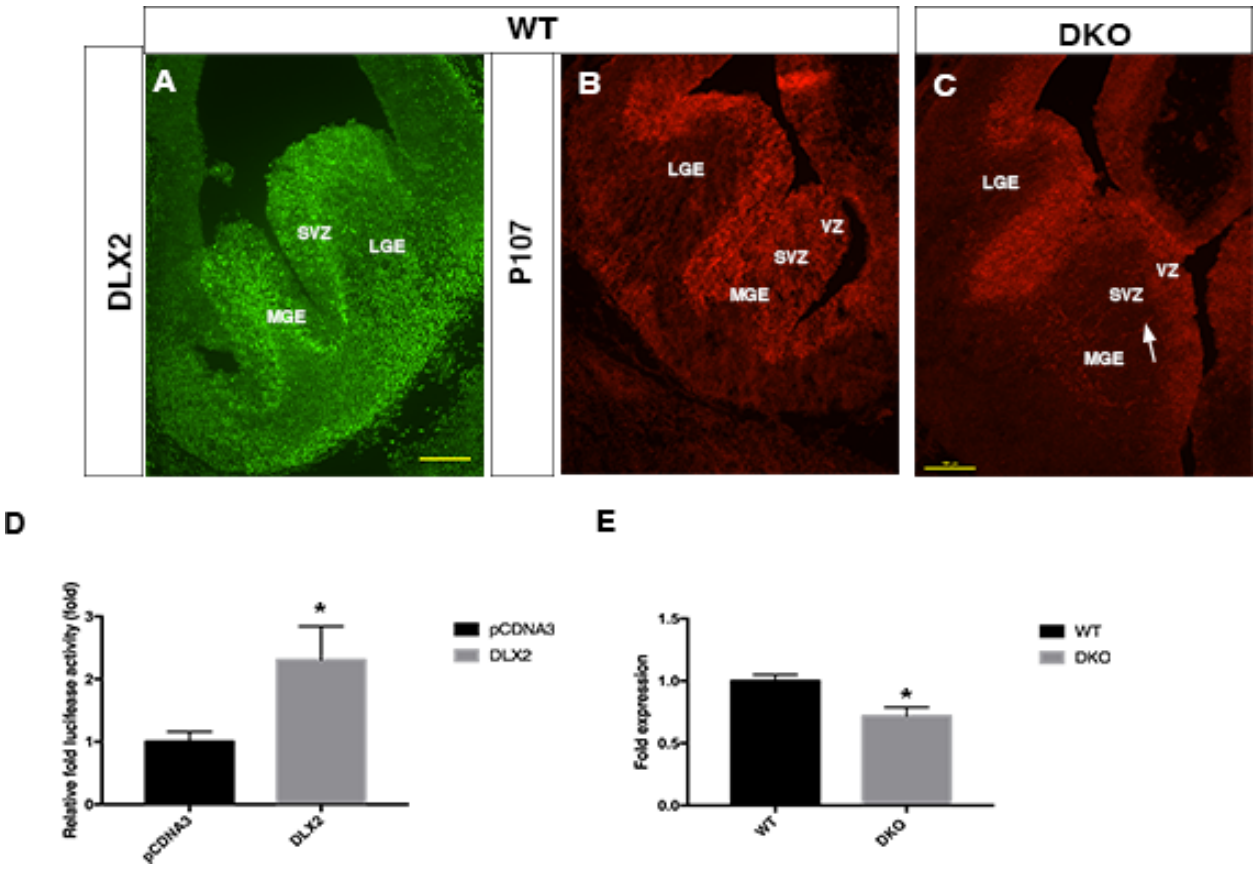

Figure 4.3 P107 expression is reduced in the *Dlx1/Dlx2* DKO forebrain.

(A) DLX2 is highly expressed in the SVZ of the MGE and LGE in the WT E13 subpallium. (B) P107 expression was also observed in the SVZ and VZ of the WT E13 subpallium. (C) In the absence of *Dlx1/Dlx2*, specific reduction of *p107* was observed in the SVZ of the MGE (white arrow). (D) Upon co-transfection of a *Dlx2* expression plasmid with *p107* reporter vectors into HEK 293 cells, significant activation of luciferase reporter gene expression was observed compared to empty pCDNA3 controls. (E) Quantification of *p107* transcript levels in the *Dlx1/Dlx2* DKO forebrain reveals a reduction in *p107* expression in the *Dlx1/Dlx2* GE compared to WT littermate controls.

[LGE; lateral ganglionic eminence, MGE; medial ganglionic eminence, SVZ; subventricular zone, VZ; ventricular zone. Scale = 100 μm *=P<0.05]

4.2.4 Notch signalling is upregulated in the Dlx1/Dlx2 DKO GE but is unchanged in the retinas of Dlx1/Dlx2 DKO mice.

As described previously, GABAergic interneurons born in the *Dlx1*/*Dlx2* DKO subpallium fail to differentiate. While Notch pathway genes were not identified in the E13 forebrain ChIP-chip, P107 has been shown to regulate neural differentiation in the developing cortex by restricting expression of *Hes1* (Vanderluit et al. 2004, Vanderluit et al. 2007). In addition, previous ISH experiments have shown that *Notch1* is elevated in the *Dlx1*/*Dlx2* DKO forebrain (Yun et al. 2002). Utilizing qRT-PCR we examined transcript levels of *Notch1*, *Hes1*, and *Hes5* in the *Dlx1*/*Dlx2* DKO GE and retina at E13 and E18, respectively. In the DKO GE, significant elevation of *Notch1* (1.76 fold), *Hes1* (2.25 fold), and *Hes5* (1.57 fold) was observed compared to WT littermate controls (Figure 4.4A) (N=3). In the retina, however, there was no change in Notch expression observed, nor was any change in *p107* expression observed (Figure 4.4B) (N=3). These findings demonstrate that elevation of the Notch pathway contributes to the failed differentiation of GABAergic interneurons observed in the *Dlx1*/*Dlx2* DKO forebrain. In the retina, Notch signalling has long been shown to have a crucial role in RPC multipotency and proliferation (Ahmad, Zaqouras, and Artavanis-Tsakonas 1995, Austin et al. 1995, Ahmad, Dooley, and Polk 1997, Bao and Cepko 1997). Since no change in Notch signalling was observed in the *Dlx1*/*Dlx2* DKO retina, this may suggest that Notch is upstream of *Dlx1*/*Dlx2*, restricting *Dlx* expression and inhibiting RPC from adopting RGC fates (Austin et al. 1995, Mu and Klein 2004) and therefore, loss of *Dlx1*/*Dlx2* expression has no effect on Notch signalling in this tissue.

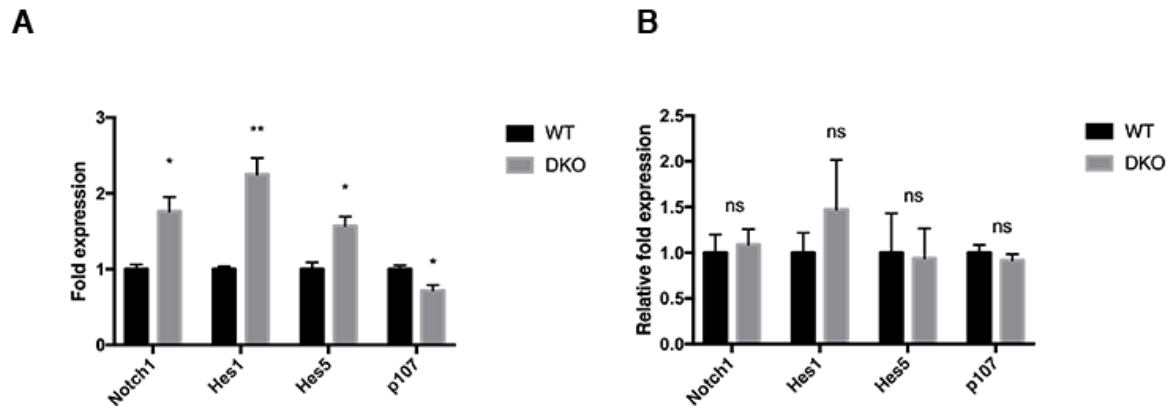

Figure 4.4 Significant elevation of Notch signalling in the *Dlx1*/*Dlx2* DKO forebrain.

Expression of genes critical for Notch signalling were examined in the *Dlx1*/*Dlx2* DKO forebrain to determine if aberrant Notch1 signalling may contribute to lack of differentiation observed in *Dlx1*/*Dlx2* DKO forebrains. (A) Significant elevation of *Notch1*, *Hes1*, and *Hes5* expression was observed in the *Dlx1*/*Dlx2* DKO forebrain compared to WT littermate controls (N=3). P107 expression was significantly reduced in the *Dlx1*/*Dlx2* DKO forebrain (N=3). (B) In the developing retina, however, Notch pathway gene expression was unchanged in the absence of *Dlx1*/*Dlx2* as was expression of *p107* compared to WT littermate controls (N=3). Statistical significance was determined by carrying out unpaired t-tests.

[ns; not significant, *=P<0.05, **=P<0.01]

4.2.5 Dlx2 gain-of-function in WERI-Rb-1 cells drives p107 expression whereas Dlx2 knockdown reduces p107 expression in vitro

To complement the *Dlx1*/*Dlx2* DKO studies carried out in mice, we transfected Dlx2-GFP plasmids into WERI-Rb-1 cells to examine the expression of *p107* when ectopic *Dlx2* is added. WERI-Rb-1 cells are derived from human retinoblastomas. In human retinoblastomas, *Rb* loss is sufficient for the development of retinoblastoma and no upregulation of *p107* expression is observed to compensate for the loss of *Rb*. In mice, on the other hand, upon the loss of *Rb*, *p107* is transcriptionally upregulated, supressing tumour formation. Because there is no upregulation of *p107* observed in the WERI-Rb-1 retinoblastoma cells, we concluded they would be a suitable cell line to examine *p107* expression upon transfection of DLX2-GFP. Transfection of Dlx2-EGFP resulted in a significant upregulation of *p107* expression compared to empty GFP controls (Figure 4.5A) (N=3). We also performed *Dlx2* knockdown experiments in SK-N-BE(2) cells. SK-N-BE(2) cells were chosen for the *Dlx2* knockdown experiments as a high level of endogenous *Dlx2* expression is observed in these human neuroblastoma cells. Transient knockdown of *Dlx2* expression resulted in reduction of *p107* expression *in vitro* (N=3) (Figure 4.5B). These results further support that DLX2 is critical for the transcriptional activation of *p107* expression in the developing CNS.

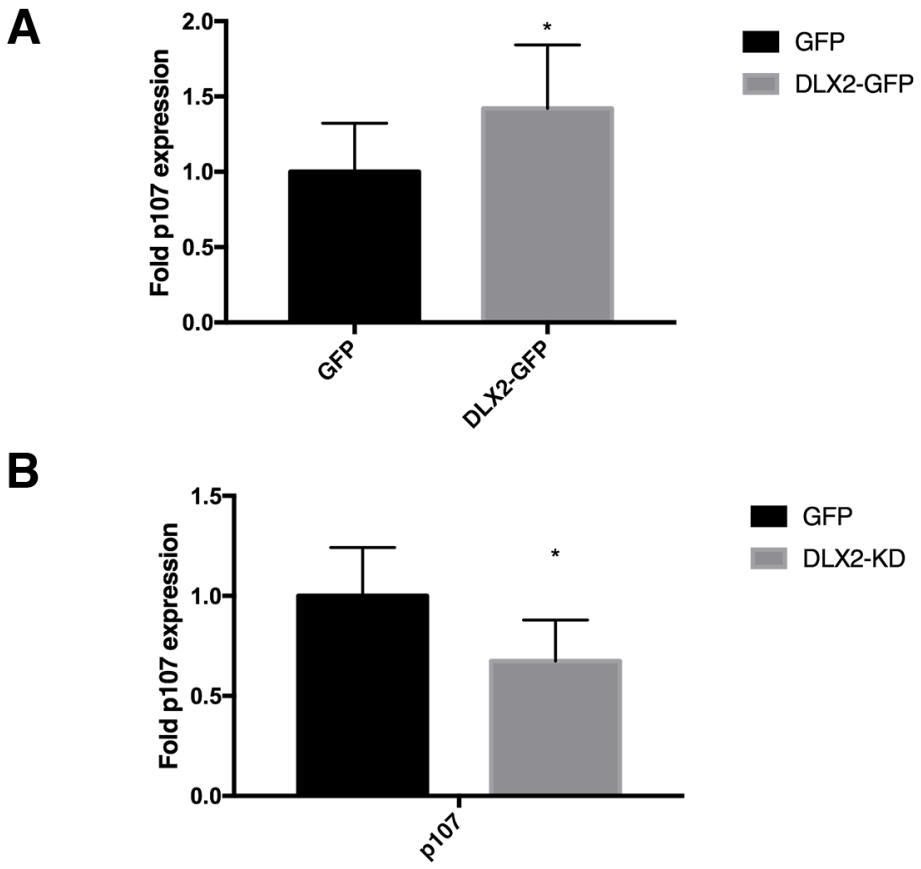

Figure 4.5 p107 expression is increased upon *Dlx2* gain of function and reduced with *Dlx2* knockdown.

(A) *Dlx2*-GFP expression plasmids and empty GFP vector controls were transfected into WERI-Rb-1 cells and p107 expression was examined. In *Dlx2*-GFP gain of function transfections a significant upregulation of *p107* was observed compared to empty GFP controls. (B) Transient knockdown of *Dlx2* expression in SK-N-BE(2) cells resulted in significant reduction of *p107* expression *in vitro* as determined by carrying out unpaired t-test (N=3).

4.3 Discussion

4.3.1 Dlx1/Dlx2 indirectly regulates Notch signalling through activation of p107 to promote neuronal differentiation in the subpallium

ChIP-chip is a powerful technique to identify protein/DNA interactions *in vivo* (Ren et al. 2000). We utilized this technology to identify transcriptional targets of DLX2 in the E13 forebrain. We expected Notch pathway genes to be identified as direct targets of DLX2 in the ChIP-chip since *Hes5* and *Notch1* are upregulated in the E13 *Dlx1*/*Dlx2* DKO forebrain (Yun et al. 2002), and neuronal differentiation is arrested in the SVZ of the *Dlx1*/*Dlx2* DKO forebrain. However, Notch pathway genes were not observed in the DLX2 forebrain ChIP-chip. Among the targets identified, *p107* has previously been shown to regulate Notch signalling the cortex by binding to and restricting expression of *Hes1* (Vanderluit et al. 2004, Vanderluit et al. 2007). We propose that DLX2 indirectly regulates Notch signalling in the forebrain through *p107* activation, which then in turn restricts Notch signalling to promote interneuron differentiation in the developing subpallium. It is potentially possible, however, that DLX2 directly regulates the Notch pathway. While our CpG island ChIP-chip covers areas corresponding to annotated promoters, ChIP-seq has several advantages including greater coverage (Park 2009). Therefore, in the future a DLX2 ChIP-seq could identify additional regulatory targets, including members of the Notch signalling pathway.

P107 is believed to regulate gene expression by binding to and recruiting the transcriptional repressor E2F4 to target genes (Dyson et al. 1993, Ginsberg et al. 1994, Moberg, Starz, and Lees 1996, Wirt and Sage 2010). Furthermore, a number of binding sites for E2F transcription factors have been identified upstream of *Hes1*, *Hes5*, and *Notch1* (Julian et al. 2016, Vanderluit et al. 2004, Vanderluit et al. 2007). Further experiments will need to be carried out to confirm that P107 directly restricts Notch signalling in the subpallium. For instance, examination of *p107* null forebrains would allow us to examine if Notch signalling is elevated in the subpallium upon the loss of *p107*. Because *Hes1* was elevated in the developing neocortex in

p107 null mice (Vanderluit et al. 2007), we expect that similar findings would be observed in the developing subpallium.

While the first wave of neurogenesis from the LGE and the MGE of the subpallium in the *Dlx1*/*Dlx2* DKO forebrain is unaffected (taking place between E10-E12), differentiation of later-born GABAergic interneurons is arrested (Anderson, Qiu, et al. 1997, Eisenstat et al. 1999, Panganiban and Rubenstein 2002). This defect in late differentiation leads to defects in the development of the SVZ, including aberrant expression of the neuronal progenitor marker *Lhx2* in the SVZ of the *Dlx1*/*Dlx2* DKO forebrain (Anderson, Qiu, et al. 1997, Panganiban and Rubenstein 2002). We determined that the block in differentiation was also partially due to the significant elevation of Notch signalling (*Notch1*, *Hes1*, and *Hes5* expression) in the E13 GE of the *Dlx1*/*Dlx2* DKO, where upregulation of *Hes1* expression was the highest, and a significant reduction in *p107* expression was also observed (Figure 4.4). In addition, we observed specific loss of *p107* expression in the SVZ of the MGE in *Dlx1*/*Dlx2* DKO forebrains (Figure 4.3). Specific loss of p107 in the SVZ with maintained expression in the VZ suggests that similar to *Dlx1*/*Dlx2*, p107 is also critical in maintaining neuronal differentiation of the secondary wave of interneuron differentiation in the SVZ.

Previous reports have stated that *Hes1* expression is unchanged in the *Dlx1*/*Dlx2* DKO forebrain (Yun et al. 2002) while our findings showed a significant increase in Hes1 expression in the *Dlx1*/*Dlx2* DKO GE. The difference between our findings and that of the previous study could possibly be attributed to the developmental time point in which *Hes1* expression was examined in the two studies. We quantified *Hes1* transcript level in the GE at E13 when neuronal differentiation defects are first observed in the *Dlx1*/*Dlx2* DKO forebrain using qRT-PCR, while the previous study utilized ISH to examine *Hes1* expression no earlier than E15. By E15, *Dlx1/Dlx2* expression is significantly reduced in the WT subpallium (Porteus et al. 1994). Therefore, it is possible that by E15, the authors did not observe an appreciable change in *Hes1* expression in the *Dlx1*/*Dlx2* DKO GE that they may have otherwise observed had they carried

out their ISH experiments with *Hes1* at E13 when *Dlx1*/*Dlx2* expression is at its peak in the subpallium. It is worth noting that the authors did carry out ISH on *Dll1* and *Hes5* at E11, but only carried out *Hes1* and *Notch1* ISH in addition to *Dll1* and *Hes5* at E15. It is unclear why the authors did not examine *Hes1* expression prior to E15 in the *Dlx1*/*Dlx2* forebrain sections.

Collectively, our results demonstrate that *Dlx1*/*Dlx2* directly activates *p107* expression in the developing subpallium. We propose that P107 restricts Notch signalling in the SVZ primarily through the restriction of *Hes1* expression in the SVZ, driving neural differentiation of GABAergic interneurons (Figure 4.6A). In the absence of *Dlx1*/*Dlx2, p107* expression is reduced in the SVZ while the *Hes1* expression domain is expanded into the SVZ blocking differentiation of GABAergic interneurons.

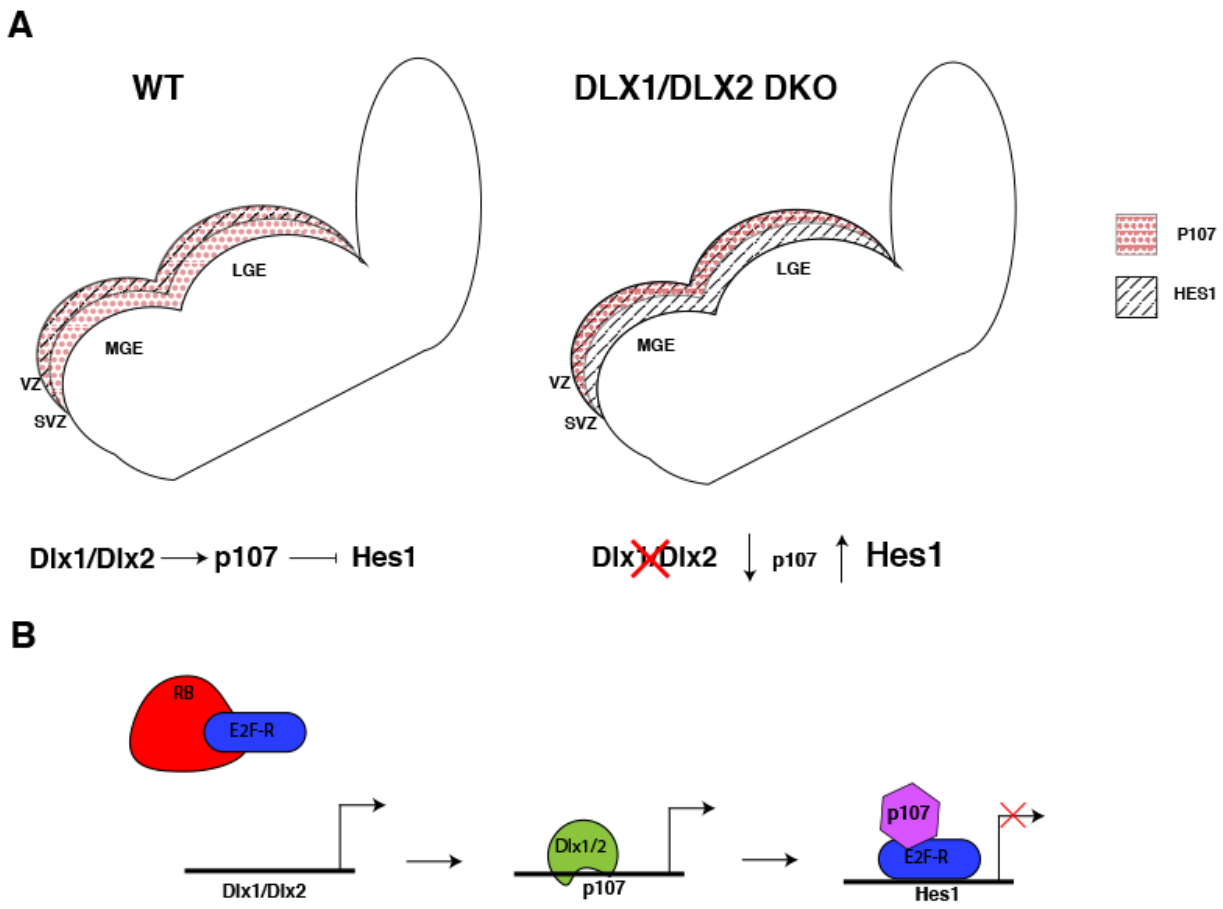
A
WT
DLX1/DLX2 DKO
LGE
MGE
VZ
SVZ
P107
HES1
Dlx1/Dlx2 → p107 ⊣ Hes1
Dlx1/Dlx2 ↓ p107 ↑ Hes1
B
RB
E2F-R
Dlx1/Dlx2
Dlx1/2
p107
Hes1

Figure 4.6 Proposed model for Dlx1/Dlx2 regulation of *p107* expression and interneuron differentiation during forebrain development.

We propose that in the WT forebrain, *Dlx1*/*Dlx2* promotes *p107* expression (dotted region of expression) in the developing subpallium, which in turn restricts Notch signalling in the SVZ by inhibiting *Hes1* expression (cross-hatched expression region). In the *Dlx1*/*Dlx2* DKO forebrain, the *Hes1* expression domain increases into the SVZ (increased cross-hatched expression area) at the expense of *p107* expression in the SVZ (dotted area no longer found in the SVZ). (B) Rb family regulates interneuron differentiation both up- and downstream of *Dlx1*/*Dlx2*. Active Rb binds to and prevents repressor E2F from binding to the *Dlx1*/*Dlx2* intergenic enhancer, allowing for upregulation of *Dlx1*/*Dlx2* expression in GABAergic interneurons. *Dlx1*/*Dlx2* then binds to and upregulates *p107* expression in the subpallium. P107, in turn, perhaps in combination with repressor E2F, binds to conserved E2F binding site in the *Hes1* regulatory regions to restrict *Hes1* expression in the SVZ to further promote differentiation of GABAergic interneurons.

4.3.2 Rb family regulates GABAergic interneuron differentiation both up- and downstream of Dlx1/Dlx2

Additional members of the Rb family have been shown to play a role in interneuron differentiation by regulation of *Dlx1*/*Dlx2*. Rb has been shown to directly regulate expression of *Dlx1*/*Dlx2* in the developing forebrain through the *Dlx1*/*Dlx2* intergenic enhancer (Ghanem et al. 2012). The authors showed that in the absence of *Rb*, expression of the repressor E2F7 was elevated, which then bound to and restricted the expression of *Dlx1*/*Dlx2* through binding to E2F consensus sites in the *Dlx1*/*Dlx2* intergenic enhancer. Mutation of the E2F binding sites rescued *Dlx1*/*Dlx2* expression, confirming the E2F repressors restrict *Dlx1*/*Dlx2* expression through this enhancer. This reduction in *Dlx1*/*Dlx2* expression in the absence of Rb consequently resulted in failed GABAergic interneuron differentiation and migration. The authors unfortunately did not examine the expression of *p107* in the *Rb* null brains. Given that p107 has the ability to compensate for Rb loss (Donovan et al. 2006), it would be interesting to determine if *p107* is elevated in the *Rb* null forebrain. Of the Rb family members, *p107* expression is the most highly transcriptionally regulated (Burkhart et al. 2010, Wirt and Sage 2010). In fact, *p107* contains two E2F binding sites in its upstream regulatory region (Zhu et al. 1995). It is possible that in the *Rb* null brain, activator E2Fs are no longer inhibited by RB allowing them to bind to consensus E2F sites and upregulate *p107* expression. However, while the authors did not look at alterations of *p107* expression in the absence of *Rb* specifically, some of their data suggests that p107 expression is not elevated in response to Rb loss. For instance, they analyzed expression of a number of repressor E2Fs in response to *Rb* loss. The preferential E2F binding partners for p107, E2F4 and E2F5 were unchanged in the Rb null brain compared to controls. In addition, because the repressor E2F7 was significantly upregulated in the *Rb* null brain, E2F7 may bind to the two consensus E2F sites in the *p107* promoter and restrict expression of *p107* in the absence of *Rb*. Furthermore, in conjunction with our findings in the *Dlx1*/*Dlx2* DKO forebrain, elevated expression of *p107* in response to *Rb* loss would be expected

to compensate for the loss of *Rb*, and rescue the differentiation defects observed in the *Rb* null brain, possibly by restricting Notch signalling, which would likely be elevated in the *Rb* null brain due to reduced *Dlx1*/*Dlx2* expression. This apparent lack of compensation by *p107* in the *Rb* null brain would be interesting considering the compensation that has been observed in other tissues (Donovan et al. 2006). Collectively, the findings in the *Rb* null forebrain in conjunction with our findings indicate that the Rb family is regulating interneuron differentiation both up- and downstream of *Dlx1*/*Dlx2* (Figure 4.6B). First, active RB binds to and prevents repressor E2F from binding to the *Dlx1*/*Dlx2* intergenic enhancer, allowing for upregulation of *Dlx1*/*Dlx2* in differentiating progenitors in the GE SVZ. *Dlx1*/*Dlx2* in turn upregulates expression of *p107* in the SVZ, which further drives interneuron differentiation by restricting Notch signalling.

4.3.3 Reduction of p107 in the MGE may lead to specific reduction in cortical interneurons

The loss of *Dlx1*/*Dlx2* results in defective differentiation and migration of GABAergic interneurons from both the MGE and the LGE. The interneurons generated from the GE populate distinct anatomical structures where interneurons born in the LGE migrate and primarily populate the olfactory bulb, while interneurons born in the MGE populate the striatum and the cortex (Anderson, Eisenstat, et al. 1997, Anderson, Qiu, et al. 1997, Marin, Anderson, and Rubenstein 2000, Panganiban and Rubenstein 2002). In our study, we observed specific reduction of *p107* expression in the SVZ of the MGE in the *Dlx1*/*Dlx2* DKO subpallium while *p107* expression in the LGE appeared unchanged (Figure 4.3). Because *p107* is known to regulate neurogenesis in the developing cortex and cortical interneurons are born in the MGE (Anderson et al. 2001, Vanderluit et al. 2004, Vanderluit et al. 2007), perhaps reduction in *p107* expression in the MGE contributes specifically to loss of cortical interneurons in the *Dlx1*/*Dlx2* DKO brain. Again, examination of a p107 null mouse model would be informative to determine if differentiation of cortical interneurons born in the MGE are specifically affected in the absence of *p107*. It would also be interesting to carryout neuronal migration assays to determine

if neuronal migration would also be affected in the absence of p107 since migration defects are observed in both *Dlx1*/*Dlx2* DKO and *Rb* null forebrains.

CHAPTER 5: PERSISTENT FETAL VASCULATURE IN THE NRP2 KNOCKOUT EYE

5 Chapter 5. Persistent fetal vasculature in the *Nrp2* knockout eye

5.1 Introduction

5.1.1 Ocular vascular systems

The mature retina, while small, has a high metabolic demand with the highest oxygen consumption of any tissue (Saint-Geniez and D'Amore 2004, Schmidt et al. 2003, Wangsa-Wirawan and Linsenmeier 2003). As such, two distinct vascular networks, the choroid and the retina vessels, are required to sustain the metabolic demands of the mature retina. The embryonic retina, on the other hand, is supplied by the choroid and the transient hyaloid vascular system. The choroid is generated from the ocular mesenchyme that surrounds the nascent optic cup and supplies oxygen and nutrients to the outer retina. In addition to the endothelial cells derived from the mesenchyme, the choroid is also made up of neural crest-derived melanocytes, stromal cells and pericytes (Etchevers et al. 2001, Nickla and Wallman 2010, Saint-Geniez and D'Amore 2004). Both FGF and vascular endothelial growth factor (VEGF) play a role in the development of the choroid. FGF signalling must be reduced in order for the choroid to properly differentiate, while upregulation of VEGF expression in the RPE is essential for choroidal development (Gogat et al. 2004, Nickla and Wallman 2010, Saint-Geniez and D'Amore 2004, Zhao and Overbeek 2001, Marneros et al. 2005).

While the choroid is responsible for nourishing the outer retina, the retinal vessels provide nutrients to the mature inner retina. The retinal vessel network emerges from the optic nerve head and spreads across the nerve fibre layer of the retina toward the periphery of the retina. Before this retinal vascular network emerges, retinal astrocytes invade the retina and migrate toward the retinal periphery (Fruttiger 2007, Fruttiger et al. 1996, Ling and Stone 1988). These astrocytes act as a template upon which the retinal blood vessels will be created. RGC secrete platelet-derived growth factor (PDGF), which promotes the proliferation of retinal

astrocytes expressing PDGF receptor alpha (Fruttiger, Calver, and Richardson 2000, Mudhar et al. 1993). When retinal astrocytes have reached the retinal periphery, hypoxic conditions stimulate the astrocytes to produce a peripheral to central gradient of VEGF, promoting angiogenesis of the primary vascular plexus along the retinal surface (Fruttiger 2007, Stone et al. 1995, West, Richardson, and Fruttiger 2005). Neuronal expression of vascular endothelial growth factor receptor 2 (VEGFR2) also promotes retinal angiogenesis along the surface of the retina by titrating the levels of VEGF (Okabe et al. 2014). When the retinal vessels (primary plexus) have reached the retinal periphery, new vessels sprout from the primary plexus and grow vertically into the neural retina generating the intermediate deep plexus and outer deep plexus, which extends into the outer IPL and the inner OPL, respectively (Tata, Ruhrberg, and Fantin 2015, Fruttiger 2007). Contrary to the primary plexus, angiogenesis of the deep plexus occurs independent of astrocytes; however, the specific molecular mechanisms guiding deep plexus angiogenesis are poorly understood.

The leading cause of blindness in the Western world results from the pathological neovascularization of the retina (Centers for Disease Control and Prevention). Both the choroid and retinal vessels are subject to pathological neovascularization. Choroidal neovascularization can arise as a complication of age-related macular degeneration (AMD) (neovascular AMD or wet AMD), while retinal vessel neovascularization arise from ischemic retinopathies including diabetic retinopathy and retinal vein occlusion (Campochiaro 2015, Fruttiger 2007). In addition to its critical role in ocular vascular development, the upregulation of VEGF plays an important role in the pathological neovascularization of both retinal vessels and the choroid. Mouse models of retinal ischemia have shown that under hypoxic conditions, hypoxia-inducible factor 1 (HIF-1) activates the expression of VEGF, which in turn drives neovascularization (Campochiaro 2013, Kelly et al. 2003, Ozaki et al. 1999, Pierce et al. 1995). Following disruption of Bruch's membrane in animal models, upregulation of VEGF is observed and followed by choroidal neovascularization (Campochiaro 2013, Oshima et al. 2005, Yamada et al. 2000).

5.1.2 Hyaloid vasculature and persistent fetal vasculature

Prior to the development of the mature retinal vasculature, the hyaloid vasculature is the primary blood supply to the developing retina. The hyaloid vasculature is a transient blood vessel network that delivers nutrients to the developing lens and surrounding ocular tissues (Figure 5.1A). At approximately E10 the hyaloid artery enters the eye through the choroid fissure in the optic stalk (Ito and Yoshioka 1999, Saint-Geniez and D'Amore 2004). The hyaloid vasculature is organized into several anatomical structures including the hyaloid artery, tunica vasculosa lentis (TVL), the vasa hyaloidea propria, and the pupillary membranes. The TVL and the pupillary membrane cover the developing lens posteriorly and anteriorly, respectively. The hyaloid artery extends through the optic disc, and the vitreous before making contact with the posterior lens. The hyaloidea propria branches off the hyaloid artery and extends peripherally into the vitreous. Prior to birth, these embryonic structures must regress in order to have a clear visual path through the vitreal space. In mice, regression of the hyaloid vasculature begins around P14 starting with the hyaloidea propria and ends at approximately P30 with regression of the TVL (Brown et al. 2005, Hegde and Srivastava 2016, Ito and Yoshioka 1999, Mitchell, Risau, and Drexler 1998, Saint-Geniez and D'Amore 2004). In humans, the hyaloid vasculature is first observed during the 4th gestational week and has fully regressed by the 39th gestation week. As hyaloid regression begins, the mature retinal vasculature begins to emerge in order to replace the hyaloid system as the oxygen supply to the inner retina.

Failure of hyaloid vessel regression results in the development of a condition referred to as persistent fetal vasculature (PFV, previously persistent hyperplastic primary vitreous (PHPV)) (Figure 5.1B). PFV can lead to the development of a number of additional secondary pathologies including cataracts, detached retina, retinal folding, and intraocular haemorrhage (Hobbs and Hartnett 2014). In addition, PFV patient's eyes are often microphthalmic. PFV accounts for approximately 5% of cases of reported blindness in the United States (Mets 1999, Hobbs and Hartnett 2014, Hegde and Srivastava 2016). While the majority of PFV cases are

sporadic, a small number of genetic cases have been described. A handful of mutations in *Atoh7* have been identified in families with ocular defects that include PFV (Khan et al. 2012, Prasov et al. 2012, Khaliq et al. 2001). These mutations are found in the bHLH domain of *Atoh7* that binds DNA and regulates transcription. Prasov and colleagues tested the ability of the ATOH7 variant they identified to bind to DNA. They determined that the ATOH7 variant was unable to bind DNA and activate transcription (Prasov et al. 2012). In *Atoh7* mutant mice, in addition to RGC loss, persistence of the hyaloid vasculature is also observed (Edwards et al. 2012). The loss of RGC coupled with PFV in *ATOH7* mutants suggests that RGC may be playing a critical role in the timely regression of the hyaloid vasculature. While the specific regulatory mechanisms that mediate hyaloid regression are not well understood, a number of genetic PFV models have been generated that indicate that induction of apoptosis, increased vitreal anti-angiogenic factors, and the reduction of growth factors and their downstream signalling all play a role. The most commonly described mechanism of hyaloid regression involves macrophage-induced apoptosis of the endothelial cells of the hyaloid (Lang and Bishop 1993). Mouse models with deletions in *βA3/A1-crystallin*, *Ephrin-A5* (*Efna5*), and lens-specific *Smoothened* (*Smo*) have altered migration of cells into the vitreous and develop PFV in the form of a retrolental mass (Sinha et al. 2008, Son et al. 2014, Choi et al. 2014). A number of mutations in the Wnt pathway including *Lrp5*, *Wnt7b*, Frizzled-5 (*Fzd5)*, *Pu.1*, and *Lef1* develop PFV and apoptotic defects preventing the regression of the PFV (Kato et al. 2002, Lobov et al. 2005, van Genderen et al. 1994, Liu and Nathans 2008, Zhang, Fuhrmann, and Vetter 2008, McKercher et al. 1996). Mice with deletions of the tumour suppressor genes $p19^{Arf}$ and *p53*, and mice with double-deletions of the pro-apoptotic genes *Bax* and *Bak* develop retrolental PFV masses (Thornton et al. 2007, Freeman-Anderson et al. 2009, Silva et al. 2005, Reichel et al. 1998, Hahn et al. 2005). Finally, aberrant expression of growth factors and growth factor receptors including over-expression of VEGF, VEGF-A(188), deletion of *Vegfr2*, and deletion of transforming growth factor β (*Tgfβ2*) in the

eye also lead to the development of PFV (Rutland et al. 2007, Freeman-Anderson et al. 2009, Yoshikawa et al. 2016).

A

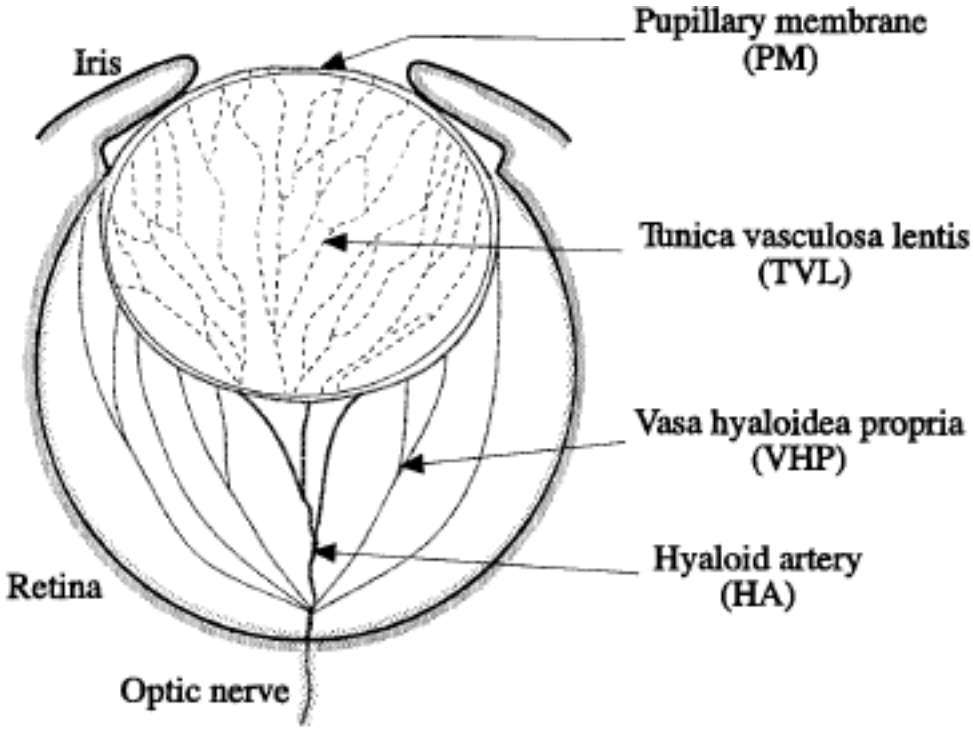
Pupillary membrane
(PM)
Iris
Tunica vasculosa lentis
(TVL)
Vasa hyaloidea propria
(VHP)
Hyaloid artery
(HA)
Retina
Optic nerve

B

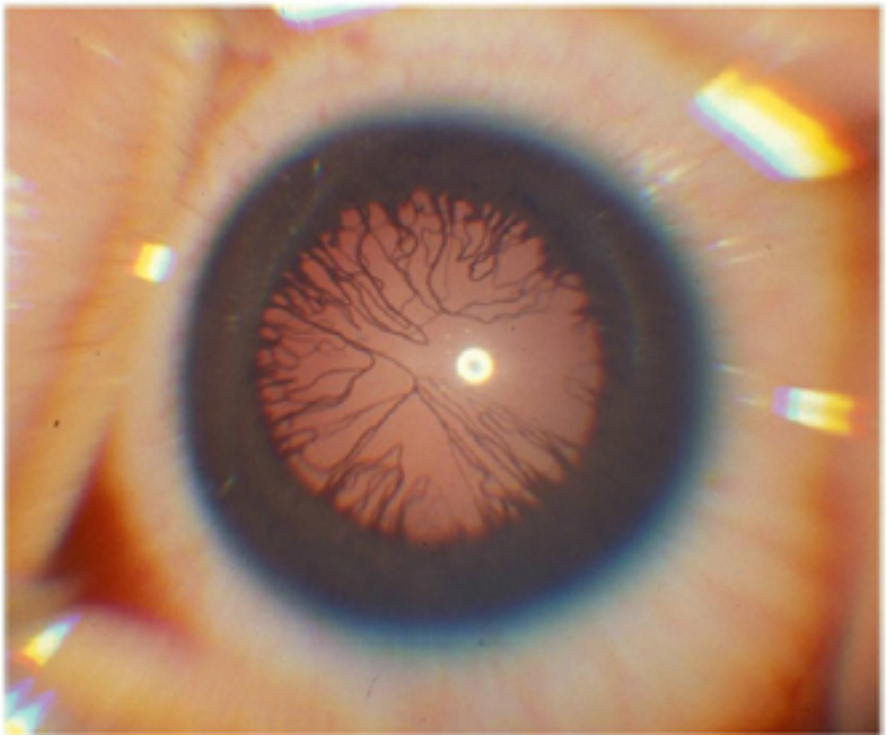

Figure 5.1 Hyaloid vasculature and PFV.

(A) The transient hyaloid vasculature system is comprised of several parts. The hyaloid artery enters the eye through the choroid fissure and extends to the posterior of the lens. The hyaloidea propria branches peripherally off the hyaloid artery into the vitreous. The tunica vasculosa lentis and the pupillary membrane cover the posterior and anterior of the developing lens, respectively. (B) PFV is a congenital malformation that develops when the hyaloid vasculature fails to regress. PFV can result from failed regression of the structures posterior to the lens and/or those covering the lens such as the tunica vasculosa lentis, and pupillary membrane as demonstrated in this figure. Figure (A) is from (Ito and Yoshioka 1999), reproduced with permission. Figure (B) is from (Hobbs and Hartnett 2014), reproduced with permission.

5.1.3 Neuropilins

Neuropilins are classically described as non-catalytic co-receptors for VEGF and class-3 semaphorins (Sema3), mediating functional responses to these ligands by forming receptor complexes with VEGF receptors (VEGFR) and Plexins, respectively. These functional responses mediated by neuropilin co-receptor interactions include axonal guidance when signalling through Sema3 binding, and angiogenesis when signalling through VEGF binding (Chen et al. 2000, Chen, Chedotal, et al. 1997, Giger et al. 2000, He and Tessier-Lavigne 1997, Kolodkin et al. 1997, Neufeld and Kessler 2008, Soker et al. 1998). However, in the last decade a number of additional non-classical ligands and their receptors have been identified including Tgfβ, hepatocyte growth factor, and platelet-derived growth factor (Ball et al. 2010, Banerjee et al. 2006, Glinka and Prud'homme 2008, Glinka et al. 2011, Matsushita, Gotze, and Korc 2007, Prud'homme and Glinka 2012). The neuropilin homologues, neuropilin-1 (Nrp1) and neuropilin-2 (Nrp2) share many of the same ligands with some exceptions, but also have differing ligand affinities and specificities. For instance, Nrp1 preferentially binds to Sema3a and Sema3C, while Nrp2 prefers Sema3F and Sema3C (Figure 5.2) (Pellet-Many et al. 2008, Raimondi et al. 2016, Raper 2000, Sharma, Verhaagen, and Harvey 2012).

Neuropilins are critical for vascular, cardiovascular, and neuronal development as demonstrated through loss of function mutations for *Nrp1* and *Nrp2*. *Nrp1* mutants die at mid-embryonic stages due to numerous cardiac defects including failed development of the great vessels, branchial arches, and dorsal aorta (Kawasaki et al. 1999, Gu et al. 2003). In addition, lack of *Nrp1* expression leads to severe defasciculation and aberrant projection of both spinal and cranial neurons (Gu et al. 2003, Kitsukawa et al. 1997). *Nrp2* mutants, on the other hand, survive to adulthood where significant axonal guidance and fasciculation defects of the cranial nerves are observed, reduction of the small lymphatic vessels, but without cardiac defects (Chen et al. 2000, Giger et al. 2000, Yuan et al. 2002). Compound *Nrp1*/*Nrp2* mutants have severe vascular abnormalities with large avascular areas of the head and trunk, and absent blood vessel

connections (Takashima et al. 2002). Given their critical roles in angiogenesis and migration, it is unsurprising that neuropilins are also highly expressed in cancer. Numerous cancers including breast, colon, prostate, and kidney carcinomas, leukemia, melanoma, and glioblastomas over-express *Nrp1*, *Nrp2*, or both (Prud'homme and Glinka 2012).

Neuropilins, particularly *Nrp1*, have been identified as potential novel therapeutic target for retinal diseases that can lead to pathological neovasculatization such as wet AMD, and diabetic retinopathy. Nrp1 expression is observed in fibrovascular tissue from diabetic retinopathy patients, and in choroidal neovascular membranes (Ishida et al. 2000, Lim et al. 2005). In addition, reduction in choroidal and retinal neovascularization is observed in endothelial cell-specific *Nrp1* knockout mice and *Nrp2* knockout mice (Shen et al. 2004, Fernandez-Robredo et al. 2017, Cui et al. 2003).

While there are reports indicating that *Nrp1* and *Nrp2* are involved in contralateral RGC axon projection at the midline, and development of the mature retinal vasculature, it is unknown what role neuropilins play in neural retina development and embryonic retinal vasculature development. The overwhelming majority of reports studying the role of neuropilins in the retina are studies on the role of *Nrp1*, but very little is known about the role of *Nrp2*. Here we investigated the role of *Nrp2* in the developing neural retina and embryonic retinal vasculature. Given the importance of neuropilins in angiogenesis and migration, we hypothesized that *Nrp2* may also be necessary for development of the embryonic retinal vasculature.

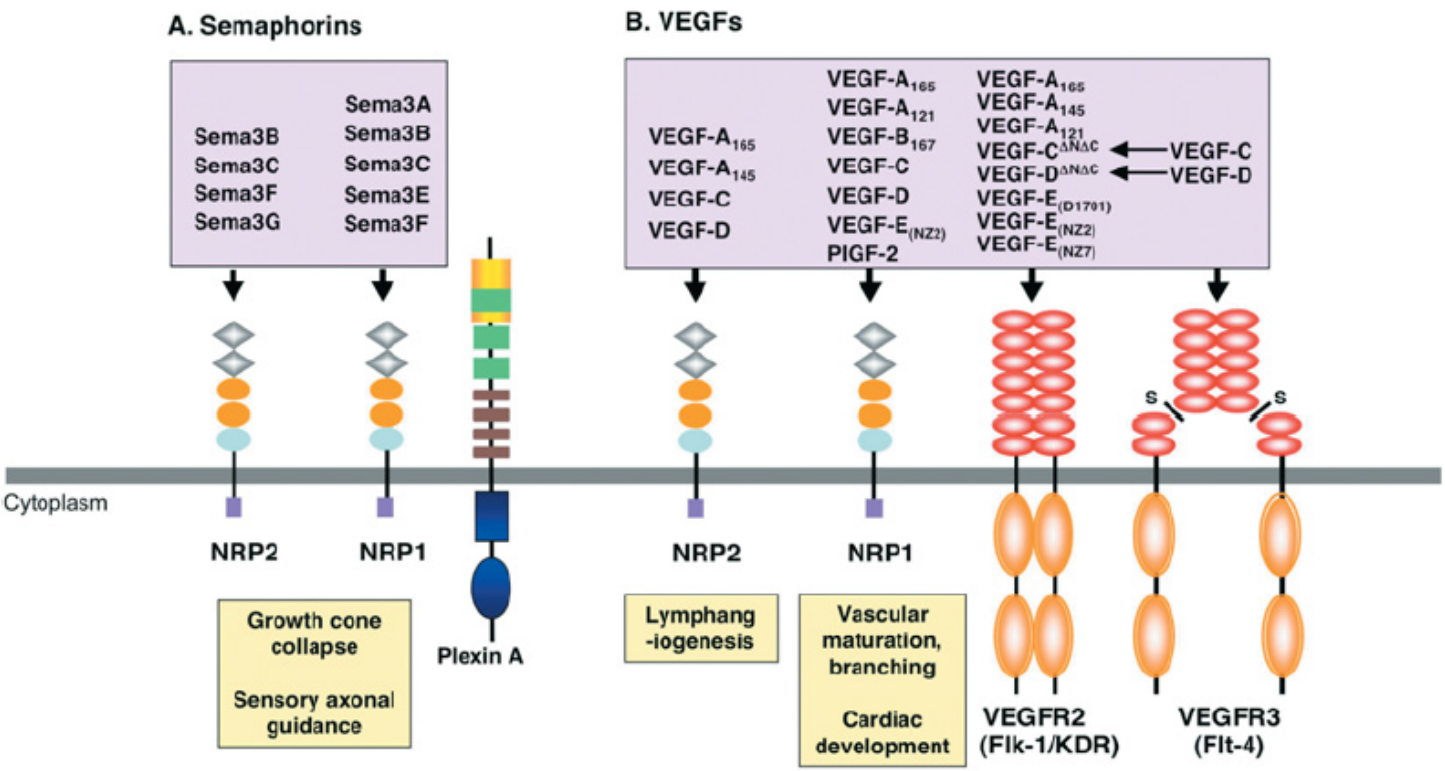
A. Semaphorins
Sema3B
Sema3C
Sema3F
Sema3G
Sema3A
Sema3B
Sema3C
Sema3E
Sema3F
B. VEGFs
VEGF-A165
VEGF-A145
VEGF-C
VEGF-D
VEGF-A165
VEGF-A121
VEGF-B167
VEGF-C
VEGF-D
VEGF-E(NZ2)
PIGF-2
VEGF-A165
VEGF-A145
VEGF-A121
VEGF-CΔNΔC
VEGF-DΔNΔC
VEGF-E(D1701)
VEGF-E(NZ2)
VEGF-E(NZ7)
VEGF-C
VEGF-D
Cytoplasm
NRP2
NRP1
Plexin A
NRP2
NRP1
S
S
Growth cone collapse
Sensory axonal guidance
Lymphang-iogenesis
Vascular maturation, branching
Cardiac development
VEGFR2 (Flk-1/KDR)
VEGFR3 (Flt-4)

Figure 5.2 Neuropilin receptors and ligands.

Neuropilins (Nrp1 and Nrp2) are non-catalytic co-receptors for Plexins, VEGFR, and others including TGFβ (not pictured). (A) Nrp1 and Nrp2 have both overlapping and specific affinities for class 3 semaphorin ligands. Neuropilins bind Sema3 and complex with Plexin receptors to mediate repulsion guidance cues and axonal growth cone collapse. (B) Like the Sema3 ligands, VEGF can bind to Nrp1 and Nrp2 with overlapping and specific affinities. Neuropilins are co-receptors for VEGF and can complex with VEGFR, enhancing VEGF signalling and promoting vasculogenesis, angiogenesis, lymphangiogenesis, and axonal guidance.

[Figure from (Pellet-Many et al. 2008), reproduced with permission]

5.2 Results

5.2.1 Expression of Neuropilins in the developing retina

Only a limited examination of the temporal and spatial expression patterns of *Nrp1* and *Nrp2* in the developing retina has been explored previously and the results of these studies are conflicting. Temporal expression of *Nrp1*, *Nrp2*, and class 3 semaphorin transcripts in whole retinas has shown that *Nrp2* increases steadily from E16 to adulthood (Sharma et al. 2014). *Nrp1* expression was approximately two-fold higher than *Nrp2* expression at all developmental stages examined. Two separate studies examined the spatial expression of *Nrp1* and *Nrp2* and each study showed that *Nrp1* is expressed in the RGC, hyaloid, and choroid (Erskine et al. 2011, McKenna, Munjaal, and Lwigale 2012). However, the results of these studies differed in regards to *Nrp2* expression. Erskine and colleagues did not observe *Nrp2* expression in the hyaloid or choroid from E12.5 to E17.5 (all time-points examined in their study). They observed Nrp2 expression initiation in RGC at E17.5 (Erskine et al. 2011). Contrary to the findings of the Erskine group, McKenna and colleagues discovered *Nrp2* expression in the hyaloid and periocular mesenchyme at E12.5 (McKenna, Munjaal, and Lwigale 2012). To better understand the temporal and spatial expression of neuropilins during development of the vertebrate ocular structures, we performed immunostaining on E13 and E18 retinas using NRP1 and NRP2 specific antibodies. We also utilized the β-galactosidase cassette present in our *Nrp2* gene-trap mouse to act as a reporter gene to examine the spatial expression pattern of *Nrp2* in the adult retina. In the E13 eye structures, NRP2 expression was absent from the neural retina (Figure 5.3A). In accordance with the findings of McKenna and colleagues, we observed NRP2 expression in the transient hyaloid vasculature structures and the choroidal vasculature surrounding the optic cup at E13. At E18, NRP2 expression was observed in the GCL of the neural retina and in the remnants of the hyaloid vasculature (Figure 5.3B). Expression of NRP2 was also maintained in the choroid vasculature. NRP1 was expressed at high levels throughout

the GCL and nerve fibre layer at E13 (Figure 5.3C). Much like the expression of NRP2, NRP1 was also observed in the hyaloid and choroidal vasculature during early embryonic retinal development. NRP1 expression is reduced in the GCL at E18 but maintained in the choroid and remaining hyaloid vessels (Figure 5.3D). Expression of *Nrp2* in the adult retina has not been described previously. To examine *Nrp2* expression in the adult retina, we utilized our *Nrp2* gene-trap mouse. The *Nrp2* null mouse was generated through the insertion of a gene trap vector containing a β-galactosidase reporter gene into the *Nrp2* coding sequence (inserts in the cDNA at nucleotide 2069), generating non-functional NRP2 protein (Chen et al. 2000). Therefore, to report the expression of *Nrp2* in the adult retina, X-gal staining was performed on mice heterozygous for the *Nrp2* gene trap. First, in order to verify that β-galactosidase expression is consistent with the NRP2 expression we observed using immunostaining in the WT retina, we examined β-galactosidase expression in E13 *Nrp2* gene-trap heterozygous eyes to compare with our E13 NRP2 immunostaining results. In accordance with our immunostaining findings, β-galactosidase expression was observed in the hyaloid, and choroid in the E13 eye demonstrating that β-galactosidase expression in the adult retina can be utilized as reliable read-out of *Nrp2* expression (Figure 5.4A). In the mature adult retina, β-galactosidase expression was observed in the GCL as well as the inner INL, which is the laminar location of amacrine cells (Figure 5.4B). Together, our findings demonstrate that *Nrp1* and *Nrp2* are expressed in the inner retinal cells. Not only is *Nrp2* expressed in the GCL as described previously, but for the first time, we also demonstrate that *Nrp2* is expressed in the GCL and amacrine cells of the adult retina. We also confirmed that *Nrp2* is expressed in the embryonic hyaloid vasculature as demonstrated by previous studies (McKenna, Munjaal, and Lwigale 2012), and in the choroidal vasculature. The expression pattern of *Nrp2* suggests that *Nrp2* is required in multiple areas of ocular development including the development of inner retinal cells, and hyaloid vasculature development.

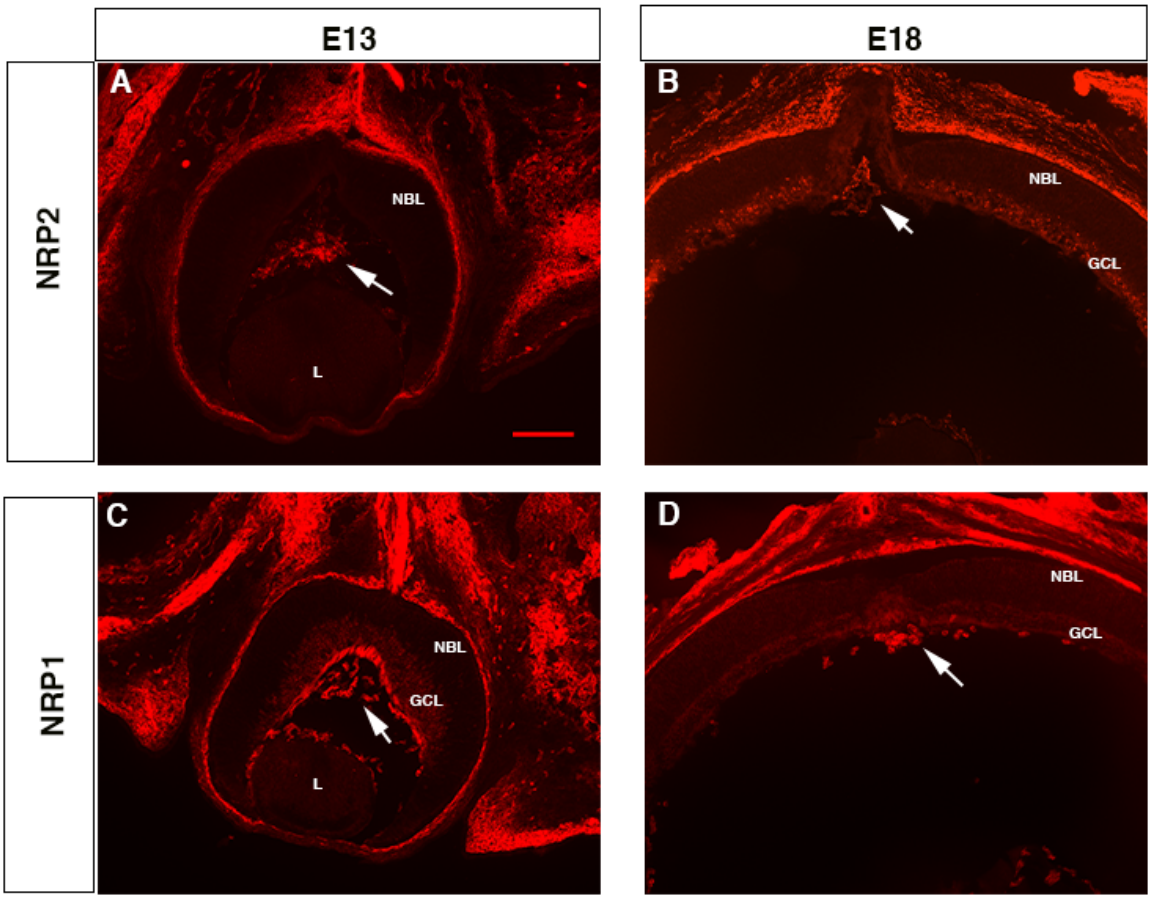

Figure 5.3 Neuropilin expression during embryonic ocular development.

Expression of NRP1 and NRP2 was examined during embryonic retinal development using NRP2 and NRP1 specific antibodies. (A) NRP2 expression in the WT E13 retina was observed in the hyaloid (white arrow) and in the choroid surrounding the optic cup. (B) At E18, NRP2 expression is observed in the GCL, remnants of the hyaloid (white arrow) and the choroid. (C) NRP1 expression was observed in the GCL and the nerve fibre layer at E13. Similar to NRP2 expression, NRP1 was also observed in the hyaloid and the choroid. (D) Nrp1 expression in the GCL decreases, but is maintained in hyaloid remnants (white arrow) and the choroid.

[GCL; ganglion cell layer, L; lens, NBL; neuroblastic layer. Scale = 100 μm]

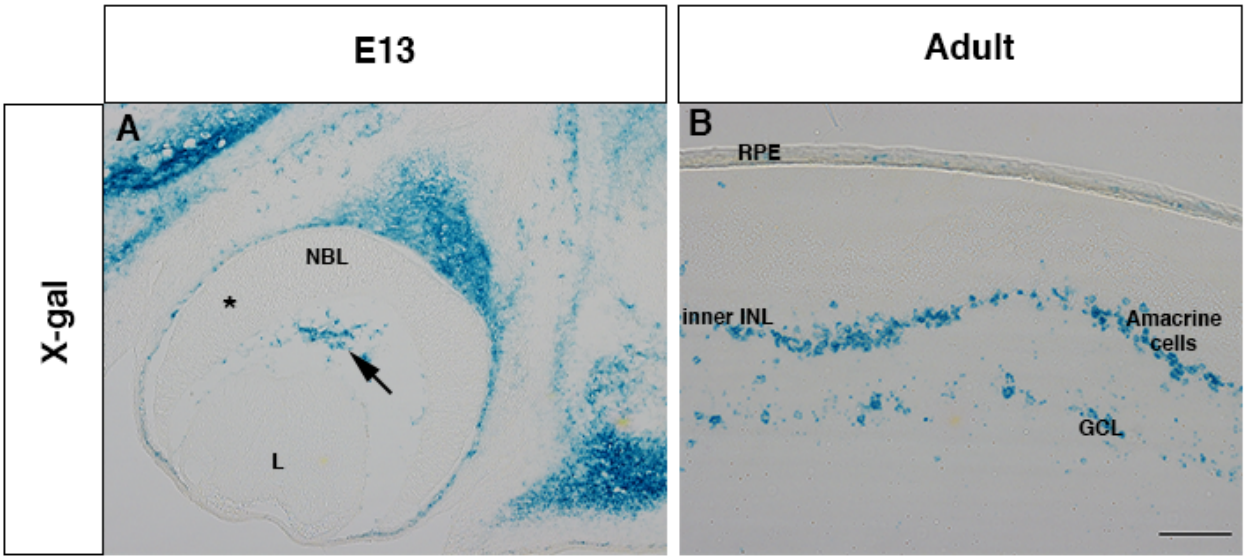

Figure 5.4 *Nrp2* is expressed in the inner cell layers of the adult retina.

X-gal staining was used to examine *Nrp2* expression in the adult retina. (A) As was demonstrated in NRP2 immunostaining, *Nrp2* is expressed in the hyaloid (black arrow) while the optic cup (asterisk) is devoid of *Nrp2* expression. (B) In the adult retina, *Nrp2* expression is observed in the GCL and in the inner INL, which is the laminar location of amacrine cells.

[GCL; ganglion cell layer, INL; inner nuclear layer, L; lens, NBL; neuroblastic layer, RPE; retinal pigment epithelium. Scale = 100 μm]

5.2.2 PFV and inner retina expansion in the embryonic Nrp2 null eye

The brains of *Nrp2* knockout mice have been extensively characterized. These studies demonstrate that a loss of *Nrp2* eliminates axonal response to repulsive guidance cues from class 3 semaphorins resulting in aberrant cranial nerve axon fasciculation and projections (Chen et al. 2000, Giger et al. 2000). While the role of *Nrp2* in CNS axonal guidance is well established, the role of *Nrp2* expression in the retina has not been examined previously. To study the role of *Nrp2* in ocular development, we utilized a homozygous gene-trap *Nrp2* null mouse, which was generated as described above (5.2.1). *Nrp2* gene-trap null mice are both viable and fertile. We examined the overall histology of the *Nrp2* knockout retina compared to WT littermate controls using CV staining techniques during embryonic stages of retina development. In WT E13 eyes (N=3), hyaloid vasculature is observed in the vitreal space, as would be expected at this developmental time point (Figure 5.5A). In the E13 Nrp2 null retina (N=3), the NBL was expanded compared to WT controls and an accumulation of hyaloidal cells was observed in the vitreal space (Figure 5.5B). In addition, the lens of the *Nrp2* knockout eye was significantly smaller in size compared to the WT control lens (Figure 5.5C) By late embryonic development (E18), the posterior hyaloid vasculature in the WT retina has noticeably regressed with few hyaloidal cells remaining near the optic disc (Figure 5.5D) (N=3). In the *Nrp2* null retina, however, a large retrolental (localized posterior to the lens) mass is present in the vitreous and the GCL is expanded particularly in the area surrounding the optic disc (Figure 5.5E) (N=3). To determine if the differentiation of the lens was affected by the loss of *Nrp2* in E13 retina, and therefore contributing to the reduction in size observed, we performed immunostaining for PROX1 in E13 WT and *Nrp2* knockout retinas. Prox1 is critical for the differentiation and elongation of lens fibres (Wigle et al. 1999). Prox1 immunostaining revealed that the expression of PROX1 in the *Nrp2* knockout is unchanged compared to the WT control (Figure 5.6). Therefore, the reduction in lens size does not appear to be due defects in lens differentiation, but may be due to the overall increase in retina size and decrease in vitreal space

in the *Nrp2* knockout. These results demonstrate that the loss of *Nrp2* results in expansion of the inner retina suggesting that *Nrp2* is playing a role in the development of the inner retinal cells, which include the RGC and amacrine cells. In addition, expression of *Nrp2* appears to be critical for the development of the hyaloid vasculature system. Future experiments will include BrdU proliferation analysis and apoptosis in the *Nrp2* null retina to address the mechanism underlying the increased cellularity observed.

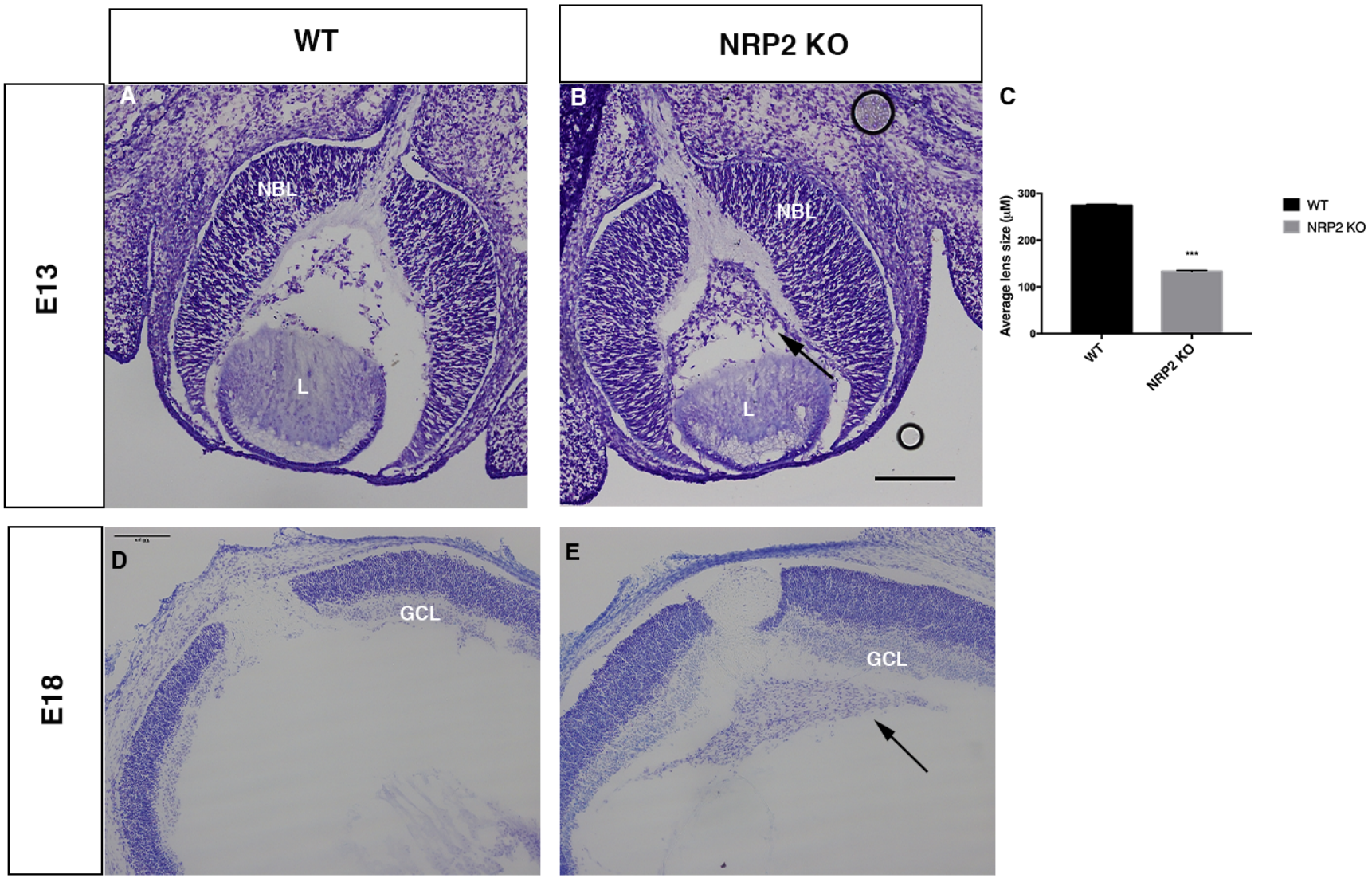
WT
NRP2 KO
E13
E18
A
B
C
D
E
NBL
L
GCL
Average lens size (μM)
300
200
100
0
WT
NRP2 KO
***

Figure 5.5 Expanded inner retina and retrolental mass in the embryonic *Nrp2* null eye.

The overall histology of the *Nrp2* null eye at embryonic developmental stages was examined using CV staining techniques. (A, B) At E13, the *Nrp2* null retina (B) contained a significant accumulation of hyaloidal cells (black arrow) in the vitreous compared to WT littermate controls (A). The lens of the E13 *Nrp2* null mouse appeared smaller and increased cellularity of the NBL was observed. (C, D) At E18, a significant retrolental mass (black arrow) was observed in the vitreous of the *Nrp2* null mouse (D) compared to WT controls (C), which was devoid of such a structure. Increased GCL cellularity at the optic disc was also observed in the *Nrp2* null retina compared to WT controls. Lens size was calculated using Image-J software.

[GCL; ganglion cell layer, KO; knockout, NBL; neuroblastic layer. Scale = 100 μm]

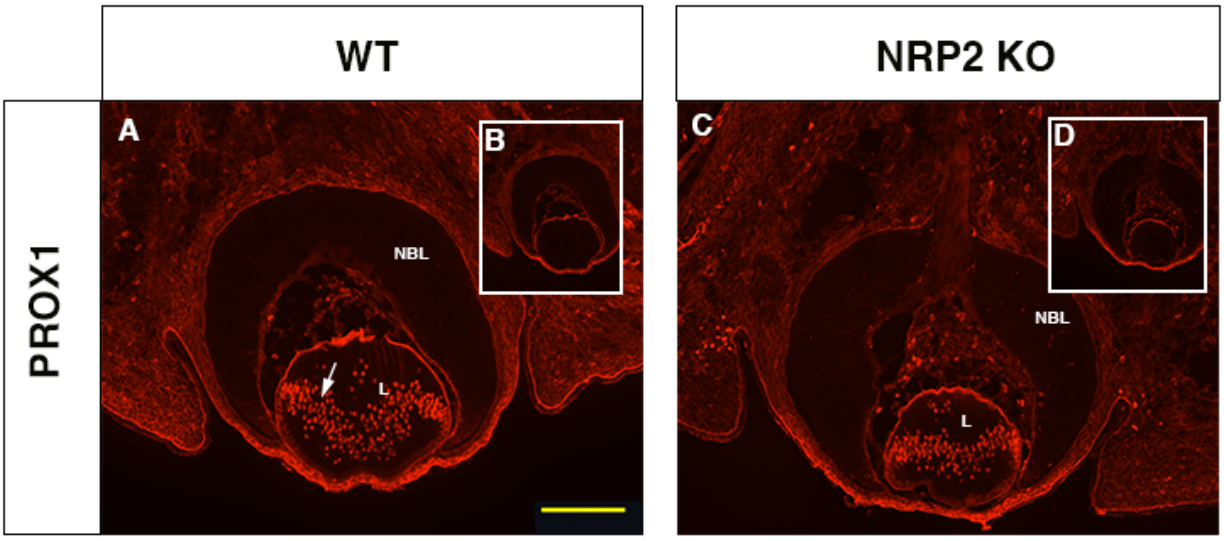

Figure 5.6 Lens differentiation is unaffected in the absence of *Nrp2*.

PROX1 immunostaining was performed to determine if the reduced lens size observed in the early *Nrp2* embryonic null retina was due lens differentiation defects. (A) PROX1 immunostaining was present in the lens fibres (white arrow). Negative controls (B) demonstrate that fluorescence observed in the hyaloid and lens epithelium represents background staining. (C) PROX1 immunostaining was maintained in the *Nrp2* null lens. (D) As was shown in the WT retina, the negative control insert demonstrates the background staining observed in the hyaloid and lens epithelium.

[L; lens, KO; knockout, NBL; neuroblastic layer. Scale = 100 μM]

5.2.3 Reduced vitreal space and retinal folding in the Nrp2 null eye

Two common secondary ocular pathologies observed in PFV patients are microphthalmia and retinal folding (Goldberg 1997, Pollard 1997). To examine the overall histology of the eyes in postnatal (P7, P14, and P28) *Nrp2* knockouts, we performed H&E staining. Prior to collecting postnatal eyes for histological analysis, we noted that *Nrp2* knockout mice were significantly smaller than the WT littermate controls at P28 (*Nrp2* KO: 11.74g ±0.68g, WT: 19.73g ±1.09g at P28) (Figure 5.7). *Nrp2* knockout mice were also significantly smaller than WT littermates at P7 and P14 (data not shown). In the P7 *Nrp2* null eye there was a reduction in the overall size of the eye and a significant reduction in the vitreal space compared to WT littermate controls (N=3) (Figure 5.8A-C, G-I). In addition to the reduced vitreal space, the *Nrp2* knockout eye had substantial retinal folding compared to the WT control (Figure 5.8G-I). Interestingly, the severe ocular phenotype observed in the *Nrp2* knockout appears to be asymmetrical (i.e only one eye severely affected). The other *Nrp2* knockout eye isolated from the same animal had a less severe phenotype compared to the other mutant eye but unlike the severely folded retina, the less severe mutant eye appears to have PFV (Figure 5.8D-F). This observation was consistent throughout the later stages of postnatal retinal development. At both P14 (N=2) and P28 (N=2), the *Nrp2* knockout retina had asymmetric retinal folding (Figure 5.9D-F, Figure 5.10D-F). In the more severe *Nrp2* knockout eye at each postnatal stage of retinal development, the IPL was expanded compared to the WT controls. We also examined the corneas of the *Nrp2* null eyes. In the severe *Nrp2* null eye at P7 and P14, the cornea was significantly thicker when compared to WT littermate controls (Figure 5.11). It also appears that, unlike the embryonic *Nrp2* knockout retinas (Figure 5.5), the lens of the postnatal *Nrp2* knockout retina recovers to a size comparable to WT controls. Collectively, our results indicate that the loss of *Nrp2* expression results in significant ocular abnormalities that are typically observed secondary to PFV including microphthalmia and retinal folding. Our results also

indicate that *Nrp2* knockout retinal phenotypes are unilateral or asymmetrical in the *Nrp2* null mice.

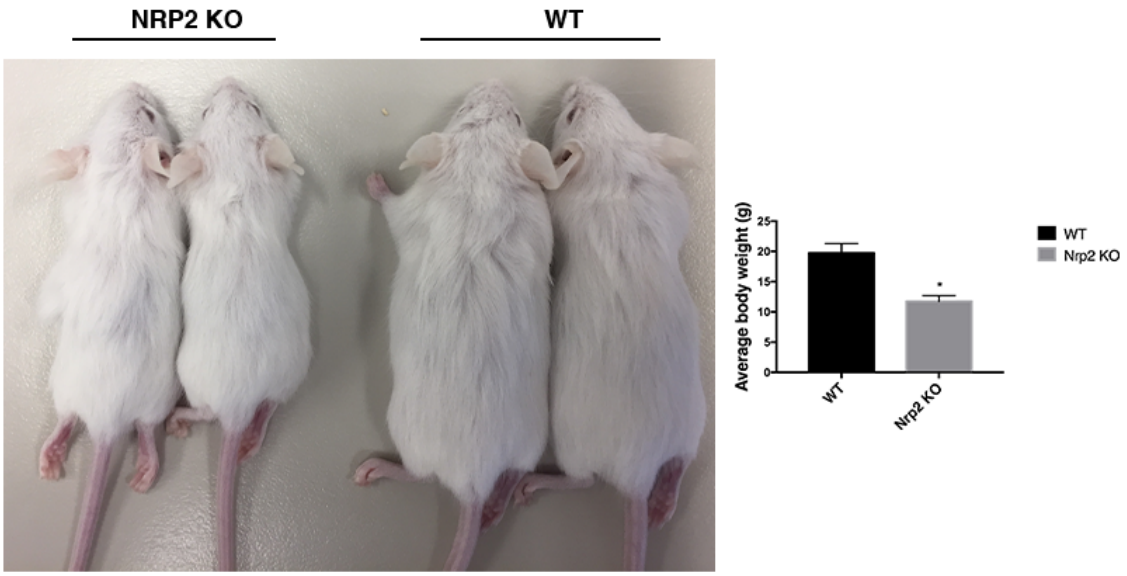

Figure 5.7 *Nrp2* knockout mice are significantly smaller than WT littermate controls at P28.

In the absence of *Nrp2* expression, mice are significantly reduced in size compared to WT littermate controls. Animals were weighed and the mean body weight for WT and *Nrp2* KO mice was calculated. Unpaired t-tests were used to determine statistical significance.

[KO; knockout, *P=0.05]

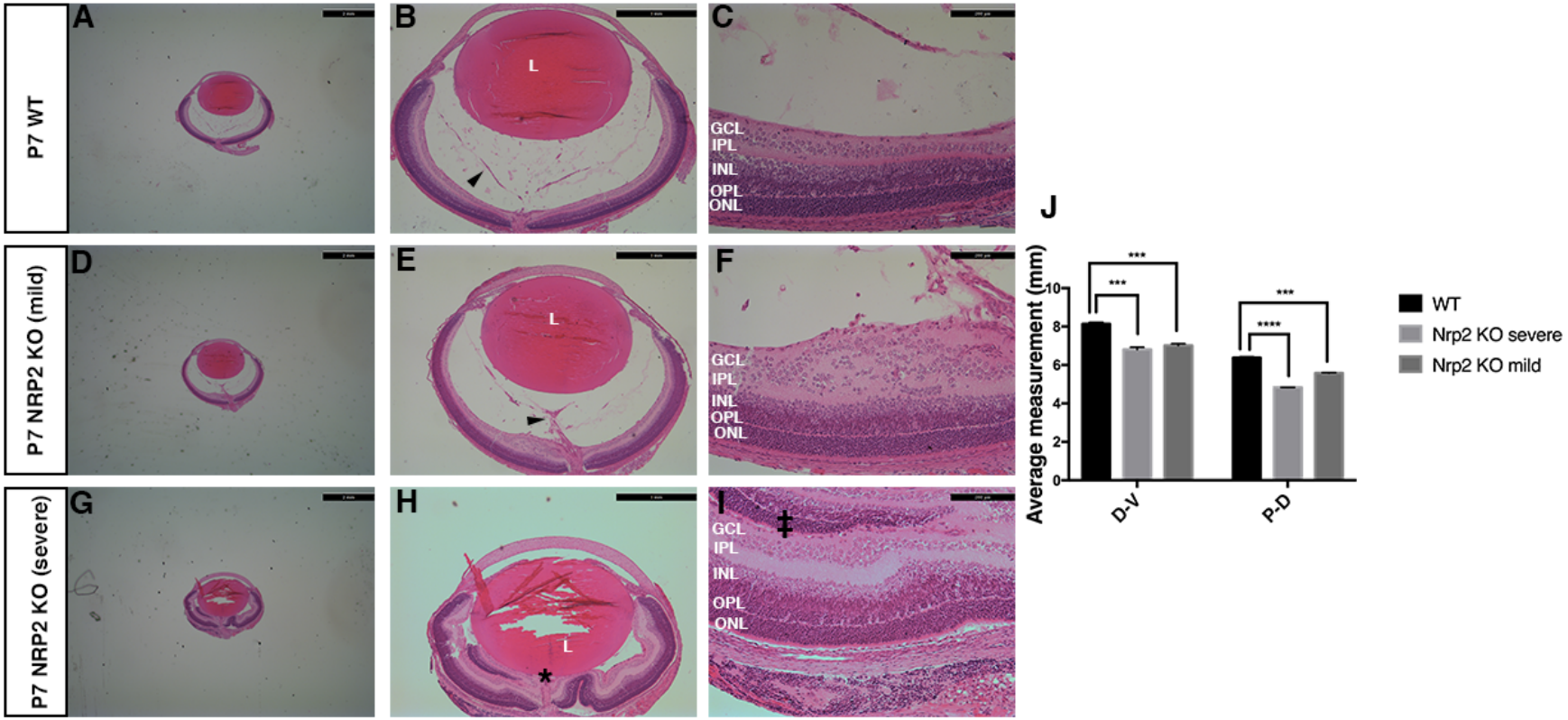
P7 WT
P7 NRP2 KO (mild)
P7 NRP2 KO (severe)
A
B
C
D
E
F
G
H
I
L
GCL
IPL
INL
OPL
ONL
J
Average measurement (mm)
D-V
P-D
WT
Nrp2 KO severe
Nrp2 KO mild

Figure 5.8 Microphthalmia, retinal folding, and PFV in the *Nrp2* knockout eye at P7.

Significant secondary ocular defects were observed in the *Nrp2* null eye compared to WT controls. (A-C) In the P7 WT eye (N=3), remnants of the hyaloid vasculature (vasa hyaloidea propria, black arrowhead) are visible. (G-I) In the severe *Nrp2* knockout mouse (N=3), significant retinal folding is observed (indicated by ‡). In addition, the vitreal space is significantly reduced and the overall size of the eye was significantly smaller (indicated by *). (D-F) The *Nrp2* null phenotype is asymmetric as the other eye from the same *Nrp2* null animal does not have significant retinal folding but is significantly smaller and has increased presence of the hyaloid artery (black arrow) compared to controls (*Nrp2* KO mild). (J) Measurements of the eye from dorsal to ventral retina and proximal to distal eye (i.e cornea to RPE) were collected and statistically analysed. H&E staining was performed by P. Baddam.

[KO; knockout, P-D; proximal-distal, D-V; dorsal-ventral. *** P=<0.001, ****P=<0.0001]

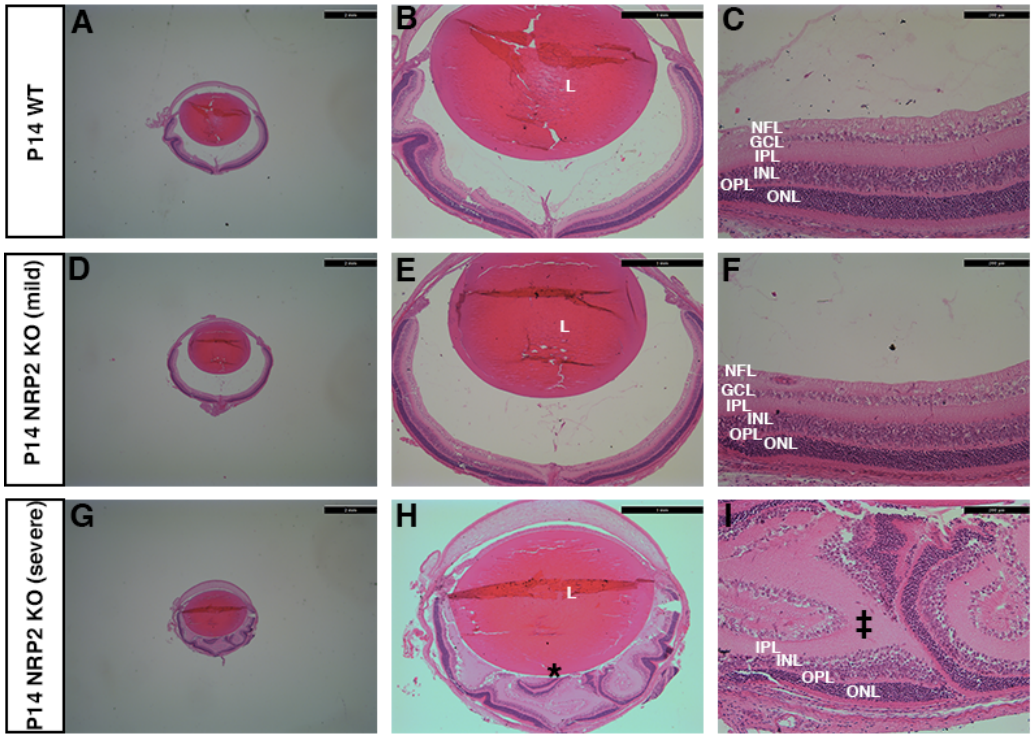
P14 WT
P14 NRP2 KO (mild)
P14 NRP2 KO (severe)
A
B
C
D
E
F
G
H
I
L
NFL
GCL
IPL
INL
OPL
ONL
*
‡

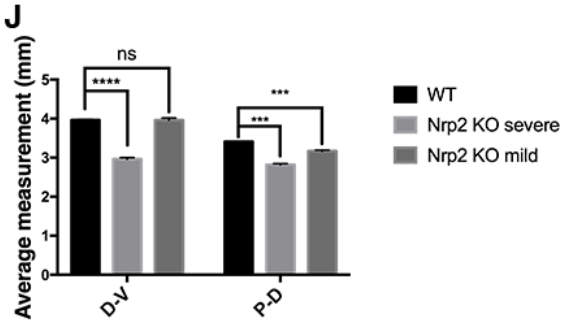
J
Average measurement (mm)
ns
****
***
***
D-V
P-D
WT
Nrp2 KO severe
Nrp2 KO mild

Figure 5.9 Microphthalmia and retinal folding in the *Nrp2* knockout eye at P14.

Significant secondary ocular defects were observed in the *Nrp2* null eye compared to WT controls. (A-C) In the P14 WT eye (N=2), remnants of the hyaloid vasculature are visible. (G-I) In the severe *Nrp2* knockout mouse (N=2), significant retinal folding is observed (indicated by ‡). In addition, the vitreal space is significantly reduced and the overall size of the eye was significantly smaller (indicated by *). (D-F) Severity of *Nrp2* null phenotype varies and/or is asymmetric as the other eye from the same *Nrp2* null animal (*Nrp2* knockout mild) does not have significant retinal folding but is significantly smaller on the P-D axis (i.e cornea to RPE) compared to controls. (J) Measurements of ocular size from dorsal to ventral retina (D-V) and proximal to distal (P-D) in the WT, more severe, and less severe *Nrp2* null eye. H&E staining was performed by P.Baddam.

[KO; knockout, ns; not significant, P-D; proximal-distal, D-V; dorsal-ventral. *** P=<0.001, ****P=<0.0001]

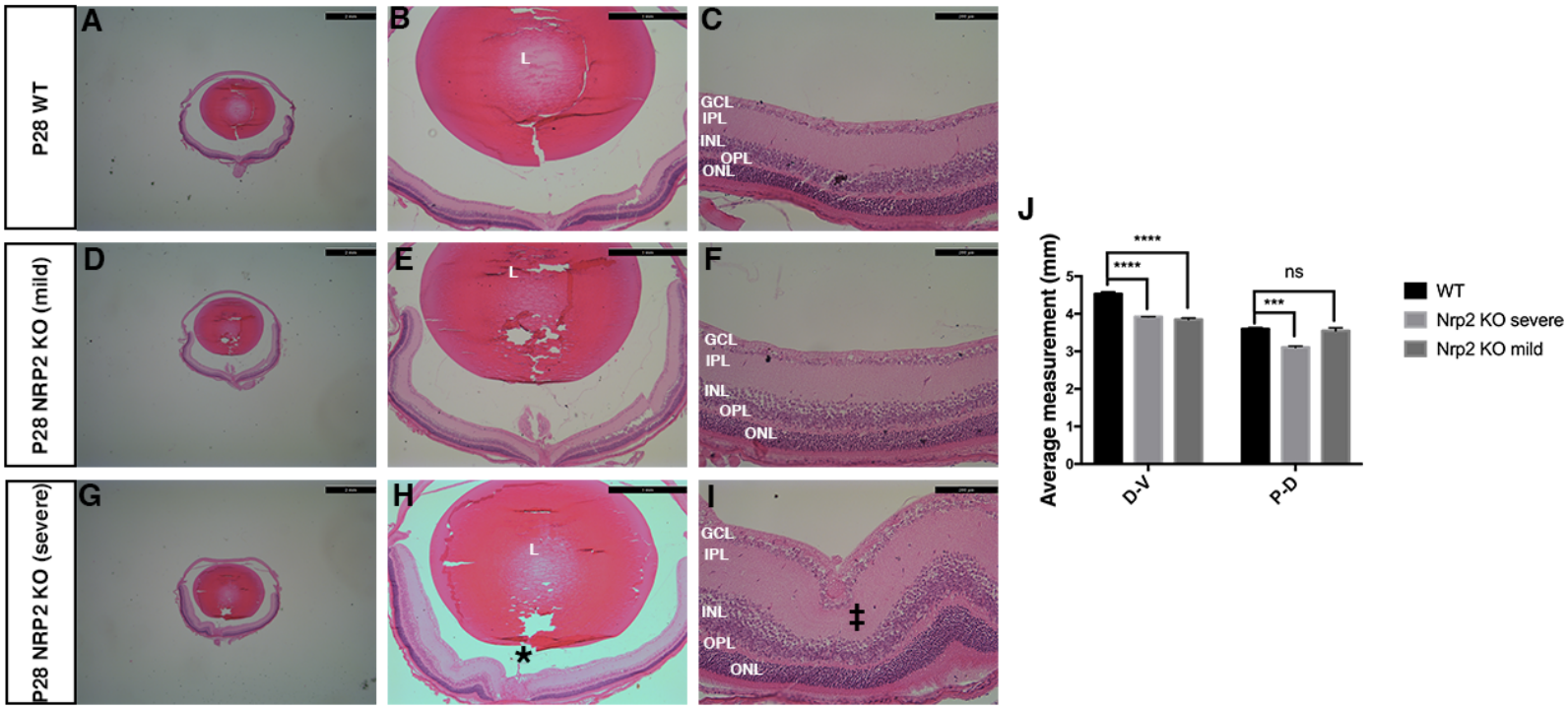
P28 WT
P28 NRP2 KO (mild)
P28 NRP2 KO (severe)
A
B
C
D
E
F
G
H
I
L
GCL
IPL
INL
OPL
ONL
*
‡
J
Average measurement (mm)
****
****
ns
***
D-V
P-D
WT
Nrp2 KO severe
Nrp2 KO mild

Figure 5.10 Microphthalmia, retinal folding, and PFV in the *Nrp2* knockout eye at P28.

Significant secondary ocular defects were observed in the Nrp2 null eye compared to WT controls. (A-C) In the P28 WT eye (N=2), the hyaloid vasculature has largely regressed. (G-I) In the severe *Nrp2* knockout mouse (N=2), significant retinal folding is observed (indicated by ‡). In addition, the vitreal space is significantly reduced and the overall size of the eye was significantly smaller (indicated by *). (D-F) Severity of *Nrp2* null phenotype varies and/or is asymmetric as the other eye from the same *Nrp2* null animal (*Nrp2* knockout mild) does not have significant retinal folding but is significantly smaller on the D-V axis. (H) Measurements of ocular size from dorsal to ventral retina (D-V) and proximal to distal (P-D) in the WT, severe, and mild *Nrp2* null eye performed with Image-J software. H&E staining was performed by P. Baddam.

[KO, knockout, ns; not significant. *** P=<0.001, ****P=<0.0001]

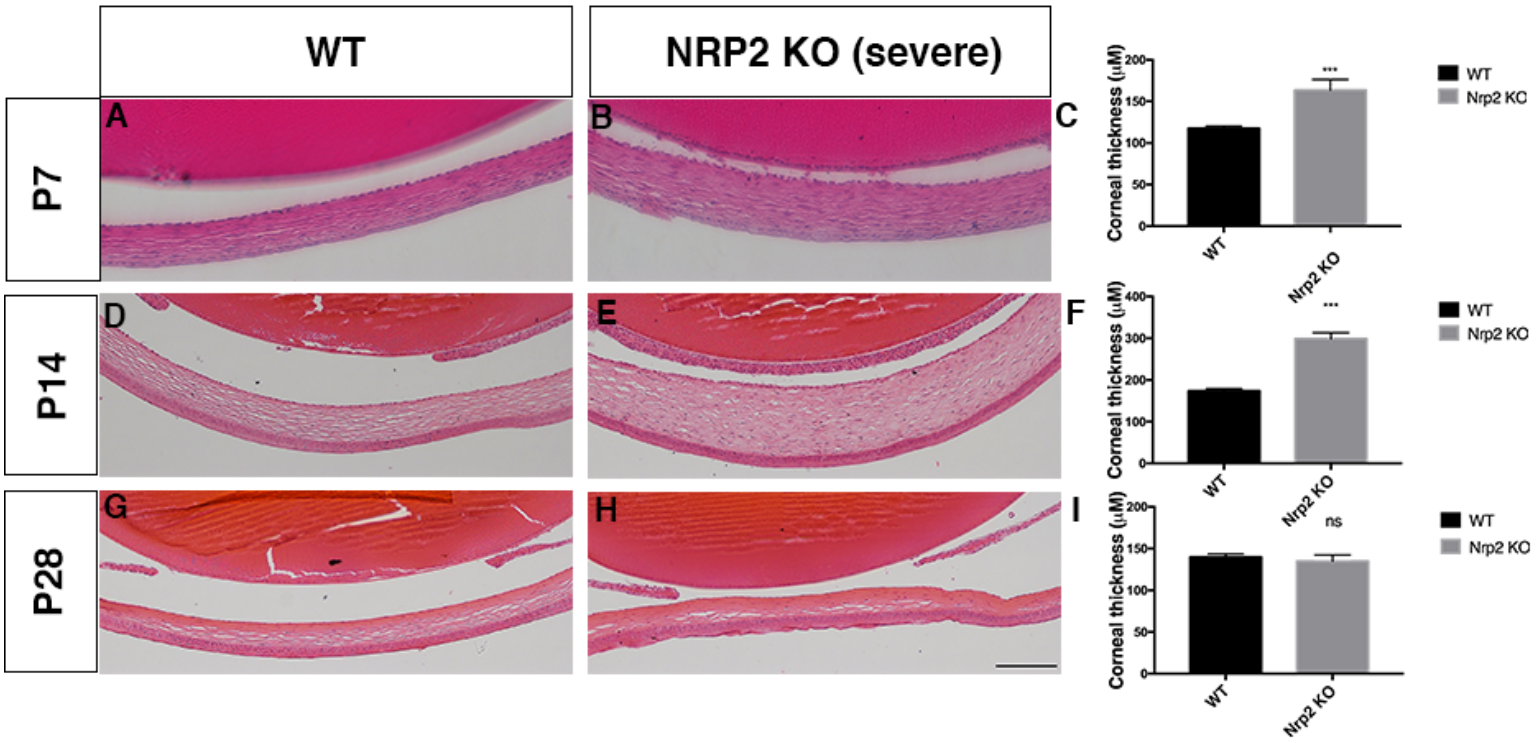

Figure 5.11 Increased corneal thickness in the *Nrp2* knockout eye.

Corneas from the *Nrp2* knockout (B, E) mice were significantly thicker when compared to WT (A, D) littermate controls at P7 and P14. (C, F) Measurements and statistical analysis for P7 and P14 corneas, respectively. There is no significant change in the thickness of *Nrp2* knockout (H) corneas compared to WT (G) littermate controls at P28. (I) Measurements and statistical analysis for P28 corneas were performed using Image-J software . H&E staining was performed by P. Baddam.

[KO; knockout, ns; not significant. *** P=<0.001, ****P=<0.0001]

5.2.4 Optical coherence tomography also shows aberrations in the retinal cell layers

Since the *Nrp2* null mice are viable and fertile into adulthood, their retinas can also be live-imaged using non-invasive OCT imaging techniques. We performed preliminary OCT (N=1) to investigate retinal lamination in the *Nrp2* knockout animals and have also carried out OCT on *Nrp2* heterozygous mice (N=3). Concordant with what we observed in the less severe *Nrp2* null retina, the *Nrp2* null retina appears to have an expanded IPL compared to the WT littermate controls and may demonstrate some dysplasia near the optic disc (Figure 5.12 A, B), however this may be due to the angle of imaging, and additional OCT will need to be performed to eliminate this possibility. In the *Nrp2* heterozygous mice, we observed that 1/3 of the animals examined had expansion of the inner retinal layers (Figure 5.12 C, D). We are currently in the process of generating several more litters of *Nrp2* knockout mice and *Nrp2* heterozygous mice (P28) to repeat OCT imaging. In addition to further OCT imaging of the retina, we will also image the anterior segment to determine if the cornea is thickened in accordance with the H&E staining results.

5.2.5 Persistent pupillary membrane in the Nrp2 heterozygous eye

In addition to preliminary OCT, we carried out preliminary fundoscopic imaging and fluorescent angiography on WT mice and *Nrp2* heterozygous mice to examine the mature retinal vasculature (N=2). We did not have *Nrp2* knockouts available at the time of analysis. Interestingly, however, both the *Nrp2* heterozygous animals examined appeared to have PFV in the form of persistent pupillary membranes (Figure 5.13). In addition, during the fundoscopic imaging and angiography we were unable to image the mature retinal vasculature in the *Nrp2* heterozygous animals; opacity of the lens was observed inhibiting our ability to image (Figure 5.13E). These results are interesting since cataracts are a common secondary ocular pathology observed in PFV patients (Hobbs and Hartnett 2014). However, the opacity could also be attributed to the imaging process. Again, these results are preliminary and we will repeat the

fundoscopy and angiography on WT and *Nrp2* knockout eyes. These preliminary findings also illustrate that the *Nrp2* heterozygous animals may also have ocular phenotypes and will need to be examined further in future experiments.

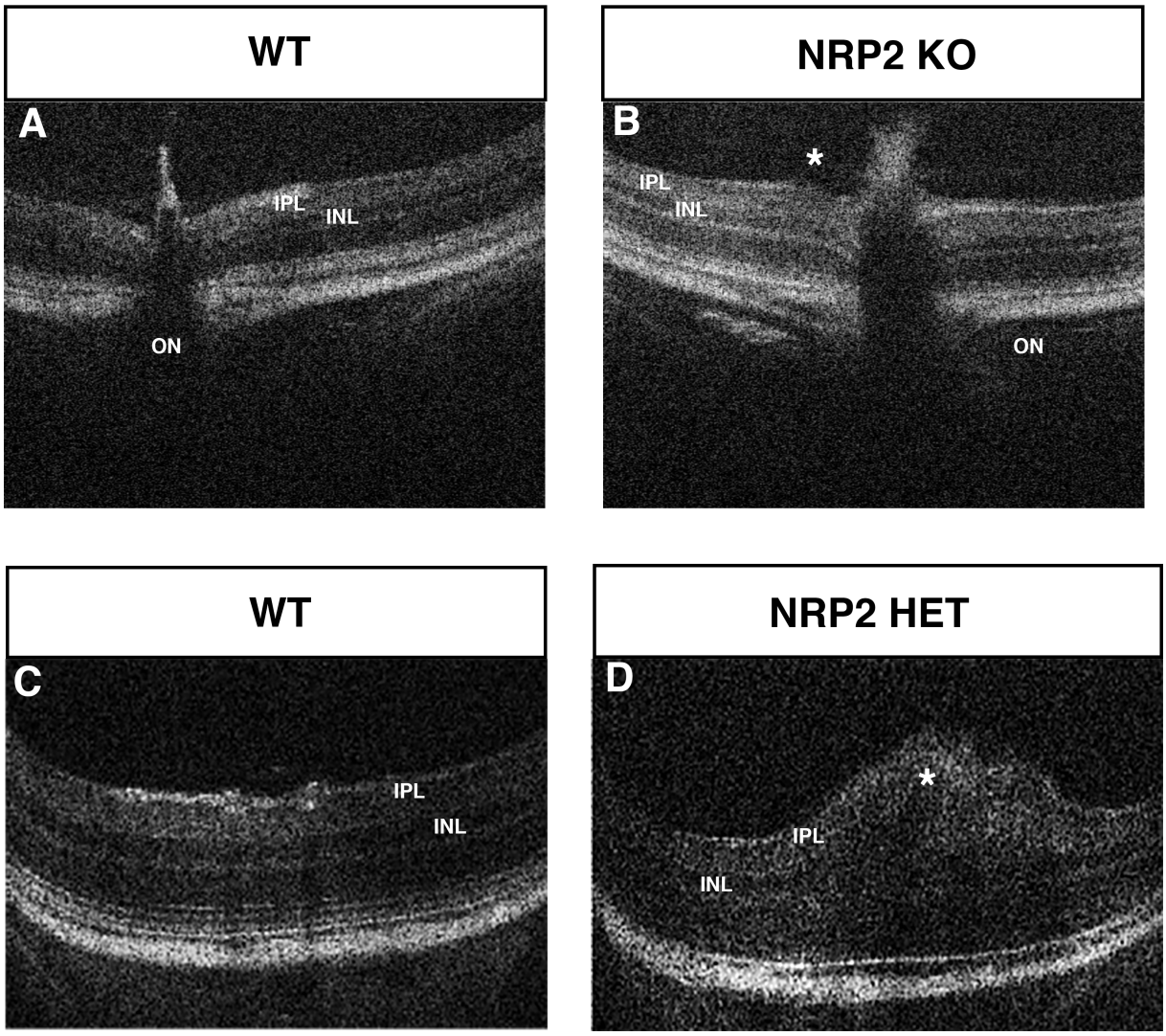

Figure 5.12 OCT imagining shows expanded IPL in *Nrp2* knockout retinas.

(A, B) Preliminary OCT imaging demonstrates that the IPL in the *Nrp2* knockout retina is increased compared to WT controls (N=1). There may also be some dysplasia near the optic disc similar to that observed in the less severe mutant *Nrp2* null retina (asterisk). (C, D) One of three Nrp2 heterozygous mice (N=3) also had expansion of inner retinal layers compared to controls.

[HET, heterozygous, INL; inner nuclear layer, IPL; inner plexiform layer, KO, knockout,ON; optic nerve]]

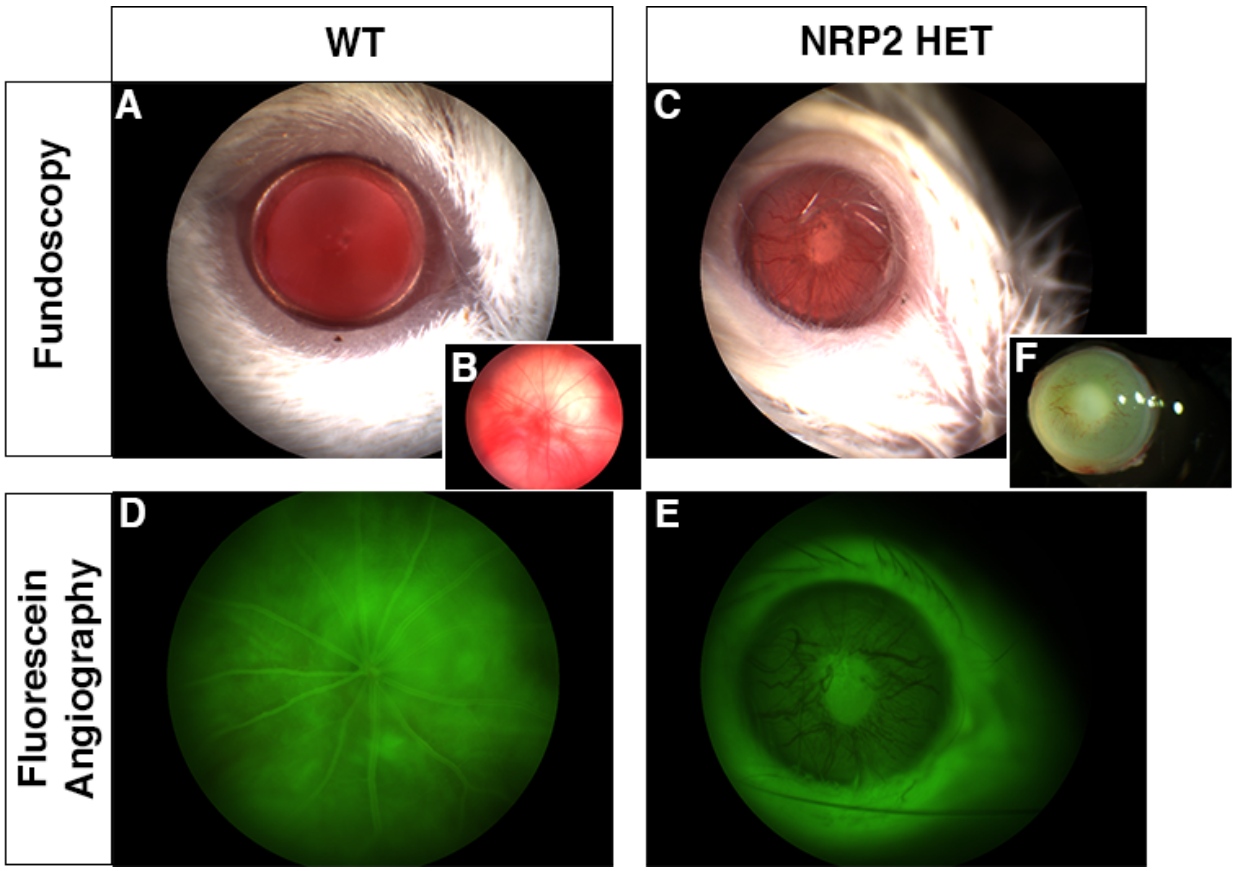

Figure 5.13 PFV in the *Nrp2* heterozygous eye.

In order to image the mature retina vasculature, fundoscopy and fluorescence angiography was performed. (A, B, D) The *Nrp2* WT mouse has a clear anterior segment (A) and normal retinal vasculature (C). (C, F, E) The mature retinal vasculature in the *Nrp2* heterozygous mouse, however, could not be imaged as lens opacity obstructed imaging. The *Nrp2* heterozygous mouse appeared to have PFV in the form of persistent pupillary membranes.

5.2.6 Retrolental mass contains vascular and neural crest cells

While the localization of the retrolental cell mass in the *Nrp2* knockout vitreous is reminiscent of PFV, we sought to confirm that the retrolental mass in the vitreous of *Nrp2* knockout mice contained vascular cells. Immunostaining was carried out on *Nrp2* knockout retinas using a widely used endothelial cell marker, IB4, and a blood vessel marker, Collagen IV. Collagen IV is present in basement membranes of blood vessels and has been previously used to examine mature retinal vessels (Mao et al. 2015, Bai et al. 2009), the hyaloid vasculature system (Sarthy 1993, Snead et al. 2002), and the lens capsule (Kelley, Sado, and Duncan 2002). In both the WT and *Nrp2* null eyes at E13 (N=3) and E18 (N=3), IB4 was highly expressed in the lens, likely as part of the TVL/pupillary membrane capillary network (Figure 5.14). In the E13 WT eye, IB4 was expressed in the hyaloid vasculature as would be expected at this early developmental time point (Figure 5.14A). In the WT E18 eye, IB4 expression was observed in the remnants of the regressing hyaloid artery (Figure 5.14C). In the *Nrp2* knockout eye at both E13 and E18, IB4 expression was increased in the hyaloid compared to the hyaloid vasculature system in the WT littermate control eyes (Figure 5.14B, D). Collagen IV had a similar expression pattern in the hyaloid vasculature to that observed with IB4 immunostaining. Collagen IV expression was observed in the WT hyaloid vasculature, the choroid, and in the basement membrane surrounding the developing lens (lens capsule) at E13 (N=3) and E18 (N=3) (Figure 5.15). In the E13 and E18 *Nrp2* knockout eyes, Collagen IV expression was elevated in the retrolental mass in the vitreous of the *Nrp2* knockout eye (Figure 5.15B, D) (N=3). In addition, we carried out co-expression analysis of NRP1 and Collagen IV in both WT and *Nrp2* knockout retinas to further verify the presence of increased vascular cells in the vitreous of the *Nrp2* null eye. *Nrp1* is expressed in retinal blood vessels (Kawasaki et al. 1999, Fantin et al. 2014) and is also expressed in the developing hyaloid vasculature as observed in our NRP1 immunostaining results above (Figure 5.3). In the WT retina, NRP1 and Collagen IV expressing cells co-localize in the hyaloid vasculature as expected (Figure 5.16A-C). In the *Nrp2* null eye, an increase in the

number of cells expressing both NRP1 and Collagen IV was observed in the vitreal space, further confirming the increase in hyaloid vasculature cells present in the *Nrp2* null eye (Figure 5.16D-F).

We also examined expression of the non-functional NRP2 protein in the *Nrp2* null eye at E13. Because our *Nrp2* knockout mouse is created using a gene trap that disrupts the MAM (Meprin-A5 antigen-μ tyrosine phosphatase) domain of the NPR2 protein (Chen et al. 2000), we were able to use a NRP2 antibody recognizing an epitope upstream of the gene trap insertion site to identify expression of the non-functional NRP2 protein. We performed double immunostaining of NRP2 and IB4 to determine if non-functional NPR2 co-localized with endothelial cells in the hyaloid vasculature. Interestingly, we observed that there was an increase in cells expressing non-functional NRP2 present in the vitreous of the *Nrp2* knockout eye compared to cells expressing WT NRP2 in WT littermate controls (Figure 5.17). We also determined that cells expressing either WT NRP2 (control) or non-functional NRP2 (Nrp2 knockout) did not co-localize with IB4 positive cells, indicating that Nrp2 is not expressed in endothelial cells of the hyaloid vasculature (Figure 5.17). However, in addition to vascular endothelial cells, the hyaloid also contains cells derived from the cranial neural crest (Gage et al. 2005). *Nrp2* is known to be expressed in neural crest cells and therefore the accumulation of non-functional NRP2 expressing cells in the vitreous of the *Nrp2* knockout eye is possibly of neural crest origin (Gammill, Gonzalez, and Bronner-Fraser 2007, Choi et al. 2014). Overall, our results confirm that the retrolental mass observed in the vitreous of the *Nrp2* knockout eyes contains increased vascular cells and neural crest cells, confirming the presence of a PFV-like phenotype in the *Nrp2* knockout eye as suggested by our histological findings explained above.

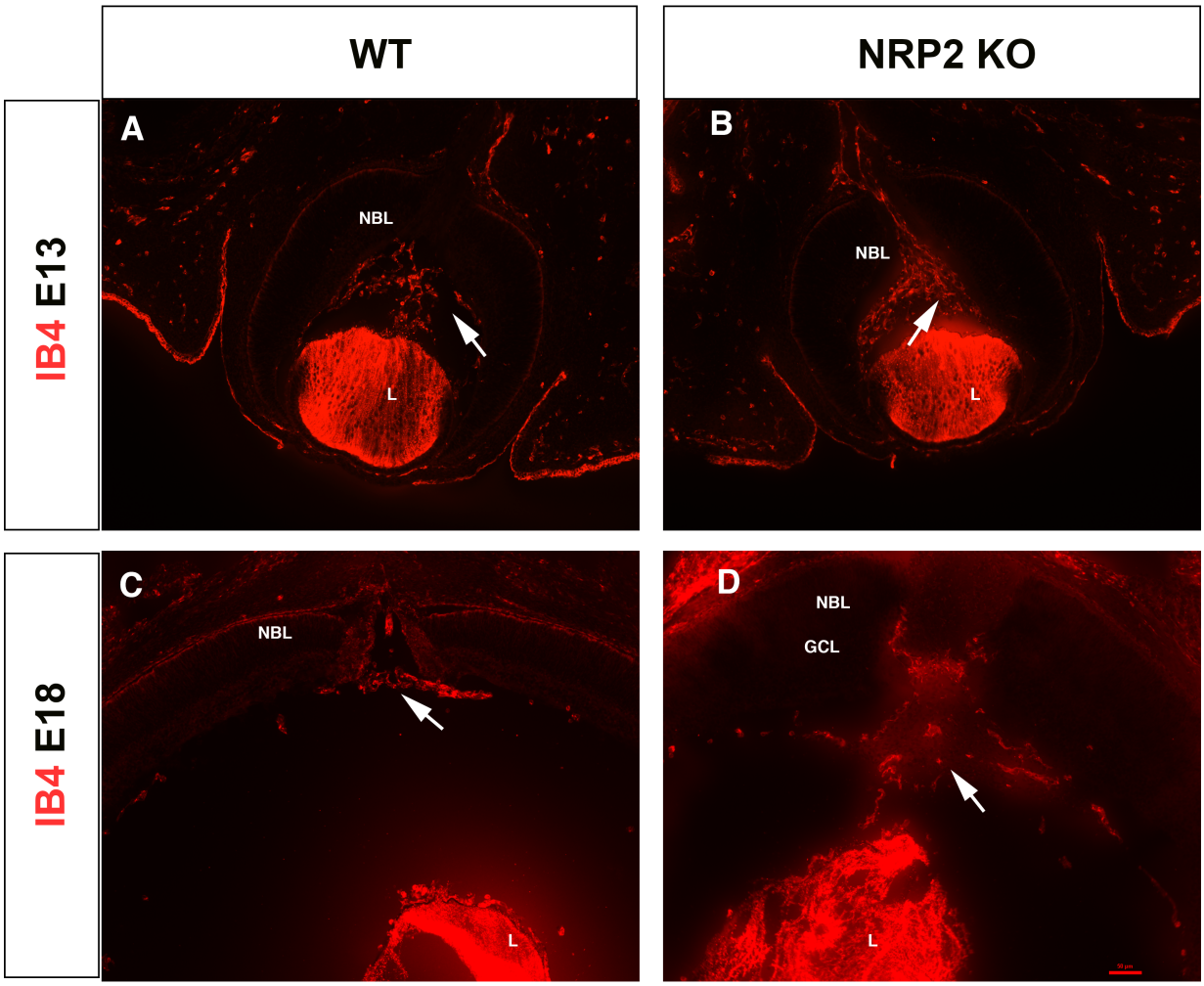
WT
NRP2 KO
IB4 E13
IB4 E18
A
B
C
D
NBL
GCL
L

Figure 5.14 Retrolental mass in the *Nrp2* knockout eye contains IB4 positive endothelial cells.

The retrolental mass in the *Nrp2* knockout eye was examined for the presence of endothelial cells by staining with IB4. (A) IB4 staining was observed in the WT hyaloid vasculature (white arrow) and the lens (TVL). (B) In the *Nrp2* knockout, an increase in cells expressing IB4 in the hyaloid vasculature is observed (white arrow). IB4 staining is also observed in the TVL in the *Nrp2* knockout (C) In the WT E18 eye, IB4 expression is observed in the TVL and is present in the remnants of the regressing hyaloid vasculature. (D) In the *Nrp2* knockout eye, many cells expressing IB4 are observed in the retrolental vitreal mass compared to WT littermate controls.

[L; lens, NBL; neuroblastic layer. Scale = 100 μm]

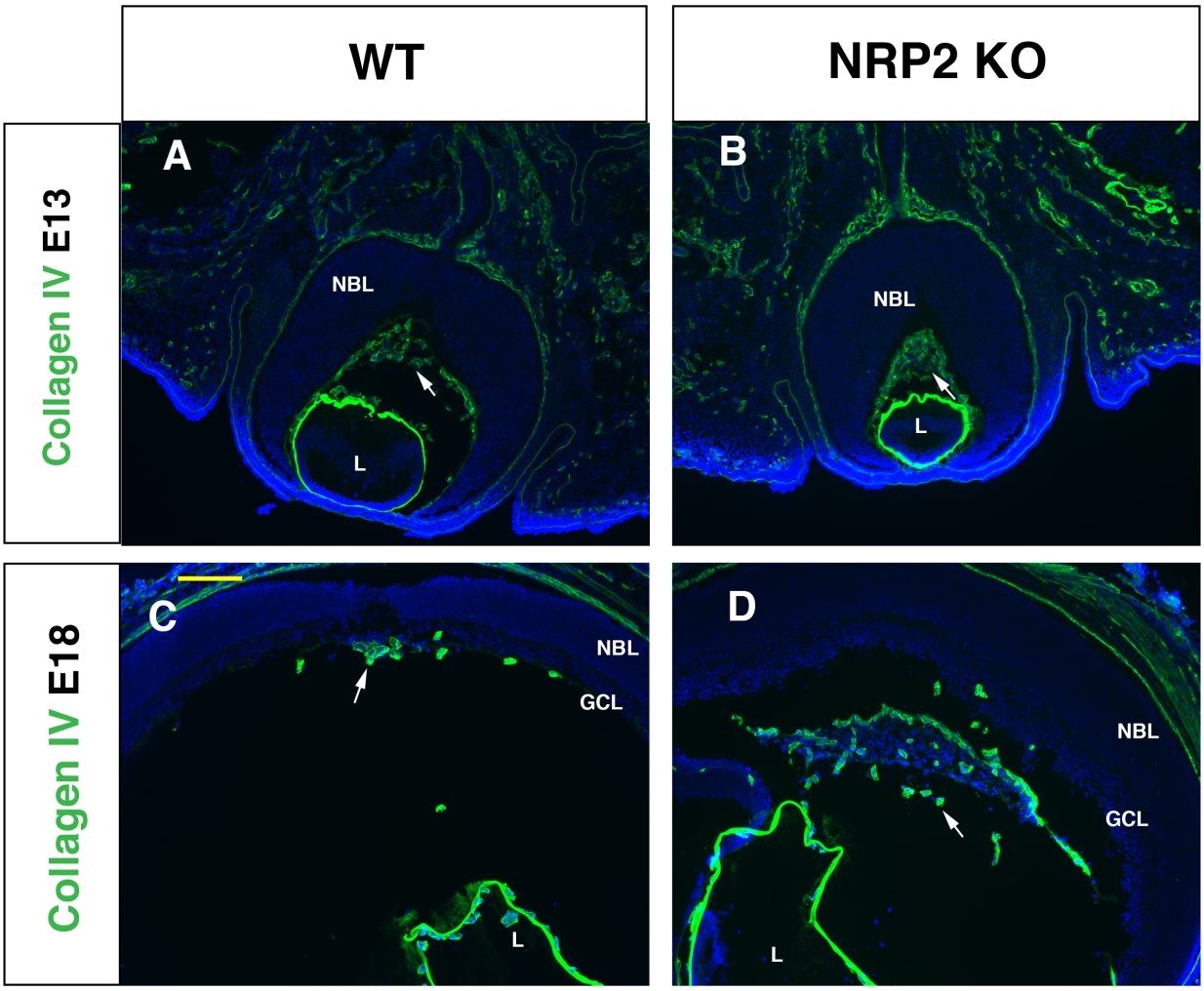
WT
NRP2 KO
Collagen IV E13
Collagen IV E18
A
B
C
D
NBL
GCL
L

Figure 5.15 Collagen IV is expressed in *Nrp2* knockout retrolental mass.

Collagen IV is a marker for blood vessels. (A) In the E13 WT eye, Collagen IV is expressed in the hyaloid (white arrow), the choroid, and the lens capsule. (B) In the E13 *Nrp2* knockout, an increase in collagen IV expression is observed in the hyaloid. Collagen IV is also present in the lens capsule and choroid. (C) At E18, Collagen IV is observed in the few remaining hyaloid vascular cells that have not yet regressed from the vitreous (white arrow). (D) The E18 *Nrp2* knockout has increased Collagen IV expression in the large vitreal hyaloid mass compared to WT littermate controls.

[GCL; ganglion cell layer, L; lens, NBL; neuroblastic layer. Scale = 100 μm]

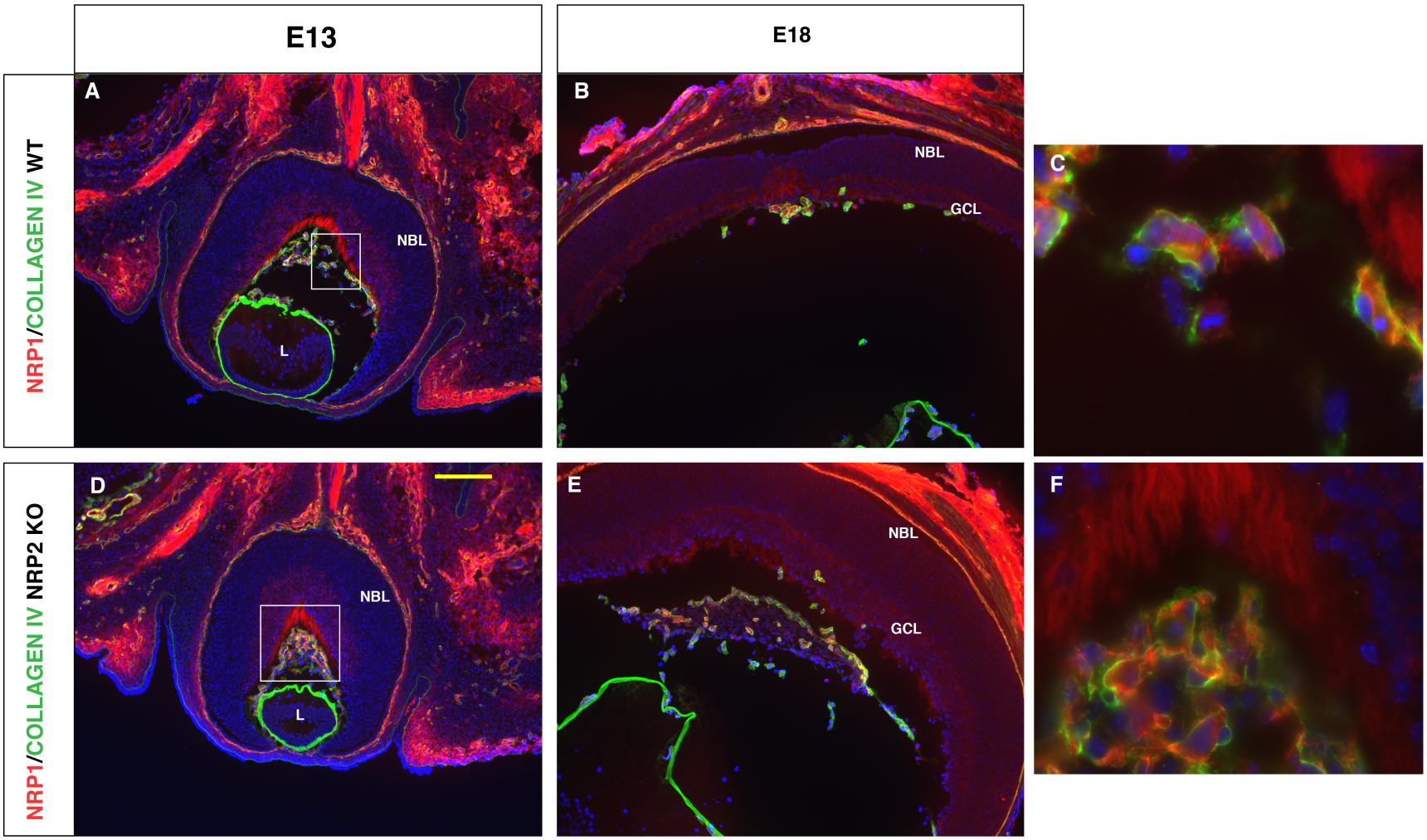
E13
E18
NRP1/COLLAGEN IV WT
NRP1/COLLAGEN IV NRP2 KO
A
B
C
D
E
F
NBL
GCL
L

Figure 5.16 Co-localization of NRP1 and Collagen IV in the vitreal mass in the *Nrp2* knockout.

Nrp1 and Collagen IV are both expressed in the ocular vasculature. (A) NRP1 expression (red) is present in the GCL, nerve fibre layer, and the hyaloid while Collagen IV (green) co-localizes with NRP1 in the hyaloid. The boxed region is magnified in (C) to demonstrate the co-localization of NRP1 and Collagen IV. (B) Co-localization of NRP1 and Collagen IV is also observed in the remnants of the hyaloid at E18. (D) At E13 in the *Nrp2* knockout, increased expression of NRP1 and Collagen IV is observed in the retrolental mass. The boxed region is magnified in (F) to demonstrate co-localization of NRP1 and Collagen IV in the *Nrp2* knockout. (E) An increase in the number of cells co-expressing NRP1 and Collagen IV was also observed in the E18 *Nrp2* knockout hyaloid.

[GCL; ganglion cell layer, NBL; neuroblastic cell layer. Scale = 100 μm]

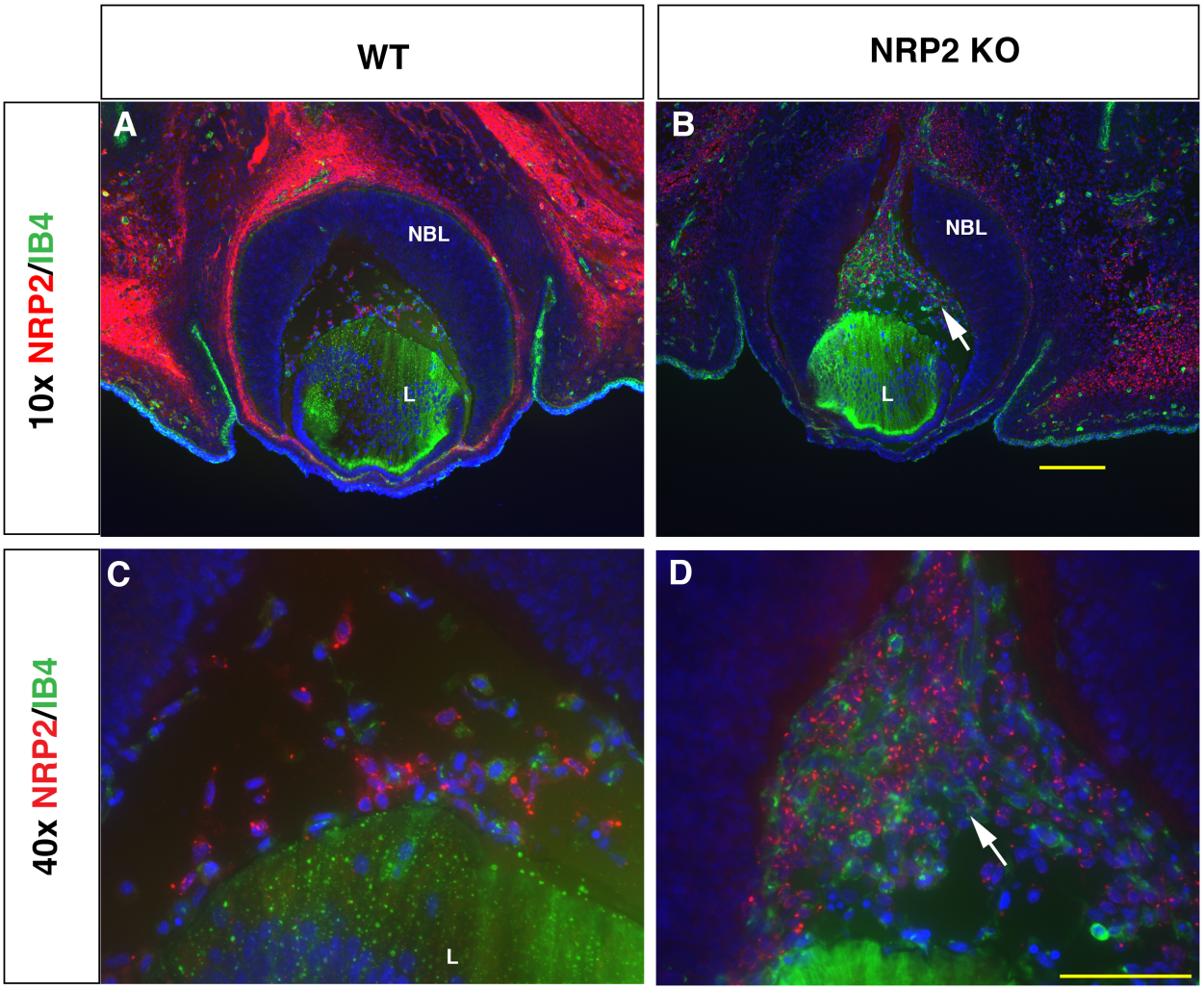

Figure 5.17 Accumulation of non-functional NRP2 positive cells in the vitreous of the *Nrp2* knockout mouse.

Co-localization of NRP2 and IB4 was examined to determine if NRP2 positive cell in the hyaloid were of endothelial origin. (A, C) In the WT control retina, few WT NRP2 (red) expressing cells were observed in the vitreous. These cells did not co-localize with IB4 positive endothelial cells (green). (B, D) In the *Nrp2* null retina, an increase in cells that expressed non-functional NRP2 (red) was observed in the vitreous. An increase in IB4 positive cells (green) was also observed, but like the WT eye, co-localization of non-functional NRP2 and IB4 was not observed.

[L; lens, NBL; neuroblastic layer. Scale = 100 µm]

5.2.7 Nrp2 negatively regulates amacrine cell differentiation

CV and H&E staining demonstrated that the IPL of the *Nrp2* knockout retina was significantly expanded compared to WT littermate controls. Visual information is relayed through the IPL via bipolar cells that synapse onto amacrine and RGC (Kolb 1995). To determine if expansion of the IPL in the *Nrp2* knockout retina was due to increased genesis of inner retinal cells including RGC and amacrine cells, immunostaining was performed using neuronal, RGC, and amacrine cell markers at different embryonic and postnatal stages of retinogenesis. Starting at E13, immunostaining was performed with the RGC-specific marker BRN3B, amacrine cell marker PAX6, and neural marker TUJ1 that stains both RGC and amacrine cells (N=3). At early embryonic development, there is no significant increase in RGC and amacrine cells in the *Nrp2* knockout retina compared to WT littermate controls (Figure 5.18). We next examined RGC and amacrine cells at later stages of embryonic retinal development. In the E18 retina, calretinin and syntaxin were each used as markers for amacrine cells, while Brn3b was again used as a RGC marker. Increases in both amacrine cells and RGC were observed at E18 in the *Nrp2* knockout compared to WT controls (Figure 5.19) (N=3). In addition, amacrine cell localization defects were observed in the *Nrp2* knockout retina, which were particularly apparent when examining syntaxin expression (Figure 5.19). In postnatal stages of retinal development (P7 (N=3), P14 (N=2), and P28 (N=2)), calretinin and TUJ1 expression was increased, and a significant expansion of the IPL was observed in the absence of *Nrp2* expression (Figure 5.20**,** Figure 5.21**,** Figure 5.22). Future qRT-PCR utilizing amacrine cell (calretinin, syntaxin, *Pax6*) and RGC (*Brn3a*, *Brn3b*) markers will allow us to quantify changes in expression of genes critical for amacrine cell and RGC development in the *Nrp2* knockout compared to WT littermate controls. These results demonstrate that during early retinal development, amacrine and RGC genesis is not initially affected. However, at later embryonic retinal development and into adulthood, an increase in amacrine cells was observed leading to marked expansion of the IPL. Our findings suggest that *Nrp2* may be dispensable for early

amacrine cell specification but is possibly required to restrict RPC from specifying additional amacrine cells to regulate the proper complement of cells in the mature retina.

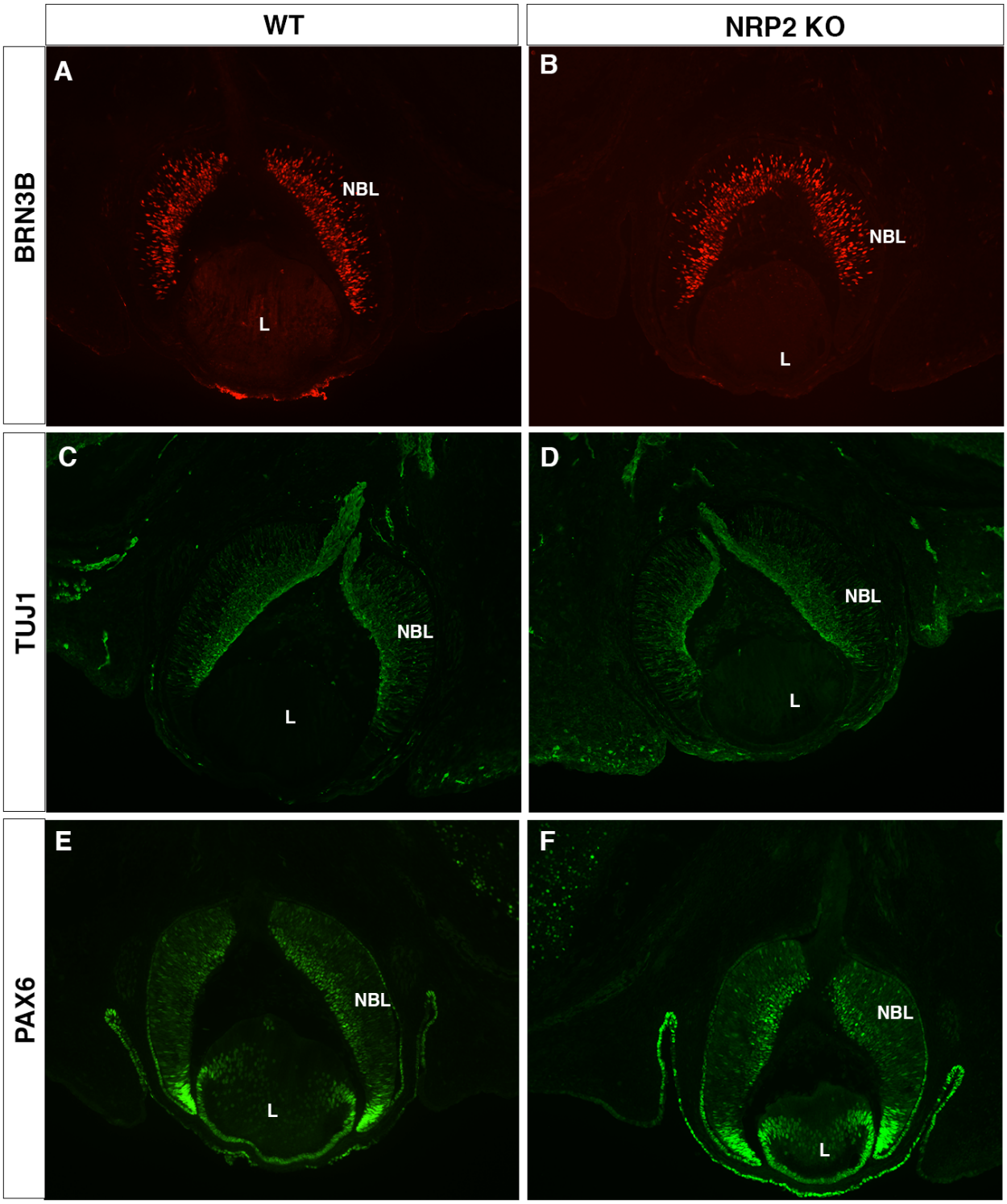
WT
NRP2 KO
BRN3B
TUJ1
PAX6
A
B
C
D
E
F
NBL
L

Figure 5.18 No change in RGC and amacrine cells is observed during early retinal development in the *Nrp2* knockout.

RGC and amacrine cell genesis was examined in the absence of *Nrp2*. (A, B) No change in RGC differentiation at E13 was observed. (C, D) Expression of the neuronal marker TUJ1 was also unchanged in the absence of *Nrp2* expression compared to control. (E, F) Early amacrine cell differentiation was also not affected in the absence of *Nrp2*.

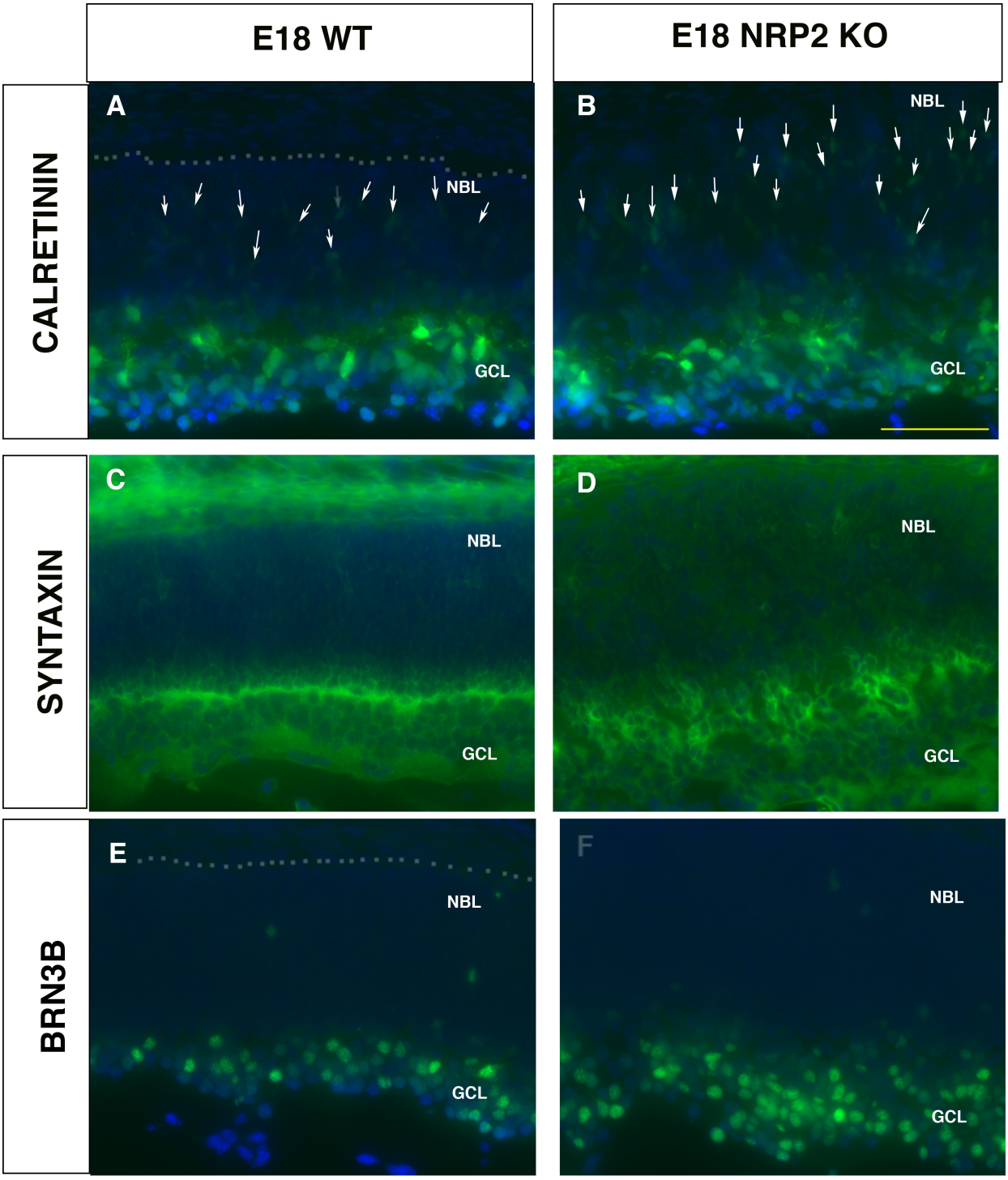
E18 WT
E18 NRP2 KO
CALRETININ
SYNTAXIN
BRN3B
A
B
C
D
E
F
NBL
GCL

Figure 5.19 Increased amacrine and RGC in the *Nrp2* knockout retina at E18.

(A, B) Calretinin expression is increased in the *Nrp2* knockout retina (arrows demonstrate increased caltretinin expressing cells in the outer NBL) (B) compared to controls (arrows demonstrate calretinin expressing cells in the outer NBL) (A) indicating an increase in amacrine cells in the absence of *Nrp2*. (C, D) Syntaxin expression is also increased in the *Nrp2* knockout (D) and showed disrupted localization of the amacrine cells within the INL. (E, F) RGC are increased in the *Nrp2* knockout retina (F) compared to WT controls (E).

[GCL; ganglion cell layer, NBL; neuroblastic layer. Scale = 100 μm. Dotted line in the WT images represent the boundary between the NBL and the RPE. This boundary is not observed in the *Nrp2* KO due to the increased retina cellularity]

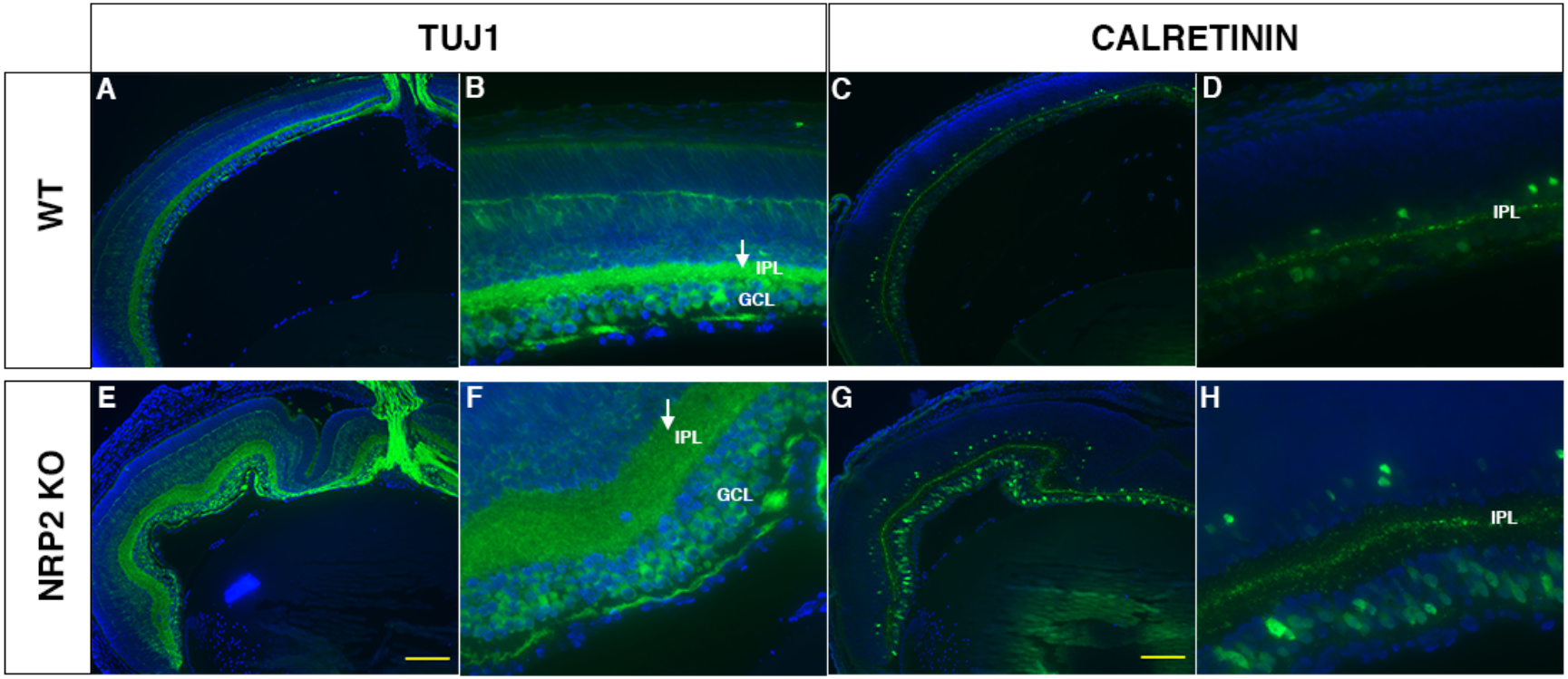

Figure 5.20 Increased amacrine cells in the P7 *Nrp2* knockout retina.

(A, B) Tuj1 is expressed in neurons in the WT retina and also marks the IPL as shown at 10x (A) and 40x (B) magnification. The white arrow in panel (B) indicates the IPL. (C, D) Calretinin stains for amacrine cells shown at 10x (C) and 40x (D) magnification. (E-H) In the *Nrp2* knockout retina, increased amacrine cells and an expanded IPL is observed in addition to retinal folding.

[GCL; ganglion cell layer, IPL; inner plexiform layer. Scale = 100 μm]

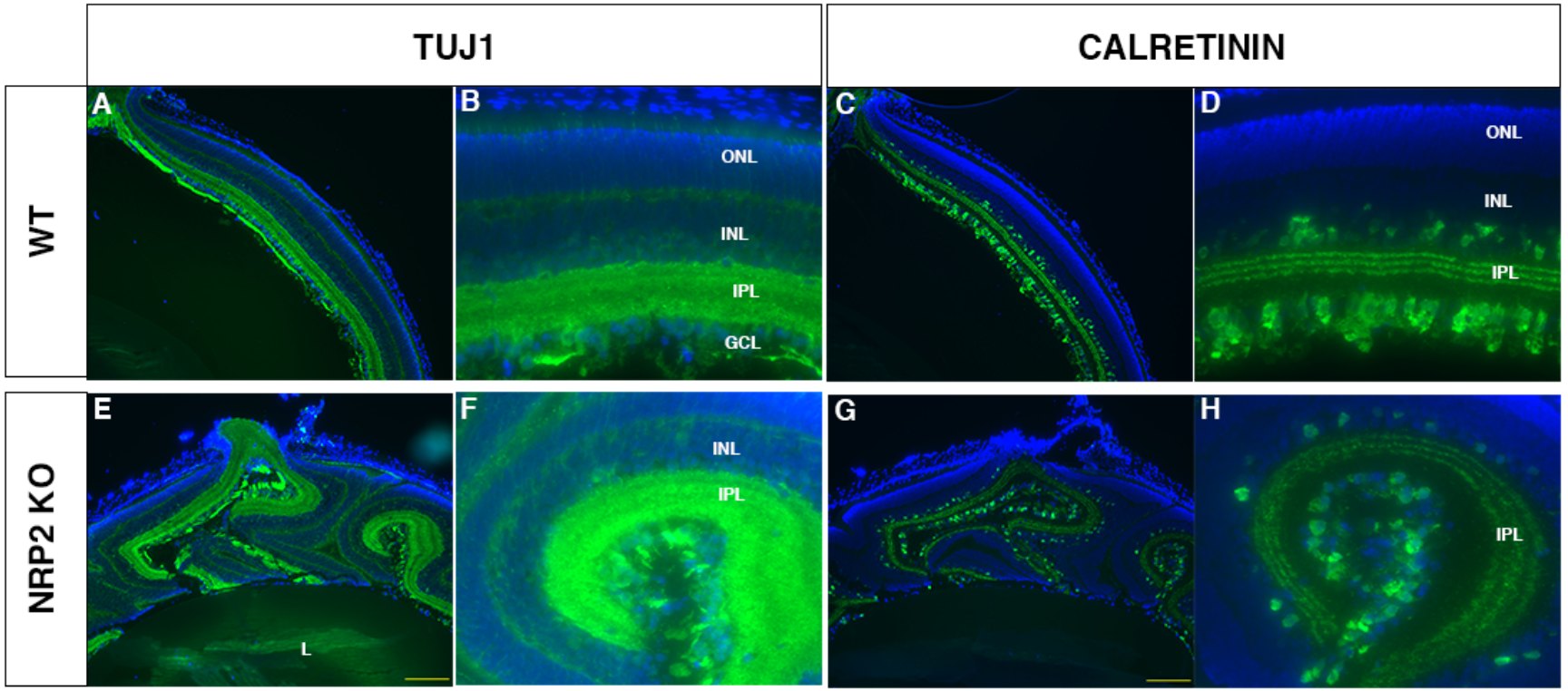

Figure 5.21 Increased amacrine cells in the P14 *Nrp2* knockout retina.

(A, B) Tuj1 is expressed in neurons in the WT retina and also marks the IPL as shown at 10x (A) and 40x (B) magnification. (C, D) Calretinin stains for amacrine cells shown at 10x (C) and 40x (D) magnification. (E-H) In the *Nrp2* knockout retina, increased amacrine cells and an expanded IPL are observed in addition to retinal folding.

[GCL; ganglion cell layer, INL; inner nuclear layer, IPL; inner plexiform layer, ONL; outer nuclear layer. Scale = 100 μm]

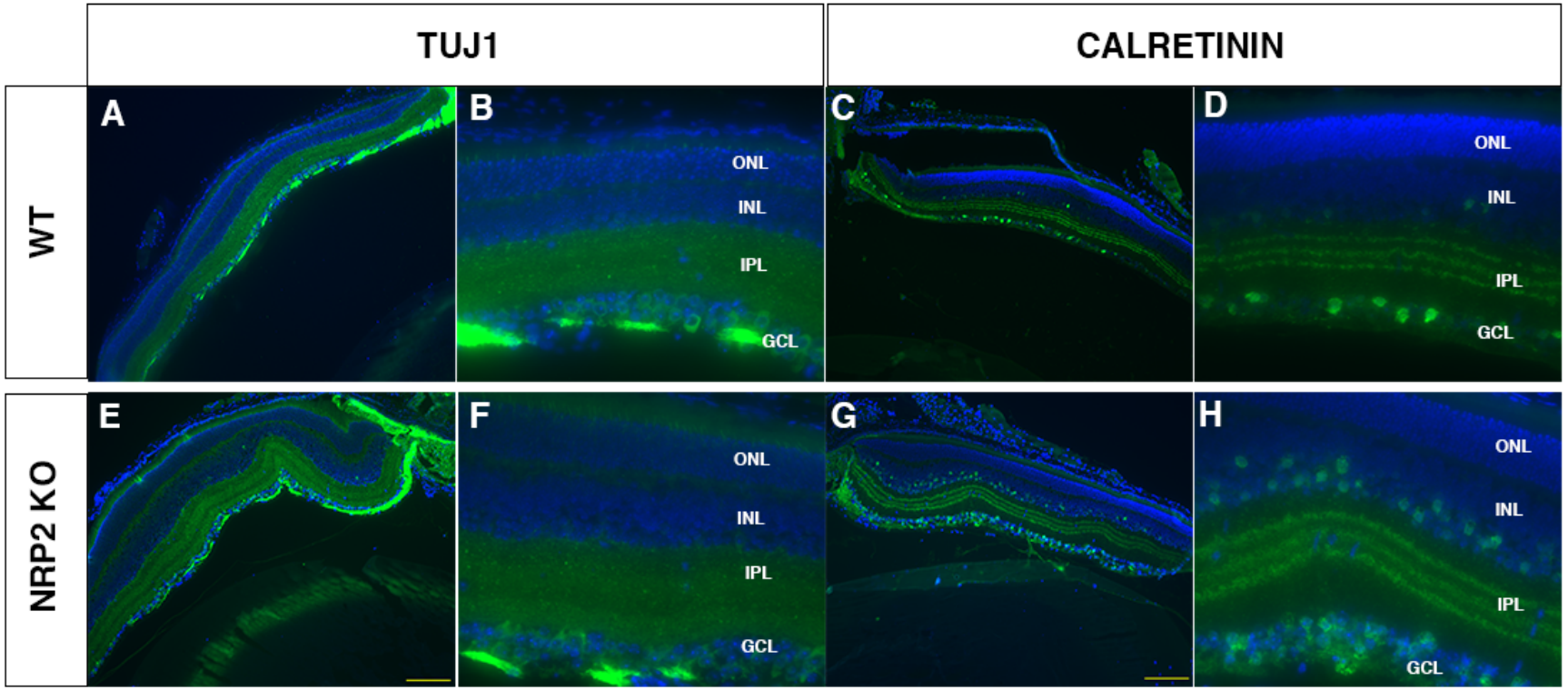

Figure 5.22 Increased amacrine cells in the P28 *Nrp2* knockout retina.

(A, B) Tuj1 is expressed in neurons in the WT retina and also marks the IPL as shown at 10x (A) and 40x (B) magnification. (C, D) Calretinin stains for amacrine cells shown at 10x (C) and 40x (D) magnification. (E-H) In the *Nrp2* knockout retina, increased amacrine cells and an expanded IPL are observed in addition to retinal folding.

[GCL; ganglion cell layer, INL; inner nuclear layer, IPL; inner plexiform layer, ONL; outer nuclear layer. Scale = 100 μm]

5.2.8 Intraretinal axonal guidance defects in the Nrp2 null retina

Nrp2 is necessary for the proper axon fasciculation and axonal guidance in the developing brain (Giger et al. 2000, Chen et al. 2000). Axonal guidance in the *Nrp2* mutant eye has not been examined. There is, however, limited information regarding the role of *Nrp1* in retinal axonal guidance. *Nrp1* expression is critical for contralateral projections at the optic chiasm (Erskine et al. 2011). Interestingly, the guidance cue that mediates axonal crossing via Nrp1 is VEGF164 instead of the class III semaphorins, which are primarily associated with axonal guidance through their interactions with neuropilins. Because *Nrp2* expression was not observed in the RGC until E18 (Figure 5.3), it is unlikely to play a significant role in RGC axon crossing at the chiasm, as the majority of RGC crossing has already occurred at this late embryonic developmental time point (Godement et al. 1987, Erskine et al. 2011). Therefore, we carried out preliminary studies on intraretinal axonal guidance in the *Nrp2* knockout retinas at E18 and adulthood to determine if *Nrp2* was involved in the fasciculation of axons in the retina. We did not examine earlier than E18, as we did not observe *Nrp2* expression in the RGC at earlier time points. RGC axons were visualized in whole-mount retinas by immunostaining with a neuron-specific β-tubulin (TUJ1). In the E18 retina, axon fasciculation is disorganized in the *Nrp2* knockout, particularly toward the optic disc compared to WT controls (Figure 5.23) (N=1). In the *Nrp2* adult knockout retina, the axon bundles appear thinner than the WT counterpart (Figure 5.23). These findings demonstrate that there may also be a role for *Nrp2* in intraretinal axonal guidance, which will be an interesting avenue of investigation for future studies into the role of *Nrp2* genes in retinal development.

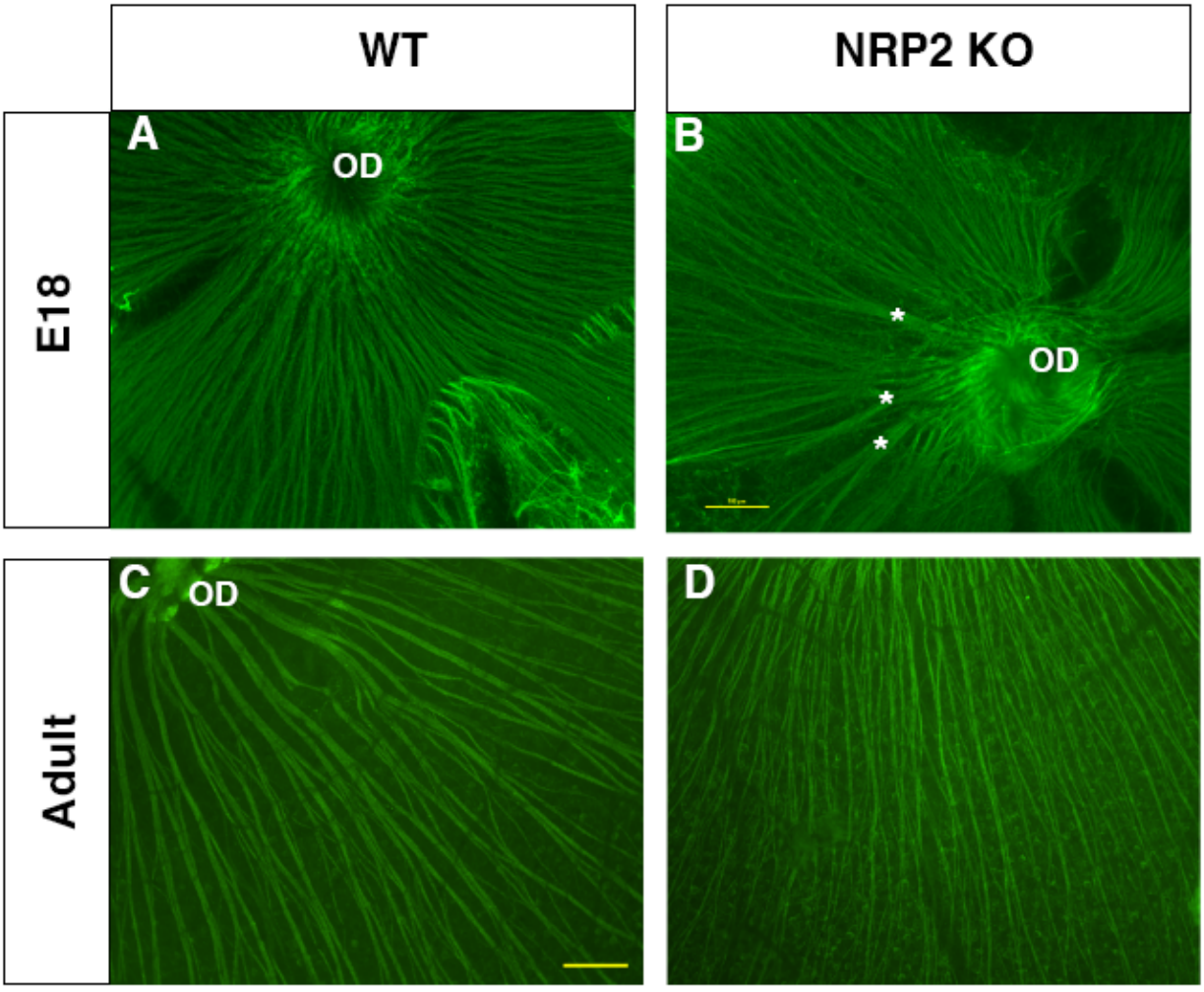

Figure 5.23 Intraretinal axonal guidance defects may be present in the *Nrp2* null retina.

Nrp2 null mice were examined for intraretinal axonal guidance defects using a TUJ1 antibody. (A, B) At E18, fasciculation of axonal bundles appears disrupted, particularly toward the optic disc (asterisks). (C, D) In the adult retina, bundles appeared much thinner and more numerous in the *Nrp2* knockout retina compared to WT controls.

[OD; optic disc. Scale = 100 μm]

5.2.9 Shh signalling is not affected in the absence of Nrp2 expression in the retina

Several different genetic mutations have led to the development of PFV in mice (Hegde and Srivastava 2016). One such mutation is a lens-specific deletion of smoothened (Smo) (Choi et al. 2014). When *Smo* expression is absent from the lens, a number of ocular abnormalities are present including smaller lenses, thickened corneas, and a retrolental mass. Both Nrp2 and Nrp1 are positive regulators of the Hedgehog pathway and contribute to vascularization and proliferation of medulloblastomas through activation of Shh signalling (Hayden Gephart et al. 2013, Hillman et al. 2011). Therefore, we considered that *Nrp2* loss could result in reduced Shh signalling, and lead to the development of a retrolental mass and thicker cornea as observed in the lens-specific *Smo* mutant. We performed qRT-PCR on RNA extracted from E13 *Nrp2* mutant retinas using primers for the downstream Shh transcription factors *Gli1*, *Gli2*, and *Gli3*. There was no significant change observed in *Gli1*, *Gli2*, or *Gli3* expression in the heterozygous and *Nrp2* knockout retinas (Figure 5.24) (N=3) suggesting that the PFV phenotype observed in the *Nrp2* mutant retina is independent of Shh signalling.

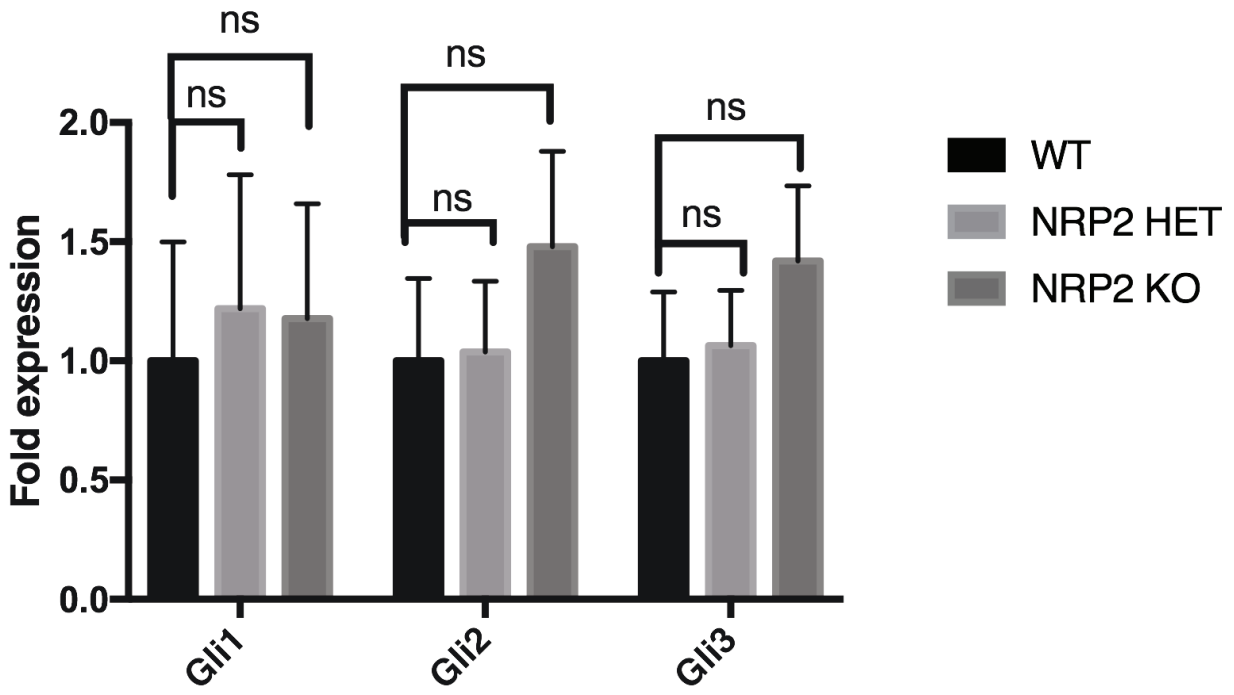

Figure 5.24 Shh signalling is not affected in the absence of *Nrp2* during early retinal development.

The lack of *Smo* in the developing lens results in the development of a retrolental mass. Neuropilins have been described to regulate Shh signalling and therefore we examined expression of downstream Shh transcription factors *Gli1*, *Gli2*, and *Gli3* in the *Nrp2* null eye at E13. There was no significant change in Shh signalling in the *Nrp2* heterozygous eye or *Nrp2* null eye compared to WT littermate controls (N=3). Unpaired t-tests were used to determine statistical significance.

5.3 Discussion

5.3.1 Nrp2 is critical for the development of the hyaloid vasculature

To our knowledge, this study shows for the first time that *Nrp2* is essential for development of the hyaloid vascular system. While the precise molecular mechanisms governing hyaloid vessel regression remain unclear, several gene knockout models have been generated which develop PFV, many of which have a similar phenotype to that observed in the Nrp2 knockout mouse (Table 5). These models provide some clues as to the potential mechanisms contributing to the PFV observed in the *Nrp2* knockout. As described above, *Nrp2* has been shown to positively regulate Shh signalling, and lens-specific *Smo* mutations generate a PFV phenotype (Choi et al. 2014, Hillman et al. 2011). However, our findings determined that Shh signalling was not affected in the absence of *Nrp2* (Figure 5.24). It is plausible that Nrp2 may affect Shh signalling at later developmental time points, as E13 was the only pup age examined to date. Future qRT-PCR investigating Shh signalling at later developmental time points (E18, P7, P14) could clarify whether Shh signalling is temporally affected in the absence of *Nrp2*. Next, it has recently been shown that RGC-specific expression of VEGFR2 in neonatal retinas is required for regression of the hyaloid (Yoshikawa et al. 2016). Neuronal expression of VEGFR2 gradually increases at postnatal stages and is required to sequester VEGF from the vitreous, triggering regression of the hyaloid. Therefore, failure to sequester VEGF results in excessive vitreal VEGF and persistent hyaloid vasculature. Since Nrp2 is a co-receptor for VEGFR2, perhaps Nrp2 could also be playing a critical role in sequestering VEGF from the vitreous. Future experiments assessing the vitreal expression of VEGF in the absence of *Nrp2* expression would help determine whether Nrp2 is playing a role in sequestering VEGF from the vitreous. If Nrp2 was in fact critical for this process, we would expect to see elevated levels of VEGF in the vitreous of *Nrp2* knockout mice compared to WT littermate controls. In addition, should Nrp2 be involved in sequestering vitreal VEGF, it would be interesting to examine a DKO of *Nrp2* and retinal neuron-specific deletion of VEGF (*Vegfa*) to determine if the PFV and retinal folding

observed in the *Nrp2* null retina can be rescued by the removal of VEGF. This DKO would provide evidence that excessive vitreal VEGF in the absence of *Nrp2* contributes to the mechanism of PFV generation in the *Nrp2* knockout model.

Another potential mechanism for the persistent hyaloid observed in the *Nrp2* null eye is reduction of TgfβII signalling. Two mouse knockouts have been generated that indicate TgfβII signalling is involved in the development of PFV. The first model is an *Arf* null mouse model. In the absence of *Arf* expression, an accumulation of hyaloid cells in the vitreous at levels exceeding that of the WT eye were observed during embryonic development (Silva et al. 2005). Postnatal time points were not examined in the *Arf* study. A follow-up study by the same group determined TgfβII signalling is required for *Arf* expression (Freeman-Anderson et al. 2009). TgfβRII knockout eyes have a similar phenotype to the *Arf* mutant animals with a retrolental mass present at E13 and E18. Again, no postnatal time points were examined. Interestingly, TgfβRII has been shown to form protein complexes with neuropilins but binds with higher affinity to NRP2 (Glinka et al. 2011). In addition, Nrp1 has been shown to both positively and negatively regulate Tgfβ signalling (Aspalter et al. 2015, Rizzolio and Tamagnone 2011). Therefore, a possible mechanism for hyaloid regression in the murine retina may involve Nrp2-mediated upregulation of TgfβII signalling or a requirement for Nrp2 co-receptor binding to TgfβRII to mediate TgfβII signalling in the ocular structures. Therefore, future investigation of TgfβRII expression in the absence of *Nrp2* and examination of downstream pSMAD2/3 signalling would allow us to determine if the TgfβRII pathway is disrupted in the absence of *Nrp2*, contributing to the PFV observed in the *Nrp2* knockout eye. Disruption of TgfβII signalling may also contribute to the amacrine cell differentiation defect observed in the *Nrp2* knockout retina and will be discussed below.

Lastly, the hyaloid vascular system contains both vascular cells and cells derived from the neural crest (Gage et al. 2005). Our study determined that *Nrp2* expression is observed in the hyaloid but not in endothelial cells (Figure 5.17). In addition, we observed an accumulation

of non-functional NRP2 expressing cells in the vitreous of the *Nrp2* knockout mouse. Previous studies have determined *Nrp2* is expressed in neural crest cells, and has even been utilized as a neural crest cell marker for the retrolental mass observed in the lens-specific *Smo* mutant (Choi et al. 2014, Lumb et al. 2014). The increase in non-functional NRP2 expressing cells observed in the vitreous of the *Nrp2* knockout eye may suggest that there is aberrant migration of neural crest cells into the vitreous in the absence of *Nrp2* expression. Double immunostaining experiments in the *Nrp2* null eye with NRP2 and neural crest markers such as SOX10 and/or AP2 would provide further evidence for this hypothesis. *Nrp2* expression has also been observed in the periocular mesenchyme, which is derived from the neural crest and is also highly expressed in the mesenchyme that surrounds the optic nerve (McKenna, Munjaal, and Lwigale 2012, Gammill, Gonzalez, and Bronner-Fraser 2007, Gage et al. 2005, Cvekl and Tamm 2004, Erskine et al. 2011). Migration of cranial neural crest cells that express *Nrp2* respond to repulsive guidance cues from Sema3F and loss of either *Nrp2* or *Sem3F* results in aberrant neural crest cell migration (Gammill, Gonzalez, and Bronner-Fraser 2007). However, the migration of neural crest cells into the ocular structures in the absence of *Nrp2* or *Sema3F* has not been examined. *Sema3F* expression is observed throughout the neural retina, periocular mesenchyme, and presumptive cornea at low levels at E12.5 (McKenna, Munjaal, and Lwigale 2012). It is possible that loss of *Nrp2* expression in neural crest cells render them unresponsive to the restrictive guidance cues present in the neural retinal and periocular mesenchyme, allowing the neural crest cells to migrate aberrantly into the vitreous. This lack of negative guidance response and elevation of neural crest cells into the periocular region may also be a contributing factor to the increase in corneal thickness observed in the *Nrp2* knockout retina (Cvekl and Tamm 2004, Sowden 2007). To determine if the increased hyaloid vasculature observed in the *Nrp2* knockout mouse is due to increased migration of neural crest cells into the vitreous, neural crest cell specific knockouts of *Nrp2* could be examined in the future. *Wnt1*-Cre drivers have been widely utilized for neural crest-specific gene deletion (Lewis et al. 2013, Chai

et al. 2000, Brewer et al. 2004). These mice could then be bred to *Nrp2*-flox mice to specifically delete *Nrp2* in neural crest cells.

In addition to PFV, several secondary ocular defects were observed in the *Nrp2* knockout retinas that are consistent with congenital PFV diagnosed in humans, including retinal folding and microphthalmia (Pollard 1997, Goldberg 1997). Several other murine genetic models of PFV also have retinal folding and microphthalmia similar to the *Nrp2* knockout mouse (Table 5). Future directions for examination of the *Nrp2* knockout eye include performing additional OCT live-imaging of the retina to conclusively demonstrate that the retinal folding observed is due to the loss of *Nrp2* expression and to further determine if *Nrp2* mutations result in unilateral development of PFV and/or reduced penetrance.

While severe retinal folding and reduction in ocular size was observed in the *Nrp2* knockout mice, the severity of this phenotype was asymmetrical. It is possible that the unilateral phenotype observed is due to the nature of the insertion *Nrp2* gene trap utilized to generate the *Nrp2* null mouse. Again, the *Nrp2* knockout mouse studied in our laboratory was generated by an insertional gene trap mutation that inserts into a *Nrp2* intron at cDNA position 2069, disrupting the MAM domain (Chen et al. 2000). Because the gene trap inserts into an intron, there is the possibility of alternative splicing, which can result in the formation of hypomorphic alleles and low levels of WT transcripts (McClive et al. 1998, Stanford, Cohn, and Cordes 2001). The *Nrp2* gene trap null mouse has been described as a severe Nrp2 hypomorph with some remaining WT *Nrp2* expression observed (Chen et al. 2000). It is therefore possible that the gene trap vector could be spliced out upon transcript processing, resulting in elevated WT transcript levels in one eye of the *Nrp2* knockout. This hypomorphic expression of *Nrp2* may contribute to the asymmetrical phenotype observed in the *Nrp2* null animals. A hypomorph of *Nrp1* was recently generated in which retinal angiogenesis was delayed compared to WT controls (Fantin et al. 2014). At P7, the primary vascular plexus in the *Nrp1* hypomorph failed to

reach the retinal margin. By P21 angiogenesis in the *Nrp1* hypomorph had recovered and the primary vascular plexus had reached the retinal margin. Therefore, perhaps elevated levels of WT Nrp2 transcript present in one eye of the Nrp2 hypomorphic mouse is sufficient to produce the mild *Nrp2* knockout phenotype. Alternatively, the differences in severity could be due to random somatic mutations occurring in one of the eyes of the *Nrp2* knockout mouse that is sufficient to "tip the balance" toward a more severe phenotype in the absence of *Nrp2* expression. It would be interesting to determine if similar findings were observed in the complete *Nrp2* null mouse model (Giger et al. 2000) eliminating the possibility of alternative splicing problems that may potentially arise when using the gene trap.

In the less severe *Nrp2* postnatal knockout eye, PFV was observed. However, due to the significant retinal folding and reduction in vitreal space observed in the more severe postnatal *Nrp2* knockout eye it is difficult to determine if the hyaloid has in fact regressed. It is plausible that the persistence of the hyaloid vasculature directly contributes to the reduction in the vitreal space observed in the *Nrp2* null eye. Embryonic development of the vitreous occurs in three stages, which include development of the primary vitreous, secondary vitreous, and the tertiary vitreous. Primary vitreous development is equivalent to the transient hyaloid vasculature (hence persistent hyperplastic primary vitreous as the previous disease nomenclature) (Ponsioen, Hooymans, and Los 2010). The secondary vitreous is an avascular network of collagen fibrils and hyaluronan that produce and maintain the clear gel of the vitreal body (Bishop 2000, Ponsioen, Hooymans, and Los 2010). The tertiary vitreous is generated from the developing ciliary body (Ponsioen, Hooymans, and Los 2010). During development of the secondary vitreous, the collagen fibrils remodel the regressing hyaloid vessels into a scaffold upon which the secondary vitreous is developed (Los 2008). While very little is known regarding the mechanisms that direct hyaloid remodelling into the secondary vitreous, perhaps the lack of regression of the embryonic hyaloid observed in the *Nrp2* knockout mouse inhibits the

generation of the secondary vitreous, resulting in a significantly reduced vitreal space postnatally.

To date, no human *NRP2* mutations have been described in PFV or other ocular diseases. PFV can also occur with other ocular disorders including Norrie disease and familial exudative vitreoretinopathy (FEVR) (Dhingra et al. 2006, Downey et al. 2006). Both Norrie disease and FEVR are due to mutations in canonical Wnt signalling, where Norrie disease results from mutations in the ligand Norrin, and FEVR arises from mutations in FZD4 or low-density lipoprotein receptor-related protein 5 (LRP5), both of which are co-receptors for Norrin (Ye et al. 2009). Recently, inhibition of Wnt signalling was shown to result in downregulation of *Nrp2* expression (Ji et al. 2015). Therefore, perhaps loss of downstream *Nrp2* expression phenocopies the PFV defects observed in Norrin/FZD4/LRP5 mutations. While we did not examine the mature retinal vasculature in the *Nrp2* null mouse, future directions would include examination of the mature retinal vasculature to determine if there is a delay in mature retinal vessel development as this process is concurrent with the regression of the hyaloid vasculature. It would also be of great interest to examine PFV patient DNA to potentially identify novel mutations in *NRP2*.

Table 5: Genetic models with phenotypes similar to Nrp2 KO

KO model	**Ocular defects**	**Reference**
Nrp2	Retrolental mass, retinal folding, microphthalmia, small embryonic lens, thickened corneas	
Arf	Retrolental mass, microphthalmia	(Thornton et al. 2007)
Bax/Bak	Retrolental mass, cataract, retinal folding	(Hahn et al. 2005)

CryβA3/A1	Retrolental mass, cataract, microphthalmia	(Sinha et al. 2008)
Ephrin-A5	Retrolental mass, cataract, retinal folding,	(Son et al. 2014)
Smo	Retrolental mass, small embryonic lens, thickened corneas	(Choi et al. 2014)
TgfβRII	Retrolental mass	(Freeman-Anderson et al. 2009)

5.3.2 Increased RGC may be due to lack of apoptosis through Semaphorin signalling.

The number of RGC born in the developing murine retina far exceeds the final number of RGC present in the mature murine retina. During retinal development, a period of perinatal RGC apoptosis occurs in order to prune the population of RGC to the numbers observed at adulthood (Dallimore et al. 2010, Crespo, O'Leary, and Cowan 1985, Potts, Dreher, and Bennett 1982, Horsburgh and Sefton 1987). Therefore, an increase in RGC could plausibly be due to a defect in this apoptotic epoch. *Nrp2* is expressed in the WT retina in RGC at a time point that corresponds to this apoptotic event. The loss of *Nrp2* expression may therefore inhibit apoptosis of RGC. The class 3 Semaphorin ligands for Nrp2 have previously been associated with neuronal apoptosis (Bagnard et al. 2004, Goshima et al. 2000, Shirvan et al. 1999, Gagliardini and Fankhauser 1999, Ben-Zvi et al. 2008). The class 3 semaphorin ligands for Nrp2, including Sema3C and Sema3F, are both expressed in the GCL of the postnatal retina (de Winter et al. 2004). Therefore, the increase in RGC observed in the embryonic *Nrp2* null retina could be attributed to a lack of Sema3 signalling in the RGC, which in the WT retina would lead to apoptosis of excess RGC. However, the GCL cellularity appears to have recovered to a thickness comparable to WT littermate controls at postnatal stages. Perhaps the hypomorphic expression of *Nrp2* results in delayed RGC apoptosis instead of an outright inhibition or expression of other factors such as *Nrp1* is able to compensate postnatally. Future directions include further

examination of the GCL using RGC specific markers, including BRN3A and BRN3B, to determine if there is any change in RGC numbers in the absence of *Nrp2* in the postnatal retina.

5.3.3 Increased amacrine cells/IPL in the Nrp2 null retina may be due to misregulation of TgfβII signalling

While *Nrp2* expression has been previously identified in the GCL of the embryonic retina, the function of *Nrp2* in retinal development is unknown. In accordance with published findings (Erskine et al. 2011) we have also identified Nrp2 expression in the GCL of the neural retina during late embryonic retinal development. We also demonstrated, for the first time, that *Nrp2* is expressed in amacrine cells of the mature retina and *Nrp2* loss results in increased production of amacrine cells and a significantly expanded IPL at late embryonic retinal development. Future experiments include carrying out whole retina qRT-PCR on *Nrp2* knockout mice to quantify expression of genes important for amacrine cell development including calretinin, syntaxin, and *Pax6*. Utilizing cell counting to quantify increases in amacrine cell production observed in the *Nrp2* knockout retina may be difficult in the postnatal retinal developmental stages due to the substantial retinal folding observed. One potential explanation for the increased production of amacrine cells during late retinogenesis could be reduction of TgfβII signalling. As described above, Nrp2 may promote TgfβII signalling either through direct regulation or influence signalling though co-receptor interactions with TgfβRII. Upregulation of TgfβII expression by Zic1 expressed in post-mitotic amacrine cells controls amacrine cell differentiation though a negative feedback loop by restricting RPC from generating additional amacrine cells during the amacrine cell genesis window (Ma et al. 2007). In addition, PI3K/Akt signalling in RPC contributes to restriction of amacrine cells genesis by enhancing RPC responsiveness to TgfβII (Tachibana et al. 2016). Amacrine cell genesis in the *Zic1* null mouse model is only affected at later developmental stages, much like that observed in the *Nrp2* null retina (Ma et al. 2007). Therefore, it would be of interest to examine the expression of TgfβRII and/or pSMAD2/3 in *Nrp2* knockout retinas to determine if TgfβII

signalling is affected in the absence of *Nrp2*. It is possible that the increase in amacrine cell production, combined with the microphthalmia could contribute to the retina folding, and reduction in vitreal space that is observed in the *Nrp2* knockout retina. Reduced or absent TgfβII signalling is an attractive mechanism for the increased amacrine cell production observed in the *Nrp2* null retina since, in addition to the elevated amacrine cell production in the conditional TgfβRII knockout retina (Ma et al. 2007), TgfRβII knockout mice also have PFV. Therefore, the findings in the TgfRβII knockout strongly resemble our observations in the *Nrp2* knockout retina and we could hypothesize that TgfβII expression is downstream of or interacts with Nrp2.

5.3.4 Neuropilins may play a role in intraretinal axon guidance

A number of guidance cues are required in the retina and along the optic tract to guide RGC axons from the retina to the superior colliculus. *Nrp2* is widely known to be critical for axonal guidance and fasciculation in the CNS (Chen et al. 2000, Giger et al. 2000). Our preliminary studies suggest that *Nrp2* may be involved in intraretinal axonal pathfinding, where RGC axons are organized before they project out of the optic disc. There has been some limited evidence to suggest that neuropilins play a role in this stage of RGC pathfinding as well as in mapping of RGC axons to the superior colliculus. First, a pair of studies from Alan Harvey's laboratory has examined the expression of neuropilins and semaphorins in the retina and superior colliculus. These studies identified that several members of the class 3 semaphorins and Nrp1 and Nrp2 were expressed in the retina with temporal changes in expression patterns observed over the course of retina development (de Winter et al. 2004, Sharma et al. 2014). Sharma and colleagues quantified transcript levels of Sema3 and neuropilins in both the retina and superior colliculus. The authors determined that *Nrp2* expression increased gradually beginning at E16 to adulthood. Sema3c expression gradually increased from E19 to adulthood while Sema3f expression peaked at P0, decreased, and then was significantly elevated again from P21 to adulthood (Sharma et al. 2014). The elevated expression of *Nrp2* and its preferred

ligands Sema3c and Sema3f at late embryonic and postnatal stages of retinal development would be consistent with *Nrp2* being required for intraretinal axonal guidance at these time-points as was observed in our preliminary studies. In their earlier work, the Harvey lab carried out ISH and determined that *Nrp2*, and *Sema3c* and *Sema3f* are expressed in RGC at postnatal stages (earlier developmental time points were not examined)(de Winter et al. 2004). Co-expression of a repulsive guidance ligand and its receptors has been documented in the RGC before with known roles in intraretinal axonal guidance. The repulsive guidance ligands Slit1 and Slit2 and their receptor Robo2 are each expressed in the RGC (Thompson et al. 2006, Thompson et al. 2009). Mutations in either *Slit1*/*Slit2* or *Robo2* result in intraretinal pathfinding errors, but projections of axons to the optic disc are not perturbed. Specifically, the authors found that Slit/Robo signalling was required to restrict RGC axons to the optic fibre layer. Perhaps Nrp2 and also Nrp1 are similarly involved in restricting RGC to the OFL. Indeed we observed that RGC axon fasciculation is disrupted in the *Nrp2* knockout retina at E18. In addition to carrying out more repetitions of the retinal flatmounts, it would also be interesting to examine coronal sections of the retinal flatmounts to determine if any RGC axons are aberrantly projecting in the retina. If Nrp2/Sema3 signalling maintains organization of the RGC in the nerve fibre layer, it is possible that lack of this signalling no longer restricts RGC axons to the nerve fibre layer, resulting in aberrant axon projections into the retina, as is observed in *Slit* mutants (Thompson et al. 2006).

While previous studies suggest that *Nrp2* is likely not involved in RGC crossing at the optic chiasm due its late embryonic expression in RGC (Erskine et al. 2011), as discussed above expression of *Nrp2* and its preferred ligands *Sema3c* and *Sema3f* has been identified in the superior colliculus. Neurogenesis of the superior colliculus occurs between E12 and E17 (Sharma et al. 2014). In accordance with this developmental window, *Nrp2* and *Sema3c* expression increases significantly from E16 to P0 (Sharma et al. 2014). This expression pattern suggests that *Nrp2* could be critical for mapping of RGC to the superior colliculus. In the future, axonal

projections from the *Nrp2* null retina could be examined using anterograde lipophilic DiI tracing. This would not only allow us to examine projection of RGC into the superior colliculus, but also allow us to examine if aberrant RGC crossing at the optic chiasm is observed, and if RGC exit from the optic disc is impaired in the absence of *Nrp2* expression.

To date, our preliminary intraretinal axonal guidance experiments in the *Nrp2* knockout retina suggest that *Nrp2* may be playing a role in proper bundling of RGC axons before exiting the optic disc. While our findings are preliminary, these results encourage future in-depth study into the role of *Nrp2* of RGC axon fasciculation and projection throughout the optic pathway.

CHAPTER 6: OVERALL DISCUSSION AND CONCLUSIONS

6 Chapter 6. Overall Discussion and Conclusions

One of the primary goals in our laboratory is to elucidate the role of the *Dlx* homeobox genes in the regulation of retina cell fate decisions. Specifically, this thesis focused on evaluating the role of *Dlx* genes in restricting photoreceptor cell fates through the transcriptional repression of genes involved in photoreceptor differentiation, with emphasis on *Olig2*. In our study, we determined that *Olig2* is expressed specifically in photoreceptor precursors, indicating that *Olig2* may be important for the specification of photoreceptors. We also determined that DLX2 binds to the regulatory region of *Olig2* in the developing retina, *in vivo* and *in vitro*. Binding of DLX2 to *Olig2* regulatory elements resulted in the transcriptional repression of *Olig2*, supporting our hypothesis that *Dlx* genes restrict *Dlx1*/*Dlx2* positive RPC from adopting photoreceptor cell fates and demonstrating for the first time, transcriptional regulation of *Olig2* expression in the developing retina. In the future, our laboratory will be characterizing the postnatal retinas from *Dlx2* conditional knockout mice to determine if postnatal photoreceptor development is affected as the majority of photoreceptors are born during this period. Importantly, during our study, we also uncovered the impact of genetic background for the study of photoreceptor development in the mouse model system, which will be critical in planning future experiments examining the role of *Dlx* homeobox genes in photoreceptor development.

We also examined the role of *Dlx* genes in the developing forebrain to further our understanding of the role of *Dlx* genes in neuronal differentiation. In both the developing forebrain and retina, *Dlx1*/*Dlx2* has a critical function in regulating cell fate decisions. Interestingly, *Dlx* genes also control binary cell fate decisions in the developing forebrain by regulating the expression of *Olig2,* much like in the developing retina. As shown in previous studies, Dlx1/Dlx2 restricts *Olig2* in the developing forebrain, favouring GABAergic interneuron fates over oligodendrocytes (Petryniak et al. 2007). Where the role of *Dlx* genes in the brain and

the retina appear to differ is in the restriction of neural progenitor self-renewal to promote differentiation. In the forebrain, loss of *Dlx1*/*Dlx2* expression results in upregulation of Notch signalling in the SVZ, which contributes to the failed differentiation of GABAergic interneurons. In the *Dlx1*/*Dlx2* DKO retina, Notch signalling appears to be unchanged and yet, differentiation and survival of RGC is affected in the absence of *Dlx1*/*Dlx2*. A recent study determined the *Atoh7*, *Dlx1,* and *Dlx2* are highly expressed in *Notch1* receptor-positive RPC that have diminished Notch expression, thereby promoting these RPC to adopt RGC fates (Dvoriantchikova et al. 2015). These results suggest that *Dlx1*/*Dlx2* may inhibit Notch to maintain RGC fate. There are two potential explanations for why Notch signalling was not affected in the *Dlx1*/*Dlx2* DKO retina. First, our examination of Notch signalling in the *Dlx1*/*Dlx2* retina was not carried out until E18. This time point is perhaps too late to examine regulation of Notch signalling by *Dlx1*/*Dlx2* as Notch receptor-positive RPC specify RGC at early embryonic stages. Alternatively, *Atoh7* is sufficient to restrict Notch signalling in the retina despite *Dlx1*/*Dlx2* loss, while in the forebrain, *Dlx1*/*Dlx2* is indispensible for restricting Notch signalling. We also determined that the regulation of Notch signalling by *Dlx* genes in the developing forebrain occurs indirectly though activation of *p107*. Reduction in p107 expression in the absence of *Dlx1*/*Dlx2* was observed specifically in the SVZ of the GE, while Notch expression is specifically elevated in SVZ (Yun et al. 2002) leading to defects in SVZ development. Like Notch signalling, p107 expression was also unchanged in the *Dlx1/Dlx2* DKO retina. Again, this could possibly be due to the developmental time point in which p107 transcript levels were examined in the *Dlx1*/*Dlx2* DKO retina. At E18, DLX2 is expressed in differentiated GCL, amacrine, and horizontals cells (de Melo et al. 2003). Of the RB family members, P107 is the most highly expressed in the embryonic retina (Donovan et al. 2006, Wirt and Sage 2010). Hes1 is highly expressed in RPC during retinal development (Marquardt et al. 2001, Wang et al. 2005). It would be interesting to determine whether DLX2 and P107 expressing cells co-localize during early embryonic retinal development. If co-localization is

observed during this early developmental time-point, it is plausible that DLX2 drives p107 expression to allow for RPC to differentiate into RGC through restriction of *Hes1* expression and activation of RGC differentiation genes, similar to the role observed for *Dlx* genes in promoting GABAergic interneuron differentiation in the developing forebrain.

Very little is known about the role of Nrp2 in the developing ocular structures. Our study has uncovered novel functions for *Nrp2* in both the development of the embryonic vasculature and retina. For the first time, we have demonstrated that *Nrp2* is involved in hyaloid vessel development. In the absence of *Nrp2* expression, a large retrolental mass was observed in the vitreous of the embryonic *Nrp2* knockout mice. This mass is made up of both endothelial cells and cells expressing non-functional *Nrp2*, which may be of neural crest origin and are no longer responsive to semaphorin guidance cues. In the postnatal retina, the *Nrp2* knockout mice display a number of secondary ocular defects that are commonly associated with PFV, including microphthalmia and retinal folding. Increased corneal thickness was also observed in the postnatal *Nrp2* knockout, further suggesting defects in neural crest cell migration is perturbed in the absence of *Nrp2* expression. Taken together, our *Nrp2* knockout mouse could perhaps be a new model for the study of PFV. A critical next step in the study of *Nrp2* in hyaloid vessel development is uncovering the molecular mechanism(s) by which the hyaloid vessels accumulate or fail to regress in the absence of *Nrp2* expression. Currently, there are several genetic models that develop PFV. As mentioned above, these models may provide clues as to the molecular mechanisms governing persistence of hyaloid vessels in *Nrp2* knockout eyes. Overall, studying hyaloid vasculature development in the *Nrp2* model may contribute to the currently limited understanding of the mechanisms governing the development and regression of the transient hyaloid vascular system.

Not only have we uncovered a role for *Nrp2* in hyaloid development, but we have also determined that *Nrp2* plays a role in amacrine cell differentiation in the developing retina. We

observed an increase in amacrine cells in the late embryonic and postnatal retina in the absence of *Nrp2* expression. The overall cellularity of the retina was also increased in the absence of Nrp2 expression. Proliferation and apoptosis in the absence of *Nrp2* expression will be examined in future studies to uncover the mechanism contributing to the increased cellularity observed in the *Nrp2* knockout eye. Like the PFV in the *Nrp2* knockout, the next important step in studying the amacrine cell defect is to uncover the mechanism contributing to the elevation in amacrine cells observed in the absence of *Nrp2* expression. We are interested in examining TgfβII signalling in the absence of Nrp2 since TgfβII signalling negatively regulates amacrine cell genesis and has been shown to interact with Nrp2. This observation of *Nrp2* in retinal cell differentiation adds another dimension to our laboratory's primary retina studies investigating the role of DLX transcription factors in retina cell fate specification and differentiation. Retinal cell differentiation requires the coordinated activity of numerous transcription factors, including *Dlx1*/*Dlx2* and signalling proteins including *Nrp2*. It may also be interesting to investigate whether DLX2 transcriptionally regulates *Nrp2* expression in the developing retina. Our laboratory has previously examined the repression of *Nrp2* expression by *Dlx* genes in the developing forebrain (Le et al. 2007). Therefore, with additional studies in the future, perhaps we can integrate *Nrp2* into the genetic regulatory networks we have established for *Dlx1*/*Dlx2* in specifying retinal cell fate as outlined in Chapter 3 of this thesis.

Moving forward, our *Nrp2* study represents several exciting avenues of study to explore including the role of *Nrp2* in hyaloid vessel development, axonal guidance, and in amacrine cell differentiation.

BIBLIOGRAPHY

7 Bibliography

Abouzeid, H., M. A. Youssef, N. Bayoumi, N. ElShakankiri, I. Marzouk, P. Hauser, and D. F. Schorderet. 2012. "RAX and anophthalmia in humans: evidence of brain anomalies." *Mol Vis* 18:1449-56.

Ahmad, I., C. M. Dooley, and D. L. Polk. 1997. "Delta-1 is a regulator of neurogenesis in the vertebrate retina." *Dev Biol* 185 (1):92-103. doi: 10.1006/dbio.1997.8546.

Ahmad, I., P. Zaqouras, and S. Artavanis-Tsakonas. 1995. "Involvement of Notch-1 in mammalian retinal neurogenesis: association of Notch-1 activity with both immature and terminally differentiated cells." *Mech Dev* 53 (1):73-85.

Akhmedov, N. B., N. I. Piriev, B. Chang, A. L. Rapoport, N. L. Hawes, P. M. Nishina, S. Nusinowitz, J. R. Heckenlively, T. H. Roderick, C. A. Kozak, M. Danciger, M. T. Davisson, and D. B. Farber. 2000. "A deletion in a photoreceptor-specific nuclear receptor mRNA causes retinal degeneration in the rd7 mouse." *Proc Natl Acad Sci U S A* 97 (10):5551-6.

Akimenko, M. A., M. Ekker, J. Wegner, W. Lin, and M. Westerfield. 1994. "Combinatorial expression of three zebrafish genes related to distal-less: part of a homeobox gene code for the head." *J Neurosci* 14 (6):3475-86.

Akimoto, M., H. Cheng, D. Zhu, J. A. Brzezinski, R. Khanna, E. Filippova, E. C. Oh, Y. Jing, J. L. Linares, M. Brooks, S. Zareparsi, A. J. Mears, A. Hero, T. Glaser, and A. Swaroop. 2006. "Targeting of GFP to newborn rods by Nrl promoter and temporal expression profiling of flow-sorted photoreceptors." *Proc Natl Acad Sci U S A* 103 (10):3890-5. doi: 10.1073/pnas.0508214103.

Amores, A., A. Force, Y. L. Yan, L. Joly, C. Amemiya, A. Fritz, R. K. Ho, J. Langeland, V. Prince, Y. L. Wang, M. Westerfield, M. Ekker, and J. H. Postlethwait. 1998. "Zebrafish hox clusters and vertebrate genome evolution." *Science* 282 (5394):1711-4.

Anderson, S. A., D. D. Eisenstat, L. Shi, and J. L. Rubenstein. 1997. "Interneuron migration from basal forebrain to neocortex: dependence on Dlx genes." *Science* 278 (5337):474-6.

Anderson, S. A., O. Marin, C. Horn, K. Jennings, and J. L. Rubenstein. 2001. "Distinct cortical migrations from the medial and lateral ganglionic eminences." *Development* 128 (3):353-63.

Anderson, S. A., M. Qiu, A. Bulfone, D. D. Eisenstat, J. Meneses, R. Pedersen, and J. L. Rubenstein. 1997. "Mutations of the homeobox genes Dlx-1 and Dlx-2 disrupt the striatal subventricular zone and differentiation of late born striatal neurons." *Neuron* 19 (1):27-37.

Andrusiak, M. G., K. A. McClellan, D. Dugal-Tessier, L. M. Julian, S. P. Rodrigues, D. S. Park, T. E. Kennedy, and R. S. Slack. 2011. "Rb/E2F regulates expression of neogenin during neuronal migration." *Mol Cell Biol* 31 (2):238-47. doi: 10.1128/MCB.00378-10.

Artavanis-Tsakonas, S., M. D. Rand, and R. J. Lake. 1999. "Notch signaling: cell fate control and signal integration in development." *Science* 284 (5415):770-6.

Asano, M., Y. Emori, K. Saigo, and K. Shiokawa. 1992. "Isolation and characterization of a Xenopus cDNA which encodes a homeodomain highly homologous to Drosophila Distal-less." *J Biol Chem* 267 (8):5044-7.

Ashery-Padan, R., and P. Gruss. 2001. "Pax6 lights-up the way for eye development." *Curr Opin Cell Biol* 13 (6):706-14.

Ashery-Padan, R., T. Marquardt, X. Zhou, and P. Gruss. 2000. "Pax6 activity in the lens primordium is required for lens formation and for correct placement of a single retina in the eye." *Genes Dev* 14 (21):2701-11.

Aspalter, I. M., E. Gordon, A. Dubrac, A. Ragab, J. Narloch, P. Vizan, I. Geudens, R. T. Collins, C. A. Franco, C. L. Abrahams, G. Thurston, M. Fruttiger, I. Rosewell, A. Eichmann, and H. Gerhardt. 2015. "Alk1 and Alk5 inhibition by Nrp1 controls vascular sprouting downstream of Notch." *Nat Commun* 6:7264. doi: 10.1038/ncomms8264.

Aspock, G., and T. R. Burglin. 2001. "The Caenorhabditis elegans distal-less ortholog ceh-43 is required for development of the anterior hypodermis." *Dev Dyn* 222 (3):403-9. doi: 10.1002/dvdy.1201.

Austin, C. P., D. E. Feldman, J. A. Ida, Jr., and C. L. Cepko. 1995. "Vertebrate retinal ganglion cells are selected from competent progenitors by the action of Notch." *Development* 121 (11):3637-50.

Avanesov, A., and J. Malicki. 2010. "Analysis of the retina in the zebrafish model." *Methods Cell Biol* 100:153-204. doi: 10.1016/B978-0-12-384892-5.00006-2.

Bagnard, D., N. Sainturet, D. Meyronet, M. Perraut, M. Miehe, G. Roussel, D. Aunis, M. F. Belin, and N. Thomasset. 2004. "Differential MAP kinases activation during semaphorin3A-

induced repulsion or apoptosis of neural progenitor cells." *Mol Cell Neurosci* 25 (4):722-31. doi: 10.1016/j.mcn.2003.12.007.

Bai, X., D. J. Dilworth, Y. C. Weng, and D. B. Gould. 2009. "Developmental distribution of collagen IV isoforms and relevance to ocular diseases." *Matrix Biol* 28 (4):194-201. doi: 10.1016/j.matbio.2009.02.004.

Bailey, T. J., H. El-Hodiri, L. Zhang, R. Shah, P. H. Mathers, and M. Jamrich. 2004. "Regulation of vertebrate eye development by Rx genes." *Int J Dev Biol* 48 (8-9):761-70. doi: 10.1387/ijdb.041878tb.

Balasubramanian, R., and L. Gan. 2014. "Development of Retinal Amacrine Cells and Their Dendritic Stratification." *Curr Ophthalmol Rep* 2 (3):100-106. doi: 10.1007/s40135-014-0048-2.

Ball, S. G., C. Bayley, C. A. Shuttleworth, and C. M. Kielty. 2010. "Neuropilin-1 regulates platelet-derived growth factor receptor signalling in mesenchymal stem cells." *Biochem J* 427 (1):29-40. doi: 10.1042/BJ20091512.

Banerjee, S., K. Sengupta, K. Dhar, S. Mehta, P. A. D'Amore, G. Dhar, and S. K. Banerjee. 2006. "Breast cancer cells secreted platelet-derived growth factor-induced motility of vascular smooth muscle cells is mediated through neuropilin-1." *Mol Carcinog* 45 (11):871-80. doi: 10.1002/mc.20248.

Bao, Z. Z., and C. L. Cepko. 1997. "The expression and function of Notch pathway genes in the developing rat eye." *J Neurosci* 17 (4):1425-34.

Baribault, H., J. Price, K. Miyai, and R. G. Oshima. 1993. "Mid-gestational lethality in mice lacking keratin 8." *Genes Dev* 7 (7A):1191-202.

Baumer, N., T. Marquardt, A. Stoykova, D. Spieler, D. Treichel, R. Ashery-Padan, and P. Gruss. 2003. "Retinal pigmented epithelium determination requires the redundant activities of Pax2 and Pax6." *Development* 130 (13):2903-15.

Ben-Zvi, A., O. Manor, M. Schachner, A. Yaron, M. Tessier-Lavigne, and O. Behar. 2008. "The Semaphorin receptor PlexinA3 mediates neuronal apoptosis during dorsal root ganglia development." *J Neurosci* 28 (47):12427-32. doi: 10.1523/JNEUROSCI.3573-08.2008.

Bernstein, B. E., A. Meissner, and E. S. Lander. 2007. "The mammalian epigenome." *Cell* 128 (4):669-81. doi: 10.1016/j.cell.2007.01.033.

Bernstein, B. E., T. S. Mikkelsen, X. Xie, M. Kamal, D. J. Huebert, J. Cuff, B. Fry, A. Meissner, M. Wernig, K. Plath, R. Jaenisch, A. Wagschal, R. Feil, S. L. Schreiber, and E. S. Lander. 2006. "A bivalent chromatin structure marks key developmental genes in embryonic stem cells." *Cell* 125 (2):315-26. doi: 10.1016/j.cell.2006.02.041.

Bhansali, P., I. Rayport, A. Rebsam, and C. Mason. 2014. "Delayed neurogenesis leads to altered specification of ventrotemporal retinal ganglion cells in albino mice." *Neural Dev* 9:11. doi: 10.1186/1749-8104-9-11.

Bishop, P. N. 2000. "Structural macromolecules and supramolecular organisation of the vitreous gel." *Prog Retin Eye Res* 19 (3):323-44.

Boije, H., S. Shirazi Fard, P. H. Edqvist, and F. Hallbook. 2016. "Horizontal Cells, the Odd Ones Out in the Retina, Give Insights into Development and Disease." *Front Neuroanat* 10:77. doi: 10.3389/fnana.2016.00077.

Bone-Larson, C., S. Basu, J. D. Radel, M. Liang, T. Perozek, N. Kapousta-Bruneau, D. G. Green, M. Burmeister, and M. H. Hankin. 2000. "Partial rescue of the ocular retardation phenotype by genetic modifiers." *J Neurobiol* 42 (2):232-47.

Bonyadi, M., S. A. Rusholme, F. M. Cousins, H. C. Su, C. A. Biron, M. Farrall, and R. J. Akhurst. 1997. "Mapping of a major genetic modifier of embryonic lethality in TGF beta 1 knockout mice." *Nat Genet* 15 (2):207-11. doi: 10.1038/ng0297-207.

Brewer, S., W. Feng, J. Huang, S. Sullivan, and T. Williams. 2004. "Wnt1-Cre-mediated deletion of AP-2alpha causes multiple neural crest-related defects." *Dev Biol* 267 (1):135-52. doi: 10.1016/j.ydbio.2003.10.039.

Bringmann, A., I. Iandiev, T. Pannicke, A. Wurm, M. Hollborn, P. Wiedemann, N. N. Osborne, and A. Reichenbach. 2009. "Cellular signaling and factors involved in Muller cell gliosis: neuroprotective and detrimental effects." *Prog Retin Eye Res* 28 (6):423-51. doi: 10.1016/j.preteyeres.2009.07.001.

Bringmann, A., T. Pannicke, J. Grosche, M. Francke, P. Wiedemann, S. N. Skatchkov, N. N. Osborne, and A. Reichenbach. 2006. "Muller cells in the healthy and diseased retina." *Prog Retin Eye Res* 25 (4):397-424. doi: 10.1016/j.preteyeres.2006.05.003.

Brown, A., M. McKie, V. van Heyningen, and J. Prosser. 1998. "The Human PAX6 Mutation Database." *Nucleic Acids Res* 26 (1):259-64.

Brown, A. S., M. Zhang, V. Cucevic, C. J. Pavlin, and F. S. Foster. 2005. "In vivo assessment of postnatal murine ocular development by ultrasound biomicroscopy." *Curr Eye Res* 30 (1):45-51.

Brown, N. L., S. Patel, J. Brzezinski, and T. Glaser. 2001. "Math5 is required for retinal ganglion cell and optic nerve formation." *Development* 128 (13):2497-508.

Brox, A., L. Puelles, B. Ferreiro, and L. Medina. 2003. "Expression of the genes GAD67 and Distal-less-4 in the forebrain of Xenopus laevis confirms a common pattern in tetrapods." *J Comp Neurol* 461 (3):370-93. doi: 10.1002/cne.10688.

Brzezinski, J. A., and T. A. Reh. 2015. "Photoreceptor cell fate specification in vertebrates." *Development* 142 (19):3263-73. doi: 10.1242/dev.127043.

Brzezinski, J. A. th, D. A. Lamba, and T. A. Reh. 2010. "Blimp1 controls photoreceptor versus bipolar cell fate choice during retinal development." *Development* 137 (4):619-29. doi: 10.1242/dev.043968.

Brzezinski, J. A. th, K. Uoon Park, and T. A. Reh. 2013. "Blimp1 (Prdm1) prevents re-specification of photoreceptors into retinal bipolar cells by restricting competence." *Dev Biol* 384 (2):194-204. doi: 10.1016/j.ydbio.2013.10.006.

Bumsted, K. M., and C. J. Barnstable. 2000. "Dorsal retinal pigment epithelium differentiates as neural retina in the microphthalmia (mi/mi) mouse." *Invest Ophthalmol Vis Sci* 41 (3):903-8.

Bunt, J., N. A. Hasselt, D. A. Zwijnenburg, J. Koster, R. Versteeg, and M. Kool. 2013. "OTX2 sustains a bivalent-like state of OTX2-bound promoters in medulloblastoma by maintaining their H3K27me3 levels." *Acta Neuropathol* 125 (3):385-94. doi: 10.1007/s00401-012-1069-2.

Burkhart, D. L., S. E. Wirt, A. F. Zmoos, M. S. Kareta, and J. Sage. 2010. "Tandem E2F binding sites in the promoter of the p107 cell cycle regulator control p107 expression and its cellular functions." *PLoS Genet* 6 (6):e1001003. doi: 10.1371/journal.pgen.1001003.

Burmeister, M., J. Novak, M. Y. Liang, S. Basu, L. Ploder, N. L. Hawes, D. Vidgen, F. Hoover, D. Goldman, V. I. Kalnins, T. H. Roderick, B. A. Taylor, M. H. Hankin, and R. R. McInnes. 1996. "Ocular retardation mouse caused by Chx10 homeobox null allele: impaired retinal progenitor proliferation and bipolar cell differentiation." *Nat Genet* 12 (4):376-84. doi: 10.1038/ng0496-376.

Burrill, J. D., and S. S. Easter, Jr. 1994. "Development of the retinofugal projections in the embryonic and larval zebrafish (Brachydanio rerio)." *J Comp Neurol* 346 (4):583-600. doi: 10.1002/cne.903460410.

Campochiaro, P. A. 2013. "Ocular neovascularization." *J Mol Med (Berl)* 91 (3):311-21. doi: 10.1007/s00109-013-0993-5.

Campochiaro, P. A. 2015. "Molecular pathogenesis of retinal and choroidal vascular diseases." *Prog Retin Eye Res* 49:67-81. doi: 10.1016/j.preteyeres.2015.06.002.

Cao, L., B. Faha, M. Dembski, L. H. Tsai, E. Harlow, and N. Dyson. 1992. "Independent binding of the retinoblastoma protein and p107 to the transcription factor E2F." *Nature* 355 (6356):176-9. doi: 10.1038/355176a0.

Carl, M., F. Loosli, and J. Wittbrodt. 2002. "Six3 inactivation reveals its essential role for the formation and patterning of the vertebrate eye." *Development* 129 (17):4057-63.

Chai, Y., X. Jiang, Y. Ito, P. Bringas, Jr., J. Han, D. H. Rowitch, P. Soriano, A. P. McMahon, and H. M. Sucov. 2000. "Fate of the mammalian cranial neural crest during tooth and mandibular morphogenesis." *Development* 127 (8):1671-9.

Chellappan, S. P., S. Hiebert, M. Mudryj, J. M. Horowitz, and J. R. Nevins. 1991. "The E2F transcription factor is a cellular target for the RB protein." *Cell* 65 (6):1053-61.

Chen, B., W. H. Piel, and A. Monteiro. 2016. "Distal-less homeobox genes of insects and spiders: genomic organization, function, regulation and evolution." *Insect Sci* 23 (3):335-52. doi: 10.1111/1744-7917.12327.

Chen, H., A. Bagri, J. A. Zupicich, Y. Zou, E. Stoeckli, S. J. Pleasure, D. H. Lowenstein, W. C. Skarnes, A. Chedotal, and M. Tessier-Lavigne. 2000. "Neuropilin-2 regulates the development of selective cranial and sensory nerves and hippocampal mossy fiber projections." *Neuron* 25 (1):43-56.

Chen, H., A. Chedotal, Z. He, C. S. Goodman, and M. Tessier-Lavigne. 1997. "Neuropilin-2, a novel member of the neuropilin family, is a high affinity receptor for the semaphorins Sema E and Sema IV but not Sema III." *Neuron* 19 (3):547-59.

Chen, S., Q. L. Wang, Z. Nie, H. Sun, G. Lennon, N. G. Copeland, D. J. Gilbert, N. A. Jenkins, and D. J. Zack. 1997. "Crx, a novel Otx-like paired-homeodomain protein, binds to and transactivates photoreceptor cell-specific genes." *Neuron* 19 (5):1017-30.

Cheng, C. W., R. L. Chow, M. Lebel, R. Sakuma, H. O. Cheung, V. Thanabalasingham, X. Zhang, B. G. Bruneau, D. G. Birch, C. C. Hui, R. R. McInnes, and S. H. Cheng. 2005. "The Iroquois homeobox gene, Irx5, is required for retinal cone bipolar cell development." *Dev Biol* 287 (1):48-60. doi: 10.1016/j.ydbio.2005.08.029.

Chiang, C., Y. Litingtung, E. Lee, K. E. Young, J. L. Corden, H. Westphal, and P. A. Beachy. 1996. "Cyclopia and defective axial patterning in mice lacking Sonic hedgehog gene function." *Nature* 383 (6599):407-13. doi: 10.1038/383407a0.

Choi, J. J., C. T. Ting, L. Trogrlic, S. V. Milevski, M. Familari, G. Martinez, and R. U. de Iongh. 2014. "A role for smoothened during murine lens and cornea development." *PLoS One* 9 (9):e108037. doi: 10.1371/journal.pone.0108037.

Chow, R. L., and R. A. Lang. 2001. "Early eye development in vertebrates." *Annu Rev Cell Dev Biol* 17:255-96. doi: 10.1146/annurev.cellbio.17.1.255.

Chow, R. L., B. Volgyi, R. K. Szilard, D. Ng, C. McKerlie, S. A. Bloomfield, D. G. Birch, and R. R. McInnes. 2004. "Control of late off-center cone bipolar cell differentiation and visual signaling by the homeobox gene Vsx1." *Proc Natl Acad Sci U S A* 101 (6):1754-9. doi: 10.1073/pnas.0306520101.

Classon, M., and N. Dyson. 2001. "p107 and p130: versatile proteins with interesting pockets." *Exp Cell Res* 264 (1):135-47. doi: 10.1006/excr.2000.5135.

Cohen, S. M., and G. Jurgens. 1989. "Proximal-distal pattern formation in Drosophila: cell autonomous requirement for Distal-less gene activity in limb development." *EMBO J* 8 (7):2045-55.

Corbo, J. C., and C. L. Cepko. 2005. "A hybrid photoreceptor expressing both rod and cone genes in a mouse model of enhanced S-cone syndrome." *PLoS Genet* 1 (2):e11. doi: 10.1371/journal.pgen.0010011.

Crespo, D., D. D. O'Leary, and W. M. Cowan. 1985. "Changes in the numbers of optic nerve fibers during late prenatal and postnatal development in the albino rat." *Brain Res* 351 (1):129-34.

Cui, J. Z., B. J. Hinz, M. D. Greve, M. J. Potter, D. Hornan, A. Samad, E. To, and J. A. Matsubara. 2003. "Expression of neuropilin-1 in choroidal neovascular membranes." *Can J Ophthalmol* 38 (1):41-5.

Cvekl, A., and E. R. Tamm. 2004. "Anterior eye development and ocular mesenchyme: new insights from mouse models and human diseases." *Bioessays* 26 (4):374-86. doi: 10.1002/bies.20009.

Dallimore, E. J., K. K. Park, M. A. Pollett, J. S. Taylor, and A. R. Harvey. 2010. "The life, death and regenerative ability of immature and mature rat retinal ganglion cells are influenced by their birthdate." *Exp Neurol* 225 (2):353-65. doi: 10.1016/j.expneurol.2010.07.007.

de Melo, J., B. S. Clark, and S. Blackshaw. 2016. "Multiple intrinsic factors act in concert with Lhx2 to direct retinal gliogenesis." *Sci Rep* 6:32757. doi: 10.1038/srep32757.

de Melo, J., G. Du, M. Fonseca, L. A. Gillespie, W. J. Turk, J. L. Rubenstein, and D. D. Eisenstat. 2005. "Dlx1 and Dlx2 function is necessary for terminal differentiation and survival of late-born retinal ganglion cells in the developing mouse retina." *Development* 132 (2):311-22. doi: 10.1242/dev.01560.

de Melo, J., X. Qiu, G. Du, L. Cristante, and D. D. Eisenstat. 2003. "Dlx1, Dlx2, Pax6, Brn3b, and Chx10 homeobox gene expression defines the retinal ganglion and inner nuclear layers of the developing and adult mouse retina." *J Comp Neurol* 461 (2):187-204. doi: 10.1002/cne.10674.

de Melo, J., Q. P. Zhou, Q. Zhang, S. Zhang, M. Fonseca, J. T. Wigle, and D. D. Eisenstat. 2008. "Dlx2 homeobox gene transcriptional regulation of Trkb neurotrophin receptor expression during mouse retinal development." *Nucleic Acids Res* 36 (3):872-84. doi: 10.1093/nar/gkm1099.

de Melo, J., C. Zibetti, B. S. Clark, W. Hwang, A. L. Miranda-Angulo, J. Qian, and S. Blackshaw. 2016. "Lhx2 Is an Essential Factor for Retinal Gliogenesis and Notch Signaling." *J Neurosci* 36 (8):2391-405. doi: 10.1523/JNEUROSCI.3145-15.2016.

de Winter, F., Q. Cui, N. Symons, J. Verhaagen, and A. R. Harvey. 2004. "Expression of class-3 semaphorins and their receptors in the neonatal and adult rat retina." *Invest Ophthalmol Vis Sci* 45 (12):4554-62. doi: 10.1167/iovs.04-0173.

Deaton, A. M., and A. Bird. 2011. "CpG islands and the regulation of transcription." *Genes Dev* 25 (10):1010-22. doi: 10.1101/gad.2037511.

Depew, M. J., T. Lufkin, and J. L. Rubenstein. 2002. "Specification of jaw subdivisions by Dlx genes." *Science* 298 (5592):381-5. doi: 10.1126/science.1075703.

Depew, M. J., C. A. Simpson, M. Morasso, and J. L. Rubenstein. 2005. "Reassessing the Dlx code: the genetic regulation of branchial arch skeletal pattern and development." *J Anat* 207 (5):501-61. doi: 10.1111/j.1469-7580.2005.00487.x.

Dhawan, R. R., T. J. Schoen, and D. C. Beebe. 1997. "Isolation and expression of homeobox genes from the embryonic chicken eye." *Mol Vis* 3:7.

Dhingra, S., D. J. Shears, V. Blake, H. Stewart, and C. K. Patel. 2006. "Advanced bilateral persistent fetal vasculature associated with a novel mutation in the Norrie gene." *Br J Ophthalmol* 90 (10):1324-5. doi: 10.1136/bjo.2005.088625.

Diamond, E., M. Amen, Q. Hu, H. M. Espinoza, and B. A. Amendt. 2006. "Functional interactions between Dlx2 and lymphoid enhancer factor regulate Msx2." *Nucleic Acids Res* 34 (20):5951-65. doi: 10.1093/nar/gkl689.

Ding, Q., H. Chen, X. Xie, R. T. Libby, N. Tian, and L. Gan. 2009. "BARHL2 differentially regulates the development of retinal amacrine and ganglion neurons." *J Neurosci* 29 (13):3992-4003. doi: 10.1523/JNEUROSCI.5237-08.2009.

Dixit, R., F. Lu, R. Cantrup, N. Gruenig, L. M. Langevin, D. M. Kurrasch, and C. Schuurmans. 2011. "Efficient gene delivery into multiple CNS territories using in utero electroporation." *J Vis Exp* (52). doi: 10.3791/2957.

Doetschman, T. 2009. "Influence of genetic background on genetically engineered mouse phenotypes." *Methods Mol Biol* 530:423-33. doi: 10.1007/978-1-59745-471-1_23.

Dong, P. D., J. Chu, and G. Panganiban. 2000. "Coexpression of the homeobox genes Distal-less and homothorax determines Drosophila antennal identity." *Development* 127 (2):209-16.

Donovan, S. L., B. Schweers, R. Martins, D. Johnson, and M. A. Dyer. 2006. "Compensation by tumor suppressor genes during retinal development in mice and humans." *BMC Biol* 4:14. doi: 10.1186/1741-7007-4-14.

Dowling, J. E. 1970. "Organization of the vertebrate retina." *Nihon Seirigaku Zasshi* 32 (8):546-7.

Downey, L. M., H. M. Bottomley, E. Sheridan, M. Ahmed, D. F. Gilmour, C. F. Inglehearn, A. Reddy, A. Agrawal, J. Bradbury, and C. Toomes. 2006. "Reduced bone mineral density and hyaloid vasculature remnants in a consanguineous recessive FEVR family with a mutation in LRP5." *Br J Ophthalmol* 90 (9):1163-7. doi: 10.1136/bjo.2006.092114.

Dryja, T. P., S. Friend, and R. A. Weinberg. 1986. "Genetic sequences that predispose to retinoblastoma and osteosarcoma." *Symp Fundam Cancer Res* 39:115-9.

Dvoriantchikova, G., I. Perea-Martinez, S. Pappas, A. F. Barry, D. Danek, X. Dvoriantchikova, D. Pelaez, and D. Ivanov. 2015. "Molecular Characterization of Notch1 Positive Progenitor Cells in the Developing Retina." *PLoS One* 10 (6):e0131054. doi: 10.1371/journal.pone.0131054.

Dyer, M. A., F. J. Livesey, C. L. Cepko, and G. Oliver. 2003. "Prox1 function controls progenitor cell proliferation and horizontal cell genesis in the mammalian retina." *Nat Genet* 34 (1):53-8. doi: 10.1038/ng1144.

Dyson, N., M. Dembski, A. Fattaey, C. Ngwu, M. Ewen, and K. Helin. 1993. "Analysis of p107-associated proteins: p107 associates with a form of E2F that differs from pRB-associated E2F-1." *J Virol* 67 (12):7641-7.

Edwards, M. M., D. S. McLeod, R. Li, R. Grebe, I. Bhutto, X. Mu, and G. A. Lutty. 2012. "The deletion of Math5 disrupts retinal blood vessel and glial development in mice." *Exp Eye Res* 96 (1):147-56. doi: 10.1016/j.exer.2011.12.005.

Eisenstat, D. D., J. K. Liu, M. Mione, W. Zhong, G. Yu, S. A. Anderson, I. Ghattas, L. Puelles, and J. L. Rubenstein. 1999. "DLX-1, DLX-2, and DLX-5 expression define distinct stages of basal forebrain differentiation." *J Comp Neurol* 414 (2):217-37.

Ekker, M., M. A. Akimenko, R. Bremiller, and M. Westerfield. 1992. "Regional expression of three homeobox transcripts in the inner ear of zebrafish embryos." *Neuron* 9 (1):27-35.

Erkman, L., R. J. McEvilly, L. Luo, A. K. Ryan, F. Hooshmand, S. M. O'Connell, E. M. Keithley, D. H. Rapaport, A. F. Ryan, and M. G. Rosenfeld. 1996. "Role of transcription factors Brn-3.1 and Brn-3.2 in auditory and visual system development." *Nature* 381 (6583):603-6. doi: 10.1038/381603a0.

Erskine, L., S. Reijntjes, T. Pratt, L. Denti, Q. Schwarz, J. M. Vieira, B. Alakakone, D. Shewan, and C. Ruhrberg. 2011. "VEGF signaling through neuropilin 1 guides commissural axon crossing at the optic chiasm." *Neuron* 70 (5):951-65. doi: 10.1016/j.neuron.2011.02.052.

Erter, C. E., T. P. Wilm, N. Basler, C. V. Wright, and L. Solnica-Krezel. 2001. "Wnt8 is required in lateral mesendodermal precursors for neural posteriorization in vivo." *Development* 128 (18):3571-83.

Etchevers, H. C., C. Vincent, N. M. Le Douarin, and G. F. Couly. 2001. "The cephalic neural crest provides pericytes and smooth muscle cells to all blood vessels of the face and forebrain." *Development* 128 (7):1059-68.

Euler, T., S. Haverkamp, T. Schubert, and T. Baden. 2014. "Retinal bipolar cells: elementary building blocks of vision." *Nat Rev Neurosci* 15 (8):507-19.

Fantin, A., B. Herzog, M. Mahmoud, M. Yamaji, A. Plein, L. Denti, C. Ruhrberg, and I. Zachary. 2014. "Neuropilin 1 (NRP1) hypomorphism combined with defective VEGF-A binding reveals novel roles for NRP1 in developmental and pathological angiogenesis." *Development* 141 (3):556-62. doi: 10.1242/dev.103028.

Fausett, B. V., and D. Goldman. 2006. "A role for alpha1 tubulin-expressing Muller glia in regeneration of the injured zebrafish retina." *J Neurosci* 26 (23):6303-13. doi: 10.1523/JNEUROSCI.0332-06.2006.

Feng, L., X. Xie, P. S. Joshi, Z. Yang, K. Shibasaki, R. L. Chow, and L. Gan. 2006. "Requirement for Bhlhb5 in the specification of amacrine and cone bipolar subtypes in mouse retina." *Development* 133 (24):4815-25. doi: 10.1242/dev.02664.

Fernandez-Robredo, P., S. Selvam, M. B. Powner, D. A. Sim, and M. Fruttiger. 2017. "Neuropilin 1 Involvement in Choroidal and Retinal Neovascularisation." *PLoS One* 12 (1):e0169865. doi: 10.1371/journal.pone.0169865.

Ferrari, D., L. Sumoy, J. Gannon, H. Sun, A. M. Brown, W. B. Upholt, and R. A. Kosher. 1995. "The expression pattern of the Distal-less homeobox-containing gene Dlx-5 in the developing chick limb bud suggests its involvement in apical ectodermal ridge activity, pattern formation, and cartilage differentiation." *Mech Dev* 52 (2-3):257-64.

Freeman-Anderson, N. E., Y. Zheng, A. C. McCalla-Martin, L. M. Treanor, Y. D. Zhao, P. M. Garfin, T. C. He, M. N. Mary, J. D. Thornton, C. Anderson, M. Gibbons, R. Saab, S. H. Baumer, J. M. Cunningham, and S. X. Skapek. 2009. "Expression of the Arf tumor suppressor gene is controlled by Tgfbeta2 during development." *Development* 136 (12):2081-9. doi: 10.1242/dev.033548.

Freund, C. L., C. Y. Gregory-Evans, T. Furukawa, M. Papaioannou, J. Looser, L. Ploder, J. Bellingham, D. Ng, J. A. Herbrick, A. Duncan, S. W. Scherer, L. C. Tsui, A. Loutradis-Anagnostou, S. G. Jacobson, C. L. Cepko, S. S. Bhattacharya, and R. R. McInnes. 1997. "Cone-rod dystrophy due to mutations in a novel photoreceptor-specific homeobox gene (CRX) essential for maintenance of the photoreceptor." *Cell* 91 (4):543-53.

Friend, S. H., R. Bernards, S. Rogelj, R. A. Weinberg, J. M. Rapaport, D. M. Albert, and T. P. Dryja. 1986. "A human DNA segment with properties of the gene that predisposes to retinoblastoma and osteosarcoma." *Nature* 323 (6089):643-6. doi: 10.1038/323643a0.

Fruttiger, M. 2007. "Development of the retinal vasculature." *Angiogenesis* 10 (2):77-88. doi: 10.1007/s10456-007-9065-1.

Fruttiger, M., A. R. Calver, W. H. Kruger, H. S. Mudhar, D. Michalovich, N. Takakura, S. Nishikawa, and W. D. Richardson. 1996. "PDGF mediates a neuron-astrocyte interaction in the developing retina." *Neuron* 17 (6):1117-31.

Fruttiger, M., A. R. Calver, and W. D. Richardson. 2000. "Platelet-derived growth factor is constitutively secreted from neuronal cell bodies but not from axons." *Curr Biol* 10 (20):1283-6.

Fu, Y., H. Liu, L. Ng, J. W. Kim, H. Hao, A. Swaroop, and D. Forrest. 2014. "Feedback induction of a photoreceptor-specific isoform of retinoid-related orphan nuclear receptor beta by the rod transcription factor NRL." *J Biol Chem* 289 (47):32469-80. doi: 10.1074/jbc.M114.605774.

Fuhrmann, S. 2010. "Eye morphogenesis and patterning of the optic vesicle." *Curr Top Dev Biol* 93:61-84. doi: 10.1016/B978-0-12-385044-7.00003-5.

Fuhrmann, S., E. M. Levine, and T. A. Reh. 2000. "Extraocular mesenchyme patterns the optic vesicle during early eye development in the embryonic chick." *Development* 127 (21):4599-609.

Fujimura, N., M. M. Taketo, M. Mori, V. Korinek, and Z. Kozmik. 2009. "Spatial and temporal regulation of Wnt/beta-catenin signaling is essential for development of the retinal pigment epithelium." *Dev Biol* 334 (1):31-45. doi: 10.1016/j.ydbio.2009.07.002.

Fujitani, Y., S. Fujitani, H. Luo, F. Qiu, J. Burlison, Q. Long, Y. Kawaguchi, H. Edlund, R. J. MacDonald, T. Furukawa, T. Fujikado, M. A. Magnuson, M. Xiang, and C. V. Wright. 2006. "Ptf1a determines horizontal and amacrine cell fates during mouse retinal development." *Development* 133 (22):4439-50. doi: 10.1242/dev.02598.

Furukawa, T., C. A. Kozak, and C. L. Cepko. 1997. "rax, a novel paired-type homeobox gene, shows expression in the anterior neural fold and developing retina." *Proc Natl Acad Sci U S A* 94 (7):3088-93.

Furukawa, T., E. M. Morrow, and C. L. Cepko. 1997. "Crx, a novel otx-like homeobox gene, shows photoreceptor-specific expression and regulates photoreceptor differentiation." *Cell* 91 (4):531-41.

Gage, P. J., W. Rhoades, S. K. Prucka, and T. Hjalt. 2005. "Fate maps of neural crest and mesoderm in the mammalian eye." *Invest Ophthalmol Vis Sci* 46 (11):4200-8. doi: 10.1167/iovs.05-0691.

Gagliardini, V., and C. Fankhauser. 1999. "Semaphorin III can induce death in sensory neurons." *Mol Cell Neurosci* 14 (4-5):301-16. doi: 10.1006/mcne.1999.0787.

Gaiano, N., and G. Fishell. 2002. "The role of notch in promoting glial and neural stem cell fates." *Annu Rev Neurosci* 25:471-90. doi: 10.1146/annurev.neuro.25.030702.130823.

Gammill, Laura S., Constanza Gonzalez, and Marianne Bronner-Fraser. 2007. "Neuropilin 2/semaphorin 3F signaling is essential for cranial neural crest migration and trigeminal ganglion condensation." *Developmental Neurobiology* 67 (1):47-56. doi: 10.1002/dneu.20326.

Gan, L., M. Xiang, L. Zhou, D. S. Wagner, W. H. Klein, and J. Nathans. 1996. "POU domain factor Brn-3b is required for the development of a large set of retinal ganglion cells." *Proc Natl Acad Sci U S A* 93 (9):3920-5.

Gao, Z., C. A. Mao, P. Pan, X. Mu, and W. H. Klein. 2014. "Transcriptome of Atoh7 retinal progenitor cells identifies new Atoh7-dependent regulatory genes for retinal ganglion cell formation." *Dev Neurobiol* 74 (11):1123-40. doi: 10.1002/dneu.22188.

Ghanem, N., M. G. Andrusiak, D. Svoboda, S. M. Al Lafi, L. M. Julian, K. A. McClellan, Y. De Repentigny, R. Kothary, M. Ekker, A. Blais, D. S. Park, and R. S. Slack. 2012. "The Rb/E2F pathway modulates neurogenesis through direct regulation of the Dlx1/Dlx2 bigene cluster." *J Neurosci* 32 (24):8219-30. doi: 10.1523/JNEUROSCI.1344-12.2012.

Ghanem, N., O. Jarinova, A. Amores, Q. Long, G. Hatch, B. K. Park, J. L. Rubenstein, and M. Ekker. 2003. "Regulatory roles of conserved intergenic domains in vertebrate Dlx bigene clusters." *Genome Res* 13 (4):533-43. doi: 10.1101/gr.716103.

Ghanem, N., M. Yu, J. Long, G. Hatch, J. L. Rubenstein, and M. Ekker. 2007. "Distinct cis-regulatory elements from the Dlx1/Dlx2 locus mark different progenitor cell populations in the ganglionic eminences and different subtypes of adult cortical interneurons." *J Neurosci* 27 (19):5012-22. doi: 10.1523/JNEUROSCI.4725-06.2007.

Ghosh, K. K., S. Bujan, S. Haverkamp, A. Feigenspan, and H. Wassle. 2004. "Types of bipolar cells in the mouse retina." *J Comp Neurol* 469 (1):70-82. doi: 10.1002/cne.10985.

Giger, R. J., J. F. Cloutier, A. Sahay, R. K. Prinjha, D. V. Levengood, S. E. Moore, S. Pickering, D. Simmons, S. Rastan, F. S. Walsh, A. L. Kolodkin, D. D. Ginty, and M. Geppert. 2000. "Neuropilin-2 is required in vivo for selective axon guidance responses to secreted semaphorins." *Neuron* 25 (1):29-41.

Gillis, J. A., M. S. Modrell, and C. V. Baker. 2013. "Developmental evidence for serial homology of the vertebrate jaw and gill arch skeleton." *Nat Commun* 4:1436. doi: 10.1038/ncomms2429.

Ginsberg, D., G. Vairo, T. Chittenden, Z. X. Xiao, G. Xu, K. L. Wydner, J. A. DeCaprio, J. B. Lawrence, and D. M. Livingston. 1994. "E2F-4, a new member of the E2F transcription factor family, interacts with p107." *Genes Dev* 8 (22):2665-79.

Glinka, Y., and G. J. Prud'homme. 2008. "Neuropilin-1 is a receptor for transforming growth factor beta-1, activates its latent form, and promotes regulatory T cell activity." *J Leukoc Biol* 84 (1):302-10. doi: 10.1189/jlb.0208090.

Glinka, Y., S. Stoilova, N. Mohammed, and G. J. Prud'homme. 2011. "Neuropilin-1 exerts co-receptor function for TGF-beta-1 on the membrane of cancer cells and enhances responses to both latent and active TGF-beta." *Carcinogenesis* 32 (4):613-21. doi: 10.1093/carcin/bgq281.

Godement, P., J. Vanselow, S. Thanos, and F. Bonhoeffer. 1987. "A study in developing visual systems with a new method of staining neurones and their processes in fixed tissue." *Development* 101 (4):697-713.

Goding, C. R. 2000. "Mitf from neural crest to melanoma: signal transduction and transcription in the melanocyte lineage." *Genes Dev* 14 (14):1712-28.

Gogat, K., L. Le Gat, L. Van Den Berghe, D. Marchant, A. Kobetz, S. Gadin, B. Gasser, I. Quere, M. Abitbol, and M. Menasche. 2004. "VEGF and KDR gene expression during human embryonic and fetal eye development." *Invest Ophthalmol Vis Sci* 45 (1):7-14.

Goldberg, M. F. 1997. "Persistent fetal vasculature (PFV): an integrated interpretation of signs and symptoms associated with persistent hyperplastic primary vitreous (PHPV). LIV Edward Jackson Memorial Lecture." *Am J Ophthalmol* 124 (5):587-626.

Goldman, D. 2014. "Muller glial cell reprogramming and retina regeneration." *Nat Rev Neurosci* 15 (7):431-42. doi: 10.1038/nrn3723.

Gordon, C. T., I. M. Brinas, F. A. Rodda, A. J. Bendall, and P. G. Farlie. 2010. "Role of Dlx genes in craniofacial morphogenesis: Dlx2 influences skeletal patterning by inducing ectomesenchymal aggregation in ovo." *Evol Dev* 12 (5):459-73. doi: 10.1111/j.1525-142X.2010.00432.x.

Gordon, P. J., S. Yun, A. M. Clark, E. S. Monuki, L. C. Murtaugh, and E. M. Levine. 2013. "Lhx2 balances progenitor maintenance with neurogenic output and promotes competence state progression in the developing retina." *J Neurosci* 33 (30):12197-207. doi: 10.1523/JNEUROSCI.1494-13.2013.

Gorfinkiel, N., G. Morata, and I. Guerrero. 1997. "The homeobox gene Distal-less induces ventral appendage development in Drosophila." *Genes Dev* 11 (17):2259-71.

Goshima, Y., Y. Sasaki, T. Nakayama, T. Ito, and T. Kimura. 2000. "Functions of semaphorins in axon guidance and neuronal regeneration." *Jpn J Pharmacol* 82 (4):273-9.

Green, E. S., J. L. Stubbs, and E. M. Levine. 2003. "Genetic rescue of cell number in a mouse model of microphthalmia: interactions between Chx10 and G1-phase cell cycle regulators." *Development* 130 (3):539-52.

Grindley, J. C., D. R. Davidson, and R. E. Hill. 1995. "The role of Pax-6 in eye and nasal development." *Development* 121 (5):1433-42.

Gu, C., E. R. Rodriguez, D. V. Reimert, T. Shu, B. Fritzsch, L. J. Richards, A. L. Kolodkin, and D. D. Ginty. 2003. "Neuropilin-1 conveys semaphorin and VEGF signaling during neural and cardiovascular development." *Dev Cell* 5 (1):45-57.

Hafler, B. P., N. Surzenko, K. T. Beier, C. Punzo, J. M. Trimarchi, J. H. Kong, and C. L. Cepko. 2012. "Transcription factor Olig2 defines subpopulations of retinal progenitor cells biased toward specific cell fates." *Proc Natl Acad Sci U S A* 109 (20):7882-7. doi: 10.1073/pnas.1203138109.

Hagglund, A. C., L. Dahl, and L. Carlsson. 2011. "Lhx2 is required for patterning and expansion of a distinct progenitor cell population committed to eye development." *PLoS One* 6 (8):e23387. doi: 10.1371/journal.pone.0023387.

Hahn, P., T. Lindsten, M. Tolentino, C. B. Thompson, J. Bennett, and J. L. Dunaief. 2005. "Persistent fetal ocular vasculature in mice deficient in bax and bak." *Arch Ophthalmol* 123 (6):797-802. doi: 10.1001/archopht.123.6.797.

Haider, N. B., W. Zhang, R. Hurd, A. Ikeda, A. M. Nystuen, J. K. Naggert, and P. M. Nishina. 2008. "Mapping of genetic modifiers of Nr2e3 rd7/rd7 that suppress retinal

degeneration and restore blue cone cells to normal quantity." *Mamm Genome* 19 (3):145-54. doi: 10.1007/s00335-008-9092-2.

Hatakeyama, J., Y. Bessho, K. Katoh, S. Ookawara, M. Fujioka, F. Guillemot, and R. Kageyama. 2004. "Hes genes regulate size, shape and histogenesis of the nervous system by control of the timing of neural stem cell differentiation." *Development* 131 (22):5539-50. doi: 10.1242/dev.01436.

Hayden Gephart, M. G., Y. S. Su, S. Bandara, F. C. Tsai, J. Hong, N. Conley, H. Rayburn, L. Milenkovic, T. Meyer, and M. P. Scott. 2013. "Neuropilin-2 contributes to tumorigenicity in a mouse model of Hedgehog pathway medulloblastoma." *J Neurooncol* 115 (2):161-8. doi: 10.1007/s11060-013-1216-1.

He, Z., and M. Tessier-Lavigne. 1997. "Neuropilin is a receptor for the axonal chemorepellent Semaphorin III." *Cell* 90 (4):739-51.

Hegde, S., and O. Srivastava. 2016. "Different gene knockout/transgenic mouse models manifesting persistent fetal vasculature: Are integrins to blame for this pathological condition?" *Life Sci*. doi: 10.1016/j.lfs.2016.12.019.

Hill, R. E., J. Favor, B. L. Hogan, C. C. Ton, G. F. Saunders, I. M. Hanson, J. Prosser, T. Jordan, N. D. Hastie, and V. van Heyningen. 1991. "Mouse small eye results from mutations in a paired-like homeobox-containing gene." *Nature* 354 (6354):522-5. doi: 10.1038/354522a0.

Hillman, R. T., B. Y. Feng, J. Ni, W. M. Woo, L. Milenkovic, M. G. Hayden Gephart, M. N. Teruel, A. E. Oro, J. K. Chen, and M. P. Scott. 2011. "Neuropilins are positive regulators of Hedgehog signal transduction." *Genes Dev* 25 (22):2333-46. doi: 10.1101/gad.173054.111.

Hobbs, R., and M. E. Hartnett. 2014. "Hyaloid Vasculature: Development, Regression, Structure, and Pathologies A2 - McManus, Linda M." In *Pathobiology of Human Disease*, edited by Richard N. Mitchell, 2126-2136. San Diego: Academic Press.

Horsburgh, G. M., and A. J. Sefton. 1987. "Cellular degeneration and synaptogenesis in the developing retina of the rat." *J Comp Neurol* 263 (4):553-66. doi: 10.1002/cne.902630407.

Horsford, D. J., M. T. Nguyen, G. C. Sellar, R. Kothary, H. Arnheiter, and R. R. McInnes. 2005. "Chx10 repression of Mitf is required for the maintenance of mammalian neuroretinal identity." *Development* 132 (1):177-87. doi: 10.1242/dev.01571.

Hu, M., and S. S. Easter. 1999. "Retinal neurogenesis: the formation of the initial central patch of postmitotic cells." *Dev Biol* 207 (2):309-21. doi: 10.1006/dbio.1998.9031.

Huang, L., F. Hu, L. Feng, X. J. Luo, G. Liang, X. Y. Zeng, J. L. Yi, and L. Gan. 2014. "Bhlhb5 is required for the subtype development of retinal amacrine and bipolar cells in mice." *Dev Dyn* 243 (2):279-89. doi: 10.1002/dvdy.24067.

Iida, A., T. Shinoe, Y. Baba, H. Mano, and S. Watanabe. 2011. "Dicer plays essential roles for retinal development by regulation of survival and differentiation." *Invest Ophthalmol Vis Sci* 52 (6):3008-17. doi: 10.1167/iovs.10-6428.

Inoue, T., M. Hojo, Y. Bessho, Y. Tano, J. E. Lee, and R. Kageyama. 2002. "Math3 and NeuroD regulate amacrine cell fate specification in the retina." *Development* 129 (4):831-42.

Ishibashi, M., K. Moriyoshi, Y. Sasai, K. Shiota, S. Nakanishi, and R. Kageyama. 1994. "Persistent expression of helix-loop-helix factor HES-1 prevents mammalian neural differentiation in the central nervous system." *EMBO J* 13 (8):1799-805.

Ishida, S., K. Shinoda, S. Kawashima, Y. Oguchi, Y. Okada, and E. Ikeda. 2000. "Coexpression of VEGF receptors VEGF-R2 and neuropilin-1 in proliferative diabetic retinopathy." *Invest Ophthalmol Vis Sci* 41 (7):1649-56.

Ito, M., and M. Yoshioka. 1999. "Regression of the hyaloid vessels and pupillary membrane of the mouse." *Anat Embryol (Berl)* 200 (4):403-11.

Iwai-Takekoshi, L., A. Ramos, A. Schaler, S. Weinreb, R. Blazeski, and C. Mason. 2016. "Retinal pigment epithelial integrity is compromised in the developing albino mouse retina." *J Comp Neurol* 524 (18):3696-3716. doi: 10.1002/cne.24025.

Jadhav, A. P., H. A. Mason, and C. L. Cepko. 2006. "Notch 1 inhibits photoreceptor production in the developing mammalian retina." *Development* 133 (5):913-23. doi: 10.1242/dev.02245.

Jadhav, A. P., K. Roesch, and C. L. Cepko. 2009. "Development and neurogenic potential of Muller glial cells in the vertebrate retina." *Prog Retin Eye Res* 28 (4):249-62. doi: 10.1016/j.preteyeres.2009.05.002.

Jelcick, A. S., Y. Yuan, B. D. Leehy, L. C. Cox, A. C. Silveira, F. Qiu, S. Schenk, A. J. Sachs, M. A. Morrison, A. M. Nystuen, M. M. DeAngelis, and N. B. Haider. 2011. "Genetic variations strongly influence phenotypic outcome in the mouse retina." *PLoS One* 6 (7):e21858. doi: 10.1371/journal.pone.0021858.

Ji, T., Y. Guo, K. Kim, P. McQueen, S. Ghaffar, A. Christ, C. Lin, R. Eskander, X. Zi, and B. H. Hoang. 2015. "Neuropilin-2 expression is inhibited by secreted Wnt antagonists and its down-regulation is associated with reduced tumor growth and metastasis in osteosarcoma." *Mol Cancer* 14:86. doi: 10.1186/s12943-015-0359-4.

Julian, L. M., Y. Liu, C. A. Pakenham, D. Dugal-Tessier, V. Ruzhynsky, S. Bae, S. Y. Tsai, G. Leone, R. S. Slack, and A. Blais. 2016. "Tissue-specific targeting of cell fate regulatory genes by E2f factors." *Cell Death Differ* 23 (4):565-75. doi: 10.1038/cdd.2015.36.

Jusuf, P. R., A. D. Almeida, O. Randlett, K. Joubin, L. Poggi, and W. A. Harris. 2011. "Origin and determination of inhibitory cell lineages in the vertebrate retina." *J Neurosci* 31 (7):2549-62. doi: 10.1523/JNEUROSCI.4713-10.2011.

Kallapur, S., I. Ormsby, and T. Doetschman. 1999. "Strain dependency of TGFbeta1 function during embryogenesis." *Mol Reprod Dev* 52 (4):341-9. doi: 10.1002/(SICI)1098-2795(199904)52:4<341::AID-MRD2>3.0.CO;2-N.

Kato, M., M. S. Patel, R. Levasseur, I. Lobov, B. H. Chang, D. A. Glass, 2nd, C. Hartmann, L. Li, T. H. Hwang, C. F. Brayton, R. A. Lang, G. Karsenty, and L. Chan. 2002. "Cbfa1-independent decrease in osteoblast proliferation, osteopenia, and persistent embryonic eye vascularization in mice deficient in Lrp5, a Wnt coreceptor." *J Cell Biol* 157 (2):303-14. doi: 10.1083/jcb.200201089.

Katoh, K., Y. Omori, A. Onishi, S. Sato, M. Kondo, and T. Furukawa. 2010. "Blimp1 suppresses Chx10 expression in differentiating retinal photoreceptor precursors to ensure proper photoreceptor development." *J Neurosci* 30 (19):6515-26. doi: 10.1523/JNEUROSCI.0771-10.2010.

Kautzmann, M. A., D. S. Kim, M. P. Felder-Schmittbuhl, and A. Swaroop. 2011. "Combinatorial regulation of photoreceptor differentiation factor, neural retina leucine zipper gene NRL, revealed by in vivo promoter analysis." *J Biol Chem* 286 (32):28247-55. doi: 10.1074/jbc.M111.257246.

Kawasaki, T., T. Kitsukawa, Y. Bekku, Y. Matsuda, M. Sanbo, T. Yagi, and H. Fujisawa. 1999. "A requirement for neuropilin-1 in embryonic vessel formation." *Development* 126 (21):4895-902.

Kelley, P. B., Y. Sado, and M. K. Duncan. 2002. "Collagen IV in the developing lens capsule." *Matrix Biol* 21 (5):415-23.

Kelly, B. D., S. F. Hackett, K. Hirota, Y. Oshima, Z. Cai, S. Berg-Dixon, A. Rowan, Z. Yan, P. A. Campochiaro, and G. L. Semenza. 2003. "Cell type-specific regulation of angiogenic growth factor gene expression and induction of angiogenesis in nonischemic tissue by a

constitutively active form of hypoxia-inducible factor 1." *Circ Res* 93 (11):1074-81. doi: 10.1161/01.RES.0000102937.50486.1B.

Khaliq, S., A. Hameed, M. Ismail, K. Anwar, B. Leroy, A. M. Payne, S. S. Bhattacharya, and S. Q. Mehdi. 2001. "Locus for autosomal recessive nonsyndromic persistent hyperplastic primary vitreous." *Invest Ophthalmol Vis Sci* 42 (10):2225-8.

Khan, K., C. V. Logan, M. McKibbin, E. Sheridan, N. H. Elcioglu, O. Yenice, D. A. Parry, N. Fernandez-Fuentes, Z. I. Abdelhamed, A. Al-Maskari, J. A. Poulter, M. D. Mohamed, I. M. Carr, J. E. Morgan, H. Jafri, Y. Raashid, G. R. Taylor, C. A. Johnson, C. F. Inglehearn, C. Toomes, and M. Ali. 2012. "Next generation sequencing identifies mutations in Atonal homolog 7 (ATOH7) in families with global eye developmental defects." *Hum Mol Genet* 21 (4):776-83. doi: 10.1093/hmg/ddr509.

Kiecker, C., and C. Niehrs. 2001. "A morphogen gradient of Wnt/beta-catenin signalling regulates anteroposterior neural patterning in Xenopus." *Development* 128 (21):4189-201.

Kim, H. T., and J. W. Kim. 2012. "Compartmentalization of vertebrate optic neuroephithelium: external cues and transcription factors." *Mol Cells* 33 (4):317-24. doi: 10.1007/s10059-012-0030-5.

Kitsukawa, T., M. Shimizu, M. Sanbo, T. Hirata, M. Taniguchi, Y. Bekku, T. Yagi, and H. Fujisawa. 1997. "Neuropilin-semaphorin III/D-mediated chemorepulsive signals play a crucial role in peripheral nerve projection in mice." *Neuron* 19 (5):995-1005.

Klimova, L., B. Antosova, A. Kuzelova, H. Strnad, and Z. Kozmik. 2015. "Onecut1 and Onecut2 transcription factors operate downstream of Pax6 to regulate horizontal cell development." *Dev Biol* 402 (1):48-60. doi: 10.1016/j.ydbio.2015.02.023.

Koike, C., A. Nishida, S. Ueno, H. Saito, R. Sanuki, S. Sato, A. Furukawa, S. Aizawa, I. Matsuo, N. Suzuki, M. Kondo, and T. Furukawa. 2007. "Functional roles of Otx2 transcription factor in postnatal mouse retinal development." *Mol Cell Biol* 27 (23):8318-29. doi: 10.1128/MCB.01209-07.

Kolb, H. 1995. "Inner Plexiform Layer." In *Webvision: The Organization of the Retina and Visual System*, edited by H. Kolb, E. Fernandez and R. Nelson. Salt Lake City (UT).

Kolodkin, A. L., D. V. Levengood, E. G. Rowe, Y. T. Tai, R. J. Giger, and D. D. Ginty. 1997. "Neuropilin is a semaphorin III receptor." *Cell* 90 (4):753-62.

Koo, C. Y., K. W. Muir, and E. W. Lam. 2012. "FOXM1: From cancer initiation to progression and treatment." *Biochim Biophys Acta* 1819 (1):28-37. doi: 10.1016/j.bbagrm.2011.09.004.

Kouzarides, T. 2007. "Chromatin modifications and their function." *Cell* 128 (4):693-705. doi: 10.1016/j.cell.2007.02.005.

Krupnik, V. E., J. D. Sharp, C. Jiang, K. Robison, T. W. Chickering, L. Amaravadi, D. E. Brown, D. Guyot, G. Mays, K. Leiby, B. Chang, T. Duong, A. D. Goodearl, D. P. Gearing, S. Y. Sokol, and S. A. McCarthy. 1999. "Functional and structural diversity of the human Dickkopf gene family." *Gene* 238 (2):301-13.

Lam, E. W., J. J. Brosens, A. R. Gomes, and C. Y. Koo. 2013. "Forkhead box proteins: tuning forks for transcriptional harmony." *Nat Rev Cancer* 13 (7):482-95. doi: 10.1038/nrc3539.

Lang, R. A., and J. M. Bishop. 1993. "Macrophages are required for cell death and tissue remodeling in the developing mouse eye." *Cell* 74 (3):453-62.

Lapan, S. W., and P. W. Reddien. 2011. "dlx and sp6-9 Control optic cup regeneration in a prototypic eye." *PLoS Genet* 7 (8):e1002226. doi: 10.1371/journal.pgen.1002226.

Larsen, F., G. Gundersen, R. Lopez, and H. Prydz. 1992. "CpG islands as gene markers in the human genome." *Genomics* 13 (4):1095-107.

Le, T. N., G. Du, M. Fonseca, Q. P. Zhou, J. T. Wigle, and D. D. Eisenstat. 2007. "Dlx homeobox genes promote cortical interneuron migration from the basal forebrain by direct repression of the semaphorin receptor neuropilin-2." *J Biol Chem* 282 (26):19071-81. doi: 10.1074/jbc.M607486200.

Lee, J., M. K. Shin, D. K. Ryu, S. Kim, and W. S. Ryu. 2010. "Insertion and deletion mutagenesis by overlap extension PCR." *Methods Mol Biol* 634:137-46. doi: 10.1007/978-1-60761-652-8_10.

Lee, W. H., R. Bookstein, F. Hong, L. J. Young, J. Y. Shew, and E. Y. Lee. 1987. "Human retinoblastoma susceptibility gene: cloning, identification, and sequence." *Science* 235 (4794):1394-9.

Lekven, A. C., C. J. Thorpe, J. S. Waxman, and R. T. Moon. 2001. "Zebrafish wnt8 encodes two wnt8 proteins on a bicistronic transcript and is required for mesoderm and neurectoderm patterning." *Dev Cell* 1 (1):103-14.

Lewis, A. E., H. N. Vasudevan, A. K. O'Neill, P. Soriano, and J. O. Bush. 2013. "The widely used Wnt1-Cre transgene causes developmental phenotypes by ectopic activation of Wnt signaling." *Dev Biol* 379 (2):229-34. doi: 10.1016/j.ydbio.2013.04.026.

Li, B., M. Carey, and J. L. Workman. 2007. "The role of chromatin during transcription." *Cell* 128 (4):707-19. doi: 10.1016/j.cell.2007.01.015.

Li, S., Z. Mo, X. Yang, S. M. Price, M. M. Shen, and M. Xiang. 2004. "Foxn4 controls the genesis of amacrine and horizontal cells by retinal progenitors." *Neuron* 43 (6):795-807. doi: 10.1016/j.neuron.2004.08.041.

Lim, J. I., C. Spee, M. Hangai, J. Rocha, H. S. Ying, S. J. Ryan, and D. R. Hinton. 2005. "Neuropilin-1 expression by endothelial cells and retinal pigment epithelial cells in choroidal neovascular membranes." *Am J Ophthalmol* 140 (6):1044-1050. doi: 10.1016/j.ajo.2005.07.021.

Lin, Y. P., Y. Ouchi, S. Satoh, and S. Watanabe. 2009. "Sox2 plays a role in the induction of amacrine and Muller glial cells in mouse retinal progenitor cells." *Invest Ophthalmol Vis Sci* 50 (1):68-74. doi: 10.1167/iovs.07-1619.

Ling, T. L., and J. Stone. 1988. "The development of astrocytes in the cat retina: evidence of migration from the optic nerve." *Brain Res Dev Brain Res* 44 (1):73-85.

Liu, C., and J. Nathans. 2008. "An essential role for frizzled 5 in mammalian ocular development." *Development* 135 (21):3567-76. doi: 10.1242/dev.028076.

Liu, I. S., J. D. Chen, L. Ploder, D. Vidgen, D. van der Kooy, V. I. Kalnins, and R. R. McInnes. 1994. "Developmental expression of a novel murine homeobox gene (Chx10): evidence for roles in determination of the neuroretina and inner nuclear layer." *Neuron* 13 (2):377-93.

Liu, J. K., I. Ghattas, S. Liu, S. Chen, and J. L. Rubenstein. 1997. "Dlx genes encode DNA-binding proteins that are expressed in an overlapping and sequential pattern during basal ganglia differentiation." *Dev Dyn* 210 (4):498-512. doi: 10.1002/(SICI)1097-0177(199712)210:4<498::AID-AJA12>3.0.CO;2-3.

Lobov, I. B., S. Rao, T. J. Carroll, J. E. Vallance, M. Ito, J. K. Ondr, S. Kurup, D. A. Glass, M. S. Patel, W. Shu, E. E. Morrisey, A. P. McMahon, G. Karsenty, and R. A. Lang. 2005. "WNT7b mediates macrophage-induced programmed cell death in patterning of the vasculature." *Nature* 437 (7057):417-21. doi: 10.1038/nature03928.

Loosli, F., W. Staub, K. C. Finger-Baier, E. A. Ober, H. Verkade, J. Wittbrodt, and H. Baier. 2003. "Loss of eyes in zebrafish caused by mutation of chokh/rx3." *EMBO Rep* 4 (9):894-9. doi: 10.1038/sj.embor.embor919.

Los, L. I. 2008. "The rabbit as an animal model for post-natal vitreous matrix differentiation and degeneration." *Eye (Lond)* 22 (10):1223-32. doi: 10.1038/eye.2008.39.

Lu, Q. R., T. Sun, Z. Zhu, N. Ma, M. Garcia, C. D. Stiles, and D. H. Rowitch. 2002. "Common developmental requirement for Olig function indicates a motor neuron/oligodendrocyte connection." *Cell* 109 (1):75-86.

Lu, Q. R., D. Yuk, J. A. Alberta, Z. Zhu, I. Pawlitzky, J. Chan, A. P. McMahon, C. D. Stiles, and D. H. Rowitch. 2000. "Sonic hedgehog--regulated oligodendrocyte lineage genes encoding bHLH proteins in the mammalian central nervous system." *Neuron* 25 (2):317-29.

Lumb, R., S. Wiszniak, S. Kabbara, M. Scherer, N. Harvey, and Q. Schwarz. 2014. "Neuropilins define distinct populations of neural crest cells." *Neural Dev* 9:24. doi: 10.1186/1749-8104-9-24.

Ma, L., R. Cantrup, A. Varrault, D. Colak, N. Klenin, M. Gotz, S. McFarlane, L. Journot, and C. Schuurmans. 2007. "Zac1 functions through TGFbetaII to negatively regulate cell number in the developing retina." *Neural Dev* 2:11. doi: 10.1186/1749-8104-2-11.

MacDonald, R. B., M. Debiais-Thibaud, J. C. Talbot, and M. Ekker. 2010. "The relationship between dlx and gad1 expression indicates highly conserved genetic pathways in the zebrafish forebrain." *Dev Dyn* 239 (8):2298-306. doi: 10.1002/dvdy.22365.

Macdonald, R., K. A. Barth, Q. Xu, N. Holder, I. Mikkola, and S. W. Wilson. 1995. "Midline signalling is required for Pax gene regulation and patterning of the eyes." *Development* 121 (10):3267-78.

Mao, M., R. S. Smith, M. V. Alavi, J. K. Marchant, M. Cosma, R. T. Libby, S. W. John, and D. B. Gould. 2015. "Strain-Dependent Anterior Segment Dysgenesis and Progression to Glaucoma in Col4a1 Mutant Mice." *Invest Ophthalmol Vis Sci* 56 (11):6823-31. doi: 10.1167/iovs.15-17527.

Marcucio, R. S., D. R. Cordero, D. Hu, and J. A. Helms. 2005. "Molecular interactions coordinating the development of the forebrain and face." *Dev Biol* 284 (1):48-61. doi: 10.1016/j.ydbio.2005.04.030.

Marin, O., S. A. Anderson, and J. L. Rubenstein. 2000. "Origin and molecular specification of striatal interneurons." *J Neurosci* 20 (16):6063-76.

Marneros, A. G., J. Fan, Y. Yokoyama, H. P. Gerber, N. Ferrara, R. K. Crouch, and B. R. Olsen. 2005. "Vascular endothelial growth factor expression in the retinal pigment epithelium is essential for choriocapillaris development and visual function." *Am J Pathol* 167 (5):1451-9. doi: 10.1016/S0002-9440(10)61231-X.

Marquardt, T., R. Ashery-Padan, N. Andrejewski, R. Scardigli, F. Guillemot, and P. Gruss. 2001. "Pax6 is required for the multipotent state of retinal progenitor cells." *Cell* 105 (1):43-55.

Marquardt, T., and P. Gruss. 2002. "Generating neuronal diversity in the retina: one for nearly all." *Trends Neurosci* 25 (1):32-8.

Martinez-Morales, J. R., V. Dolez, I. Rodrigo, R. Zaccarini, L. Leconte, P. Bovolenta, and S. Saule. 2003. "OTX2 activates the molecular network underlying retina pigment epithelium differentiation." *J Biol Chem* 278 (24):21721-31. doi: 10.1074/jbc.M301708200.

Martinez-Morales, J. R., M. Signore, D. Acampora, A. Simeone, and P. Bovolenta. 2001. "Otx genes are required for tissue specification in the developing eye." *Development* 128 (11):2019-30.

Mathers, P. H., A. Grinberg, K. A. Mahon, and M. Jamrich. 1997. "The Rx homeobox gene is essential for vertebrate eye development." *Nature* 387 (6633):603-7. doi: 10.1038/42475.

Matsushita, A., T. Gotze, and M. Korc. 2007. "Hepatocyte growth factor-mediated cell invasion in pancreatic cancer cells is dependent on neuropilin-1." *Cancer Res* 67 (21):10309-16. doi: 10.1158/0008-5472.CAN-07-3256.

McClellan, K. A., V. A. Ruzhynsky, D. N. Douda, J. L. Vanderluit, K. L. Ferguson, D. Chen, R. Bremner, D. S. Park, G. Leone, and R. S. Slack. 2007. "Unique requirement for Rb/E2F3 in neuronal migration: evidence for cell cycle-independent functions." *Mol Cell Biol* 27 (13):4825-43. doi: 10.1128/MCB.02100-06.

McClellan, K. A., and R. S. Slack. 2006. "Novel functions for cell cycle genes in nervous system development." *Cell Cycle* 5 (14):1506-13. doi: 10.4161/cc.5.14.2980.

McClive, P., G. Pall, K. Newton, M. Lee, J. Mullins, and L. Forrester. 1998. "Gene trap integrations expressed in the developing heart: insertion site affects splicing of the PT1-ATG vector." *Dev Dyn* 212 (2):267-76. doi: 10.1002/(SICI)1097-0177(199806)212:2<267::AID-AJA11>3.0.CO;2-1.

McKenna, C. C., R. P. Munjaal, and P. Y. Lwigale. 2012. "Distinct roles for neuropilin1 and neuropilin2 during mouse corneal innervation." *PLoS One* 7 (5):e37175. doi: 10.1371/journal.pone.0037175.

McKercher, S. R., B. E. Torbett, K. L. Anderson, G. W. Henkel, D. J. Vestal, H. Baribault, M. Klemsz, A. J. Feeney, G. E. Wu, C. J. Paige, and R. A. Maki. 1996. "Targeted disruption of the PU.1 gene results in multiple hematopoietic abnormalities." *EMBO J* 15 (20):5647-58.

Mears, A. J., M. Kondo, P. K. Swain, Y. Takada, R. A. Bush, T. L. Saunders, P. A. Sieving, and A. Swaroop. 2001. "Nrl is required for rod photoreceptor development." *Nat Genet* 29 (4):447-52. doi: 10.1038/ng774.

Mets, M. B. 1999. "Childhood blindness and visual loss: an assessment at two institutions including a "new" cause." *Trans Am Ophthalmol Soc* 97:653-96.

Mitchell, C. A., W. Risau, and H. C. Drexler. 1998. "Regression of vessels in the tunica vasculosa lentis is initiated by coordinated endothelial apoptosis: a role for vascular endothelial growth factor as a survival factor for endothelium." *Dev Dyn* 213 (3):322-33. doi: 10.1002/(SICI)1097-0177(199811)213:3<322::AID-AJA8>3.0.CO;2-E.

Mo, Z., S. Li, X. Yang, and M. Xiang. 2004. "Role of the Barhl2 homeobox gene in the specification of glycinergic amacrine cells." *Development* 131 (7):1607-18. doi: 10.1242/dev.01071.

Moberg, K., M. A. Starz, and J. A. Lees. 1996. "E2F-4 switches from p130 to p107 and pRB in response to cell cycle reentry." *Mol Cell Biol* 16 (4):1436-49.

Mochii, M., T. Ono, Y. Matsubara, and G. Eguchi. 1998. "Spontaneous transdifferentiation of quail pigmented epithelial cell is accompanied by a mutation in the Mitf gene." *Dev Biol* 196 (2):145-59. doi: 10.1006/dbio.1998.8864.

Morante, J., T. Erclik, and C. Desplan. 2011. "Cell migration in Drosophila optic lobe neurons is controlled by eyeless/Pax6." *Development* 138 (4):687-93. doi: 10.1242/dev.056069.

Mu, X., P. D. Beremand, S. Zhao, R. Pershad, H. Sun, A. Scarpa, S. Liang, T. L. Thomas, and W. H. Klein. 2004. "Discrete gene sets depend on POU domain transcription factor Brn3b/Brn-3.2/POU4f2 for their expression in the mouse embryonic retina." *Development* 131 (6):1197-210. doi: 10.1242/dev.01010.

Mu, X., X. Fu, P. D. Beremand, T. L. Thomas, and W. H. Klein. 2008. "Gene regulation logic in retinal ganglion cell development: Isl1 defines a critical branch distinct from but

overlapping with Pou4f2." *Proc Natl Acad Sci U S A* 105 (19):6942-7. doi: 10.1073/pnas.0802627105.

Mu, X., and W. H. Klein. 2004. "A gene regulatory hierarchy for retinal ganglion cell specification and differentiation." *Semin Cell Dev Biol* 15 (1):115-23. doi: 10.1016/j.semcdb.2003.09.009.

Mudhar, H. S., R. A. Pollock, C. Wang, C. D. Stiles, and W. D. Richardson. 1993. "PDGF and its receptors in the developing rodent retina and optic nerve." *Development* 118 (2):539-52.

Muto, A., A. Iida, S. Satoh, and S. Watanabe. 2009. "The group E Sox genes Sox8 and Sox9 are regulated by Notch signaling and are required for Muller glial cell development in mouse retina." *Exp Eye Res* 89 (4):549-58. doi: 10.1016/j.exer.2009.05.006.

Nakamura, K., C. Harada, K. Namekata, and T. Harada. 2006. "Expression of olig2 in retinal progenitor cells." *Neuroreport* 17 (4):345-9. doi: 10.1097/01.wnr.0000203352.44998.6b.

Naser, R., R. Vandenbosch, S. Omais, D. Hayek, C. Jaafar, S. Al Lafi, A. Saliba, M. Baghdadi, L. Skaf, and N. Ghanem. 2016. "Role of the Retinoblastoma protein, Rb, during adult neurogenesis in the olfactory bulb." *Sci Rep* 6:20230. doi: 10.1038/srep20230.

Nelson, S. M., L. Park, and D. L. Stenkamp. 2009. "Retinal homeobox 1 is required for retinal neurogenesis and photoreceptor differentiation in embryonic zebrafish." *Dev Biol* 328 (1):24-39. doi: 10.1016/j.ydbio.2008.12.040.

Neufeld, G., and O. Kessler. 2008. "The semaphorins: versatile regulators of tumour progression and tumour angiogenesis." *Nat Rev Cancer* 8 (8):632-45. doi: 10.1038/nrc2404.

Ng, L., J. B. Hurley, B. Dierks, M. Srinivas, C. Salto, B. Vennstrom, T. A. Reh, and D. Forrest. 2001. "A thyroid hormone receptor that is required for the development of green cone photoreceptors." *Nat Genet* 27 (1):94-8. doi: 10.1038/83829.

Ng, L., A. Lu, A. Swaroop, D. S. Sharlin, A. Swaroop, and D. Forrest. 2011. "Two transcription factors can direct three photoreceptor outcomes from rod precursor cells in mouse retinal development." *J Neurosci* 31 (31):11118-25. doi: 10.1523/JNEUROSCI.1709-11.2011.

Nguyen, M., and H. Arnheiter. 2000. "Signaling and transcriptional regulation in early mammalian eye development: a link between FGF and MITF." *Development* 127 (16):3581-91.

Nickla, D. L., and J. Wallman. 2010. "The multifunctional choroid." *Prog Retin Eye Res* 29 (2):144-68. doi: 10.1016/j.preteyeres.2009.12.002.

Nishida, A., A. Furukawa, C. Koike, Y. Tano, S. Aizawa, I. Matsuo, and T. Furukawa. 2003. "Otx2 homeobox gene controls retinal photoreceptor cell fate and pineal gland development." *Nat Neurosci* 6 (12):1255-63. doi: 10.1038/nn1155.

Ogata-Iwao, M., M. Inatani, K. Iwao, Y. Takihara, Y. Nakaishi-Fukuchi, F. Irie, S. Sato, T. Furukawa, Y. Yamaguchi, and H. Tanihara. 2011. "Heparan sulfate regulates intraretinal axon pathfinding by retinal ganglion cells." *Invest Ophthalmol Vis Sci* 52 (9):6671-9. doi: 10.1167/iovs.11-7559.

Ohtsuka, T., M. Ishibashi, G. Gradwohl, S. Nakanishi, F. Guillemot, and R. Kageyama. 1999. "Hes1 and Hes5 as notch effectors in mammalian neuronal differentiation." *EMBO J* 18 (8):2196-207. doi: 10.1093/emboj/18.8.2196.

Okabe, K., S. Kobayashi, T. Yamada, T. Kurihara, I. Tai-Nagara, T. Miyamoto, Y. S. Mukouyama, T. N. Sato, T. Suda, M. Ema, and Y. Kubota. 2014. "Neurons limit angiogenesis by titrating VEGF in retina." *Cell* 159 (3):584-96. doi: 10.1016/j.cell.2014.09.025.

Omori, Y., K. Katoh, S. Sato, Y. Muranishi, T. Chaya, A. Onishi, T. Minami, T. Fujikado, and T. Furukawa. 2011. "Analysis of transcriptional regulatory pathways of photoreceptor genes by expression profiling of the Otx2-deficient retina." *PLoS One* 6 (5):e19685. doi: 10.1371/journal.pone.0019685.

Oshima, Y., S. Oshima, H. Nambu, S. Kachi, K. Takahashi, N. Umeda, J. Shen, A. Dong, R. S. Apte, E. Duh, S. F. Hackett, G. Okoye, K. Ishibashi, J. Handa, M. Melia, S. Wiegand, G. Yancopoulos, D. J. Zack, and P. A. Campochiaro. 2005. "Different effects of angiopoietin-2 in different vascular beds: new vessels are most sensitive." *FASEB J* 19 (8):963-5. doi: 10.1096/fj.04-2209fje.

Ozaki, H., A. Y. Yu, N. Della, K. Ozaki, J. D. Luna, H. Yamada, S. F. Hackett, N. Okamoto, D. J. Zack, G. L. Semenza, and P. A. Campochiaro. 1999. "Hypoxia inducible factor-1alpha is increased in ischemic retina: temporal and spatial correlation with VEGF expression." *Invest Ophthalmol Vis Sci* 40 (1):182-9.

Pan, L., M. Deng, X. Xie, and L. Gan. 2008. "ISL1 and BRN3B co-regulate the differentiation of murine retinal ganglion cells." *Development* 135 (11):1981-90. doi: 10.1242/dev.010751.

Panganiban, G., S. M. Irvine, C. Lowe, H. Roehl, L. S. Corley, B. Sherbon, J. K. Grenier, J. F. Fallon, J. Kimble, M. Walker, G. A. Wray, B. J. Swalla, M. Q. Martindale, and S. B. Carroll. 1997. "The origin and evolution of animal appendages." *Proc Natl Acad Sci U S A* 94 (10):5162-6.

Panganiban, G., and J. L. Rubenstein. 2002. "Developmental functions of the Distal-less/Dlx homeobox genes." *Development* 129 (19):4371-86.

Park, P. J. 2009. "ChIP-seq: advantages and challenges of a maturing technology." *Nat Rev Genet* 10 (10):669-80. doi: 10.1038/nrg2641.

Pechmann, M., S. Khadjeh, F. Sprenger, and N. M. Prpic. 2010. "Patterning mechanisms and morphological diversity of spider appendages and their importance for spider evolution." *Arthropod Struct Dev* 39 (6):453-67. doi: 10.1016/j.asd.2010.07.007.

Pellet-Many, C., P. Frankel, H. Jia, and I. Zachary. 2008. "Neuropilins: structure, function and role in disease." *Biochem J* 411 (2):211-26. doi: 10.1042/BJ20071639.

Petryniak, M. A., G. B. Potter, D. H. Rowitch, and J. L. Rubenstein. 2007. "Dlx1 and Dlx2 control neuronal versus oligodendroglial cell fate acquisition in the developing forebrain." *Neuron* 55 (3):417-33. doi: 10.1016/j.neuron.2007.06.036.

Pierce, E. A., R. L. Avery, E. D. Foley, L. P. Aiello, and L. E. Smith. 1995. "Vascular endothelial growth factor/vascular permeability factor expression in a mouse model of retinal neovascularization." *Proc Natl Acad Sci U S A* 92 (3):905-9.

Pittack, C., G. B. Grunwald, and T. A. Reh. 1997. "Fibroblast growth factors are necessary for neural retina but not pigmented epithelium differentiation in chick embryos." *Development* 124 (4):805-16.

Poche, R. A., K. M. Kwan, M. A. Raven, Y. Furuta, B. E. Reese, and R. R. Behringer. 2007. "Lim1 is essential for the correct laminar positioning of retinal horizontal cells." *J Neurosci* 27 (51):14099-107. doi: 10.1523/JNEUROSCI.4046-07.2007.

Pollard, Z. F. 1997. "Persistent hyperplastic primary vitreous: diagnosis, treatment and results." *Trans Am Ophthalmol Soc* 95:487-549.

Pollock, G. S., R. Robichon, K. A. Boyd, K. A. Kerkel, M. Kramer, J. Lyles, R. Ambalavanar, A. Khan, D. R. Kaplan, R. W. Williams, and D. O. Frost. 2003. "TrkB receptor signaling regulates developmental death dynamics, but not final number, of retinal ganglion cells." *J Neurosci* 23 (31):10137-45.

Ponsioen, T. L., J. M. Hooymans, and L. I. Los. 2010. "Remodelling of the human vitreous and vitreoretinal interface--a dynamic process." *Prog Retin Eye Res* 29 (6):580-95. doi: 10.1016/j.preteyeres.2010.07.001.

Porter, F. D., J. Drago, Y. Xu, S. S. Cheema, C. Wassif, S. P. Huang, E. Lee, A. Grinberg, J. S. Massalas, D. Bodine, F. Alt, and H. Westphal. 1997. "Lhx2, a LIM homeobox gene, is required for eye, forebrain, and definitive erythrocyte development." *Development* 124 (15):2935-44.

Porteus, M. H., A. Bulfone, R. D. Ciaranello, and J. L. Rubenstein. 1991. "Isolation and characterization of a novel cDNA clone encoding a homeodomain that is developmentally regulated in the ventral forebrain." *Neuron* 7 (2):221-9.

Porteus, M. H., A. Bulfone, J. K. Liu, L. Puelles, L. C. Lo, and J. L. Rubenstein. 1994. "DLX-2, MASH-1, and MAP-2 expression and bromodeoxyuridine incorporation define molecularly distinct cell populations in the embryonic mouse forebrain." *J Neurosci* 14 (11 Pt 1):6370-83.

Potts, R. A., B. Dreher, and M. R. Bennett. 1982. "The loss of ganglion cells in the developing retina of the rat." *Brain Res* 255 (3):481-6.

Prasov, L., T. Masud, S. Khaliq, S. Q. Mehdi, A. Abid, E. R. Oliver, E. D. Silva, A. Lewanda, M. C. Brodsky, M. Borchert, D. Kelberman, J. C. Sowden, M. T. Dattani, and T. Glaser. 2012. "ATOH7 mutations cause autosomal recessive persistent hyperplasia of the primary vitreous." *Hum Mol Genet* 21 (16):3681-94. doi: 10.1093/hmg/dds197.

Price, M., M. Lemaistre, M. Pischetola, R. Di Lauro, and D. Duboule. 1991. "A mouse gene related to Distal-less shows a restricted expression in the developing forebrain." *Nature* 351 (6329):748-51. doi: 10.1038/351748a0.

Prud'homme, G. J., and Y. Glinka. 2012. "Neuropilins are multifunctional coreceptors involved in tumor initiation, growth, metastasis and immunity." *Oncotarget* 3 (9):921-39. doi: 10.18632/oncotarget.626.

Puschel, A. W., M. Westerfield, and G. R. Dressler. 1992. "Comparative analysis of Pax-2 protein distributions during neurulation in mice and zebrafish." *Mech Dev* 38 (3):197-208.

Qiu, M., A. Bulfone, I. Ghattas, J. J. Meneses, L. Christensen, P. T. Sharpe, R. Presley, R. A. Pedersen, and J. L. Rubenstein. 1997. "Role of the Dlx homeobox genes in proximodistal patterning of the branchial arches: mutations of Dlx-1, Dlx-2, and Dlx-1 and -2 alter morphogenesis of proximal skeletal and soft tissue structures derived from the first and second arches." *Dev Biol* 185 (2):165-84. doi: 10.1006/dbio.1997.8556.

Qiu, M., A. Bulfone, S. Martinez, J. J. Meneses, K. Shimamura, R. A. Pedersen, and J. L. Rubenstein. 1995. "Null mutation of Dlx-2 results in abnormal morphogenesis of proximal first and second branchial arch derivatives and abnormal differentiation in the forebrain." *Genes Dev* 9 (20):2523-38.

Raimondi, C., J. T. Brash, A. Fantin, and C. Ruhrberg. 2016. "NRP1 function and targeting in neurovascular development and eye disease." *Prog Retin Eye Res* 52:64-83. doi: 10.1016/j.preteyeres.2016.02.003.

Rapaport, D. H., L. L. Wong, E. D. Wood, D. Yasumura, and M. M. LaVail. 2004. "Timing and topography of cell genesis in the rat retina." *J Comp Neurol* 474 (2):304-24. doi: 10.1002/cne.20134.

Raper, J. A. 2000. "Semaphorins and their receptors in vertebrates and invertebrates." *Curr Opin Neurobiol* 10 (1):88-94.

Reese, B. E. 2011. "Development of the retina and optic pathway." *Vision Res* 51 (7):613-32. doi: 10.1016/j.visres.2010.07.010.

Reichel, M. B., R. R. Ali, F. D'Esposito, A. R. Clarke, P. J. Luthert, S. S. Bhattacharya, and D. M. Hunt. 1998. "High frequency of persistent hyperplastic primary vitreous and cataracts in p53-deficient mice." *Cell Death Differ* 5 (2):156-62. doi: 10.1038/sj.cdd.4400326.

Ren, B., F. Robert, J. J. Wyrick, O. Aparicio, E. G. Jennings, I. Simon, J. Zeitlinger, J. Schreiber, N. Hannett, E. Kanin, T. L. Volkert, C. J. Wilson, S. P. Bell, and R. A. Young. 2000. "Genome-wide location and function of DNA binding proteins." *Science* 290 (5500):2306-9. doi: 10.1126/science.290.5500.2306.

Riesenberg, A. N., T. T. Le, M. I. Willardsen, D. C. Blackburn, M. L. Vetter, and N. L. Brown. 2009. "Pax6 regulation of Math5 during mouse retinal neurogenesis." *Genesis* 47 (3):175-87. doi: 10.1002/dvg.20479.

Rivolta, C., N. E. Peck, A. B. Fulton, G. A. Fishman, E. L. Berson, and T. P. Dryja. 2001. "Novel frameshift mutations in CRX associated with Leber congenital amaurosis." *Hum Mutat* 18 (6):550-1. doi: 10.1002/humu.1243.

Rizzolio, S., and L. Tamagnone. 2011. "Multifaceted role of neuropilins in cancer." *Curr Med Chem* 18 (23):3563-75.

Roberts, M. R., A. Hendrickson, C. R. McGuire, and T. A. Reh. 2005. "Retinoid X receptor (gamma) is necessary to establish the S-opsin gradient in cone photoreceptors of the developing mouse retina." *Invest Ophthalmol Vis Sci* 46 (8):2897-904. doi: 10.1167/iovs.05-0093.

Roberts, M. R., M. Srinivas, D. Forrest, G. Morreale de Escobar, and T. A. Reh. 2006. "Making the gradient: thyroid hormone regulates cone opsin expression in the developing mouse retina." *Proc Natl Acad Sci U S A* 103 (16):6218-23. doi: 10.1073/pnas.0509981103.

Robinson, G. W., S. Wray, and K. A. Mahon. 1991. "Spatially restricted expression of a member of a new family of murine Distal-less homeobox genes in the developing forebrain." *New Biol* 3 (12):1183-94.

Robinson-Rechavi, M., O. Marchand, H. Escriva, P. L. Bardet, D. Zelus, S. Hughes, and V. Laudet. 2001. "Euteleost fish genomes are characterized by expansion of gene families." *Genome Res* 11 (5):781-8. doi: 10.1101/gr.165601.

Roger, J. E., A. Hiriyanna, N. Gotoh, H. Hao, D. F. Cheng, R. Ratnapriya, M. A. Kautzmann, B. Chang, and A. Swaroop. 2014. "OTX2 loss causes rod differentiation defect in CRX-associated congenital blindness." *J Clin Invest* 124 (2):631-43. doi: 10.1172/JCI72722.

Rohrer, B., M. M. LaVail, K. R. Jones, and L. F. Reichardt. 2001. "Neurotrophin receptor TrkB activation is not required for the postnatal survival of retinal ganglion cells in vivo." *Exp Neurol* 172 (1):81-91. doi: 10.1006/exnr.2001.7795.

Rubenstein, J. L., and P. A. Beachy. 1998. "Patterning of the embryonic forebrain." *Curr Opin Neurobiol* 8 (1):18-26.

Rutland, C. S., C. A. Mitchell, M. Nasir, M. A. Konerding, and H. C. Drexler. 2007. "Microphthalmia, persistent hyperplastic hyaloid vasculature and lens anomalies following overexpression of VEGF-A188 from the alphaA-crystallin promoter." *Mol Vis* 13:47-56.

Sabo, P. J., M. S. Kuehn, R. Thurman, B. E. Johnson, E. M. Johnson, H. Cao, M. Yu, E. Rosenzweig, J. Goldy, A. Haydock, M. Weaver, A. Shafer, K. Lee, F. Neri, R. Humbert, M. A. Singer, T. A. Richmond, M. O. Dorschner, M. McArthur, M. Hawrylycz, R. D. Green, P. A. Navas, W. S. Noble, and J. A. Stamatoyannopoulos. 2006. "Genome-scale mapping of DNase I sensitivity in vivo using tiling DNA microarrays." *Nat Methods* 3 (7):511-8. doi: 10.1038/nmeth890.

Saint-Geniez, M., and P. A. D'Amore. 2004. "Development and pathology of the hyaloid, choroidal and retinal vasculature." *Int J Dev Biol* 48 (8-9):1045-58. doi: 10.1387/ijdb.041895ms.

Samuel, A., M. Housset, B. Fant, and T. Lamonerie. 2014. "Otx2 ChIP-seq reveals unique and redundant functions in the mature mouse retina." *PLoS One* 9 (2):e89110. doi: 10.1371/journal.pone.0089110.

Sanes, J. R., and R. H. Masland. 2015. "The types of retinal ganglion cells: current status and implications for neuronal classification." *Annu Rev Neurosci* 38:221-46. doi: 10.1146/annurev-neuro-071714-034120.

Sanyanusin, P., L. A. Schimmenti, L. A. McNoe, T. A. Ward, M. E. Pierpont, M. J. Sullivan, W. B. Dobyns, and M. R. Eccles. 1995. "Mutation of the PAX2 gene in a family with optic nerve colobomas, renal anomalies and vesicoureteral reflux." *Nat Genet* 9 (4):358-64. doi: 10.1038/ng0495-358.

Sarthy, V. 1993. "Collagen IV mRNA expression during development of the mouse retina: an in situ hybridization study." *Invest Ophthalmol Vis Sci* 34 (1):145-52.

Sasagawa, S., T. Takabatake, Y. Takabatake, T. Muramatsu, and K. Takeshima. 2002. "Axes establishment during eye morphogenesis in Xenopus by coordinate and antagonistic actions of BMP4, Shh, and RA." *Genesis* 33 (2):86-96. doi: 10.1002/gene.10095.

Sato, S., T. Inoue, K. Terada, I. Matsuo, S. Aizawa, Y. Tano, T. Fujikado, and T. Furukawa. 2007. "Dkk3-Cre BAC transgenic mouse line: a tool for highly efficient gene deletion in retinal progenitor cells." *Genesis* 45 (8):502-7. doi: 10.1002/dvg.20318.

Saxonov, S., P. Berg, and D. L. Brutlag. 2006. "A genome-wide analysis of CpG dinucleotides in the human genome distinguishes two distinct classes of promoters." *Proc Natl Acad Sci U S A* 103 (5):1412-7. doi: 10.1073/pnas.0510310103.

Schmidt, M., A. Giessl, T. Laufs, T. Hankeln, U. Wolfrum, and T. Burmester. 2003. "How does the eye breathe? Evidence for neuroglobin-mediated oxygen supply in the mammalian retina." *J Biol Chem* 278 (3):1932-5. doi: 10.1074/jbc.M209909200.

Schwarz, M., F. Cecconi, G. Bernier, N. Andrejewski, B. Kammandel, M. Wagner, and P. Gruss. 2000. "Spatial specification of mammalian eye territories by reciprocal transcriptional repression of Pax2 and Pax6." *Development* 127 (20):4325-34.

Selkoe, D., and R. Kopan. 2003. "Notch and Presenilin: regulated intramembrane proteolysis links development and degeneration." *Annu Rev Neurosci* 26:565-97. doi: 10.1146/annurev.neuro.26.041002.131334.

Sharma, A., C. J. LeVaillant, G. W. Plant, and A. R. Harvey. 2014. "Changes in expression of Class 3 Semaphorins and their receptors during development of the rat retina and superior colliculus." *BMC Dev Biol* 14:34. doi: 10.1186/s12861-014-0034-9.

Sharma, A., J. Verhaagen, and A. R. Harvey. 2012. "Receptor complexes for each of the Class 3 Semaphorins." *Front Cell Neurosci* 6:28. doi: 10.3389/fncel.2012.00028.

Shen, J., R. Samul, J. Zimmer, H. Liu, X. Liang, S. Hackett, and P. A. Campochiaro. 2004. "Deficiency of neuropilin 2 suppresses VEGF-induced retinal neovascularization." *Mol Med* 10 (1-6):12-8.

Shi, Z., S. Trenholm, M. Zhu, S. Buddingh, E. N. Star, G. B. Awatramani, and R. L. Chow. 2011. "Vsx1 regulates terminal differentiation of type 7 ON bipolar cells." *J Neurosci* 31 (37):13118-27. doi: 10.1523/JNEUROSCI.2331-11.2011.

Shibasaki, K., H. Takebayashi, K. Ikenaka, L. Feng, and L. Gan. 2007. "Expression of the basic helix-loop-factor Olig2 in the developing retina: Olig2 as a new marker for retinal progenitors and late-born cells." *Gene Expr Patterns* 7 (1-2):57-65. doi: 10.1016/j.modgep.2006.05.008.

Shirvan, A., I. Ziv, G. Fleminger, R. Shina, Z. He, I. Brudo, E. Melamed, and A. Barzilai. 1999. "Semaphorins as mediators of neuronal apoptosis." *J Neurochem* 73 (3):961-71.

Silbereis, J. C., H. Nobuta, H. H. Tsai, V. M. Heine, G. L. McKinsey, D. H. Meijer, M. A. Howard, M. A. Petryniak, G. B. Potter, J. A. Alberta, S. C. Baraban, C. D. Stiles, J. L. Rubenstein, and D. H. Rowitch. 2014. "Olig1 function is required to repress dlx1/2 and interneuron production in Mammalian brain." *Neuron* 81 (3):574-87. doi: 10.1016/j.neuron.2013.11.024.

Silva, R. L., J. D. Thornton, A. C. Martin, J. E. Rehg, D. Bertwistle, F. Zindy, and S. X. Skapek. 2005. "Arf-dependent regulation of Pdgf signaling in perivascular cells in the developing mouse eye." *EMBO J* 24 (15):2803-14. doi: 10.1038/sj.emboj.7600751.

Simeone, A., D. Acampora, M. Pannese, M. D'Esposito, A. Stornaiuolo, M. Gulisano, A. Mallamaci, K. Kastury, T. Druck, K. Huebner, and et al. 1994. "Cloning and characterization of two members of the vertebrate Dlx gene family." *Proc Natl Acad Sci U S A* 91 (6):2250-4.

Sinha, D., A. Klise, Y. Sergeev, S. Hose, I. A. Bhutto, L. Hackler, Jr., T. Malpic-Llanos, S. Samtani, R. Grebe, M. F. Goldberg, J. F. Hejtmancik, A. Nath, D. J. Zack, R. N. Fariss, D. S. McLeod, O. Sundin, K. W. Broman, G. A. Lutty, and J. S. Zigler, Jr. 2008. "betaA3/A1-crystallin in astroglial cells regulates retinal vascular remodeling during development." *Mol Cell Neurosci* 37 (1):85-95. doi: 10.1016/j.mcn.2007.08.016.

Snead, M. P., D. R. Snead, A. J. Richards, J. B. Harrison, A. V. Poulson, A. H. Morris, R. M. Sheard, and J. D. Scott. 2002. "Clinical, histological and ultrastructural studies of the posterior hyaloid membrane." *Eye (Lond)* 16 (4):447-53. doi: 10.1038/sj.eye.6700198.

Sohocki, M. M., L. S. Sullivan, H. A. Mintz-Hittner, D. Birch, J. R. Heckenlively, C. L. Freund, R. R. McInnes, and S. P. Daiger. 1998. "A range of clinical phenotypes associated with mutations in CRX, a photoreceptor transcription-factor gene." *Am J Hum Genet* 63 (5):1307-15. doi: 10.1086/302101.

Soker, S., S. Takashima, H. Q. Miao, G. Neufeld, and M. Klagsbrun. 1998. "Neuropilin-1 is expressed by endothelial and tumor cells as an isoform-specific receptor for vascular endothelial growth factor." *Cell* 92 (6):735-45.

Solek, C. M., S. Feng, S. Perin, H. Weinschutz Mendes, and M. Ekker. 2017. "Lineage tracing of dlx1a/2a and dlx5a/6a expressing cells in the developing zebrafish brain." *Dev Biol* 427 (1):131-147. doi: 10.1016/j.ydbio.2017.04.019.

Son, A. I., M. Sheleg, M. A. Cooper, Y. Sun, N. J. Kleiman, and R. Zhou. 2014. "Formation of persistent hyperplastic primary vitreous in ephrin-A5-/- mice." *Invest Ophthalmol Vis Sci* 55 (3):1594-606. doi: 10.1167/iovs.13-12706.

Sowden, J. C. 2007. "Molecular and developmental mechanisms of anterior segment dysgenesis." *Eye (Lond)* 21 (10):1310-8. doi: 10.1038/sj.eye.6702852.

Square, T., D. Jandzik, M. Cattell, A. Coe, J. Doherty, and D. M. Medeiros. 2015. "A gene expression map of the larval Xenopus laevis head reveals developmental changes underlying the evolution of new skeletal elements." *Dev Biol* 397 (2):293-304. doi: 10.1016/j.ydbio.2014.10.016.

Stanford, W. L., J. B. Cohn, and S. P. Cordes. 2001. "Gene-trap mutagenesis: past, present and beyond." *Nat Rev Genet* 2 (10):756-68. doi: 10.1038/35093548.

Star, E. N., M. Zhu, Z. Shi, H. Liu, M. Pashmforoush, Y. Sauve, B. G. Bruneau, and R. L. Chow. 2012. "Regulation of retinal interneuron subtype identity by the Iroquois homeobox gene Irx6." *Development* 139 (24):4644-55. doi: 10.1242/dev.081729.

Stone, J., A. Itin, T. Alon, J. Pe'er, H. Gnessin, T. Chan-Ling, and E. Keshet. 1995. "Development of retinal vasculature is mediated by hypoxia-induced vascular endothelial growth factor (VEGF) expression by neuroglia." *J Neurosci* 15 (7 Pt 1):4738-47.

Stuhmer, T., S. A. Anderson, M. Ekker, and J. L. Rubenstein. 2002. "Ectopic expression of the Dlx genes induces glutamic acid decarboxylase and Dlx expression." *Development* 129 (1):245-52.

Stuhmer, T., L. Puelles, M. Ekker, and J. L. Rubenstein. 2002. "Expression from a Dlx gene enhancer marks adult mouse cortical GABAergic neurons." *Cereb Cortex* 12 (1):75-85.

Sturtevant, A. H. 1951. "A map of the fourth chromosome of Drosophila melanogaster, based on crossing over in triploid females." *Proc Natl Acad Sci U S A* 37 (7):405-7.

Sunkel, C. E., and J. R. Whittle. 1987. "Brista: a gene involved in the specification and differentiation of distal cephalic and thoracic structures in Drosophila melanogaster." *Roux Arch Dev Biol* 196 (2):124-132. doi: 10.1007/BF00402034.

Swaroop, A., D. Kim, and D. Forrest. 2010. "Transcriptional regulation of photoreceptor development and homeostasis in the mammalian retina." *Nat Rev Neurosci* 11 (8):563-76. doi: 10.1038/nrn2880.

Tachibana, N., R. Cantrup, R. Dixit, Y. Touahri, G. Kaushik, D. Zinyk, N. Daftarian, J. Biernaskie, S. McFarlane, and C. Schuurmans. 2016. "Pten Regulates Retinal Amacrine Cell Number by Modulating Akt, Tgfbeta, and Erk Signaling." *J Neurosci* 36 (36):9454-71. doi: 10.1523/JNEUROSCI.0936-16.2016.

Takashima, S., M. Kitakaze, M. Asakura, H. Asanuma, S. Sanada, F. Tashiro, H. Niwa, J. Miyazaki Ji, S. Hirota, Y. Kitamura, T. Kitsukawa, H. Fujisawa, M. Klagsbrun, and M. Hori. 2002. "Targeting of both mouse neuropilin-1 and neuropilin-2 genes severely impairs developmental yolk sac and embryonic angiogenesis." *Proc Natl Acad Sci U S A* 99 (6):3657-62. doi: 10.1073/pnas.022017899.

Take-uchi, M., J. D. Clarke, and S. W. Wilson. 2003. "Hedgehog signalling maintains the optic stalk-retinal interface through the regulation of Vax gene activity." *Development* 130 (5):955-68.

Takebayashi, H., S. Yoshida, M. Sugimori, H. Kosako, R. Kominami, M. Nakafuku, and Y. Nabeshima. 2000. "Dynamic expression of basic helix-loop-helix Olig family members: implication of Olig2 in neuron and oligodendrocyte differentiation and identification of a new member, Olig3." *Mech Dev* 99 (1-2):143-8.

Talbot, J. C., S. L. Johnson, and C. B. Kimmel. 2010. "hand2 and Dlx genes specify dorsal, intermediate and ventral domains within zebrafish pharyngeal arches." *Development* 137 (15):2507-17. doi: 10.1242/dev.049700.

Tata, M., C. Ruhrberg, and A. Fantin. 2015. "Vascularisation of the central nervous system." *Mech Dev* 138 Pt 1:26-36. doi: 10.1016/j.mod.2015.07.001.

Thisse, C., and B. Thisse. 2008. "High-resolution in situ hybridization to whole-mount zebrafish embryos." *Nat Protoc* 3 (1):59-69. doi: 10.1038/nprot.2007.514.

Thompson, H., W. Andrews, J. G. Parnavelas, and L. Erskine. 2009. "Robo2 is required for Slit-mediated intraretinal axon guidance." *Dev Biol* 335 (2):418-26. doi: 10.1016/j.ydbio.2009.09.034.

Thompson, H., O. Camand, D. Barker, and L. Erskine. 2006. "Slit proteins regulate distinct aspects of retinal ganglion cell axon guidance within dorsal and ventral retina." *J Neurosci* 26 (31):8082-91. doi: 10.1523/JNEUROSCI.1342-06.2006.

Thornton, J. D., D. J. Swanson, M. N. Mary, D. Pei, A. C. Martin, S. Pounds, D. Goldowitz, and S. X. Skapek. 2007. "Persistent hyperplastic primary vitreous due to somatic mosaic deletion of the arf tumor suppressor." *Invest Ophthalmol Vis Sci* 48 (2):491-9. doi: 10.1167/iovs.06-0765.

Turner, D. L., and C. L. Cepko. 1987. "A common progenitor for neurons and glia persists in rat retina late in development." *Nature* 328 (6126):131-6. doi: 10.1038/328131a0.

Tzoulaki, I., I. M. White, and I. M. Hanson. 2005. "PAX6 mutations: genotype-phenotype correlations." *BMC Genet* 6:27. doi: 10.1186/1471-2156-6-27.

van Genderen, C., R. M. Okamura, I. Farinas, R. G. Quo, T. G. Parslow, L. Bruhn, and R. Grosschedl. 1994. "Development of several organs that require inductive epithelial-mesenchymal interactions is impaired in LEF-1-deficient mice." *Genes Dev* 8 (22):2691-703.

Vanderluit, J. L., K. L. Ferguson, V. Nikoletopoulou, M. Parker, V. Ruzhynsky, T. Alexson, S. M. McNamara, D. S. Park, M. Rudnicki, and R. S. Slack. 2004. "p107 regulates neural precursor cells in the mammalian brain." *J Cell Biol* 166 (6):853-63. doi: 10.1083/jcb.200403156.

Vanderluit, J. L., C. A. Wylie, K. A. McClellan, N. Ghanem, A. Fortin, S. Callaghan, J. G. MacLaurin, D. S. Park, and R. S. Slack. 2007. "The Retinoblastoma family member p107 regulates the rate of progenitor commitment to a neuronal fate." *J Cell Biol* 178 (1):129-39. doi: 10.1083/jcb.200703176.

Vitorino, M., P. R. Jusuf, D. Maurus, Y. Kimura, S. Higashijima, and W. A. Harris. 2009. "Vsx2 in the zebrafish retina: restricted lineages through derepression." *Neural Dev* 4:14. doi: 10.1186/1749-8104-4-14.

Voronina, V. A., E. A. Kozhemyakina, C. M. O'Kernick, N. D. Kahn, S. L. Wenger, J. V. Linberg, A. S. Schneider, and P. H. Mathers. 2004. "Mutations in the human RAX homeobox gene in a patient with anophthalmia and sclerocornea." *Hum Mol Genet* 13 (3):315-22. doi: 10.1093/hmg/ddh025.

Walther, C., and P. Gruss. 1991. "Pax-6, a murine paired box gene, is expressed in the developing CNS." *Development* 113 (4):1435-49.

Wang, F., C. B. Marshall, G. Y. Li, K. Yamamoto, T. W. Mak, and M. Ikura. 2009. "Synergistic interplay between promoter recognition and CBP/p300 coactivator recruitment by FOXO3a." *ACS Chem Biol* 4 (12):1017-27. doi: 10.1021/cb900190u.

Wang, H., R. Wang, T. Thrimawithana, P. J. Little, J. Xu, Z. P. Feng, and W. Zheng. 2014. "The Nerve Growth Factor Signaling and Its Potential as Therapeutic Target for Glaucoma." *Biomed Res Int* 2014:759473. doi: 10.1155/2014/759473.

Wang, S., C. Sengel, M. M. Emerson, and C. L. Cepko. 2014. "A gene regulatory network controls the binary fate decision of rod and bipolar cells in the vertebrate retina." *Dev Cell* 30 (5):513-27. doi: 10.1016/j.devcel.2014.07.018.

Wang, S. W., B. S. Kim, K. Ding, H. Wang, D. Sun, R. L. Johnson, W. H. Klein, and L. Gan. 2001. "Requirement for math5 in the development of retinal ganglion cells." *Genes Dev* 15 (1):24-9.

Wang, Y., G. D. Dakubo, S. Thurig, C. J. Mazerolle, and V. A. Wallace. 2005. "Retinal ganglion cell-derived sonic hedgehog locally controls proliferation and the timing of RGC development in the embryonic mouse retina." *Development* 132 (22):5103-13. doi: 10.1242/dev.02096.

Wangsa-Wirawan, N. D., and R. A. Linsenmeier. 2003. "Retinal oxygen: fundamental and clinical aspects." *Arch Ophthalmol* 121 (4):547-57. doi: 10.1001/archopht.121.4.547.

West, H., W. D. Richardson, and M. Fruttiger. 2005. "Stabilization of the retinal vascular network by reciprocal feedback between blood vessels and astrocytes." *Development* 132 (8):1855-62. doi: 10.1242/dev.01732.

Wigle, J. T., K. Chowdhury, P. Gruss, and G. Oliver. 1999. "Prox1 function is crucial for mouse lens-fibre elongation." *Nat Genet* 21 (3):318-22. doi: 10.1038/6844.

Williams, T. A., and L. M. Nagy. 1996. "Comparative limb development in insects and crustaceans." *Seminars in Cell & Developmental Biology* 7 (4):615-628. doi: https://doi.org/10.1006/scdb.1996.0075.

Williams, T., C. Nulsen, and L. M. Nagy. 2002. "A complex role for distal-less in crustacean appendage development." *Dev Biol* 241 (2):302-12. doi: 10.1006/dbio.2001.0497.

Wilson, S. W., and C. Houart. 2004. "Early steps in the development of the forebrain." *Dev Cell* 6 (2):167-81.

Wirt, S. E., and J. Sage. 2010. "p107 in the public eye: an Rb understudy and more." *Cell Div* 5:9. doi: 10.1186/1747-1028-5-9.

Wong, G., S. B. Conger, and M. Burmeister. 2006. "Mapping of genetic modifiers affecting the eye phenotype of ocular retardation (Chx10or-J) mice." *Mamm Genome* 17 (6):518-25. doi: 10.1007/s00335-005-0159-z.

Wu, F., T. J. Kaczynski, S. Sethuramanujam, R. Li, V. Jain, M. Slaughter, and X. Mu. 2015. "Two transcription factors, Pou4f2 and Isl1, are sufficient to specify the retinal ganglion cell fate." *Proc Natl Acad Sci U S A* 112 (13):E1559-68. doi: 10.1073/pnas.1421535112.

Wu, F., R. Li, Y. Umino, T. J. Kaczynski, D. Sapkota, S. Li, M. Xiang, S. J. Fliesler, D. M. Sherry, M. Gannon, E. Solessio, and X. Mu. 2013. "Onecut1 is essential for horizontal cell genesis and retinal integrity." *J Neurosci* 33 (32):13053-65, 13065a. doi: 10.1523/JNEUROSCI.0116-13.2013.

Yamada, H., E. Yamada, N. Kwak, A. Ando, A. Suzuki, N. Esumi, D. J. Zack, and P. A. Campochiaro. 2000. "Cell injury unmasks a latent proangiogenic phenotype in mice with increased expression of FGF2 in the retina." *J Cell Physiol* 185 (1):135-42. doi: 10.1002/1097-4652(200010)185:1<135::AID-JCP13>3.0.CO;2-Y.

Yaron, O., C. Farhy, T. Marquardt, M. Applebury, and R. Ashery-Padan. 2006. "Notch1 functions to suppress cone-photoreceptor fate specification in the developing mouse retina." *Development* 133 (7):1367-78. doi: 10.1242/dev.02311.

Ye, X., Y. Wang, H. Cahill, M. Yu, T. C. Badea, P. M. Smallwood, N. S. Peachey, and J. Nathans. 2009. "Norrin, frizzled-4, and Lrp5 signaling in endothelial cells controls a genetic program for retinal vascularization." *Cell* 139 (2):285-98. doi: 10.1016/j.cell.2009.07.047.

Yoshikawa, Y., T. Yamada, I. Tai-Nagara, K. Okabe, Y. Kitagawa, M. Ema, and Y. Kubota. 2016. "Developmental regression of hyaloid vasculature is triggered by neurons." *J Exp Med* 213 (7):1175-83. doi: 10.1084/jem.20151966.

Young, R. W. 1985. "Cell differentiation in the retina of the mouse." *Anat Rec* 212 (2):199-205. doi: 10.1002/ar.1092120215.

Yu, M., Y. Xi, J. Pollack, M. Debiais-Thibaud, R. B. Macdonald, and M. Ekker. 2011. "Activity of dlx5a/dlx6a regulatory elements during zebrafish GABAergic neuron development." *Int J Dev Neurosci* 29 (7):681-91. doi: 10.1016/j.ijdevneu.2011.06.005.

Yuan, L., D. Moyon, L. Pardanaud, C. Breant, M. J. Karkkainen, K. Alitalo, and A. Eichmann. 2002. "Abnormal lymphatic vessel development in neuropilin 2 mutant mice." *Development* 129 (20):4797-806.

Yue, T., K. Xian, E. Hurlock, M. Xin, S. G. Kernie, L. F. Parada, and Q. R. Lu. 2006. "A critical role for dorsal progenitors in cortical myelination." *J Neurosci* 26 (4):1275-80. doi: 10.1523/JNEUROSCI.4717-05.2006.

Yun, K., S. Fischman, J. Johnson, M. Hrabe de Angelis, G. Weinmaster, and J. L. Rubenstein. 2002. "Modulation of the notch signaling by Mash1 and Dlx1/2 regulates sequential specification and differentiation of progenitor cell types in the subcortical telencephalon." *Development* 129 (21):5029-40.

Yun, S., Y. Saijoh, K. E. Hirokawa, D. Kopinke, L. C. Murtaugh, E. S. Monuki, and E. M. Levine. 2009. "Lhx2 links the intrinsic and extrinsic factors that control optic cup formation." *Development* 136 (23):3895-906. doi: 10.1242/dev.041202.

Zagozewski, J. L., Q. Zhang, and D. D. Eisenstat. 2014. "Genetic regulation of vertebrate eye development." *Clin Genet* 86 (5):453-60. doi: 10.1111/cge.12493.

Zagozewski, J. L., Q. Zhang, V. I. Pinto, J. T. Wigle, and D. D. Eisenstat. 2014. "The role of homeobox genes in retinal development and disease." *Dev Biol*. doi: 10.1016/j.ydbio.2014.07.004.

Zerucha, T., and M. Ekker. 2000. "Distal-less-related homeobox genes of vertebrates: evolution, function, and regulation." *Biochem Cell Biol* 78 (5):593-601.

Zhang, J., S. Fuhrmann, and M. L. Vetter. 2008. "A nonautonomous role for retinal frizzled-5 in regulating hyaloid vitreous vasculature development." *Invest Ophthalmol Vis Sci* 49 (12):5561-7. doi: 10.1167/iovs.08-2226.

Zhang, L., P. H. Mathers, and M. Jamrich. 2000. "Function of Rx, but not Pax6, is essential for the formation of retinal progenitor cells in mice." *Genesis* 28 (3-4):135-42.

Zhang, Q., J. Zagozewski, S. Cheng, R. Dixit, S. Zhang, J. de Melo, X. Mu, W. H. Klein, N. L. Brown, J. T. Wigle, C. Schuurmans, and D. D. Eisenstat. 2017. "Regulation of Brn3b by Dlx1 and Dlx2 is required for retinal ganglion cell differentiation in the vertebrate retina." *Development*. doi: 10.1242/dev.142042.

Zhao, S., W. P. Fung-Leung, A. Bittner, K. Ngo, and X. Liu. 2014. "Comparison of RNA-Seq and microarray in transcriptome profiling of activated T cells." *PLoS One* 9 (1):e78644. doi: 10.1371/journal.pone.0078644.

Zhao, S., and P. A. Overbeek. 2001. "Regulation of choroid development by the retinal pigment epithelium." *Mol Vis* 7:277-82.

Zhou, Q. P., T. N. Le, X. Qiu, V. Spencer, J. de Melo, G. Du, M. Plews, M. Fonseca, J. M. Sun, J. R. Davie, and D. D. Eisenstat. 2004. "Identification of a direct Dlx homeodomain target in the developing mouse forebrain and retina by optimization of chromatin immunoprecipitation." *Nucleic Acids Res* 32 (3):884-92. doi: 10.1093/nar/gkh233.

Zhou, Q., S. Wang, and D. J. Anderson. 2000. "Identification of a novel family of oligodendrocyte lineage-specific basic helix-loop-helix transcription factors." *Neuron* 25 (2):331-43.

Zhu, L., S. van den Heuvel, K. Helin, A. Fattaey, M. Ewen, D. Livingston, N. Dyson, and E. Harlow. 1993. "Inhibition of cell proliferation by p107, a relative of the retinoblastoma protein." *Genes Dev* 7 (7A):1111-25.

Zhu, L., L. Zhu, E. Xie, and L. S. Chang. 1995. "Differential roles of two tandem E2F sites in repression of the human p107 promoter by retinoblastoma and p107 proteins." *Mol Cell Biol* 15 (7):3552-62.

Zuber, M. E., G. Gestri, A. S. Viczian, G. Barsacchi, and W. A. Harris. 2003. "Specification of the vertebrate eye by a network of eye field transcription factors." *Development* 130 (21):5155-67. doi: 10.1242/dev.00723.

APPENDIX

8 Appendix

The appendix section contains additional experiments carried out by Jamie Zagozewski that do not correspond with the overall subject matter detailed in the thesis chapters. These experiments will be briefly described and summarized in the appendix.

8.1 Characterization of the *Dlx1* and *Dlx2* single knockout retinas

Dlx1 and *Dlx2* single knockout mice have been previously examined for their role in forebrain development. While the *Dlx1* and *Dlx2* single knockouts (SKO) die shortly after birth, the forebrain defects are subtle and mutation of the convergent pair of *Dlx1*/*Dlx2* is required to observe severe developmental defects including aberrant interneuron differentiation and migration as discussed in Chapter 4 (Anderson, Qiu, et al. 1997, Eisenstat et al. 1999). The phenotype of *Dlx1* and *Dlx2* SKO retinas has not been previously examined. *Dlx2*-flox mice have been recently generated by Dr. John Rubenstein at the University of California, San Francisco (personal communication), which would allow us to study the role of *Dlx2* in the postnatal retina. As mentioned previously, the role of *Dlx* genes in postnatal retina development and function is unknown as the *Dlx1*/*Dlx2* DKO mouse dies at P0. Therefore, we were interested in examining individual *Dlx* gene knockouts in the developing retina to determine if a *Dlx2* conditional knockout mice would possibly be a suitable model to examine *Dlx* gene function in the postnatal retina. In the WT retina, *Dlx1* expression is not observed after P0 while *Dlx2* expression is maintained to adulthood (de Melo et al. 2003). Also, the addition of *Dlx1* expression plasmids in reporter assays where *Dlx2* expression plasmid is already present does not increase transcription of luciferase compared to *Dlx2* alone (Zhang et al. 2017). Therefore, we hypothesized that the *Dlx2* SKO mouse would have a similar phenotype to that of the *Dlx1*/*Dlx2* DKO retina. The *Dlx1* and *Dlx2* SKO embryos were kindly provided by Dr. John Rubenstein (University of California, San Francisco). *Dlx1* and *Dlx2* SKO mice were maintained

on a C57Bl/6 background. Tissue embedding and sectioning was carried out as described in Chapter 2.2. We performed preliminary CRX and Brn3B immunostaining on *Dlx1* and *Dlx2* SKO tissue sections and compared the results in the SKO retinas to results collected in the *Dlx1*/*Dlx2* DKO retina. In the DKO retina at E18, there was a significant decrease in cells expressing BRN3B, but no significant increase in cells expressing CRX was observed, perhaps due to the genetic background as discussed in Chapter 3 (Figure 8.1). In the *Dlx2* SKO retina, a trend showing a decrease in cells expressing BRN3B was observed and an increase in cells expressing CRX (N=2) (Figure 8.2). Both BRN3b and CRX expression in the *Dlx1* SKO retina did not differ significantly compared to WT controls (Figure 8.1). These results suggest that *Dlx2* SKO retinas may have a similar but less severe phenotype to that observed in the *Dlx1*/*Dlx2* DKO retina. Therefore, examination of a *Dlx2* conditional knockout retina may be an effective tool for examination of *Dlx* gene function in postnatal retinal development.

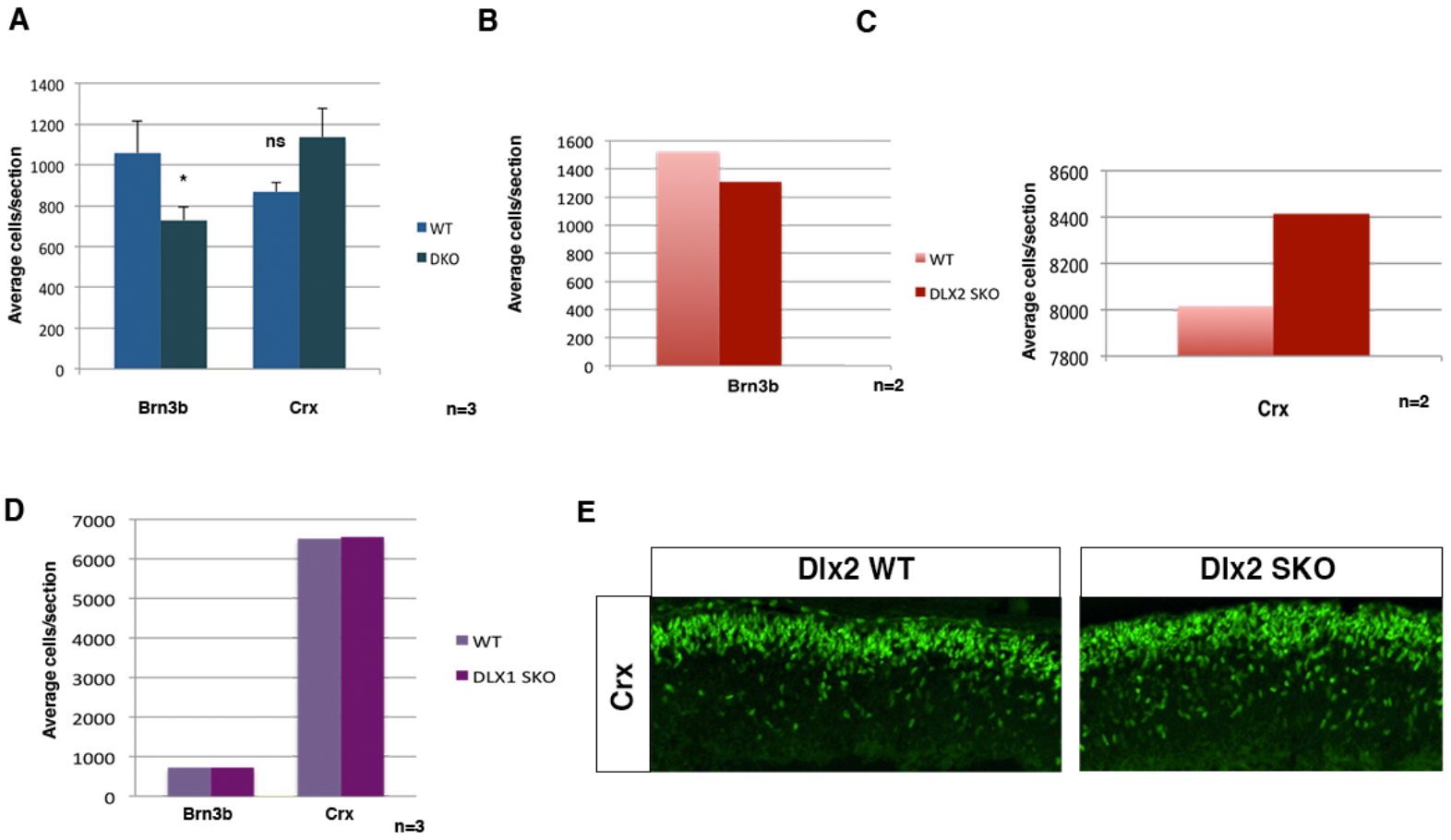
A
B
C
Average cells/section
1400
1200
1000
800
600
400
200
0
ns
*
WT
DKO
Brn3b
Crx
n=3
1600
1400
1200
1000
800
600
400
200
0
WT
DLX2 SKO
Brn3b
n=2
8600
8400
8200
8000
7800
Crx
n=2
D
E
7000
6000
5000
4000
3000
2000
1000
0
WT
DLX1 SKO
Brn3b
Crx
n=3
Dlx2 WT
Dlx2 SKO
Crx

Figure 8.1 *Dlx2* SKO retina resembles *Dlx1*/*Dlx2* DKO.

Characterization of the *Dlx1* and *Dlx2* SKO retina was performed to determine if the *Dlx2* SKO retina phenotypically resembled the *Dlx1*/*Dlx2* SKO. (A) BRN3B positive cells were significantly reduced in the *Dlx1*/*Dlx2* DKO retina compared to controls as have been reported previously. CRX positive cells were not significantly upregulated. (B) In the *Dlx2* SKO retina, there was a trend showing reduction in BRN3B positive cells. (C) An increase in CRX expressing cells was observed in the *Dlx2* SKO retina. (D) In the *Dlx1* SKO retina, no change was observed in BRN3B or CRX positive cells compared to WT controls. (E) Increase in CRX expressing cells in the *Dlx2* SKO retina.